VNIVERSITAT DE VALÈNCIA

Faculty of Medicine and Dentistry
Department of Stomatology

Doctoral Thesis

MODULATION OF SALIVARY INFLAMMATORY MARKERS AND PROTEOMIC ANALYSIS IN HNC AND OSCC PATIENTS UNDERGOING RADIOTHERAPY

Doctoral Programme in Dentistry 3143 RD 99/2011

PhD Candidate:
SARA PRINCIPE

Supervisors:
DR. JOSÉ V. BAGÁN SEBASTIÁN
DR. MANUEL M. SÁNCHEZ DEL PINO

January 2021

“LEARN FROM YESTERDAY,

LIVE FOR TODAY AND

HOPE FOR TOMORROW.

THE IMPORTANT THING IS

NOT TO STOP QUESTIONING”

Albert Einstein

AGRADECIMIENTOS

Expresar tu gratitud a las personas que lo merecen en un idioma que no es el tuyo no es algo sencillo, pero lo intentaré, espero que salga bien.

Hace casi cuatro años no podía imaginar lo que hubiera significado llegar hasta aquí, feliz de ponerme a prueba otra vez decidí emprender esta aventura con mi maleta llena de expectativas, dudas e ilusiones y ahora que esta experiencia está por terminar, puedo decir que ha sido un camino largo, en algún momento complejo y no siempre fácil, pero que ha merecido la pena.

Todo esto no hubiera sido posible sin la ayuda del Prof. Bagán, que depositó su confianza en mi desde el principio, dándome la posibilidad de formar parte de este proyecto. Muchas gracias por sus consejos, por haber compartido su gran experiencia y sabiduría, y sobre todo por su profunda humanidad hacia los pacientes, usted me ha enseñado lo que de verdad significa confiar en la medicina. Mi profunda gratitud también va al Prof. Sánchez del Pino, por el apoyo brindado, la disponibilidad en todo momento, los sabios consejos y sobre todo por su gran dedicación hacia la ciencia.

Gracias a todo el equipo de investigación de la Fundación de Investigación del Hospital General de Valencia, a la Dra. Jantus y la Dra. Calabuig, y a todos los compañeros del Laboratorio de Oncología, por haber compartido los días buenos y también los malos, por haberme ayudado en algo que parecía imposible y no lo fue, y por las risas que nunca han faltado.

Gracias a todo el Departamento de Estomatología y Cirugía Maxilofacial, por haber sido un apoyo, siempre y no solo cuando hacía falta, ha sido un placer trabajar con vosotros. Gracias a los Otorrinolaringólogos, a los Radioterapeutas, a todo el personal sanitario y también a los del Departamento de Medicina Oral de la UVEG que, con mucha paciencia, me han ayudado en el largo camino hacia la meta.

Sin embargo, el agradecimiento más grande es para todos los pacientes que han decidido involucrarse en este proyecto y compartir conmigo una pequeña parte de sus batallas contra la enfermedad, sin ellos todo esto no hubiera sido posible.

Gracias a “my partner in crime” alias Valentina Dikova, for supporting and standing me during these years, for the great time and the amazing adventures spent together, nuestra verdadera amistad es un regalo que me llevo de esta experiencia.

Gracias a “L’Ostello Principe” y a todos los que han hecho parte de esta grande familia, nunca os olvidaré.

Infine, un grazie speciale va ai miei genitori, mia sorella e al resto della grande famiglia made in Italy, i Pacifico e i De Biasi, nipotame annesso, che, nonostante la distanza, sono sempre riusciti a farmi arrivare quell’amore e il calore di cui avevo bisogno.

Last but not the least, Tonia Ripullone se non ci fossi bisognerebbe inventarti, grazie infinite per tutto l'aiuto, l'immane pazienza, l’amicizia sincera.

A Sofia,

A Michele,

"Perché ci sarà sempre luce,

Finché saremo coraggiosi abbastanza da vederla.

Finché saremo coraggiosi abbastanza da essere noi stessi luce" AG

ABSTRACT

Head and neck cancer (HNC) includes malignant tumours that most commonly arise from the oral mucosa or lining of the head and neck regions. They are characterized according to their primary site of origin as malignancies of the nasal cavity and paranasal sinuses, pharynx, larynx, salivary glands and oral cavity. The majority of these neoplasms are epithelial tumours, among them the 90% are squamous cell carcinomas (SCC). HNC including the Oral Squamous cell carcinoma (OSCC), is the sixth most common neoplasia worldwide with an incidence estimated at 650,000 cases and 330,000 deaths per year.

Despite all of the diagnostic and therapeutic advances, the 5-year survival rate remains relatively poor, around 50%. The typically late diagnosis usually requires surgical intervention, often followed by adjuvant radiotherapy (RT) and/or chemotherapy (CT) treatment. Ionizing radiation is known to increase the expression of a number of cytokines involved in inflammation and wound healing. Inflammation has become an important hallmark of cancer, the chronic inflammatory microenvironment is associated with the release of various pro-inflammatory and anti-inflammatory cytokines, chemokines and growth factors that make it more vulnerable toward tumorigenesis. Salivary cytokines have promising features to be used as biomarkers for screening and outcome prediction in this malignancy.

To date, the majority of saliva studies have focused on the levels of these inflammatory proteins comparing HNC patients with healthy individuals. However, changes from pre to post RT-treatment have not been extensively explored due to salivary glands destruction and subsequent xerostomia. Therefore, the main goals of this research project are 1) the evaluation of salivary inflammatory markers and 2) the investigation of salivary proteome before and after the irradiation process, in order to identify potential predictive biomarkers of RT response in HNC.

A panel of eight salivary inflammatory markers (IL-4, IL-6, IL-8, IL-10, MCP-1, TNF-α, VEGF, and EGF) was analysed in a group of HNC patients (N=30), pre- and post-RT, and a group of healthy subjects (N=37) as well, using immunoassays based on Multi

Analyte Profiling technology (Luminex xMAP). The investigation of the salivary proteome was carried out using liquid chromatography and tandem mass spectrometry technique with SWATH acquisition (LC-MS/MS-SWATH), which consisted of two phases: generation of a peptide spectral library using 10 HNC saliva samples and quantification of 30 individual salivary proteome profiles, selected from the two cohorts of the study.

Results concerning the salivary inflammatory markers showed a post-treatment augmentation in multiple cytokines, being the increment of IL-8 and MCP-1 statistically significant (*p-value* ≤ 0,001 and ≤ 0,0001, respectively). The comparison between the control group and the HNC patients before receiving the RT reported a significant increase of IL-6 levels (*p-value* ≤ 0,0001), to be associated with the presence of the tumour lesion. Lastly, ROC curves analysis pointed out the strong potential of IL-8 as a predictive biomarker of RT outcomes (AUC= 0.84; p-value= 0.018).

Results from the proteomic investigation demonstrated that the salivary proteome varies in saliva of HNC patients undergoing radiotherapy. Comparing pre- and post-treatment conditions a total of 21 proteins results differentially expressed. Besides, analysing the pattern followed by the control subjects and the HNC patients not yet treated, an altered salivary protein profile was detected. Among the salivary markers identified, gene NUCB2 product, gene PPIB product and gene HSPE1 product may be considered as potential predictive biomarkers of RT response, gene LTF product can help to discriminate between HNC cases pre- and post-RT, whereas gene SERPINA3 product and gene AGPAT1 product are related to the presence of HNC.

Our data support the hypothesis that screening salivary inflammatory molecules could provide a useful approach to identify biomarkers in this malignancy. Proteomic results need to be validated in a larger cohort of samples before its potential translation into clinical research. These findings may serve as the foundation of studies exploring the use of saliva as a biofluid to monitor treatment outcomes.

INDEX

Summary of the Thesis in Spanish,

according to the regulations of the University of Valencia

INTRODUCCIÓN

El cáncer de cabeza y cuello (HNC, por sus siglas en inglés) incluye tumores malignos que surgen con mayor frecuencia a partir de las células epiteliales escamosas que revisten las superficies mucosas de dicha área (por ejemplo, la boca, la nariz y la orofaringe). Se caracterizan según su origen primario como neoplasias de la cavidad nasal y senos paranasales, faringe, laringe, glándulas salivales y de la cavidad bucal. La mayoría de estas neoplasias son tumores epiteliales, entre ellos el 90% son carcinomas de células escamosas. El HNC, incluyendo el carcinoma oral de células escamosas (OSCC, por sus siglas en inglés), es la sexta neoplasia maligna más común en todo el mundo con una incidencia estimada en 650.000 casos y 330.000 muertes por año. Muchos de estos tumores tienen una evidente y demostrada relación con ciertos hábitos como el tabaquismo y el abuso de alcohol (p. ej., tumores de laringe, de la cavidad oral y tumores orofaríngeos), mientras que otros se han relacionado con infecciones virales (virus de Epstein-Barr en tumores nasofaríngeos, virus del papiloma humano en algunos carcinomas orofaríngeos).

A pesar de todos los avances diagnósticos y terapéuticos, la tasa de supervivencia a 5 los años sigue siendo relativamente baja, alrededor del 50%. El diagnóstico típicamente tardío suele requerir una intervención quirúrgica invasiva, muchas veces seguida de un tratamiento con radioterapia (RT) o quimioterapia adyuvante. Se sabe que la radiación ionizante aumenta la expresión de varias citocinas implicadas en la inflamación, y en los últimos años ésta se ha convertido en un sello importante del cáncer. El microambiente inflamatorio crónico está asociado con la liberación de diversas citocinas proinflamatorias y antiinflamatorias, quimiocinas y factores de crecimiento que lo hacen más vulnerable a la tumorigénesis. Las proteínas inflamatorias salivales tienen características con un potencial reconocido para poder ser utilizadas como biomarcadores en el diagnóstico y la predicción de resultados terapéuticos ante esta neoplasia.

Hasta la fecha, la mayoría de los estudios con saliva se han centrado en los niveles de estas citocinas comparando pacientes con HNC e individuos sanos. Sin embargo, los hallazgos diferenciales entre las condiciones antes y después del tratamiento con

RT no se han explorado ampliamente debido a la destrucción de las glándulas salivales y la consiguiente xerostomía; aunque el avance en los más recientes tratamientos radioterápicos, que protegen las glándulas salivales, ha mostrado un impacto favorable en la recuperación de la saliva. La finalidad de este proyecto de investigación es la evaluación de marcadores inflamatorios salivales y del proteoma salival antes y después del proceso de irradiación, con el fin de identificar posibles biomarcadores predictivos de la respuesta a la radioterapia en el cáncer de cabeza y cuello.

OBJETIVOS

1. Investigación de marcadores inflamatorios salivales

1.1. Comprobar si hay diferencias entre los niveles de citocinas proinflamatorias (IL-6, IL-8, TNF-α) y antiinflamatorias (IL-4, IL-10), quimiocinas (MCP-1/CCL2) y factores de crecimiento (EGF, VEGF) en las tomas salivales realizadas en pacientes con cáncer de cabeza y cuello antes y después de la RT, analizando los mismos casos. Posteriormente, valorar si hay diferencias en las citadas proteínas salivales entre el grupo de controles sanos con los casos de cáncer evaluados antes de someterse a la RT.

1.2. Verificar si existe una relación entre los niveles de los marcadores inflamatorios salivales con las variables clínicas de los pacientes con HNC, en particular la tolerancia al tratamiento (desarrollo de mucositis) y la respuesta a la RT.

1.3. Finalmente, comprobar si alguna de las citocinas, quimiocinas o factores de crecimiento analizados puede considerarse como marcador biológico predictivo de la respuesta al tratamiento radioterápico en paciente con cáncer de cabeza y cuello.

2. Investigación sobre el proteoma salival

2.1. Verificar si existen alteraciones en el proteoma salival entre el grupo de controles sanos con los casos de cáncer valorados antes y tras el someterse a la RT. Posteriormente, valorar si hay diferencias en los perfiles del proteoma salival entre los mismos pacientes con HNC, analizados antes y después del tratamiento con RT.

2.2. Examinar si entre las proteínas salivales alteradas pueden encontrarse moléculas relacionadas con la lesión tumoral, la progresión del tratamiento o la respuesta a la RT.

2.3. Comprobar si alguna de las proteínas salivales identificadas puede considerarse como marcador biológico predictivo de la respuesta al tratamiento radioterápico en paciente con cáncer de cabeza y cuello.

MATERIAL Y MÉTODOS

Diseño del estudio

El presente estudio prospectivo observacional se realizó en el Hospital General Universitario de Valencia (HGUV) entre los años 2017 al 2020. La investigación se llevó a cabo de acuerdo con los principios fundamentales establecidos en la Declaración de Helsinki y con la aprobación previa del comité ético de investigación del HGUV.

Pacientes

En este estudio se usaron dos cohortes de sujetos independientes. En la cohorte de pacientes diagnosticados de HNC que se sometieron a RT se incluyeron 30 individuos (Cohorte 1), mientras que 37 voluntarios sanos fueron seleccionados para la cohorte de controles sanos (Cohorte 2). Los pacientes provenían del Servicio de Cirugía Oral y Maxilofacial y del Servicio de Otorrinolaringología del HGUV, y en parte del Servicio de Radioterapia del Instituto Valenciano de Oncología (IVO). Los voluntarios sanos fueron recogidos en la Clínica Odontológica de la Universidad de

Valencia (UVEG). Los criterios de selección seguidos fueron los siguientes: Cohorte 1, eran pacientes con un diagnóstico histológico de HNC, tratamiento radioterápico mínimo de 30 días, ausencia de patologías a nivel de las glándulas salivales. En el caso de la Cohorte 2, se trataba de sujetos sanos, de sexo y edad similares a los del grupo de pacientes con cáncer y sin ninguna patología a nivel de las glándulas salivales. Todos los sujetos aceptaron participar voluntariamente en el estudio firmando el correspondiente consentimiento informado.

Para el grupo de pacientes, los parámetros clínicos registrados fueron: edad, sexo, diagnóstico, localización de la lesión, metástasis en el cuello, clasificación TNM, desarrollo de mucositis, respuesta al tratamiento. La última variable se registró en dos momentos: al final de la radioterapia (T = 0) y tres meses después (T = 1).

La evaluación de la respuesta clínica tras someterse al tratamiento radioterápico se basó en la siguiente clasificación:

1) Respuesta completa (RC) → desaparición de la lesión tumoral tras la RT

2) Respuesta parcial (RP) → disminución del tamaño tumoral, pero persistencia de la lesión maligna después de la RT

3) Sin respuesta (NR) → ninguna reducción del tamaño tumoral desde que comenzó el tratamiento o progresión inequívoca de las lesiones existentes

4) Recurrencia (R) → aparición de una o más lesiones nuevas en T=1

Muestras

La posibilidad de medir cambios en la saliva no estimulada antes y después del proceso de irradiación es generalmente muy baja, debido a la destrucción de las glándulas salivales causada por el tratamiento. Para superar este problema, en todos los sujetos incluidos en el proyecto se recogió la saliva estimulada. Con respecto a la Cohorte 1, la primera muestra se tomó antes del tratamiento con RT (BRT, por sus siglas en inglés), mientras que la segunda muestra fue recolectada después de la RT (ART, por sus siglas en inglés) y se obtuvo en un rango de 4/8 semanas tras finalizar el proceso de irradiación, debido a las secuelas inflamatorias esperadas posteriormente a la RT. En cuanto a la Cohorte 2, las muestras de saliva en los

voluntarios sanos se tomaron siempre en la primera visita. Todos los participantes del estudio debían evitar comer, beber, fumar y usar productos de higiene bucal durante al menos 1 hora antes de la toma. El flujo salival se estimuló masticando parafina durante 5 minutos, bajo estimulación continua, la saliva acumulada en la boca se expulsaba y vaciaba en un tubo de 15 ml a través de un embudo. Posteriormente, la muestra recogida se centrifugó a 3000 rpm durante 15 min a 4 °C y se congeló a -80 °C hasta su posterior uso. Se registró el estado periodontal de cada participante y se descartaron del estudio las muestras con rastros visibles de sangre.

Evaluación de los marcadores inflamatorios salivales

Se realizaron inmunoensayos, basados en la tecnología Luminex® xMAP (*multi-analyte profiling*) para análisis de proteínas y detección de biomarcadores, con el objetivo de cuantificar la concentración salival de IL-4, IL-6, IL-8, IL-10, MCP-1, TNF-α, VEGF y EGF. Los niveles de fluorescencia en cada estándar, control de calidad y muestra se detectaron con el uso de Luminex 200™ (Luminex Corporation, Austin, TX). Los datos se analizaron posteriormente utilizando el software de gestión Bio-plex (Bio-Rad Laboratories, Inc. Hercules, CA). Las muestras de saliva, antes de ser analizadas, se descongelaron y centrifugaron a 1500 rpm durante 15 min a 4 °C para obtener un sobrenadante transparente, desprovisto de partículas y residuos.

Evaluación del proteoma salival

El estudio proteómico se realizó mediante la técnica de cromatografía líquida y espectrometría de masas en tándem (LC-MS/MS). Se realizaron ensayos preliminares de LC-MS/MS para identificar (entre la saliva completa, el sobrenadante y el sedimento) el mejor componente salival para detectar y describir las proteínas del proteoma salival. La cuantificación de proteínas se realizó mediante la técnica SWATH que consistió en dos fases: generación de una biblioteca espectral de péptidos a partir de 10 pacientes con HNC y cuantificación de 30 perfiles proteómicos salivales, seleccionados de las dos cohortes del estudio. Una vez lograda la construcción de la "biblioteca espectral del cáncer de cabeza y cuello" utilizando la saliva completa, se realizó la investigación del proteoma salival antes y después del tratamiento

radioterápico, en conjunto, con la cuantificación dirigida de proteínas inflamatorias salivales y la comparación entre los perfiles proteómicos de pacientes y controles.

Antes de cualquier análisis proteómico, todas las muestras de saliva se descongelaron y se centrifugaron a 1500 rpm durante 15 min a 4 °C. Posteriormente, cada muestra se agitó en un vórtex para reducir la viscosidad. La resultante combinación heterogénea de secreciones serosas y mucosas se dividió en alícuotas y se utilizó para el siguiente análisis: determinación de la concentración de proteínas con el método de Bradford, separación de proteínas por electroforesis en gel de poliacrilamida-SDS unidimensional (SDS-PAGE 1D).

I. Construcción de la biblioteca de espectros

Se utilizó un conjunto de 10 muestras de saliva completa, obtenidas de 10 pacientes con cáncer de cabeza y cuello (7 en estadio avanzado y 3 en estadio inicial del cáncer, antes de cualquier tipo de tratamiento o intervención quirúrgica) para crear la biblioteca espectral. En primer lugar, se cuantificó la proteína total salival mediante Bradford, luego, combinando la misma cantidad de proteínas de cada muestra, se creó un *pool* que se separó mediante electroforesis en gel de poliacrilamida-SDS (4% *stacking gel* - 12% *resolving gel*). La carrera electroforética se cortó en cinco piezas y cada una se procesó individualmente. A continuación, las proteínas se digirieron con tripsina y los péptidos resultantes se analizaron por LC-MS/MS, usando un espectrómetro de masas TripleTOF 5600 (SCIEX) operado en modo de adquisición de datos dependiente (DDA). Las proteínas se identificaron mediante el sofware Protein Pilot (SCIEX).

II. Análisis individuales de los perfiles proteómicos salivales

Para realizar la segunda parte del estudio proteómico se emplearon 30 muestras de saliva completa. Sobre la base de criterios específicos (sexo, edad, parámetros clínicos), se realizó una selección entre las dos cohortes del estudio con el fin de identificar los mejores candidatos para la investigación de los perfiles del proteoma salival. Los sujetos incluidos se dividieron en 3 grupos distintos:

- GRUPO 1 compuesto por 10 pacientes con muestras tomadas antes de la radioterapia (BRT)
- GRUPO 2 compuesto por 10 pacientes diagnosticados de HNC cuyas muestras se obtuvieron tras la radioterapia (ART)
- GRUPO 3 constituido por 10 voluntarios sanos considerados como controles (CTRL)

Las muestras pertenecientes al Grupo 2 se obtuvieron de los mismos pacientes del Grupo 1, evaluados antes y después del tratamiento, los casos de ambos grupos están incluidos en la Cohorte 1 del estudio. Los sujetos sanos reclutados en el Grupo 3 se seleccionaron a partir de la Cohorte 2. Las muestras de saliva se procesaron como se mencionó anteriormente: tras el proceso de cuantificación mediante el ensayo de Bradford, 20 µg de proteínas de cada muestra se cargaron en un gel de poliacrilamida-SDS (4% *stacking gel* - 15% *resolving gel*) para el proceso electroforético, mediante la aplicación de 20 mA durante 20 min. Después, las proteínas se digirieron con tripsina y los péptidos generados se analizaron por LC-MS/MS usando un espectrómetro de masas TripleTOF 6600 (SCIEX) operado en modo de adquisición independiente de datos (DIA) o SWATH. Para completar el análisis, los datos obtenidos del experimento SWATH fueron analizados mediante el software Peak View (v2.1, SCIEX), utilizando la biblioteca de espectros del cáncer de cabeza y cuello como referencia.

RESULTADOS

Objetivo 1: Investigación de marcadores inflamatorios salivales

Características de los pacientes

Este estudio incluyó 30 pacientes con HNC, que fueron sometidos a radioterapia y valorados antes y tras el tratamiento, y 37 voluntarios sanos. La mediana de la edad de los pacientes con HNC (Cohorte 1) fue de 60,5 años [rango: 38-85], el 66,76% eran hombres y el 33,33% eran mujeres. La localización tumoral con mayor incidencia fue la cavidad bucal (36,67%), seguida de la laringe (33,33%). La descripción histológica

del cáncer de células escamosas se observó en el 96,76% de los casos. Además, el 60% de los pacientes fueron diagnosticados en estadio avanzado de la enfermedad (T3-T4) y el 46,67% también presentaron metástasis en el cuello. La mayoría de la población con HNC recibió RT adyuvante postoperatoria (60%). Se observó el desarrollo de mucositis oral en el 90% de los casos. La respuesta al tratamiento registrada al tiempo T = 0 (final de la RT) mostró una RC en el 96,67% de los pacientes, aunque se observó una ligera disminución en el considerado como tiempo T = 1 (tres meses después de la terapia) donde el porcentaje de RC registrado fue del 80,0%. Los sujetos de control (Cohorte 2) incluyeron 19 hombres sanos (51,35%) y 18 mujeres sanas (48,65%) con una edad mediana de 57 años [rango: 40-78].

Objetivo específico 1.1: El estudio de comparación sobre los marcadores inflamatorios salivales, se llevó a cabo primero en pacientes con HNC sometidos a radioterapia y, en segundo lugar, en controles sanos.

Con respecto a la comparación de los niveles salivales de EGF, IL-10, IL-4, IL-6, IL-8, MCP-1, TNF-α y VEGF en pacientes con HNC, antes y después del tratamiento con RT, el análisis estadístico se realizó mediante un test no paramétrico T de Wilcoxon, siendo muestras apareadas.

Los datos analizados revelaron que la concentración de IL-8 y MCP-1 aumentó significativamente en la saliva de los pacientes con HNC después de la RT, mostrando un p-valor ≤ 0,001 y ≤ 0,0001, respectivamente. Sin embargo, no se observaron cambios significativos en los niveles de expresión de IL-10, IL-4, IL-6, TNF-α y VEGF. Por último, se detectó una disminución en los niveles de EGF, aunque sin alcanzar significación estadística.

Posteriormente, se analizaron los niveles salivales de citocinas proinflamatorias (IL-6, IL-8, TNF-α) y antiinflamatorias (IL-4, IL-10), quimiocinas (MCP-1 / CCL2) y factores de crecimiento (EGF, VEGF) en controles sanos y pacientes con HNC evaluados antes (grupo BRT) y tras el proceso de irradiación (grupo ART). Debido a que las dos comparaciones debían realizarse entre grupos independientes, se utilizó una prueba U de Mann-Whitney no paramétrica.

Se observó un incremento en los niveles salivales de IL-10, IL-4, IL-8, MCP-1, TNF-α y VEGF, que se correlacionó con la presencia de la enfermedad maligna. Sin embargo, la significancia estadística se confirmó solo para los niveles de IL-6, presentando un p-valor ≤ 0,0001. Con respecto a la concentración de EGF, los resultados no mostraron diferencias entre los pacientes evaluados antes de la RT y los controles (grupo CTRL).

Objetivo específico 1.2: Comprobar si hay correlación de las proteínas salivales alteradas con las variables clínicas de los pacientes con HNC.

Para este análisis, se construyó una red bayesiana utilizando gráficos acíclicos dirigidos (DAG) y metodología de probabilidad condicional. La red bayesiana generalmente asume que los datos se distribuyen normalmente. En nuestro caso, no fue así debido al pequeño tamaño muestral. Por ello, las variables tuvieron que ser simplificadas ya que presentaban un número excesivo de condiciones en relación al número de muestras. Una vez reducidos los parámetros clínicos, se realizó el análisis de dependencia entre:

a) los datos promedios de los analitos (EGF, IL-10, IL-4, IL-6, IL-8, MCP-1, TNF-α y VEGF) del grupo de pacientes evaluados antes de la RT (grupo BRT) y las siguientes variables: diagnóstico (HNC u OSCC), localización de la lesión tumoral, metástasis en el cuello, tumor primario ("TNM.T") y extensión de la metástasis en los ganglios linfáticos regionales ("TNM.N");

b) Los datos promedios de los mencionados analitos, obtenidos del grupo de pacientes analizados después del tratamiento radioterápico (grupo ART) y las siguientes variables: tipo de tratamiento (Cirugía + RT, Quimioradioterapia (QRT), RT solo), respuesta al tratamiento (respondedores, no respondedores), tolerancia al tratamiento (dermitis, mucositis, xerostomía).

No se observó dependencia entre los analitos y la variable “TNM.T” en el caso de las muestras pertenecientes al grupo BRT, así como tampoco para las variables “tipo de tratamiento” y “mucositis” en el caso de las muestras pertenecientes al grupo ART. Esto no quiere decir que dicha dependencia no exista, sino que la muestra es demasiado pequeña para concluir algo respecto a estos parámetros clínicos. Para el

resto de variables, sí que se encontraron dependencias, directas e indirectas. Por un lado, antes del tratamiento, la red indicó que todos los analitos podrían tener valores significativos aplicables al diagnóstico de HNC u OSCC. Además, teniendo en cuenta la variable "localización del tumor", se observó una relación directa con las proteínas IL-10 e IL-6; mientras que para el parámetro "TNM.N" se detectó una conexión directa solo con la proteína MCP-1. Por otro lado, a partir de nuestros resultados sobre las variables clínicas analizadas tras la RT, "respuesta al tratamiento" y "metástasis en cuello", existe, en todos los analitos, un rango de valores que podrían ser utilizados como criterio diagnóstico para los pacientes con buena respuesta terapéutica. Finalmente, en cuanto al parámetro de "tolerancia al tratamiento" y las condiciones clínicas dermitis y xerostomía, se detectó un rango de valores diagnósticos para las proteínas IL-6 e IL-10, aunque sea solo para excluir el posible desarrollo de estos efectos secundarios. Sin embargo, debido al número limitado de muestras disponibles, debemos asumir que estos son resultados preliminares y deben ser validados en un grupo más grande de pacientes.

Objetivo específico 1.3: Comprobar si alguna de las proteínas salivales analizadas puede considerarse como marcador biológico predictivo de la respuesta al tratamiento radioterápico.

Para lograr este objetivo, se comparó la expresión de estos marcadores salivales (EGF, IL-10, IL-4, IL-6, IL-8, MCP-1, TNF-α y VEGF) en las muestras tumorales antes de recibir el tratamiento radioterápico (grupo BRT), con el fin de identificar si alguno de ellos estaba asociado con la respuesta a los tres meses de administrar la terapia (T=1). Nos centramos en la respuesta clínica registrada al tiempo T=1 y se desestimó aquella valorada al tiempo T=0 (final del tratamiento), porque ambos datos resultaron prácticamente similares. Para encontrar un biomarcador predictivo con utilidad clínica, se deben considerar las muestras recogidas antes de cualquier terapia, ya que no había un interés en encontrar un marcador en una muestra para la que los médicos ya conocen la respuesta al tratamiento. En general, la idea detrás de este análisis es que, pudiendo utilizar la primera muestra obtenida, se pudiera predecir cómo se comportará en un futuro frente al tratamiento y, por tanto, poder escoger la terapia más adecuada. Para ello, los pacientes con HNC pertenecientes al grupo

BRT se dividieron en dos subgrupos y se clasificaron en: buena respuesta (N=24), pacientes que lograron una respuesta completa al final del tratamiento y mala respuesta (N=6), los que presentaron respuesta parcial o nula a la RT al tiempo T=1. Después, se utilizó la prueba U de Mann-Whitney no paramétrica para representar a los que tenían buena respuesta frente a los que no la tenían. Los resultados revelaron una tendencia hacia un aumento de los niveles salivales de IL-10, IL-4, IL-6, MCP-1 y TNF-α en muestras de pacientes con mala respuesta, mientras que no se observaron cambios relevantes en el caso de la expresión de VEGF y se detectó una reducción de los niveles de EGF, aunque sin alcanzar valores significativos. Sin embargo, la significación estadística se confirmó solo para la proteína IL-8 (p-valor < 0,05). Posteriormente, empleando la misma base de datos, se llevó a cabo un análisis de curvas ROC (*receiver operating characteristic curve*) con el fin de evaluar la capacidad diagnóstica de estos posibles biomarcadores. De este modo, las curvas ROC confirmaron sustancialmente los resultados obtenidos de la prueba U de Mann-Whitney no paramétrica, indicando el fuerte potencial de la IL-8 como biomarcador predictivo de las respuestas al tratamiento radioterápico (AUC = 0,84; p-valor = 0,018) y sugiriendo el papel hipotético de TNF-α también (AUC = 0,768; p-valor = 0,0623).

Objetivo 2: Investigación sobre el proteoma salival

Características de los pacientes

En este estudio se incluyeron 30 individuos, seleccionados entre las dos cohortes del estudio, y divididos en tres grupos (Grupo 1 – 10 casos de HNC BRT; Grupo 2 – 10 casos de HNC ART; GRUPO 3 – 10 casos de CTRL). Las muestras pertenecientes al Grupo 2 se obtuvieron de los mismos pacientes del Grupo 1, evaluados antes (BRT) y después (ART) del tratamiento radioterápico. La mediana de la edad de ambos grupos (1 y 2) fue de 63,5 años [rango: 38-85], el 80% eran hombres y el 20% eran mujeres. La localización tumoral con mayor incidencia fue la laringe (60%), seguido de la cavidad oral (30%). La descripción histológica de carcinoma de células escamosas se observó en el 100% de los casos. Además, el 60% de los pacientes fueron diagnosticados en estadio avanzado de la enfermedad (T3-T4) y también presentaron metástasis en el cuello (50%). La mayoría de la población con HNC recibió RT adyuvante postoperatoria (60%). La respuesta al tratamiento registrada en T=0

mostró una respuesta completa (RC) en el 90% de los pacientes, aunque se observó una ligera disminución en T=1 donde el porcentaje de RC registrado fue del 70 %. El Grupo control (Grupo 3) incluyó 5 hombres (50%) y 5 mujeres sanos (50%) con una edad mediana de 61 años.

Construcción de la biblioteca de espectros

Para construir la biblioteca espectral se utilizó un conjunto de 10 muestras de saliva completa recogidas de 10 pacientes diagnosticados de HNC, no incluidas en el grupo final de las 30 muestras antes mencionadas. Los datos obtenidos del ensayo LC-MS/MS se analizaron utilizando los parámetros predeterminados de ProteinPilot. Para realizar la búsqueda en la base de datos Swissprot (versión 03-2018) se aplicó el algoritmo Paragon del software ProteinPilot v5.0 (SCIEX). Para la construcción de la biblioteca solo se utilizaron muestras de pacientes con cáncer, asumiendo que la mayoría de las proteínas exhibidas de los perfiles tumorales estarían presentes al mismo tiempo en los perfiles sanos. Finalmente, la cantidad de proteínas salivales humanas identificadas en la realización de la "biblioteca espectral del cáncer de cabeza y cuello" fue de 1053.

Objetivo específico 2.1: Evaluación de los perfiles proteómicos salivales en pacientes con HNC sometidos a radioterapia y en controles sanos.

Los datos cuantitativos resultantes del experimento LC-MS/MS-SWATH, que se llevó a cabo con las 30 muestras de saliva seleccionadas entre los dos Grupos del estudio, fueron analizados previamente por Peak View (v2.1, SCIEX) y, adicionalmente, por Marker View (SCIEX). Finalmente, en 30 muestras individuales se cuantificaron 695 proteínas (FDR <1%). Por tanto, se procedió con el análisis estadístico prefiriendo el uso de modelos de regresión penalizada, como lo es el de Elastic Net (1), a los modelos clásicos más conocidos como t-test, ANOVA o chi-cuadrado, ya que el número de variables de interés era mucho mayor que el número de observaciones disponibles. El objetivo del análisis fue identificar qué proteínas podían diferenciar los grupos considerados (Grupo1-BRT; Grupo2-ART; Grupo3-CTRL). Los resultados se presentaron utilizando la representación gráfica de los

mapas de calor o *heatmaps*, seguida del análisis discriminante por mínimos cuadrados parciales o PLS-DA.

En primer lugar, las 695 proteínas cuantificadas durante el análisis SWATH se representaron en un *Heatmap*, sin realizar ningún tipo de análisis estadístico. Las muestras y las proteínas se representaron ordenadas según el resultado de la clasificación jerárquica. Los resultados evidenciaron que las muestras no se distribuían según los grupos considerados. Sin embargo, una vez aplicado el modelo de regresión penalizada de Elastic Net, varias proteínas (N=40) expresadas diferencialmente proporcionaron una clasificación de los grupos satisfactoria. Esta tendencia también se observó cuando la comparación se realizó únicamente entre dos grupos en lugar de tres. De hecho, los resultados obtenidos al comparar las muestras pertenecientes al Grupo 1 (BRT) con las del Grupo 2 (ART) revelaron que un total de 21 proteínas se expresaban diferencialmente entre los dos grupos (BRT vs ART). Además, el mismo modelo de análisis se utilizó para determinar si existían modificaciones en los perfiles del proteoma salival entre los controles sanos (Grupo 3_CTRL) y los pacientes con HNC valorados previamente al tratamiento (Grupo 1_BRT) y después del proceso de irradiación (Grupo 2_ART). Una vez más, cuando se aplicó el modelo de regresión penalizada de Elastic Net, los resultados evidenciaron que algunas de estas proteínas (N=11 para CTRL vs BRT; N=12 para CTRL vs ART) se expresaban diferencialmente entre los grupos, pudiendo clasificarlos de manera adecuada. Igualmente, el análisis PLS-DA realizado después de cada comparación también mostró una correcta clasificación de los grupos. Además, se realizaron análisis funcionales y de enriquecimiento en GO (*Gene Ontology*) para investigar sobre la posible presencia de procesos biológicos relacionados con las proteínas expresadas diferencialmente. En conclusión, los datos mostraron que el proteoma varía en la saliva de los pacientes con cáncer sometidos a radioterapia, comparando las condiciones previas y posteriores al tratamiento y analizando el patrón seguido por los controles, observando un perfil proteico alterado. Los datos aportan nueva información sobre las proteínas salivales expresadas en pacientes con HNC y enfatizan la potencial aplicación del análisis proteómico para la identificación de biomarcadores asociados a esta enfermedad.

Objetivo específico 2.2: Verificar si entre las proteínas salivales alteradas pueden encontrarse moléculas relacionadas con la enfermedad y el tratamiento radioterápico.

Nuestro estudio para el descubrimiento de posibles marcadores salivales específicos para el cáncer de cabeza y cuello se llevó a cabo en de dos etapas. Una vez identificadas las proteínas expresadas diferencialmente en los 30 perfiles proteómicos salivales, se consideró su abundancia relativa, obtenida del experimento SWATH, para efectuar un análisis cuantitativo. Para averiguar si estas proteínas mostraban significación estadística con respecto a su abundancia salival, se utilizó una prueba t paramétrica, seguida de la aplicación de la tasa de descubrimiento falso (FDR) de Benjamini-Hochberg (2) para ajustar los valores-p. Entre las 695 proteínas totales identificadas, sólo 59 expresadas diferencialmente resultaron seleccionadas por el modelo de regresión penalizada de Elastic Net; entre ellas, según los patrones observados a partir de los resultados de la prueba t no paramétrica, fue posible diferenciar cuatro clases de proteínas:

1) CTRL vs Cáncer → proteínas alteradas en los perfiles salivales de los pacientes con HNC con respecto a los controles sanos (N=10);

2) Revertidas → proteínas expresadas diferencialmente en pacientes con HNC aún no tratados (grupo BRT) que volvían a su estado normal (niveles del grupo de control) después de la RT (N=3);

3) Tratamiento → proteínas alteradas principalmente después del tratamiento radioterápico, probablemente como consecuencia del mismo (N=12);

4) Progreso → proteínas expresadas diferencialmente en pacientes con HNC evaluados antes de la RT pero aún más representativas después del tratamiento (N=3).

Las proteínas restantes que no siguieron una tendencia particular se clasificaron como no específicas (N=31). Las cuatro clases de proteínas también se sometieron a análisis funcional y enriquecimiento en GO (*Gene Ontology*) para investigar la posible presencia de procesos biológicos relacionados.

Objetivo específico 2.3: Identificación de posibles biomarcadores predictivos de la respuesta al tratamiento radioterápico en el proteoma salival.

Para identificar las proteínas salivales que podrían usarse como marcadores para distinguir los casos de cáncer de cabeza y cuello de los controles, y los pacientes aún no tratados de los que ya habían sido tratados con RT, se realizó un análisis de curvas ROC de las proteínas expresadas diferencialmente entre los grupos.

Entre las proteínas salivales expresadas diferencialmente en la saliva de los pacientes con HNC evaluados antes y después del tratamiento con RT (Group2-ART vs Group1-BRT), ninguna de las proteínas identificadas alcanzó la mejor precisión predictiva (valor AUC = 1). El valor predictivo más alto fue alcanzado por LTF con un AUC de 0,86, seguido de NUCB2 (valor AUC = 0,83).

Con respecto a las proteínas expresadas diferencialmente entre los sujetos sanos y comparadas con los pacientes con HNC antes del tratamiento con RT (Grupo3-CTRL vs Grupo1-BRT), AGAPAT1 tuvo la mejor precisión predictiva (valor AUC = 1) pero también SERPINA3 (valor AUC = 0,93) y BPIFA1 (valor AUC = 0,88) mostraron valores predictivos importantes.

Para concluir, con respecto a las proteínas salivales expresadas diferencialmente entre los sujetos sanos y los pacientes con HNC tras el tratamiento con RT (Grupo3-CTRL vs Grupo2-ART), SERPINA3 y AGPAT1 tuvieron la mejor precisión predictiva (valor AUC = 1), seguida de LTF (valor AUC = 0,97) y LCN2 igualmente (valor AUC = 0,93). Es de destacar que SERPINA3 y AGPAT1 también fueron las principales proteínas identificadas para discriminar al grupo control de los pacientes con HNC antes de la RT, mientras que LTF fue la proteína con el valor predictivo más alto para discriminar a los pacientes con HNC aún no tratados de aquellos que ya habían sido tratados con radioterapia.

En general, los resultados del análisis de las curvas ROC mostraron que SERPINA3 y AGPAT1 podían ser consideradas como biomarcadores de HNC, pudiendo utilizarse para discriminar controles sanos de pacientes con cáncer. Además, LTF y NUCB2 podrían ayudar en distinguir entre los casos de HNC antes y tras el tratamiento radioterápico, aunque lo más importante era identificar marcadores del efecto

positivo del tratamiento (valores que vuelven a la normalidad) y los posibles marcadores de resistencia o ineficacia del tratamiento (valores que persisten alterados y que no son debidos al tratamiento). En particular, NUCB2 junto con HSPE1 y PPIB, las tres proteínas que forman parte de la clase denominada "Revertidas", se pueden considerar como posibles biomarcadores predictivos de respuesta a la RT, considerando el hecho de que la abundancia salival vuelve a su estado normal (niveles del grupo de control) después del proceso de irradiación. Sin embargo, se trata de resultados preliminares ya que no se realizó ninguna validación cruzada o validación con datos externos para respaldar nuestros resultados.

CONCLUSIONES

1. La radiación ionizante afecta la expresión salival de citocinas proinflamatorias y antiinflamatorias, quimiocinas y a los factores de crecimiento. Los niveles de IL-8 y MCP-1 aumentan significativamente en la saliva de los pacientes con cáncer de cabeza y cuello tras el tratamiento radioterápico.

2. En la saliva de los pacientes con cáncer de cabeza y cuello, antes que someterse a la RT, hay un aumento significativo de los niveles de IL-6 y, en general, un incremento de todos los marcadores inflamatorios salivales, debido a la presencia de la lesión neoplásica.

3. No hay relación entre los marcadores inflamatorios salivales alterados y el desarrollo de mucositis oral en los pacientes con cáncer de cabeza y cuello tratados con RT. Aunque, esta relación puede no existir debido al número limitado de muestras utilizadas para el análisis en nuestro estudio.

4. En la saliva de pacientes con cáncer de cabeza y cuello, la IL-8 tiene un gran potencial como biomarcador predictivo de la respuesta terapéutica a la radioterapia. Niveles reducidos de esta molécula en la saliva de pacientes con cáncer antes de recibir el tratamiento están relacionados con una respuesta positiva a la radioterapia.

5. Se observan diferencias en el proteoma salival tanto en los pacientes antes de someterse a la radioterapia como tras la misma, así como al compararlos con el grupo control.

6. Entre los perfiles proteómicos salivales de los pacientes con cáncer de cabeza y cuello, analizados antes y tras la RT, se hallaron un total de 21 proteínas que se expresaban diferencialmente. La mayoría de estas proteínas estaban relacionadas biológicamente con la respuesta inmune y la inflamación.

7. Entre los marcadores salivales identificados, NUCB2, PPIB y HSPE1 se asociaron a resultados favorables terapéuticamente tras la RT, y pueden considerarse como posibles biomarcadores predictivos de respuesta al tratamiento. LTF puede ayudar en discriminar entre los pacientes con cáncer de cabeza y cuello antes y tras la RT, mientras que SERPINA3 y AGPAT1 están relacionados con la presencia del cáncer de cabeza y cuello.

I. Introduction

1 CANCER

1.1 The Cancer concept

Conforming to the World Health Organization (WHO):

"Cancer is a generic term for a large group of diseases characterized by the growth of abnormal cells beyond their usual boundaries that can then invade adjoining parts of the body and/or spread to other organs."

Based on current evidence, it is among the leading causes of morbidity and mortality worldwide, responsible for 18.1 million new cases and 9.6 million deaths in 2018 (3,4). It can affect almost any part of the body and has many anatomic and molecular subtypes that each require specific management strategies.

1.2 The molecular biology of cancer

In general, cancer arises through the accumulation of genetic and epigenetic changes in genes acting in different signalling pathways, causing the acquisition of varied phenotypes, that have been well summarized by Hanahan and Weinberg in 2000 (5), when they suggested that there are six essential characteristics, known as the hallmarks of cancer, for the development of the disease (6). The hallmarks comprise six biological capabilities acquired during the multistep development of a tumour lesion and constitute an organizing principle for rationalizing the complexities of neoplastic disease. They include: sustaining proliferative signalling, evading growth suppressors, resisting cell death, enabling replicative immortality, inducing angiogenesis, activating invasion and metastasis (***Figure 1***) (5). Underlying these hallmarks are genome instability and inflammation (7). Some years later, in 2011, Hanahan and Weinberg (7) incorporated four new hallmarks (***Figure 2***) and pointed out the importance of the microenvironment in the disease process. These ten features are all detailed below:

1. Sustaining proliferative signalling. In normal conditions, cells require mitogenic growth signals to move from a quiescent state into a proliferative state. By the union of signalling molecules (such as soluble growth factors or extracellular matrix components) to transmembrane receptors, growth signals are transmitted into cells. In absence of these signals, normal cells are not capable of growing. However, tumoral cells grow even when these interactions do not take place because they can generate their own intrinsic growth signals (7).

2. Evading growth suppressors. In normal conditions, cells receive antiproliferative signals in order to maintain their quiescence, many of which depend on the actions of tumour suppressor genes (7). For instance, RB (retinoblastoma-associated) protein integrates signals from diverse extracellular and intracellular sources, making it a cell-cycle progression gatekeeper (8). Hence, when the RB pathway is disrupted, cells become insensitive to inhibitory growth signals and inappropriate replication continues.

3. Resisting cell death. Programmed cell death by apoptosis is a natural barrier to cancer development (7). However, different strategies can be used by tumoral cells to escape from these mechanisms. One of the most common strategies is the loss of the proapoptotic regulator TP53, which induces apoptosis when DNA damage is detected (5).

4. Enabling replicative immortality. The number of cell divisions that can occur during a lifetime in mammals is limited by an intrinsic cell program, which is known as the Hayflick limit. Once cells have achieved this limit, they stop growing and start senescing (9), which results from the loss of the protective function of telomeres. It has been shown that in neoplastic cells, telomeres maintain their length due to higher activity of the telomerase enzyme (10).

5. Inducing angiogenesis. Like normal tissues, tumours require nutrients and oxygen and need to evacuate metabolic wastes (7). Hence, the generation of new vasculature from the pre-existing one is essential for tumour growth (11). This process is known as angiogenesis and it is regulated by the equilibrium between

inducer and inhibitor factors. Tumours have the capacity to activate the angiogenesis process by stimulating inducer factors.

6. Invasion and metastasis. Neoplastic cells can escape from primary tumour masses and invade adjacent tissues or distant sites. The multistep process of invasion and metastasis has been schematized as a sequence of discrete steps, often termed the invasion-metastasis cascade (7,12). The success of this process depends on the other five characteristics and complex changes in the physiological relationship between cells and their microenvironment, beginning with local invasion, then intravasation by cancer cells into nearby blood and lymphatic vessels, the transit of cancer cells through the lymphatic and hematogenous systems, followed by escape of cancer cells from the lumina of such vessels into the parenchyma of distant tissues (extravasation), the formation of small nodules of cancer cells (micrometastases), and finally the growth of micrometastatic lesions into macroscopic tumours, this last step termed colonization (7).

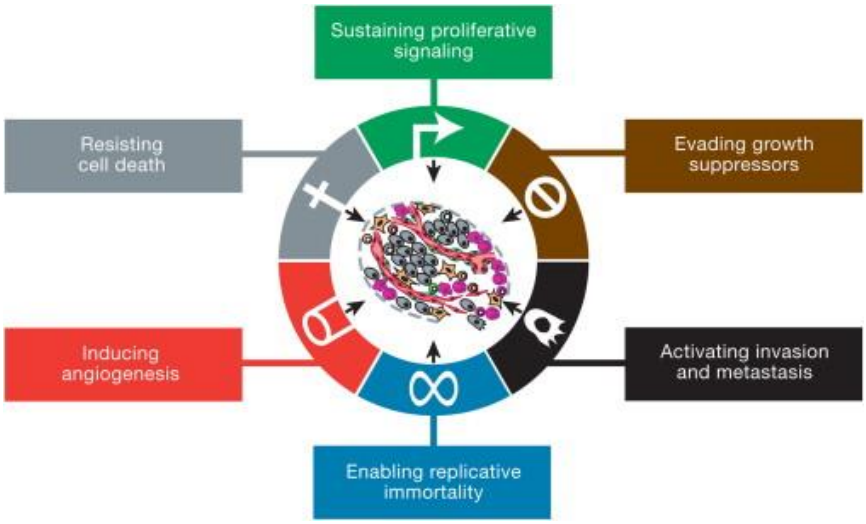

Figure 1: The Hallmarks of cancer. The illustration encompasses the six hallmark capabilities originally proposed in 2000 by Hanahan and Weinberg.

7. Genome instability and mutations. Defects affecting components of the DNA-maintenance machinery lead to the accumulation of a large number of alterations in neoplastic cells, which are related to the aforementioned characteristics. The different steps involved in tumour progression are a succession of clonal expansions

produced by the accumulation of mutations that generate selectively advantageous neoplastic cells (7).

8. Inflammation. Tumours are densely infiltrated by immune cells which were initially thought to be acting against the tumour (7). However, it has now become clear that inflammation can contribute to tumorigenesis and tumour progression by supplying different molecules to the tumour microenvironment such as growth factors, angiogenic factors, and extracellular matrix-modifying enzymes (7,13).

9. **Deregulating cellular energetics.** During the neoplastic process, changes in energy metabolism are produced to avoid apoptosis and to maintain and stimulate the growth and division of neoplastic cells (7).

10. **Avoiding immune destruction.** It has been proven that neoplastic cells have developed different strategies in order to avoid being detected by the immune system (7). For instance, inflammatory cells, such as regulatory T cells (Tregs) and myeloid-derived suppressor cells (MDSCs), which are actively immunosuppressive, are recruited to the tumour environment, where they suppress the action of cytotoxic lymphocytes against tumour cells.

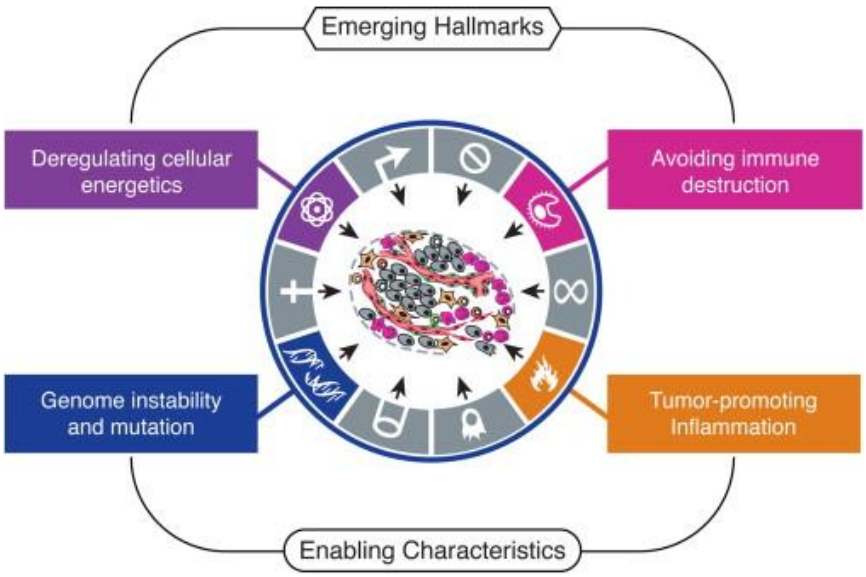

Figure 2: The next generation hallmarks of cancer. Emerging Hallmarks and Enabling Characteristics. *By Hanahan and Weinberg, 2011*

2 HEAD AND NECK CANCER

Head and Neck cancer (HNC) is a complex and heterogeneous pathology, encompassing a variety of tumours that originate from pharynx (hypopharynx, oropharynx, nasopharynx), larynx, paranasal sinuses, nasal cavity, salivary glands and oral cavity (***Figure 3***)(14). It is considered the sixth most common neoplasia worldwide with an incidence estimated at 650,000 cases and 330,000 deaths per year (4). The risk of developing these tumours increases with age and the majority of cases occur in people aged 50 or over (15). Alcohol and tobacco use are between the most common risk factors for HNC (16). Besides, a high-risk human papillomaviruses (HPV) infection, especially type 16 has recently been implicated in the malignant pathogenesis arising from the oropharynx (14). Independently from the anatomic region, men have a greater risk than women; though, this incidence has been changing over the decades as the number of female smokers has increased. Survival and cure are benefited by early diagnosis and appropriate therapy. Late diagnosis usually requires surgical intervention, often followed by adjuvant radiotherapy (RT) and/or chemotherapy (CT) treatment. Despite all of the diagnostic and therapeutic advances, the prognosis of these tumours largely depends on the stage at the time of diagnosis. The 5-year survival rate varies from early (70-90%) to advanced-metastatic stages (40-60%), improving in presence of HVP (17).

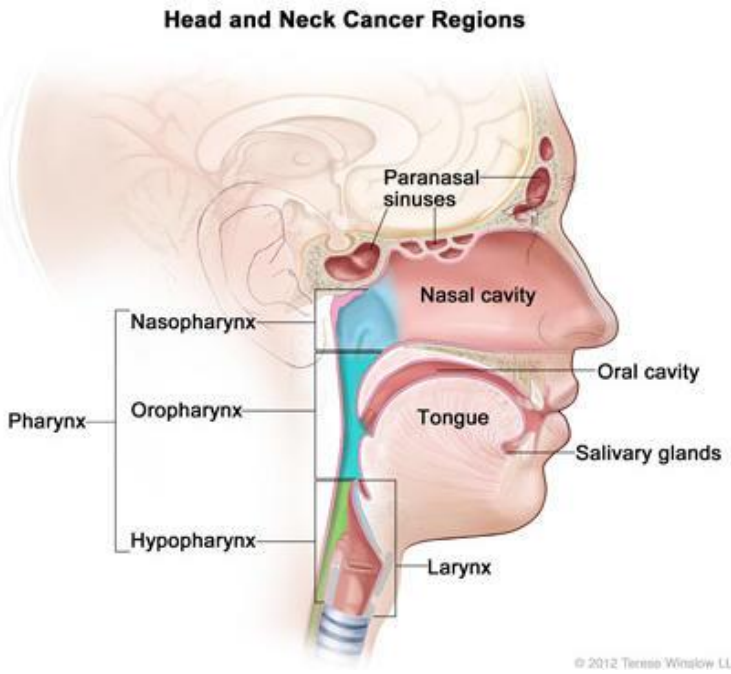

Figure 3: Head and neck cancer regions. Illustration of the location of paranasal sinuses, nasal cavity, oral cavity, tongue, salivary glands, larynx, and pharynx (including the nasopharynx, oropharynx, and hypopharynx). *By Terese Winslow,2012*

2.1 Epidemiology

In 2020, HNC is expected to affect approximately 833,000 and 151,000 new patients worldwide and in Europe, respectively (18). Although in Northern America and Europe it accounts for 5% to 10% of all new cancer cases, HNC and in particular oral squamous cell carcinoma (OSCC), is characterised by marked geographical variations in its incidence and prevalence rates (16). This variation is predominately attributed to demographic differences in habits and socioeconomic status. It is widely prevalent in developing countries and although it is less prevalent in developed western countries, recently a change in trend has been observed due to lifestyle changes (19). Among the European countries, the highest incidence of OSCC is in France, with high rates also noted in Hungary, Slovakia, and Slovenia (15). In the United States, HNC constitutes the eighth most common cancer among men, with approximately 53,600 patients diagnosed yearly, and shows considerably lower mortality with 11,500 patient deaths annually (20). The decreasing incidence of OSCC

and laryngeal SCC in the United States and other developed countries coincides with a decline in the use of tobacco products (21). By contrast, there is a recent escalation in the incidence of oropharynx tumours, which is attributed to a change in the biologic driver of SCC in this region, with an increasing frequency of an association with high-risk subtypes of human papilloma virus (HPV)(21,22). Among the ~650,000 new cases of HNC diagnosed annually all over the world, the ratio between men and women is about 3:1 (23). OSCC is the most common type of cancer in South Asian countries like India, Srilanka, Pakistan and Bangladesh due to betel quid/tobacco chewing habits, and contributes nearly one-fourth of all new cases of tumour (***Figure 4***)(15). For most countries, 5-year survival rate for cancers of the tongue, oral cavity and oropharynx is around 50%. The best outcome is for cancer of the lip, with over 90% of patients surviving for five years. The lowest survival was for hypopharyngeal tumours. In general, prognosis decreases with advanced disease and increasing inaccessibility to the tumour (15).

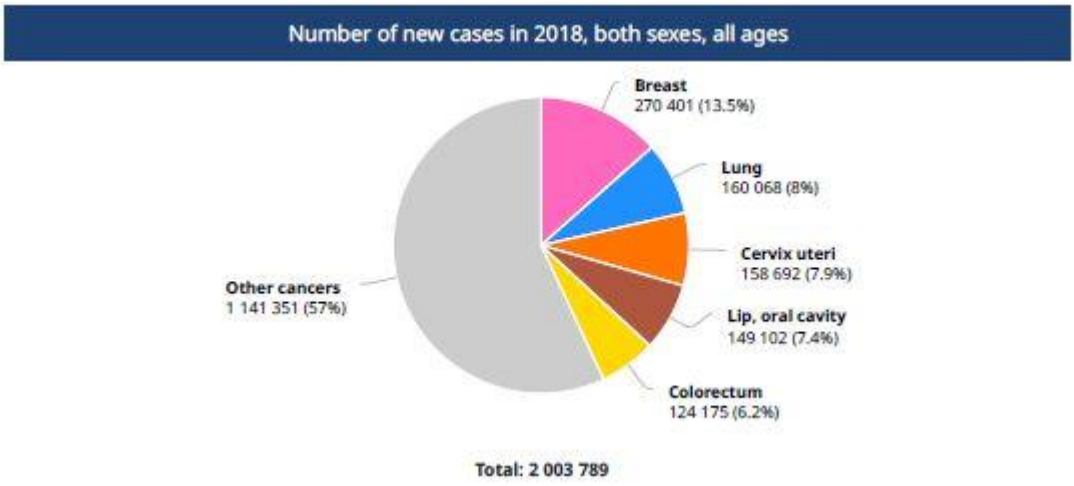

Summary statistic 2018

	Males	Females	Both sexes
Population	1 018 033 447	970 990 624	1 989 024 042
Number of new cancer cases	980 742	1 023 047	2 003 789
Age-standardized incidence rate (World)	104.9	103.1	103.4
Risk of developing cancer before the age of 75 years (%)	11.4	10.7	11.0
Number of cancer deaths	709 795	626 231	1 336 026
Age-standardized mortality rate (World)	76.5	63.6	69.7
Risk of dying from cancer before the age of 75 years (%)	8.5	6.9	7.7
5-year prevalent cases	1 686 043	2 213 865	3 899 908
Top 5 most frequent cancers excluding non-melanoma skin cancer (ranked by cases)	Lip, oral cavity Lung Colorectum Liver Stomach	Breast Cervix uteri Ovary Lung Colorectum	Breast Lung Cervix uteri Lip, oral cavity Colorectum

Figure 4: Summary of cancer statistic in the WHO South-East Asia Region (SEARO). Populations included: Bangladesh, Bhutan, India, Indonesia, Korea, Maldives, Myanmar, Nepal, Sri Lanka, Thailand, Timor-Leste. Source: Globocan 2018. WHO, World Health Organization

2.2 Etiopathogenesis

Carcinogen exposure, diet, oral hygiene, infectious agents, family history, and pre-existing medical conditions all play a role, individually or in combination, in the development of HNC (24). Many of these neoplasms have a demonstrated correlation with certain life habits such as smoking and alcohol abuse (e.g. laryngeal tumours, oral cavity and oro-hypopharyngeal tumours), or are related to specific work

activities, such as exposure to the powders of the wood and leather (intestinal adenocarcinomas of nasal cavities and ethmoid)(25), or have been related to viral infections (EBV, Epstein-Barr virus in nasopharyngeal tumours, HPV in some oropharyngeal carcinomas)(26). The risk in smokers is approximately 10 times higher than that of never-smokers, and 70–80% of new HNC diagnoses are associated with tobacco and alcohol use (27). Their synergistic effect is well known and supported by the analysis of pooled data from 17 European and American studies (28). Results showed that the population attributable risk was 72%, which included 4% for alcohol alone, 33% for tobacco alone and 35% attributable to both alcohol and tobacco. The odds ratios of developing HNC were: 2.37 for ever tobacco users among never alcohol users, 1.06, for alcohol users among never tobacco users, and 5.73 for alcohol and tobacco users (28). Smoking in non-drinkers is associated with an increased risk of developing especially laryngeal malignancies (29). Only 7% of neoplasms in this area recognize an alcohol aetiology in patients who have never been exposed to smoking (29). The longer a person smokes and the more tobacco they consume the greater their risk of developing these cancers (30). For male and female smokers, the average risk for developing HNC is ten and five times higher, respectively, compared to lifetime non-smokers (30). Heavy smokers also have up to 20 times the risk of developing laryngeal cancer compared to lifetime non-smokers. Quitting smoking can significantly reduce this risk. After about 5 years, the risk of developing oral and pharyngeal cancers is halved (30,31).

Other factors that contribute to an increased risk of developing neoplasms in the head and neck area are daily exposure to environmental pollution caused by smoking combustion of coal or wood stoves, occupational exposure to wood dust and leather working, a diet low in vegetables and fruit and particularly rich in meat and poor oral hygiene, previous bone marrow transplantation (31,32).

HPV infection, especially HPV16 and much less frequently HPV18 (32,33), may be the basis of oropharyngeal neoplasms, especially the tonsil even when the common risk factors do not coexist; however, they are less frequent in the anterior part of the mouth. The presence of HPV positivity in other subsites of the head and neck region has a less clear etiopathogenetic role compared to what is known in the oropharynx

as well as the prognostic role (34). Carcinomas that arise in patients with EBV (Epstein-Barr virus) infection usually affect young subjects. The presence of the virus in tumour cells and the finding of plasma EBV-DNA may aid in the differential diagnosis with other tumour histotypes (i.e., non-EBV-related squamous cell carcinomas)(35). The incidence of neoplasms in the cervico-cephalic district is also higher in patients with Fanconi anaemia and immunosuppressed subjects (for example HIV+ or transplanted) or in subjects with Li-Fraumeni syndrome (36–38). Advanced age is also considered to be an important risk factor for the development of these tumours; the lowering of the immune defences, the increase in mutations induced by carcinogens contained in smoking and alcohol and the reduced ability to repair DNA increase the incidence of cancer in the elderly population (39). Finally, other important factors of risk are the previous radiotherapy treatments on the head and neck area performed for others neoplasms (e.g. Hodgkin's lymphoma)(40). Since risk factors are common to neoplasms of other areas, such as oesophagus and lung, multiple primitive, synchronous or metachronous neoplasms are not uncommon (41). The distinction between primary tumour or pulmonary metastatic disease is often difficult and sometimes impossible in presence of squamous cell carcinomas. The determination of HPV status on lung cancer can identify any secondary oropharyngeal carcinoma, if HPV positive (42).

2.3 Histopathology

The majority of head and neck cancers are epithelial tumours, among them, the 90% are squamous cell carcinomas (SCC) with various degrees of differentiation (43). Histological variants of head and neck squamous cell carcinoma (HNSCC) include: basaloid SCC, spindle cell carcinoma, adenosquamous carcinoma, carcinoma cuniculatum, verrucous carcinoma, papillary SCC, acantholytic SCC, and lymphoepithelial SCC, all reported in the WHO classification of 2017 (44,45). Histologic grading of SCC into well, moderate, and poorly differentiated carcinomas is based on the degree of keratinization and cytologic maturation, as well as the growth pattern (16). Conventional/keratinizing SCC represents the vast majority

(80%) of the squamous carcinomas in the head and neck outside of the oropharynx and nasopharynx. They are most often associated with tobacco and/or alcohol (16). SCC arises from normal squamous epithelium through a stepwise process called dysplasia (46). Squamous dysplasia refers to neoplastic alterations of the surface epithelium before the invasion of the subepithelial connective tissues. These changes include abnormal cellular organization, increased mitotic activity, and nuclear enlargement with pleomorphism (24). The first and apparently earliest change is the appearance of atypical cells in the basal layers of the squamous epithelium, but this occurs alongside normal differentiation toward the prickle and keratinizing cell layers. As the lesion evolves, there is progressive involvement of several strati of the epithelium, until it is totally replaced by atypical cells, exhibiting no surface differentiation (47,48). Under the WHO classification, the atypical epithelium is divided into low and high risk of developing cancer, one that more likely progress to SCC and the other with less tendency to progression. Although the former is almost a true premalignant lesion and the latter is a reactive atypical epithelium, the concept of epithelial dysplasia includes both lesions (49). The presence of dysplastic areas in the oral and the upper aerodigestive tract epithelium is believed to be associated with a likely progression to cancer. There is evidence that in an individual lesion, the more severe the dysplasia the greater the likelihood is of progression to malignancy (50). However, rarely non-dysplastic lesions may also show malignant development (51,52). These alterations are typically graded on a scale of 1 to 3, based on the severity of the atypia or *epithelial dysplasia*. Although terminology varies, atypia limited to the lower one-third of the epithelium is generally referred as mild dysplasia, atypia limited to the lower two-thirds as moderate dysplasia, and atypia involving the full thickness of the epithelium as severe dysplasia/carcinoma in situ (24,53). With progression, the carcinoma in situ breaks through the basement membrane and infiltrates the subepithelial connective tissue as cohesive nests and cords (***Figure 5***). With advanced tumour growth, nests of invasive tumour invade skeletal muscle, craniofacial bones, and facial skin. Invasion may be associated with tumour extension along nerves (i.e., perineural invasion) and involvement of lymphatic spaces (24).

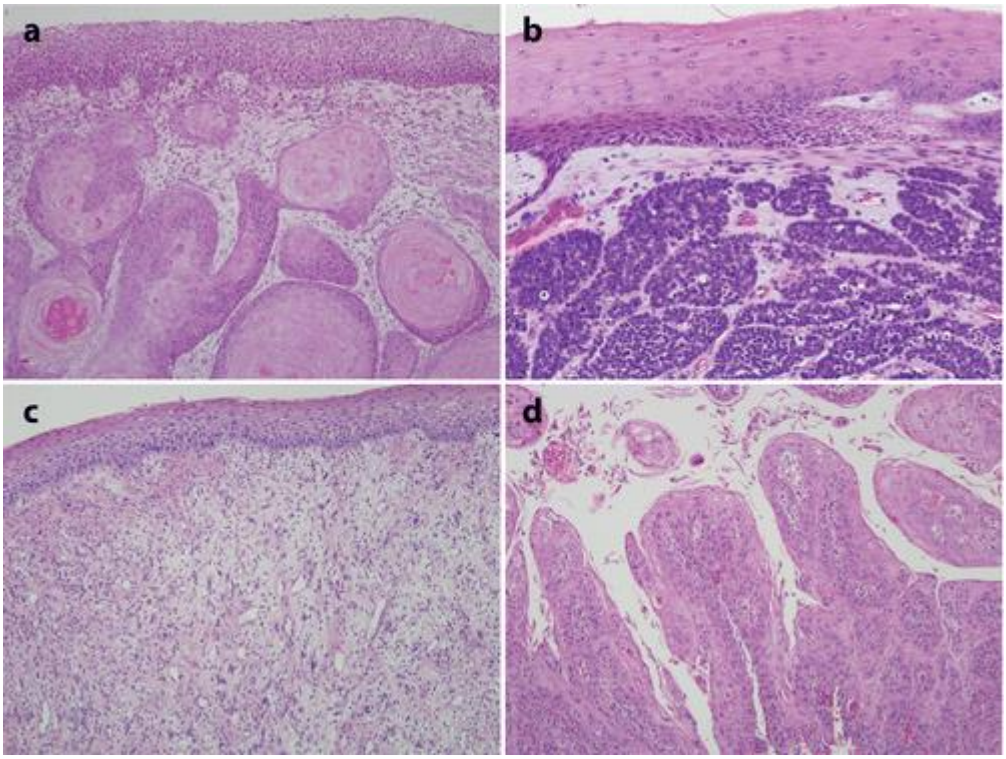

Figure 5: Histologic features of head and neck squamous cell carcinoma (HNSCC). The prototypic HNSCC is characterized by nests of squamous cells with pink cytoplasm, intercellular bridges and keratin pearl formation set in a background of stromal fibrosis (a). Subtypes of HNSCC include the basaloid variant (b), the spindle-cell variant (c), and the papillary variant (d). *By Pai and Westra 2009*

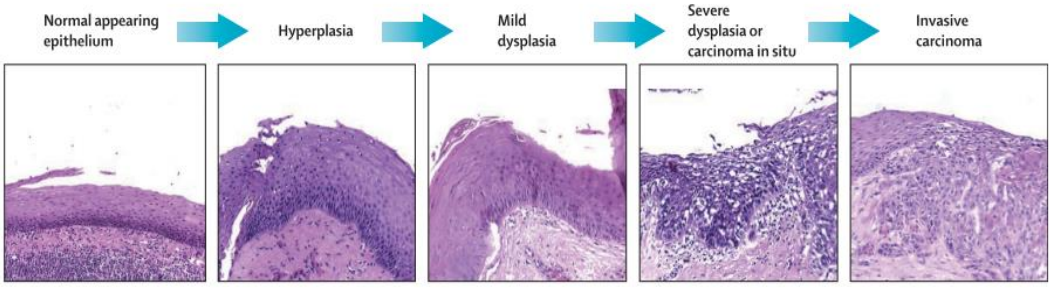

Figure 6: Cytological changes from normal mucosa to epithelial dysplasia and tumour progression. *By Argiris et al. 2008*

2.4 Field cancerization

The five-year survival rate for the advanced stages of HNSCC is ~50% and disappointingly, this has not markedly improved in the last decades, because patients frequently develop relapse at the primary site, distant metastases and second primary tumours (6). In 1953, the term "field cancerization" was proposed to explain the high propensity to develop local recurrences after treatment of HNSCC and the high likelihood that multiple independent tumours will develop in the head and neck mucosa. Owing to the developments in molecular research, the first genetic multi-step progression model for HNSCC was postulated in 1996 based on the genetic characterization of morphological changes in the squamous epithelium (54). In this model, multifocal oral cancers develop from separate, independent genetic alterations, and many of these second primary tumours have been associated with lower survival rates than occurs with the original tumour. In an updated progression model, second or multiple cancers distant from the dysplastic fields have been suggested to be clonally related and derived from the expansion of a common pre-neoplastic progenitor (55). The progressive accumulation of genetic alterations represents the basis of the progression/transformation from a normal cell to a neoplastic cell. Probably one of the earliest genetic alterations of the carcinogenesis process is the loss of chromosomal material (LOH: Loss of Heterozygosity) (***Figure 7***). In epithelial tumours such alterations occur primarily in stem cells (cells of the basal layer of the epithelium that renew themselves autonomously and produce daughter cells that will differentiate into all the other cells typical of mature tissue). Together these cells constitute the clonal unit. In the epithelium adjacent to the tumour site that appears macroscopically healthy, clonal units containing oncogenic alterations have been identified. This apparently healthy tissue around the tumour is called "field at risk" (***Figure 8***). In patients with oral and oropharyngeal carcinomas, these fields at risk were found in about one-third of cases (56). These initial clonal alterations are likely at the origin of the development of new carcinomas in the portions adjacent to the tumour already treated. Normally invisible to simple clinical inspection, these risky fields can look like white patches or plaques, known as leukoplastic lesions (16). It is necessary to consider that the malignant transformation rates of these initial

lesions range from 0.13 to 17.5% (57) with a constant ratio per year even higher for its derivatives, as *proliferative verrucous leucoplakia* (PVL).

An important clinical implication of a "field at risk" is that it may be the source of local recurrences and second primary tumours after surgical resection of the initial carcinoma (58). These two possibilities can be distinguished clinically based on their distance from the index tumour or the time interval after which they develop (whereby a local recurrence is less than 2 cm away from or occurs within 3 years of the primary tumour; a second primary tumour is more than 2 cm away from or occurs more than 3 years after the primary tumour) (59).

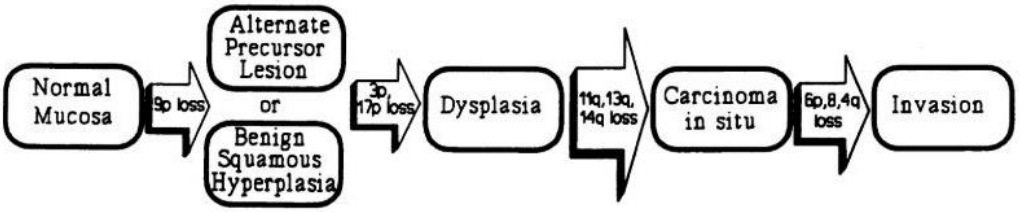

Figure 7: Genetic changes associated with the histopathological progression of HNSCC based on loss of chromosomal material (allelic loss). Loss of heterozygosity at chromosomes 3p, 9p and 17p seemed to occur in dysplasia, apparently reflecting early carcinogenesis, whereas other alterations at chromosomes 11q, 4q and of chromosome 8 were typically present in carcinomas, probably corresponding to a relatively late phase in carcinogenesis. *By J. Califano et al. 1996*

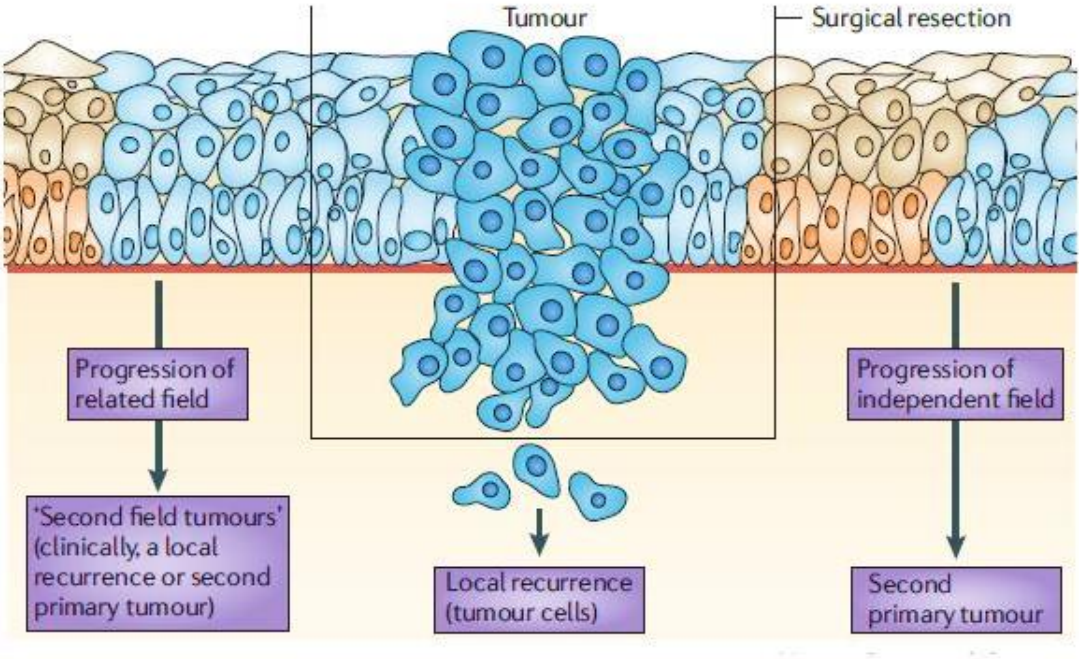

Figure 8: Field cancerization and local relapse. The relationship between field cancerization and types of relapse is shown. Based on recent molecular findings, field cancerization is defined as the presence of one or more mucosal areas consisting of epithelial cells that have cancer-associated genetic or epigenetic alterations. Tumours that do arise in a non-resected field have been described as 'second field tumours' as opposed to true local recurrences (which develop from residual tumour cells) or true second primary tumours (which have an origin that is independent of the first tumour)(58). *By Leemans et al. 2011*

2.5 Diagnosis & Prognosis

HNC typically produces symptoms referable to the oral cavity and the upper aerodigestive tract. In particular, patients can appear with: hoarseness, sore throat cough, tongue pain, mouth ulcer, mouth bleeding, dysphagia and odynophagia, otalgia and trismus (60). Early recognition of signs and symptoms is crucial for prompt diagnosis (60). No proven screening methods, except population screening with oral visual inspection in high-risk regions for oral cavity cancer, are known to exist (61). Similar to other solid malignancies, HNC development is a multistep process, often with precursors, which are commonly known as precancerous or premalignant lesions (16).

The expert Working Group of the WHO Collaborating Center for Oral Cancer and Precancer on the terminology, definitions and classification, recommended the use

of the term potentially malignant disorders (PMD), which includes premalignant lesions and conditions that have increased risk for malignant transformation (62). Tobacco and alcohol-related head and neck malignancies are often preceded by lesions that present clinically as white (leukoplakia) or red (erythroplakia) patches or plaques (16). Leukoplakia, erythroplakia, and palatal lesions in reverse smokers are considered precancerous lesions, whereas actinic keratosis, oral submucous fibrosis, and lichen planus were designated as precancerous conditions (62).

Referral criteria have been developed to expedite specialist assessment for biopsy of suspected malignant lesions, which is always needed for the confirmation of the diagnosis (63). Accurate staging, including clinical examination and radiological assessment, is the most important factor to establish the best therapeutic decision. The examination should aim to gain a clear understanding of the location and extent of the primary tumour, the presence of locoregional disease, and the presence of a synchronous primary tumour. A diagnostic imaging evaluation consisting of either computer tomography (CT) scanning or magnetic resonance imaging (MRI) is used to assess the extent of local and regional tumour spread, the depth of invasion, and the extent of lymphadenopathy (60). The most common clinical picture is to find regional neck metastasis, followed by lung, liver and bones (60). However, combined positron emission tomography (PET) and CT scans are more accurate than either method alone for identifying distant and very spread head and neck malignant lesions and also for the assessment of response and detection of persistent or recurrent pathology (64). Sometimes occurs that patients might present with neck lymphadenopathy without an apparent primary tumour, in up to 5% of cases of HNSCC the primary site remains unknown (60). Management of this entity is controversial (65).

Most of the prognostic factors rely on the evaluation of the resection specimen and the extent of disease. Specifically, pathologic factors in the primary tumour evaluation include the grade of differentiation or histologic subtypes, depth of invasion, perineural invasion, and margin status, which all carry potential significance in determining the prognosis of this malignancy (16). Regarding the molecular prognostic markers, the viral aetiology, either HPV for oropharynx carcinomas and EBV for carcinoma EBV related nasopharyngeal, are now recognized as prognostic

factors (16,66,67). Positive HPV status is also a predictive factor for increased risk of radiation therapy-induced mucositis (68). The favourable prognostic role of HPV also appears to be maintained in relapsed or metastatic disease, albeit with less evidence (69,70). The prognostic value of the mutational state of TP53 has been described both on the primary tumour and on the margins in patients undergoing surgery. In fact, not only the absence of a gene mutation constitutes a favourable prognostic factor, but also the type of mutation (functional vs non-functional) can influence the prognosis (71).

2.6 Clinical and pathological staging

Clinical and pathological staging is one of the most important procedures in the diagnosis of cancer for prognosis assessment and treatment planning. It is usually carried out using the TNM system, lastly modified in 2017 (UICC / AJCC 8th Edition).

2.6.1 TNM classification

The TNM classification evaluates the anatomical extent of malignant neoplasms based on the primary tumour margins (T category), the status of regional lymph nodes (N category) and the presence of distant metastases (M category). It is widely employed both in clinical practice and research for prognostic assessment of patients, treatment allocation and trial enrolment, as well as for epidemiological studies and data collection by cancer registries worldwide. Pathological TNM (pTNM) represents the pathological classification of a tumour, assigned after surgical resection or adequate sampling by biopsy (72). Several significant updates were made to the classification of HNC by the new edition (8th Edition). For SCC of the oral cavity, along with tumour size, the depth of invasion has been added as a new T descriptor, based on its reported correlation with lymph node metastasis (**Table 1**). Data supporting this change derived from a multicentric study involving 3149 patients with OSCC treated with surgery ± adjuvant therapies between 1990 and 2011 (73). T categories, based both on tumour size and depth of invasion, improved discrimination in terms of

disease specific survival and overall survival, and have already been validated in an independent cohort (74). The need for specific classification criteria for HPV-positive oropharyngeal carcinomas derives from their different biological characteristics and clinical behaviour, which was unreliably predicted by the previous ones (75)(**Table 2**). The 8th edition defines HPV-related tumours based on p16 expression, immunohistochemistry positivity for p16 has been demonstrated to be a reliable surrogate marker for HPV-driven tumours (76). New criteria have been also provided for cervical node metastases of unknown primary: T is classified as T0, while N categories are differently defined for viral-related and viral-unrelated tumours.

Table 1: Definition of the T category (8th edition TNM classification) by the inclusion of the "depth of invasion (DOI)" variable for SCC of the oral cavity. *By S.H. Huang and O'Sullivan 2017*

Definition of T category	
Oral cavity	
T1	• Size ≤2 cm and DOI ≤ 0.5 cm
T2	• Size ≤2 cm and DOI >0.5 but ≤1.0 cm, or • Size 2–4 cm, and DOI ≤ 1.0 cm
T3	• Size >4 cm or >1.0 cm
T4	• Moderately advanced or very advanced disease

Table 2: The 8th edition TNM classification for the HPV-mediated oropharyngeal cancer. *By S.H. Huang and O'Sullivan 2017*

HPV+ OPC	Clinical stage				Pathologic stage				
Category	T	N		M	T	N		M	
Stage I	T1, T2	N0: no regional LNs N1: ipsilateral LNs		M0	T1, T2	N0: no regional LNs N1: 1–4 LNs		M0	
Stage II	T1, T2	N2: bilateral or contralateral LNs		M0	T1, T2	N2: ≥ 5 LNs		M0	
	T3	N0: no regional LNs N1: ipsilateral LNs N2: bilateral or contralateral LNs		M0	T3, T4	N0: no regional LNs N1: 1–4 LNs		M0	
Stage III	T4	Any N		M0	T3, T4	N2: ≥ 5 LNs		M0	
	Any T	N3: >6.0 cm LN(s)		M0					
Stage IV	Any T	Any N		M1	Any T	Any N		M1	
Stage grid for non-metastatic (M0) HPV+ OPC									
Clinical stage group					Pathologic stage group				
cTcN	T1	T2	T3	T4	pTpN	T1	T2	T3	T4
N0	I	I	II	III	N0	I	I	II	II
N1	I	I	II	III	N1	I	I	II	II
N2	II	II	II	III	N2	II	II	III	III
N3	III	III	III	III	Not applicable				

LN lymph node

2.6.2 Natural history

In the early stage of the disease (T1–T2) the main clinical problem is the loco-regional control. In fact, the risk of distant metastasis is very low even if, for nasopharyngeal neoplasms and undifferentiated carcinomas in general, this should be also considered (77). The possibility for lymph nodes metastasis depends on the site (richness or not in lymphatic drainage) and, in some areas, increases in relation to the infiltration thickness of the primitive tumour; it has been defined above all for neoplasms of the oral cavity (78). A meta-analysis of the literature (16 studies, 1136 patients) (79) has better specified the relationship between the thickness of T infiltration as a predictor of metastasis to the regional lymph nodes, regarding the tumours of the oral cavity (tongue and floor), identifying a 4 mm cut-off (on a pathological sample fixed afterwards surgery). In locally advanced stages (T3-T4) the problem of distance metastasis becomes relatively more relevant. Furthermore, patients with locally advanced stages often experience relapse. To date, clinical staging is not enough to identify the population who will develop relapse and who need tailored treatment (59).

2.7 Treatment options

HNC treatment is a multidisciplinary strategy, different therapeutic approaches are combined to increase the possibility of healing the disease. The selection of sole or combined modality is based on various considerations, including disease control probability, tumour resectability, the anticipated functional and cosmetic outcomes, patient general condition and availability of resources and expertise (80). Early-stages are generally treated with single modality, either surgery or radiotherapy. The treatment for locally advanced stages is multimodal, with either surgery followed by adjuvant radiation or chemoradiation. For recurrent disease that is not suitable for a local or regional approach and in case of metastatic condition, chemotherapy, with or without a biological agent, is indicated (81).

Surgery

Primary curative surgery is reserved for resectable tumours in which clear margins can be achieved and function is preserved. It is a standard treatment for HNC but is frequently limited by the anatomical extent of the tumour. By use of modern surgical techniques, substantially improved functional outcomes are often possible for patients who need extensive surgical resections, even in the setting of salvage surgery after failure of organ-preserving treatment (60). When surgery is the primary treatment, neck dissection is carried out as part of surgical management. However, after treatment with primary chemoradiotherapy, neck dissection is usually recommended when residual disease is suspected, whereas its role remains controversial in the setting of complete response (82,83). Selective neck dissection is a reasonable therapeutic procedure for clinically uninvolved necks, which can harbour micrometastasis in up to a third of the cases (84) and a N1 status of the disease, in the absence of adverse histological features (85,86). Classic open surgery or minimally invasive procedures such as transoral robotic surgery (TORS) or laser surgery are employed depending on the anatomy and tumour characteristics (87). Currently, TORS is offered as an alternative to chemoradiation as a function-preserving strategy with or without neck dissection (88).

Radiotherapy

Radiotherapy (RT) is an integral part of the primary or adjuvant treatment of HNC. For the treatment of locally advanced disease, RT is employed as an adjunct to surgery or concurrent with chemotherapy (89,90). Usually, the radiation dose for HNC varies from 60 to 70 grays (Gy), depending from the timing and the aiming of the treatment (adjuvant vs radical) (89,90). The risk of long-term toxicity to the salivary glands, pharyngeal constrictor muscles, and thyroid gland increases with the delivery of doses exceeding 55 Gy, leading to xerostomia, dysphagia, percutaneous endoscopic gastrostomy tube dependence, chronic aspiration, and hypothyroidism (91). Recent advances with intensity-modulated radiotherapy (IMRT) allow conformal fields and the application of dose constraints to the volume of the salivary gland treated. IMRT minimizes normal organ exposure while delivering high-dose RT

to a target volume (14). Salivary gland sparing is a major benefit of IMRT, improving quality of life through the reduction of xerostomia.

Chemotherapy

The role of chemotherapy (CT) in HNC treatment has evolved from palliative care to a central component for advanced stages of this malignancy (92). Various classes of agents such as platinum compounds, antimetabolites, and taxanes have shown single-agent activity against it (93). CT has been used in the setting of induction chemotherapy (IC), concomitant with RT (CRT), and as adjuvant treatment (89,90). A comprehensive meta-analysis of clinical trials, conducted between 1965 and 2000, found an absolute benefit only for concomitant administration of cisplatin with radiation (81). The MACH (meta-analysis of chemotherapy in head and neck cancer) revealed that the absolute benefit with chemoradiation was 7% at 2 years and 8% at 5 years, with a hazard ratio (HR) of 0.81 (95% CI, 0.76-0.88; P<.0001) (94). High-dose of cisplatin remains the standard radiosensitizer in the treatment of HNC (95). Moreover, anti-epidermal growth factor receptor (EGFR) inhibition has emerged as a novel treatment strategy for this pathology, and cetuximab is the first molecularly targeted agent that has been introduced into standard practice (96).

Other Treatments

There are other therapies that, although less frequently, are used in the treatment of this pathology:

- Induction Chemotherapy (IC)

Induction (neoadjuvant) chemotherapy has the potential to reduce the incidence of distant metastases, which are increasingly recognised as sites of disease recurrence, as a result of improved locoregional control with chemoradiotherapy (97). However, the meta-analysis of *Pignon et al.* (95) revealed only a trend in favour of this treatment, without achieving statistical significance. Despite the high antitumour activity, many phase III trials that compared IC followed by locoregional

treatment (surgery or radiotherapy, or both) with locoregional treatment alone, failed to show survival benefit (98). Albeit, in 15 trials with a platinum agent plus fluorouracil, a marginal survival benefit was evident (HR 0.88, 95% CI 0.79–0.97; p=0.05) (95). The introduction of more active compounds has strengthened the rationale use of IC. The most recent MACH meta-analysis (5 randomized trials, 1772 patients) confirmed the superiority of taxane-containing chemotherapy combinations as TPF (Docetaxel, Cisplatin, 5-Fluorouracil) compared to PF (Cisplatin plus 5-FU) alone (99). Nevertheless, IC cannot be considered part of the standard treatment of locally advanced neoplasms of head and neck (100,101), it has a clearly defined role only in the organ preservation of hypopharyngeal and laryngeal tumours (102).

- Interstitial Radiotherapy (Brachytherapy)

Interstitial radiotherapy represents a traditional approach for OSCC and is an alternative to external beam radiotherapy (EBRT). Brachytherapy delivers RT by positioning radioactive sources in direct proximity to the tumour target area (80). The advantage of this therapy is its highly conformal dose distribution to a small target zone by a rapid "fall-off" within surrounding normal tissue. It can be applied as a definitive treatment for early OSCC; as a complementary treatment in combination with surgery; as a local "boost" in combination with EBRT, to enhance the local dose to the immediate tumour region, or as a salvage option for small burden persistent or recurrent disease (103).

- Immunotherapy

Immunotherapy represents a further modality of the multidisciplinary approach (14). The immune system plays a key role in cancer, as tumour cells evade immune surveillance by exploiting inhibitory checkpoints that suppress antitumor T cell responses (104,105). The increasing understanding of the mechanisms used by the immune system to control the tumour lesion (such as the presence of tumour-secreted proteins that act as inhibitory stimuli, cytokines, and T cell apoptosis), sustained the high number of novel anticancer immune-based approaches in HNC (106). The recent promise comes from the development of checkpoint blocking

antibodies, such as those against cytotoxic T-lymphocyte antigen 4 (CTLA-4) and programmed death 1 receptor (PD-1). They both function as negative regulators but play a nonredundant role in immune responses. CTLA-4 negatively regulates the early activation of naive and memory T cells; PD-1 and its ligands (PD-L1 and PD-L2) are mainly involved in the modulation of T cell activity in peripheral tissues (107). Several anti-PD-1 and anti-PD-L1 antibodies are under investigation, but two of them (Nivolumab and Pembrolizumab) were already approved, by the Food and Drug Administration (FDA), in patients progressing during or after platinum-based therapy for recurrent/metastatic HNC disease (108,109).

2.7.1 Radical treatment (Stages I and II)

About one third of all the HNC patients diagnosed at early stages (I and II) are treated with surgery or radiation therapy with the aim to eradicate it, which is achieved in up to 80% of the patients at stage I, and about 70% of those at stage II of disease (60). Treatment approach differs according to the primary tumour site. In the early stages of OSCC, surgery or radiotherapy could be used. Surgery is usually preferred, especially in the oral cavity, to avoid the late toxic effects of the irradiation and to obtained the most accurate staging (60). An exception to this is the nasopharyngeal carcinoma, whose approach is primarily non-surgical (radiotherapy or chemoradiotherapy)(110). Selective functional neck dissection of ipsilateral cervical lymph nodes, in clinically uninvolved neck , remains a standard procedure in patients with a high risk for occult neck lymphadenopathy (111). RT, as well as open or endoscopic surgery that spare the larynx, are acceptable options to treat stages I and II of laryngeal tumours; the treatment choice depends on tumour location, the treating centre's expertise and patient preference (112–114). Conventional radiotherapy has remained a mainstay in the treatment of patients with early disease for decades; the total dose of irradiation with radical intent is 66–72 Gy (1.8–2 Gy per day for 5 days a week) with conventional fractionation (115).

2.7.2 Treatment of locally advanced disease (Stages III and IV)

For locally advanced stages of HNC (III and IV) surgery is the prevalent option, especially for OSCC, although excision alone is at high risk of relapse, therefore adjuvant therapy is usually recommended (14). At these stages of the disease is often required a multimodality treatment. In this setting, chemoradiotherapy (CRT) is the standard approach, although, in some patients with bulky disease where organ preservation strategies are appropriate, IC followed by cetuximab plus RT or CRT or surgery may be used (116). The integration of RT and CT against RT alone has been tested in numerous randomized clinical studies, using platinum-based chemotherapy schemes with sequential integrations (CT followed by RT o CT followed by the association CT + RT) or concomitant (CT concurrently or alternating with RT). The best results, were obtained with the concomitant CTR treatment, with a significant advantage in terms of loco-regional control and survival (+ 6.5% at 5 years) (94,117). When the analysis is limited to platinum-containing regimens, the overall survival advantage is greater (+ 9.5% at 5 years). This advantage is confirmed in all tumour locations in the head-neck district and is also achieved in postoperative integration. Furthermore, the benefit of concomitant chemotherapy decreases with increasing age of the patients, which is practically nullified over 70 years (117–119). Obviously, the concomitant use of the two methods is burdened by greater acute and chronic toxicity. The most significant side effect is represented by severe mucositis, which occurs in about half of the patients treated and that can compromise the continuity of the radiation treatment, jeopardizing the effectiveness of the therapy (120,121). It is emphasized that prolonging the period of RT administration caused by the suspension of the therapy or delaying its beginning compromise efficacy and reduce the probability of local control (122–124).

2.7.3 Treatment management in recurrent or metastatic disease (R/M)

At least 50% of the patients with locally advanced HNC develop locoregional or distant relapses, which are usually detected within the first 2 years of treatment (60). Salvage surgery is a likely curative option for very few patients with potentially resectable locoregional recurrence (125). Investigators have also studied re-irradiation alone or in combination with CT for patients with locoregionally recurrent HNC. A randomised study that assessed re-irradiation combined with CT compared with observation after salvage surgery reported an improvement of progression-free survival (HR 1.6, 95% CI 1.1–2.4; p=0.01) with acceptable toxic effects (126). The main objective for these patients is not only to provide symptom palliation but also to extend survival. For R/M disease, CT remains the standard therapeutic option (60). Patients with R/M disease have a poor prognosis with current systemic therapy options after failure of first-line platinum-based CT, yielding an overall response rate (ORR) of ~10% and overall survival (OS) of 6 months (14). First-line treatment consists of platinum-based CT plus cetuximab, which is also used for the maintenance period. After platinum progression, no second lines that significantly improve prognosis are available (14). For this reason, molecularly targeted drugs and, more recently, immunotherapy has become very important to improve outcomes in this malignancy (127).

2.7.4 Palliative treatment

In patients that are no more suitable to treat for healing purpose, palliative medical treatment, radiotherapy and possible surgery (reserved for selected tumours with long natural history, such as adenoid cystic carcinoma (128)), can be used with the only aim of obtaining an alleviation of the symptoms. Since these are potentially toxic treatments, their use must be well assessed considering the general condition of the patient (performance status, age, comorbidities and life expectancy).

3 HNC & RADIATION THERAPY

Approximately 50% of all cancer patients require RT as part of their disease management (129–131), estimating that it contributes to about 40% of the healing treatment (132)(***Table 3***). Rapid progress in this field continues to be boosted by advances in imaging techniques, computerized treatment planning systems, radiation treatment machines (with improved X-ray production and treatment delivery) as well as improved understanding of the radiobiology behind it (133,134).

Table 3. List of common cancers treated with RT. *By Baskar et al. 2012*

Early cancers curable with radiation therapy alone	Cancers curable with radiation therapy in combination with other modalities
Skin cancers (Squamous and Basel cell)	Breast carcinomas
Prostate carcinomas	Rectal and anal carcinomas
Lung carcinomas (non-small cell)	Local advanced cervix carcinomas
Cervix carcinomas	Locally advanced head and neck carcinomas
Lymphomas (Hodgkin's and low grade Non-Hodgkin's)	Locally advanced lung carcinomas
Head and neck carcinomas	Advanced lymphomas
	Bladder carcinomas
	Endometrial carcinomas
	CNS tumors
	Soft tissue sarcomas
	Pediatric tumors

3.1 Principles of radiation therapy

Radiation is a physical agent used to destroy cancer cells (134). The radiation used is called ionizing radiation because it forms ions (electrically charged particles) and deposits energy in the cells of the tissues it passes through. This deposited energy can kill tumour cells or cause genetic changes resulting in cancer cell death (134). High-energy radiation damages cells genetic material (deoxyribonucleic acid, DNA) hence their ability to divide and proliferate is blocked (135). Normal cells usually can repair themselves and retain its normal function status at a faster rate than the

cancer cells, which are not so efficient in repairing the damage caused by radiation treatment then resulting in their death (130). Although radiation hurts both normal and cancer cells, RT aims to maximise the therapeutic ratio by delivering the highest dose possible to the tumour and minimising it in the surrounding normal tissue (136). In the era of advanced technology, there are increasingly sophisticated ways of achieving this. Depending on the tumour site, different tissues exhibit varying degrees of tolerance, which is the maximum radiation dose or intensity of fractionated RT associated with an acceptably low complication probability (usually in the order of 1–5%) (137). The structure of tissues and organs plays a major role in their response to this treatment (138). Organs in which the functional subunits (FSU), composed by a cell or a group of cells, are arranged in parallel (e.g. liver, or paired organs such as the kidneys and lungs) can sustain inactivation of many FSU without clinical manifestation of injury, due to substantial reserve capacity and compensation by the remaining functional subunits (139). In this case, tissue toxicity is caused by damage to a substantial number of chains, and functional impairment leads to complications when a significant percentage of the total tissue volume is irradiated. In general, for parallel or paired organs, there is a threshold volume dose for functional injury, above which increasing functional impairment occurs with increasing dose. These threshold doses are well established and incorporated into RT treatment planning (140). By contrast, in serial organs, FCUs are organised in chains, whereby damage to one subunit results in toxicity that affects the entire tissue, e.g. spinal cord. Thus, they have little or no functional reserve capacity and their tolerance is less dependent by the volume irradiated (137).

3.2 Biological aspects of radiotherapy

Biological effectiveness (cell-killing) of RT depends on the linear energy transfer (LET), total dose, fractionation rate and radio-sensitivity of the targeted cells or tissues (141,142). As above-mentioned, the biological target of radiation is DNA. Cancer cells whose DNA is damaged beyond repair stop dividing and die. Ionizing radiation aims to induce DNA double-strand breaks (DSBs) in these cells. DSBs are

irreparable and more effective in killing cells than the single strand DNA breaks, this is worth for tumour and surrounding normal cells as well (134). There are two ways of affecting DNA using the radiation (134):

1) Direct effect → radiation can directly interact with cellular DNA and cause damage

2) Indirect effect → free radicals formation, derived from the ionization or excitation of the water component of the cells, causes indirect DNA damage

Following the induction of DNA damage, cells respond differently and their response depends on several variables, such as cell cycle, post-translational modifications of the signalling cascade, and chromatin configurational changes (143).

3.2.1 Ionizing radiation and cell death

Radiation therapy, like most anticancer treatments, achieves its therapeutic effect by inducing different types of cell death (***Figure 9***). RT does not kill cancer cells immediately, the process takes hours, days or weeks and they continue dying for weeks to months after the treatment ends (144). Although apoptosis and mitotic catastrophe are the majority causes of cell death induced by ionizing radiation (134), the different types and characteristics of cell death are detailed below:

- Apoptosis: also known as programmed cell death is characterized by cell shrinkage and formation of apoptotic bodies. Mitochondria are important for apoptotic cell death (145). Blebbing of the cell membrane is often seen with condensed chromatin with nuclear margination and with DNA fragmentation. In general, the cellular membrane of apoptotic cells remains intact. Induction of apoptosis in cancer cells plays an important role in the efficacy of RT (144,146).
- Mitotic cell death or Mitotic catastrophe: occurs during or after aberrant mitosis (cell division) and is caused by missegregation of chromosomes leading to the formation of giant cells with aberrant nuclear morphology, multiple nuclei (147).
- Necrosis: cells visibly swell with a breakdown of the cell membrane. They have an atypical nuclear shape with vacuolization, non-condensed chromatin and disintegrated cellular organelles along with mitochondrial swelling and plasma

membrane rupture followed by the subsequent loss of intracellular contents (148). Following the irradiation process, necrosis is seen less frequently but does occur in cancer cell lines or tissues (134).

- Senescence: refers to a state of permanent loss of cell proliferative capacity. Senescent cells are viable but non-dividing, stop to synthesize DNA, become enlarged and flattened with an increased granularity. It has been reported to occur in cancer cells following extensive cellular stress in the form of DNA damage induced by radiation treatment and later die mainly by the process of apoptosis (149,150).
- Autophagy: is a genetically regulated form of programmed cell death in which the cell digests itself. It is characterized by the formation of double-membrane vacuoles in the cytoplasm, which sequesters organelles such as condensed nuclear chromatin and ribosomes (151).

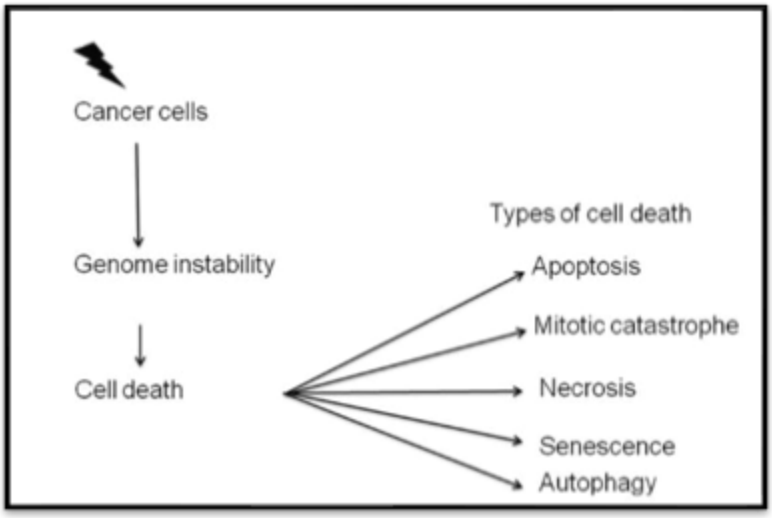

Figure 9: Types of cell death induced by radiation. *By Baskar et al. 2012*

3.3 Radiotherapy classification and techniques

In general, radiation is assigned either with a curative purpose or as palliative treatment to relieve patients from the cancer symptoms. Sometimes, the irradiation process is administrated in a single dose during the surgery (intraoperatory radiotherapy). If used before surgery (neoadjuvant therapy), radiation will aim to

shrink the tumour. If used after surgery (adjuvant therapy), radiation will destroy microscopic tumour cells that may have been left after the treatment (152). When it is applied as unique option, the purpose is to cure the disease and/or maintain the function of the organ (radical therapy). When it is administered at the same time as another treatment (concomitant therapy), to simultaneously perform the local and systemic therapy, the intent is to sum the individual effects of each treatment and have a synergistic response. Regarding the position of the irradiation source, there are two ways to deliver radiation to the tumour lesion (134):

- External beam radiation or teletherapy, the radiation is delivered from outside the body by aiming high-energy rays (photons, protons or particle radiation) to the tumour location. This is the most common approach in the clinical setting.
- Internal radiation or brachytherapy, the radiation is delivered from inside the body by radioactive sources (isotopes), sealed in catheters or seeds directly into the tumour site. It is characterized by short range effects due to the possibility to administer high doses of radiation at short distances, in a way that not all of them reach the healthy tissues surrounding the implant.

3.3.1 Impact of Advanced Technology and Altered Fractionation Regimes

Three-dimensional (3D) conformal RT has been the standard technique used in head and neck malignancies (115). However, there has been a move away from the use of 3D conformal radiotherapy towards Intensity-Modulated Radiation Therapy (IMRT) for many treatment sites (137). In general, IMRT minimizes normal organ exposure while delivering high-dose RT to a target volume (14). Toxicity can therefore be minimised, and there is the added potential to dose escalate in certain sites (153). IMRT uses inverse planning to protect healthy tissue from chronic damage by limiting the dose delivered to areas such as the salivary glands (60). Besides, the use of volumetric modulated arc therapy, which is a novel form of IMRT that delivers external beam radiotherapy through a continually rotating radiation source around the patient is especially age-appropriate (137). It makes changes in the speed of rotation, the shape of the radiation field, and the intensity of radiation, resulting in a

faster delivery of precisely targeted radiation doses (154). Since 1895 when X-ray was invented by WC Roentgen, radiation has been used for different malignant as well as benign conditions, but the concept of fractionation was not known (155). This technique, used firstly by Thor Stenbeck (Stockholm, 1900) in skin cancer administrating small doses of radiation every day, was subsequently called "fractionated radiotherapy"(155). Later on, Dr Coutard showed that, in cancers of pharynx and larynx, protracted fractionation results in better skin and mucosal tolerance and improved tumour response (155). Conventional radiation therapy for HNC treatment is typically given in daily fractions of 2·0 Gy, 5 days a week, up to a total dose of 70 Gy over 7 weeks (156). Higher dose per fraction schemas has been attempted for early-stage of SCC laryngeal tumours, with excellent results (2·25 Gy per fraction) and no increase in late toxic effects (157). The two major altered fractionation regimens used are: hyperfractionation and accelerated fractionation (158). Hyperfractionation was designed to improve treatment efficacy by delivering two to three fractions every day with a reduced dose per fraction (usually 1·10–1·25 Gy), despite an increased total dose. Accelerated fractionation was designed to increase radiation dose intensity by delivering fractions of 1·6–1·8 Gy more than once daily, with a planned dose of 10 Gy per week in a reduced period compared with hyperfractionation (159). Phase III trials showed that altered fractionation improves locoregional control, with increased infield toxic effects but with marginal effects on survival, compared with conventional radiotherapy (160). A meta-analysis of 15 randomised trials with more than 5000 participants, mostly with oropharyngeal and laryngeal tumours, showed that altered fractionation radiotherapy yielded an absolute 5-year survival benefit of 3-4% (161).

3.4 Evaluation of toxicity

Radiation toxicity manifests itself in different ways depending on the type of treatment (RT alone or concomitant chemoradiotherapy) and the irradiated region. Proper registration of toxicity is important, the various specialists, individually, have to record the acute and late toxicities by referring to a common toxicity scale; for this

purpose, the main used scoring systems are: the Common Terminology Criteria for Adverse Events (CTCAE) scale which combines both acute and negative effects in a single classification (version 5.0), the toxicity criteria of the Radiation Therapy Oncology Group (RTOG) and the WHO toxicity scale (121). For the evaluation of the side effects is also important to take into consideration the patient reported outcome (PRO) measures, through the administration of toxicity assessments directly detected by the patient (PRO-CTCAE)(162) and questionnaires about quality of life (QoL). The most used and known by HNC patients are: EORTC QLQ-HN35, FACT- HN, MDASI-HN (163,164). As RT is a localised therapy, its toxic effects (except for fatigue) are limited to the treatment site and modality employed, and are usually more tolerable compared to systemic treatment (165). Depending on the area being treated, site-specific toxicity may be more evident in the elderly population, in which can impact QoL and lead to treatment interruptions and additional supportive care or hospitalisations (137). Side effects of RT may be categorised as acute and late. Acute effects occur up to 90 days after the treatment beginning. They occur in rapidly proliferating tissues, such as skin, the gastrointestinal tract, and the haematopoietic system, and are part of the inflammatory response due to radiation exposure (166). The latency period, or time between commencement of irradiation and clinical manifestation of related side effects, varies based on the time of proliferation of precursor cells to mature cells for the irradiated endothelial tissue (167). For example, precursor skin cells in the basal layer of the epidermis usually take around two weeks to proliferate into mature cells, which is why there is approximately a two-weeks delay between onset of RT and start of radiation dermatitis (137). However, early effects are usually observed after approximately 7–10 sessions of treatment, and there is a cumulative effect with greater frequency and intensity observed at the end of RT, and for some time (weeks) after. Protracted treatment reduces acute toxicity, but can compromise tumour control (137). Late effects are those that occur beyond 90 days after the onset of RT. Late effects depend on the dose and fractionation schedule delivered during the treatment, and resultant damage to blood vessels or the extracellular matrix (168). Acute reactions are usually reversible but may have a substantial impact in older patients, in particular side effects like xerostomia. In contrast, late effects are generally irreversible and progressive, and

may have a significant impact on patient's quality of life (QoL). Late effects provide the basis for dose constraints used in RT planning (137). As part of an intervention aimed to prevent/reduce the toxicity, an odontostomatological evaluation with possible dental excision and the maintenance of an adequate level of oral hygiene along the entire treatment is recommended (169).

3.4.1 HNC Acute toxicity

Acute toxicities typically develop during the active treatment phase of either RT and CRT or CT alone (170). Common acute toxic effects are: mucositis, mild to severe xerostomia, dermatitis, oedema with related symptoms (dysphagia, pharyngodynia, dysphonia, sometimes dyspnea), loss of taste (171,172). The acute toxicity profile depends on the type of drugs used (CT or biologic drugs), the irradiated area and the patient's condition. It is more important during CRT due to its systemic toxicity, especially gastrointestinal toxicity (nausea, vomiting, diarrhoea, fatigue), haematological (anaemia, neutropenia, thrombocytopenia) and specific organ toxicity (renal, neurological etc.)(170). Regarding the acute toxicity derived from RT and cetuximab association, the only randomized trial published reports a significant increase in grade 3–4 radiodermatitis in addition to vesicular-type skin rash (typical toxicity of cetuximab); however, limited to the face and to the upper part of the trunk, whose appearance has been identified as a predictive element of the response to treatment (173).

3.4.2 HNC Late toxicity

The likelihood of late toxicity increases with age and depends on the site of the disease (larynx/hypopharynx vs oral cavity/oropharynx), T size and emptying nodal neck (174). Apart from xerostomia, that is also responsible for the difficulty in swallowing, nutritional deficiency, compromised oral hygiene, altered taste sensation, impaired speech function and poor sleep quality; the possible late

sequelae of RT include: osteoradionecrosis, dental caries, subcutaneous fibrosis, trismus, thyroid dysfunction, hearing loss, pharyngeal or oesophageal stenosis and the most severe are the neurologic complications (175).

3.5 Effects of RT on the oral cavity

As the radiation field for HNC patients usually includes the tissues of the oral cavity or salivary glands, oral complications are quite common. Oral toxicity tracks with both cumulative radiation dose and daily fraction size. Acute direct toxicities such as dry mouth and mucositis are often triggered by cumulative radiation doses of 10-20 Gy (170). The risk of more substantial injury continues to increase with higher doses of radiation. The chance of chronic injuries such as fibrosis or permanent salivary gland changes is likely with cumulative doses of 60 Gy (176). Indirect side effects are noted as a secondary consequence of radiation injury. Radiation caries provides an excellent example. Direct radiation damage to the salivary glands, particularly the parotid, results in changes in both salivary flow and composition (170). Likewise, radiation-induced vascular changes of the jaws, especially the mandible, predisposes to osteoradionecrosis (ORN) for years after the completion of active treatment (177,178).

Oral Mucositis

Oral mucositis (OM) is a common and often dose-limiting side effect of RT for HNC patients, with or without CT (179). Up to 90% of the patients are diagnosed with OM, 60–70% of those suffering severe OM characterized by ulceration and pseudomembranous formations (179,180). The association between RT and CT increases the incidence, severity and duration of OM, especially when combinations of different drugs and altered fractionation schedules are used (171). Mucositis causes significant pain, dysphagia and weight loss due to chewing and swallowing difficulties (171,172). It is considered the most debilitating acute reaction during HNC treatment (181). The severity of the symptoms or the fear that higher grade OM

might progress to necrosis can lead to unplanned RT interruptions or reduced CRT compliance, resulting in poorer outcome (180). Severe mucositis in which patients develop deep, confluent ulcers of the oral and oropharyngeal mucosa has been described in almost three-quarters of individuals treated with concomitant chemoradiation for cancers of the mouth and oropharynx, and two-thirds of patients with cancers of the hypopharynx or larynx (170,182). While other side effects of anticancer treatments, such as emesis, anaemia, and neutropenia, are relatively well controlled with validated supportive care, the therapeutic measures towards mucositis are still scarce (183). At present, there is no radioprotectant with proven efficacy in decreasing the severity of mucositis during CRT for HNC patients (60). Therefore, OM is associated with a negative impact on QoL and presents a major clinical and economic problem (184,185). Risk factors of OM include the volume of the irradiated mucosa, treatment dose, concurrent radiochemotherapy agent(s) and the treatment schedule (171,185). Oral health, use of tobacco and alcohol, comorbidities, age, sex and genetic predisposition (186), as well as changes in salivary flow and oral bacterial flora also influence the development of OM (187). However, the mechanisms of how risk factors impact on its development in HNC patients have not been sufficiently defined (184). In clinical terms, OM starts as an inflammatory process of the mucosa, predisposition to opportunistic infection and, depending on its intensity, can evolve to ulceration (188). The condition usually begins in the first week of treatment with symptoms of burning sensation and mucosal erythema (170). Although patients describe some discomfort at this stage, palliation can usually be achieved with topical barrier or analgesic agents and non-narcotics. However, within 2 weeks, breaks in the mucosa appear as irregular ulcers, usually on the movable mucosa of the lips, cheeks, lateral or ventral tongue, or soft palate (170). The ulcers are frequently covered by necrotic fibrinous pseudomembranes which act as a repository for oral microorganisms. Symptoms increase as to require an opioid analgesic and diet may be limited to soft solids or liquids (189). When a cumulative dose of 40 Gy is reached, almost at the end of the treatment, the pain became more severe and deep ulcerative lesions are present. These lesions persist until 2-4 weeks following the last day of radiation, pain is often so severe as to be refractory to opioids (170). On the other hand, the molecular mechanism that explain the

development of OM is based on the presence of high levels of mitotic activity and high cell turnover (188). Due to the high degree of cell desquamation, there is a continuous need for cell multiplication to recover the oral mucosa. Tissues with high levels of mitotic activity respond rapidly to the radiation, as the most sensitive phases of the cell cycle are G2 and mitosis. Thus, the mucosa is rapidly affected (182). Reactive oxygen species also play a central role in the pathogenesis of OM, because they can directly damage the genetic content of epithelial cells, leading to cell death and upregulation of several transcriptional factors such as nuclear factor-kB (NF-kB) (190). This is followed by the production of pro-inflammatory cytokines, such as tumour necrosis factor (TNF-α), interleukin (IL)-1β and IL-6, and chemotactic agents (190).

Xerostomia

Xerostomia is a common acute and late side effect in HNC patients treated with RT (175,191). The term is used to describe the subjective symptoms of dry mouth deriving from a lack of saliva (192), whereas hyposalivation is the physiological reduction in salivary flow (193). Hyposalivation is defined as unstimulated whole saliva flow of ≤0.2 mL/min, and symptoms of xerostomia often become evident when saliva flow is below 0.1–0.2 mL/min (191,193). It usually occurs by the third week of RT and persists after the completion of treatment, being very common in long-term survivors (175,194). The degree of xerostomia is largely dependent on the radiation dose and the volume of the major salivary glands within the radiation fields. Loss of function of salivary glands is usually permanent after radiation doses of 35 Gy (175). Oral dryness may be secondary to true salivary gland hypofunction or qualitative changes of saliva (194). RT may lead to hyposalivation (within a week), decreased saliva pH, and altered saliva consistency (170). Animal studies showed that as the radiation treatment progresses, there is a damage to the plasma membrane of acinar cells with disruption of intracellular signal transduction leading to changes in salivary composition (195). The severity and incidence of xerostomia in patients receiving IMRT are lower compared to the patients with HNC receiving conventional radiotherapy (196,197). According to the RTOG, there are four grades of radiation-

associated xerostomia to the salivary glands: grade I, slight mouth dryness; grade II, moderate mouth dryness; grade III, complete mouth dryness; grade IV, gland fibrosis)(198). Grades I and II (slight and moderate xerostomia) are the most common, affecting 60%-75% of patients. In these patients, there is a significant reduction of both stimulated and unstimulated salivary flow rates (170). One year after the completion of RT only 20%-30% of patients recover (170). Many efforts have been made to prevent or treat this complication, including the surgical transfer of salivary glands (199), the use of radioprotective agents such as amifostine (200,201) and radiation techniques that spare the salivary glands, but with very few good results (175).

Dysgeusia

Patients with HNC may experience taste alteration (dysgeusia), loss of taste (ageusia), heightened sensitivity (hypergeusia), or reduced taste sensitivity (hypogeusia). Dysgeusia is an early complication of RT and may precede mucositis (170). Radiation has a direct cytotoxic and antiproliferative effect on the epithelium of the tongue and the gustatory nerves (202). It may also lead to a reduction of taste pores with consequent loss of sour taste (203). Another factor that can explain the taste alteration is the dry mouth secondary to RT, as saliva dissolves food particles allowing the presentation of tastants to the receptors (204). Besides, surgical procedures for HNC may provoke direct surgical trauma to glossopharyngeal, facial, or chorda tympani nerves with a subsequent loss or changes in taste (170). Severe taste changes result in malnutrition, weight loss, and poor QoL (205).

Osteoradionecrosis of the jaw

Osteoradionecrosis (ORN) is delayed radiation-induced injury, with bone necrosis and failure to heal for at least 3 months (206). It is a severe complication, which occurs in approximately 4% of patients receiving radiation of the head and neck region (170). Bone radiation (50 Gy or more) may lead to hypovascularity and osteocytes apoptosis, which causes infection, poor wound healing, and bone necrosis (170). ORN can develop spontaneously in one-third of all cases but usually occurs

after local trauma or dental extraction (207). The patient may complain of oral pain and swelling. In most cases, the condition is chronic, progresses gradually and becomes more extensive and painful (208). At the beginning, it remains clinically latent and without symptoms until the lesions are visually detected with bone exposure or the patient begins to experience discomfort, with denuded bone, pain, swelling, suppuration and the formation of a cutaneous fistula or pathological fracture (209). Initial treatment includes control of infections, surgical debridement, and local sequestrectomy. Preventative strategies include a comprehensive dental evaluation before RT with the elimination of infectious foci and extraction of any non-restorable tooth 2-3 weeks before the treatment (210).

4 BIOMARKERS IN CANCER

To reduce cancer morbidity and mortality, as well as to facilitate the evolution from the traditional "one size fits all" strategy to a new "personalized" cancer therapy (i.e., the right treatment to the right patient at the right time, using the right dose and schedule), there is an urgent need of reliable, robust, accurate and validated biomarkers (211). Firstly, is necessary to define the concept of *biomarker or biological marker*: it is a feature that can be objectively measured and evaluated as an indicator of normal biological processes, pathogenic processes or pharmacologic responses to a therapeutic intervention (212). Unfortunately, despite the impressive advances in tumour biology research and in high-powerful "omics" technologies (genomic, proteomic, metabolomic), the translation of candidate cancer biomarkers from bench to clinical practice is slow and challenging, and only a few tumour markers have been adopted successfully into routine clinical care (211). To become a clinically approved test, a potential biomarker should be confirmed and validated using hundreds of specimens and should be reproducible, specific and sensitive (213). In general, biological markers include gene expression products (either RNA or proteins), metabolites, polysaccharides and other molecules such as circulating nucleic acids, single-nucleotide polymorphism and gene variants (214). These markers can be produced by the same tumour or by other tissues in response to its presence, so they can be found in different biofluids (serum, plasma, cerebrospinal fluid, urine, saliva, etc.) and/or tissues (5,215).

4.1 Characteristics of a biomarker

The ideal biomarker should be easily detectable, highly sensitive and specific for its target phenotype as well as economically feasible (213). *Sensitivity* is the ability to detect a disease in patients in whom the pathology is truly present (*i.e.*, a true positive); *specificity* is the ability to rule out the disease in patients in whom it is truly absent (*i.e.*, a true negative)(216). Besides, to be translated into clinical practice other features are essential for a biological marker (213,217):

- ✓ to be assessed non-invasively
- ✓ to be readily quantifiable in a reliable and stable test
- ✓ to be significantly increased (or decreased) in the related disease condition
- ✓ to be specifically correlated to the physiological effect studied

A biomarker should be used in clinical practice only if it reliably adds to a clinician's judgment, resulting in a more favourable clinical outcome for the target population. Its accuracy alone is not enough to imply clinical utility. Clinical decisions based on misleading biomarker results may expose the patient to adverse consequences and increase the cost of care (218).

4.2 The utility of biomarkers in oncology

Biomarkers have many potential applications in oncology, including risk assessment, screening, differential diagnosis, determination of prognosis, prediction of response to treatment, and monitoring the disease progression (219)(***Figure 10***). Although, the two types of markers most considered in the clinical practice are predictive and prognostic markers (220). *Predictive biomarkers* are able to predict response to specific therapeutic interventions; on the other hand, a *prognostic biomarker* may not be directly linked to or trigger specific therapeutic decisions, but aim to inform regarding the risk of clinical outcomes such as cancer recurrence or disease progression. Besides, another class of markers, known as diagnostic biomarkers, is also important to identify whether a patient has a specific disease condition (221).

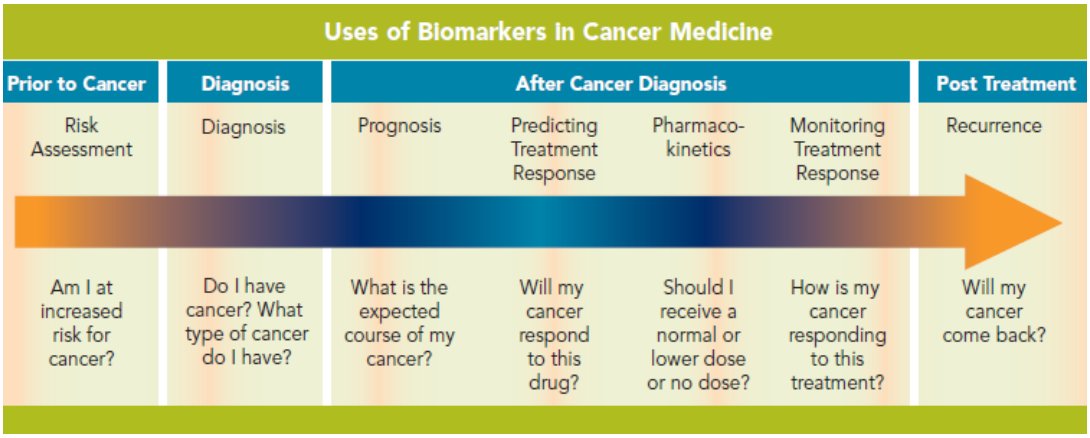

Figure 10: Potential clinical uses of biomarkers. Biomarkers can be used for patient assessment in multiple clinical settings: 1) before cancer growth, including estimating the risk of disease, screening for occult primary cancers, distinguishing benign from malignant findings or one type of malignancy from another; 2) at time of diagnosis; 3) after tumour diagnosis, determining prognosis and prediction of the cancer patient and monitoring status of the disease; 4) at the end of the therapy, either to detect recurrence or determine response or progression to therapy. *By (Google images, n.d.)*

The identification of new biomarkers with diagnostic value in cancer disease may help to significantly increase the percentage of patients who can benefit from the therapies administered, which tend to be much more effective in the early stages of the pathology. Furthermore, biomarkers with a prognostic and predictive value play a very important role in the development of personalized therapies, facilitating the patient stratification (222). This strategy seeks, retrospectively, the identification of biological markers characteristic of a specific group of patients who respond better to a certain therapy. Once identified, this information is used prospectively to select the most appropriate therapy for each patient (223). Thus, the most effective treatment is administered to each patient from the first moment, avoiding inappropriate therapy and treatment-related toxicity.

4.3 Cancer biomarkers currently available in clinic

Despite all the efforts, only a few markers are recommended by the guidelines of the European (ESMO) and American oncological societies (ASCO)(219). Among the biomarkers used in clinic as "predictive factors" for a specific therapy or for determining which treatment is likely to be most effective, KRAS and HER2 need to be cited. The first one is a predictive biomarker in colorectal cancer because somatic mutations in KRAS gene are associated with poor response to anti-epidermal growth factor receptor (EGFR) directed therapies (224). Similarly, overexpression or gene amplification of HER2 gene in breast cancer predicts for response to anti-Her2 agents such as trastuzumab (225–227). It has been shown, in pivotal phase III trials in breast cancer, that subjects with HER2 overexpression (approximately 20% of patients) treated with anti-HER2 therapy have improved disease-free and overall survival (225–227). HER2 overexpression is similarly predictive of response to trastuzumab in oesophagogastric adenocarcinoma (221). Other major predictive biomarkers include BCR-ABL in chronic myeloid leukaemia, EGFR (HER1) and ALK mutations in non-small cell lung cancer (NSCLC) and BRAF mutation in melanoma (221). Moreover, Mammaprint is one of the first gene expression signature-based assays, based on the measurement of 70 genes ,to predict breast cancer recurrence after CT (228). Similar tests are also available for colon and prostate cancer, all of which analyse gene expression in tumour tissue (229). A 186-gene expression signature in non-tumour stromal liver tissue has been validated to predict hepatocellular carcinoma development and recurrence, as well as liver cirrhosis progression (230,231). Despite the numerous prognostic biomarkers reported in the literature, only few of them have been approved by the FDA. One of the major reasons is that prognostic prediction itself often does not directly change clinical decision, making unless coupled to specific therapeutic options (221). Notwithstanding, many other prognostic biomarkers are available through the LDT (Laboratory Developed Test) pathway, a type of in vitro diagnostic test that is designed, manufactured and used within a single laboratory (232). Diagnostic markers are one of the most diverse classes of biomarkers, ranging from assays developed for cancer screening to diagnostic tests assessing the progression of known tumour (221). Recently, there

has also been increased interest in developing minimally invasive diagnostic tumour biomarkers, using the measurement of circulating DNA or microRNA by liquid biopsy (221). To date, scientists are continually searching for novel HNC biomarker panels. Despite a long list of prognostic and predictive biomarker candidates that can be found in the literature, *not one molecular marker has been widely accepted for routine use in managing patients with head and neck cancer* (220,233). Several body fluids have been evaluated as new sources for cancer biomarker discovery. In particular, salivary and serum proteomics seem promising diagnostic and predictive tools for head and neck disease (234).

5 HUMAN SALIVA AS A FUTURE DIAGNOSTIC TOOL

Monitoring health and disease status and treatment outcome through non-invasive means is a desirable aim in promoting health. In this context, human body fluids, such as saliva, plasma, serum and urine, provide several key advantages compared with tissue biopsy and other body fluids, including low invasiveness and cost, easy sample collection and processing, as well as reduced anxiety and discomfort for patients, especially when longitudinal monitoring overtime is necessary (234). Oral fluid, or saliva, is a clear, slightly acidic (pH = 6.0–7.0), and heterogeneous biological fluid consisting of secretions from the parotid, submandibular, and sublingual glands (235). The average daily flow of the whole saliva is between 1 and 1.5 L. Physiologically, the function of saliva includes oral digestion, taste, lubrication, antibacterial protection, and buffering (235–237). Saliva contains enzymes, hormones, antibodies, antimicrobial constituents, and cytokines—all of which are constituents gathered within the salivary glands and subsequently released into the oral cavity through small ducts by a cluster of cells called acini (236). Because each of the salivary glands is encapsulated by capillaries, each gland allows free exchange molecules from blood to the adjacent acinus cells (238). Previous research has suggested that circulating biomolecules that originate from a disease process, may be eventually transported from the bloodstream into the salivary glands, which will consequently modify and change the composition of saliva (238–240). Many constituents reach saliva from the blood by transcellular (e.g., passive and active transport) or paracellular means (e.g., extracellular ultrafiltration), as part of the endocrine system (241,242). Hence, in diagnostic medicine, it is of recent interest to locate saliva-based targets to evaluate an individual's current state of health (238).

5.1 Emerging of salivary biomarkers

Comparably to other human body fluids such as plasma and urine, which are in direct contact to tissues and organs and are routinely used in clinical diagnostics

(185), saliva may act as an indicator of oral disease status and allow sensitive and/or specific protein biomarker discovery (243). Mass spectrometry-based proteomics approaches and the respective analysis pipelines allow reproducible and reliable peptide-based quantification of protein levels, even in large sample series (244). Examples of the successful application of proteomics include Sjögren's syndrome (245), diabetes mellitus (246), periodontitis (247) and oral cancer (248). Proteins are attractive as potential biomarkers since they arguably more diversely participate in cellular activities than DNA and RNA, particularly those which are regulatory molecules in relevant cellular pathways (249). Considering that the transformation of oral mucosal epithelial cells to malignant, particularly in OSCC, is surrounded by saliva, and also that salivary secretions are mixtures of complex proteins, carbohydrates, lipids, electrolytes and water (250), this human biofluid is a great choice matrix to detect salivary protein markers for HNC. Especially cytokine levels have been repeatedly proven to be increased in saliva of tumour patients (251). The best-investigated candidates are EGF, interleukin 6 and 8, and to a lesser extent other NFκB-derived members such as TNF-α or interleukin 1, further VEGF, interleukin 4 and 10, endothelin (251–254). The majority of investigations have targeted EGF. This growth factor not only positively influences cell proliferation, but its levels are also correlated with the invasive behaviour of oral cancer cells (251,255). Overexpression of this marker was found to be linked to the development, growth advantage and metastasis of numerous different neoplasia, including the oral cavity and upper digestive tract (251). Consequently, EGF and its receptors have become important targets in anti-tumour therapy, as in breast cancer (256), malignancies of the head and neck (257), lung and colorectal tumours (258,259).

5.2 Salivary cytokines in cell proliferation and cancer

Cytokines are intercellular signalling proteins that play a role in regulating growth, cellular proliferation, angiogenesis and tissue repair (260). They also have a function in immune responses to infection, injury and inflammation (261). These signalling proteins differ not only in their function, but also have a wide variety of molecular

weight ranges from approximately 6–70 kDa (262). Even if some overlap in the terminology exists, the term “cytokines” refers to a diverse group of soluble proteins and peptides as interleukins (IL), chemokines, interferons (IFNs), tumour necrosis factors (TNFs) and lymphokines, but not growth factors or hormones (263,264). They are produced by a broad range of cells, including immune cells like macrophages, B lymphocytes, T lymphocytes and mast cells, as well as endothelial cells, fibroblasts, and various stromal cells (265). Cytokines can be generally classified as pro-inflammatory (including IL1, IL6, IL8, IL15, IL17, IL23 and TNFα) or anti-inflammatory [including IL4, IL10, IL13, transforming growth factor (TGFβ) and interferon (IFN)α] (266). They interact with each other in complex ways that may be additive, synergistic or antagonistic, or may involve the induction of one cytokine by another (262). These molecules levels are generally kept within a specified range and time; if not properly maintained, they can lead to induction of tissue damage (254). Depending on their balance, the collective effect can be either pro- or anti-tumorigenic (266). Chemokines are released from various cells after stimulation by pro-inflammatory cytokines (266). Tumours usually have increased expression levels of chemokines, resulting in the recruitment of leukocytes to neoplasm lesions by chemotaxis (267). IL-8 or IL-6 can stimulate several signal transduction pathways and depending on the cellular context lead to cell proliferation, cell survival, tumour invasion or angiogenesis (266). In general, it has been suggested that excess of pro-inflammatory cytokines increases growth and survival of tumour cells (266,268), TNFα is one of these inflammatory proteins for which there is convincing evidence of a role in tumour promotion (269). Cytokine production is often transient and tightly regulated. Due to the high biological activity of most cytokines, their homeostatic concentration in body fluids is low, e.g., picomolar concentrations. However, if required, the concentration of cytokines can increase up to 1000-fold (262). In healthy individuals, cytokines are either not detectable or present at pg mL^{-1} concentrations in body fluid or tissues. Elevated concentrations of cytokines indicate activation of cytokine pathways associated with inflammation or disease progression (270). For this reason, these proteins are widely used as biomarkers to understand and predict disease progression and to monitor treatment effects (271). Besides, since they work in networks, it is significantly important to be able to measure

multiple cytokines in a single sample (262). A complex relationship exists between pro-inflammatory and anti-inflammatory cytokines, which are secreted in the tumour microenvironment not only by immune cells but also by tumour cells (268). In HNC, the tumour and surrounding lymphocytes may produce altered cytokine levels (272). Alterations in immune, inflammatory and angiogenetic responses within the HNC microenvironment play a critical role in tumour aggressiveness and its response to chemo- and radiation therapies as well as its influence on the immune system. Furthermore, ionizing radiation is known to increase the expression of a number of cytokines which are involved in inflammation and wound healing (273). Thus, the better understanding of secretion and regulation pathways of immune suppressive and proangiogenic cytokines is essential to increase the clinical perspective of this tumour type, with respect to an immunomodulatory intervention in HNC patients (272). The use of body fluids like saliva, serum or plasma for the measurement of these proteins, has shown considerable promise for the early diagnosis of cancers, including breast cancer, prostate cancer and lung cancer, among others (274–276). Usually, plasma sampling requires a consistent and rapid collection, processing and storage techniques to minimize the risk of platelet deregulation, which may falsely elevate the levels of a number of cytokines (277,278), that can also be impacted by a variety of conditions in patients with inflammatory comorbidities (273). By contrast, saliva collection is a simple, non-invasive method to detect local expression of cytokines and may avoid many of these logistical and technical challenges. Besides, the assessment of local salivary cytokine levels via longitudinal sampling, in patients undergoing therapy, may allow for a better understanding of the temporal nature of cytokine elevation during the cancer treatment and correlation with tumour response and toxicity (273). However, the correlation between saliva and plasma/serum cytokine levels remains unclear. *Brailo et al.* (279) reported that altered cytokine levels produced in presence of oral cancer are not reflected in serum cytokine concentrations. Some cytokines that could not be detected or were present at a low concentration in serum were found at a higher concentration in saliva (279). The majority of the literature available has addressed immune deregulation in OSCC by utilizing serum as a source of cytokines (280–282), while saliva has not been investigated in much detail. In addition, even though a few studies have reported

derangement of salivary cytokine levels in OSCC patients, their major focus was on pro-inflammatory cytokines (283–285).

5.3 Proteomics as a potential field for biomarker discovery

Proteomics has been utilized for biomarker discovery of various diseases (215,233,286). In the cancer research field, different studies (185,234,248,287,288) have been carried out using various proteomics approaches, to identify potential biological markers for HNC and especially for OSCC, where the study of the salivary proteome is rapidly advancing and evolving (250). The term "proteome" refers to all the individual proteins that may make up a biological system and, considering the oral biofluid as it, a collection of 1166 diverse proteins was recorded within the human salivary proteome in 2007 (289,290). The research was conducted using mass spectroscopy and 2D gel-electrophoresis, comparing that results with previously gathered protein databases. Some years later, in 2013, *Schulz et al.* while investigating the differences among saliva and plasma protein composition, found that approximately 30% of the whole salivary proteins were present in plasma as well (291). In fact, comparative proteomic analysis of fluids or cancerous and control tissues is considered as a useful approach for biomarker discovery (249). By comparing salivary protein markers from patients receiving different treatments with different outcomes, proteomics may be also used to monitor treatment response (292). Due to its high-sensitivity and high-accuracy mass measurement of peptides, mass spectrometry (MS) technique has become the core technology for protein identification (292). Large-scale MS-based proteomics has been widely accepted for studies of protein expression profile, protein interactions and post-translational modifications (293). Various technical platforms have been used for protein expression studies including qualitative and quantitative approaches (249). So far, electrospray ionization (ESI) and liquid chromatography-mass spectrometry (LC-MS/MS), a chromatographic separation technique coupled with high resolution mass spectrometer, was the best recommended for proteomic analysis (294,295). The term quantitative proteomics usually refers to measuring the changes in the level of

abundance of proteins in different samples, with the intent to evaluate protein expression profiles as their cellular activity status (296,297).

Typical studies include the quantitative comparison of samples from 'different biological conditions,' with the underlying assumption that the proteins showing different abundance are functionally related to the processes affected by the applied conditions (297). In particular, labelling based quantitative methods were illustrated as the most accurate and reliable approach to measure the relative abundance of a single protein or a set of proteins among various disease samples (249). However, the more recent developments in proteomics technology increased the use of label-free methods as a quantitative technique which does not require any isotope labelling (298). Label-free proteomics has been successfully applied to various neoplasms including cancer of ovary, lung, skin, colon, bladder, and prostate (249), providing an accurate, reproducible and consistent results. In some cases, these results have been successfully validated. Normal validation processes are usually antibody-based methods and time consuming (286). Therefore, it is not possible to confirm the expression of all proteins via antibody interaction techniques like immunohistochemistry (IHC), western blot analysis (WB) and ELISA (249,286). Recently, selected reaction monitoring (SRM) also known as multiple reaction monitoring (MRM), a highly specific and sensitive mass spectrometry technique that can selectively quantify compounds within complex mixtures, has been introduced to specifically select and quantify promising protein biomarkers in serum or tissue (299,300); its application in saliva samples may provide a direct and feasible method for the validation of differentially expressed proteins in the salivary proteome (286).

II. Objectives

HNC is a complex and heterogeneous disease, characterized by different epidemiology, aetiology and therapies. Monitoring illness status and treatment outcome through non-invasive means is a desired goal in aiding health. In this context, salivary inflammatory proteins have promising features to be used as biomarkers for screening and outcome prediction in this malignancy. The majority of saliva studies have focused on the levels of these biomolecules between HNC patients and healthy individuals. However, changes from pre- to post-RT treatment have not been extensively explored due to salivary glands destruction and subsequent xerostomia. Therefore, **the aim of this doctoral thesis** is firstly to evaluate the levels of salivary inflammatory markers and the salivary proteome before and after the irradiation process, secondly, to study their modulation and association with RT outcomes, in order to identify potential predictive biomarkers for HNC.

As specific objectives

- **<u>Investigation of salivary inflammatory markers</u>**

1) To compare the levels of pro-inflammatory (IL-6, IL-8, TNF-α) and anti-inflammatory cytokines (IL-4, IL-10), chemokines (MCP-1/CCL2) and growth factors (EGF, VEGF) in saliva samples of HNC patients, evaluated pre- and post–RT treatment.

2) To analyse if there are differences in the levels of the above salivary cytokines, chemokines and growth factors among the group of healthy volunteers, recruited as controls, and the HNC patients valued before the RT treatment.

3) To determine if there is a relationship within altered inflammatory protein profiles and clinical parameters of the HNC patients, in particular treatment tolerance (development of mucositis) and response to the therapy.

4) To verify whether any of these salivary proteins can be considered as a putative biomarker of RT response.

- **Investigation of the salivary proteome**

1) To determine if there are modifications in the salivary proteome profiles between the control group and the HNC patients valued before and after the RT treatment.

2) To evaluate if there are differences in the salivary proteome findings among the same group of HNC patients, analysed pre- and post-RT treatment.

3) To identify salivary altered proteins linked to wound healing, tumour control and response to the therapy.

4) To define whether any of these specific biomolecules can be considered as a putative biomarker of RT response.

III. Materials & Methods

1 STUDY DESIGN

The present prospective observational study was carried out at the General University Hospital of Valencia (HGUV) between 2017 and 2020. The research was conducted in accordance with the fundamental principles established in the Declaration of Helsinki and with prior approval of the Ethical Committee review board of the HGUV on 19th April 2017.

2 PATIENTS

Study population consisted of two independent cohorts: Cohort 1, composed by 42 patients diagnosed with head and neck cancer, Cohort 2 comprised 40 healthy volunteers, involved as controls. Patients were partly recruited from the Oral and Maxillofacial Surgery Department and the ENT (Ear, Nose and Throat) Department of the HGUV, and partly from the Radiotherapy Department of the Valencian Institute of Oncology (IVO). Control subjects were enrolled at the Dental Clinic of the University of Valencia (UVEG). A written informed consent form was obtained from each participant. The inclusion criteria followed for the selection of the population of the two cohorts are presented in ***Figure 11***.

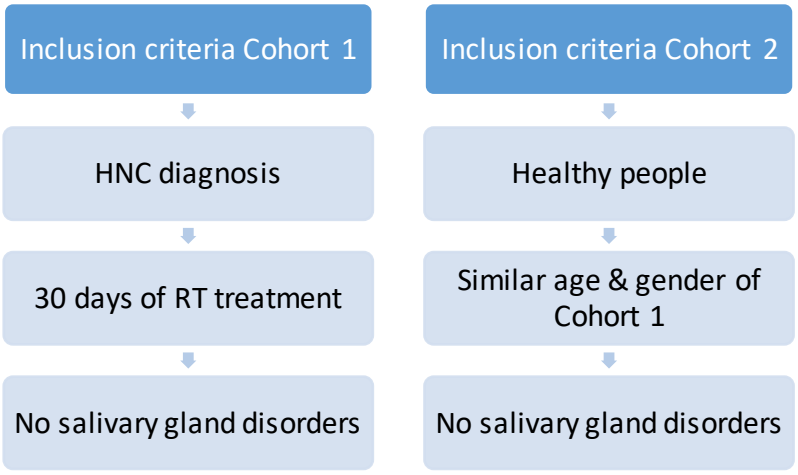

Figure 11: **Inclusion criteria followed by the two cohorts of the study.** HNC patients belong to Cohort 1 were recruited at General University Hospital of Valencia (HGUV) and at the Valencian Institute of Oncology (IVO), whereas control subjects belong to Cohort 2 were enrolled at the Dental Clinic of the University of Valencia (UVEG). Both groups were age and gender-matched.
HNC, Head and neck cancer; RT, Radiotherapy treatment.

For the HNC patients being part of Cohort 1, the clinical parameters recorded were: age, gender, diagnosis, location of the lesion, neck metastasis, TNM classification, development of mucositis, response to the treatment. The last variable was reported at two-time points: at the end of radiotherapy (T=0) and three months later (T=1).

The evaluation of the clinical response, after the use of the ionizing radiation was based on the following classification:

1) Complete Response (CR) → disappearance of tumour lesion following the RT treatment
2) Partial Response (PR) → diminution of tumour size but persistence of malignant lesion after the irradiation process
3) No Response (NR) → no reduction of tumour size since the treatment started or unequivocal progression of existing lesions
4) Recurrence (R) → appearance of one or more new lesions at T=1

3 SAMPLE COLLECTION

The chance to measure changes in non-stimulated saliva before and after the irradiation process is generally very low due to destruction of salivary glands caused by the treatment. To overcome this impasse, whole stimulated saliva was collected from all the subjects included in the project. Concerning the Cohort 1, the first sample was obtained before starting the radiotherapy treatment, while the second sample, collected post-RT, was gained in a range of 4/8 weeks after the irradiation process, due to the expected inflammatory sequels subsequent to the therapy. Regarding Cohort 2, saliva specimens were always acquired at the beginning of the dental check-up. Participants had to avoid eating, drinking, smoking, and using oral hygiene products for at least 1 hour before the procedure. The salivary flow was stimulated by chewing parafilm for five minutes, under continued stimulation the saliva accumulated in the mouth was expectorated into a 15mL tube through a funnel (301). Afterwards, the gathered sample was centrifuged at 3000 rpm for 15min at 4 °C and

frozen at −80 °C until further use. Periodontal status was recorded for each participant and specimens with visible traces of blood were discarded from the study. To characterize the periodontal status of the entire study population, a basic periodontal examination (BPE) was performed after the collection process. The clinical exploration documented the location and extent of bacterial plaque accumulation, the presence of calculus, the extent of attachment loss and the presence or absence of bleeding on probing (302,303). Tooth examination consisted of a general assessment of the dentition, focused on the registration of missing teeth, restorations and caries.

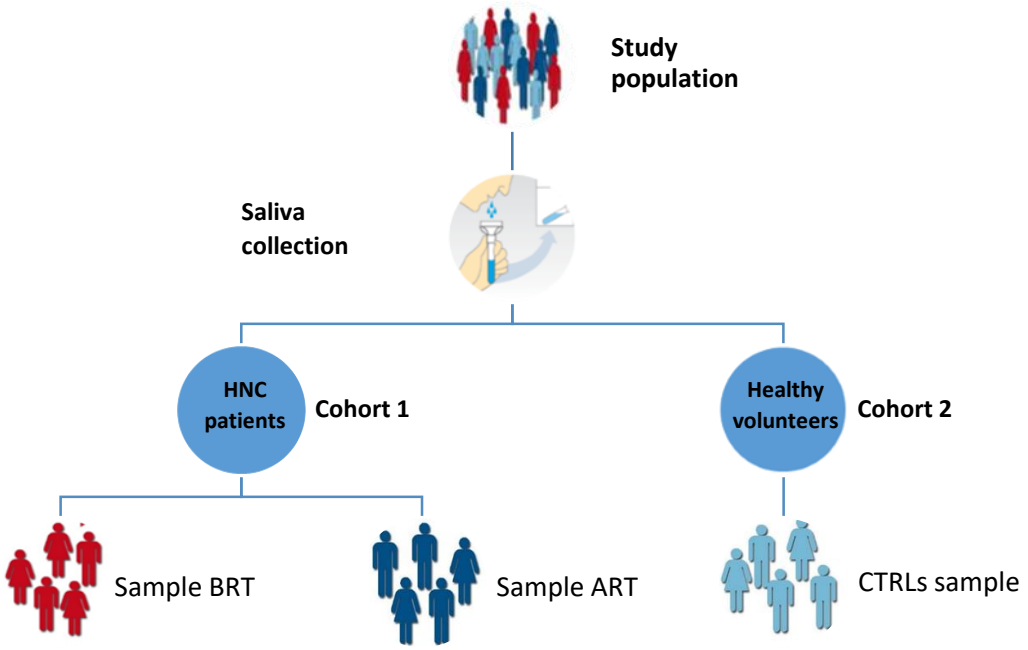

Figure 12: Flow chart showing the salivary process collection valid for the two cohorts of the study. Referring to Cohort1, the first sample was obtained before the radiotherapy treatment (BRT Group), while the second sample, collected from the same patient after the radiotherapy treatment, was gained in a range of 4/8 weeks following the irradiation process (ART Group). Only one specimen was necessary to collect from healthy donors belong to Cohort2 (CTRL group). HNC, Head and neck cancer; BRT, before radiotherapy treatment; ART, after radiotherapy treatment.

4 EVALUATION OF SALIVARY INFLAMMATORY MARKERS LEVELS

Immunoassay based on Multi Analyte Profiling technology (Luminex xMAP) for protein analysis and biomarker screening was used to quantify the salivary concentration of IL-4, IL-6, IL-8, IL-10, MCP-1, TNF-α, VEGF, and EGF. The levels of fluorescence in each standard, quality control and sample were detected with the Luminex 200™ (Luminex Corporation, Austin, TX)(273). Data were subsequently analysed using the Bio-plex manager software (Bio-Rad Laboratories, Inc. Hercules, CA).

Luminex® xMAP® is a technology that uses proprietary techniques to internally colour-code microspheres with two fluorescent dyes (***Figure 13***)(284). Through precise concentrations of these dyes, distinctly coloured bead sets of 500 5.6 µm polystyrene microspheres or 80 6.45 µm magnetic microspheres can be created and each of them is coated with a specific capture antibody. Then, an analyte from a test sample is captured by the bead and a biotinylated detection antibody is introduced. The reaction mixture is then incubated with Streptavidin-PE conjugate, the reporter molecule, to complete the reaction on the surface of each microsphere (284,304). Each microsphere is identified and the result of its bioassay is quantified based on fluorescent reporter signals. The capability of adding multiple conjugated beads to every sample results in the ability to obtain multiple results from each sample (268,305,306).

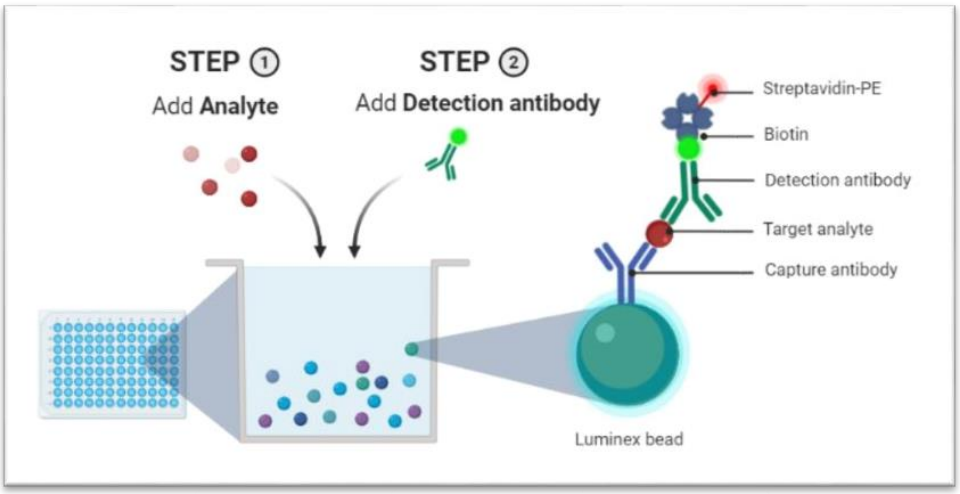

Figure 13: General overview of Luminex xMAP technology.

4.1 Sample preparation

Before performing the assay, saliva specimens were thawed and centrifuged at 1500 rpm for 15min at 4 °C to obtain a clear supernatant, devoid of any particles and debris. Supernatants were collected and aliquoted, the pellet was discarded. Generally, samples were freeze-thawed twice before the analysis.

4.2 Luminex Bead-based Multiplex Assay

The Human Cytokine/Chemokine Magnetic Bead Panel (Cat.# HCYTOMAG-60K) was performed according to the manufacturer's protocol (EMD Millipore Corporation, Billerica, MA, USA). The clear supernatant obtained after the second centrifugation was the salivary component applied for the analysis. A two-fold dilution was made per each sample, using as a diluent the assay buffer included in the kit. All reagents were warmed at room temperature (rt) before starting the experiment. Human cytokine standards were prepared according to assay protocol. In brief, the Human cytokine standard was reconstituted with 250 µL deionized water to give a 10,000 pg/mL concentration of standard for all analytes. The vial was inverted several times, vortexed for 10 sec and allowed to settle for 5-10 min. The reconstituted mixture was used as the maximum/top standard for serial dilutions (***Figure 14***). Meanwhile, individual bead vials were sonicated for 30 sec and vortexed for 1 min. 60 µL from each antibody bead vial were added in a mixing bottle, followed by the addition of a bead diluent, necessary to bring the final volume to 3 mL. Prior to use, the 96-well plate was washed with 200 µL of 1X wash buffer, sealed and mixed on a plate shaker for 10 min at rt. When the wash buffer was discarded, 25 µL of each standard, quality control and background solution were added to correspondingly wells, followed by 25 µL of assay buffer placed in all wells. Later on, 25µL of each diluted sample were added into the appropriate wells and 25 µL of mixed magnetic beads were set into the whole plate, that was finally wrapped with aluminium foil and incubated overnight at 4°C on a plate shaker with agitation. The next day, after the washing process (200 µL per well of 1X wash buffer, repeated twice) 25 µL of

detection antibodies were added in all wells and the plate was incubated for 1 hour at rt on the shaker. Afterwards, 25 µL of streptavidin-phycoerythrin (PE) were added, without aspirating the detection antibodies, and the plate was incubated on a plate shaker for 30 min at rt. The well content was gently removed and the washing process was repeated twice. The final step was the addition of 150 µL of sheath fluid to the whole plate, shaken for 5 min and subsequently run on Luminex® 200™ (Luminex Corporation, Austin, TX) with xPONENT® software. Following the manufacturer's instructions, samples were run in duplicate. The obtained results were expressed as the Median Fluorescent Intensity (MFI). Data were analyzed using a 5-parameter logistic (5-PL) method for calculating cytokine concentrations in all specimens (268). The assay sensitivity expressed as minimum detectable concentrations ([MinDC], pg/mL), ranged from 0.4 pg/ml (IL-8 MinDC) to 26.3 pg/ml (VEGF MinDC) for our panel of inflammatory markers.

Standard Concentration (pg/mL)	Volume of Deionized Water to Add	Volume of Standard to Add
10,000	250 µL	0

Standard Concentration (pg/mL)	Volume of Assay Buffer to Add	Volume of Standard to Add
2,000	200 µL	50 µL of 10,000 pg/mL
400	200 µL	50 µL of 2000 pg/mL
80	200 µL	50 µL of 400 pg/mL
16	200 µL	50 µL of 80 pg/mL
3.2	200 µL	50 µL of 16 pg/mL

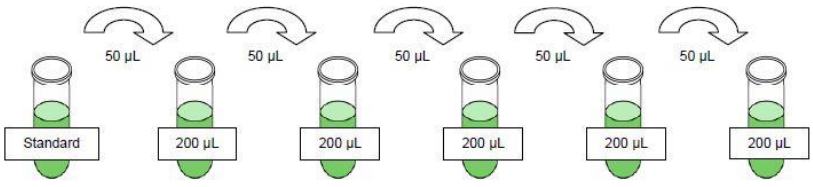

Figure 14: Preparation of Human Cytokine Standard. The 0 pg/mL standard (Background) was Assay Buffer.

5 EVALUATION OF SALIVARY PROTEOME

The proteomic study was carried out using the liquid chromatography and tandem mass spectrometry technique (LC-MS/MS) (185,249,307). Preliminary LC-MS/MS assays were performed to identify (among whole saliva, supernatant and pellet) the best salivary component for detecting and describing proteins as part of the salivary proteome. The process consisted of two phases: I) generation of a peptide spectral library from 10 Head and Neck squamous cell carcinoma (HNSCC) patients using a data dependent acquisition (DDA) approach also called shotgun proteomics and II) quantification of 30 individual salivary proteome profiles applying SWATH, a data independent analysis (DIA) procedure. Once accomplished the construction of the "HNSCC spectral library" using the whole saliva, the investigation of the proteome before and after the irradiation treatment was achieved along with the comparison between patients and control proteome profiles.

A spectral library is a database which contains mass spectrometric and chromatographic parameters such as precursor and fragment m/z value, fragment type, charge and elution time for each individual peptide in the analysed sample. Usually, these specific spectral libraries are generated by extensive DDA-based proteomic characterization of the same samples prior to analysis by DIA-MS. The library will contain information of all the proteins that will be quantitated in the second phase of the investigation. Thus, it is important to include as many proteins as possible representing all the sample groups to be analysed. Subsequently, to quantify the protein abundance of the samples, the SWATH analysis has to be performed (***Figure 15***).

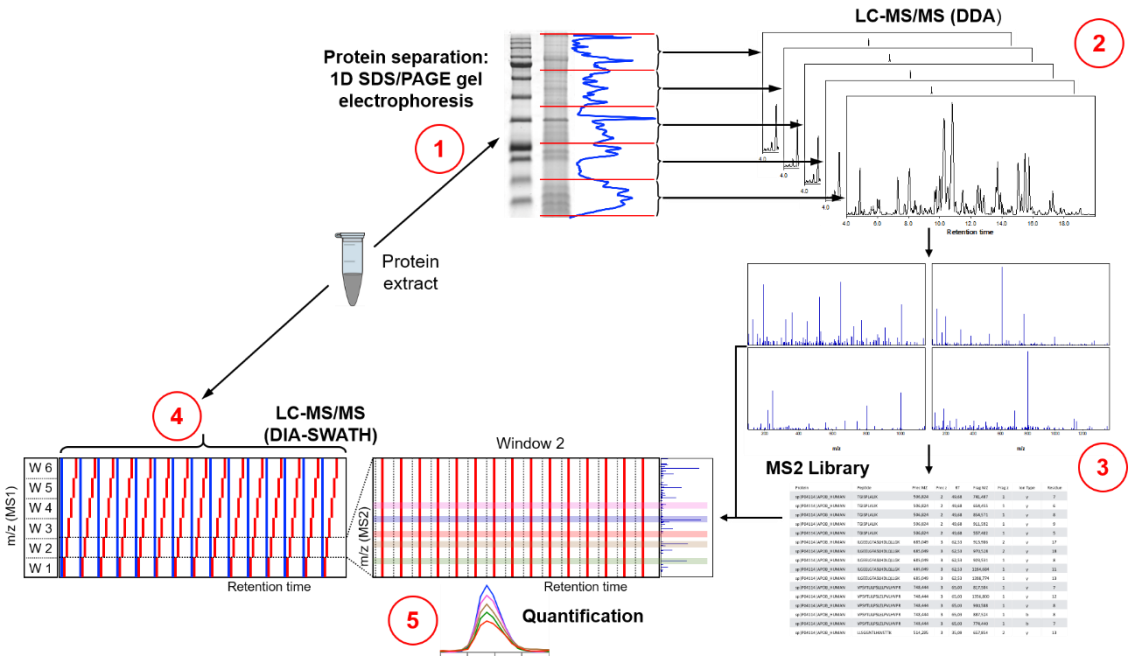

Figure 15: Schematic workflow of the LC-MS/MS SWATH quantification process. 1) Proteins are extracted and fractionated; 2) Generation of peptides and LC-MS / MS analysis by DDA acquisition; 3) Protein identification and generation of the MS2 spectral library, only the best spectra used for the identification of each protein will be selected; 4) Protein extraction (without fractionation), digestion and LC-MS / MS analysis by DIA-SWATH acquisition; 5) Generation of chromatographic profiles from the MS2 fragments of the spectral library and quantification.

5.1 Sample preparation

Before performing the assay, the whole saliva specimens were thawed and centrifuged at 1500 rpm for 15min at 4 ˚C. Afterwards, each sample was mixed and vortexed to mechanically destroy the mucins components and reduce the viscosity. The resultant heterogeneous combination of serous and mucinous secretions was aliquoted and used for the following analysis: determination of protein concentration with Bradford Assay and proteins separation by one-dimensional SDS-Polyacrylamide Gel Electrophoresis (1D SDS-PAGE). Overall, the samples were freeze-thawed twice before the analysis.

5.1.1 Bradford assay

The Bradford protein assay is a simple procedure to determine total protein concentrations in solutions that depend on the change in absorbance based on the proportional binding of the dye Coomassie Blue G250 to proteins. The assay is based on the observation that the absorbance maximum for an acidic solution of Coomassie Brilliant Blue G-250 shifts from 465 nm to 595 nm when binding to protein occurs. Both hydrophobic and ionic interactions stabilize the anionic form of the dye, causing a visible colour change. The intensity of the blue complex is proportional to the protein abundance in the sample and can be easily measured by spectrophotometer or plate reader at 595 nm. Briefly, a 20-fold dilution was made per each sample analyzed, MilliQ water (MQH_20) was used as a diluent and subsequently as a "blank". Immunoglobulin G (IgG - gamma globulin) 2 mg/ml was the protein standard used for building the curve. In a 96-well plate, 50 µL of each standard or unknown samples were combined with 250 µL of Coomassie Reagent and mixed. The absorbance was detected at 450 nm and 595 nm without any prior incubation (308), using a Perkin Elmer VICTOR X3 MultiLabel plate reader. The ratios of the two measurements were used to calculate the final protein concentrations.

5.1.2 1D SDS-PAGE Gel Electrophoresis

One-dimensional sodium dodecyl sulfate-polyacrylamide gel electrophoresis (1D SDS-PAGE) was used to separate the proteins according to their molecular weight. Before sample loading, proteins were denatured with 5X Laemmli buffer containing β-mercaptoethanol (1:1) for 5 min at 95 °C. Afterwards, 20 µg of denatured protein samples along with a molecular weight protein marker (Pink Prestained Protein Marker, NIPPON Genetics Europe) were loaded onto a 4% stacking gel - 12% acrylamide resolving gel and run through it by application of 20 mA for 1 h. After the electrophoresis process, the gel was stained with Coomassie solution for 20 min and then washed several times with distilled water (dH_20) to remove stain excess. Finally,

proteins were fixed by incubation of the gel in a de-stain solution for approximately 2 h.

5.1.3 Quality control of saliva samples by LC-MS/MS analysis

A preliminary LC-MS/MS assay was performed with the specimens to be used for the final protein relative quantitation. A pool was done per each group of samples (BRT, ART, CTRL) and analysed. The wiff files gained from the quality control assay were then combined with those resulting from the LC-MS/MS analysis performed to build the "HNSCC spectral library" (Section 5.2.1), once updated, the library was subsequently applied for the SWATH analysis.

5.2 Spectral library construction

A pool of 10 whole saliva samples, obtained from 10 HNSCC patients (7 at advanced stage and 3 at early stage of cancer, before any kind of treatment or surgical intervention) was quantified, loaded onto a 4% stacking gel - 12% acrylamide resolving gel and run as mentioned-above. Following the staining and de-staining process, the electrophoretic lane was sliced in 5 pieces containing approximately the same amount of protein (***Figure 16***).

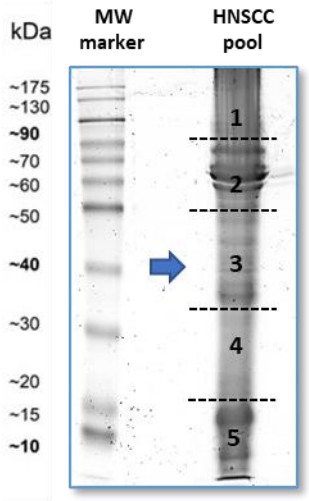

Figure 16: The pool of HNSCC samples (selected between early and late stages) quantified and separated by 1D SDS/PAGE gel electrophoresis. Proteins were loaded in triplicates and the best run was selected to be processed to build the HNSCC Spectral Library.

Each gel piece was processed individually according to the procedure described by *Shevchenko A et al* (309), proteins were digested with sequencing grade trypsin (Promega). The digestion mixture was dried in a vacuum centrifuge and re-suspended in 20 µL of 2% acetonitrile (ACN), 0.1% TFA. Peptides were then analysed by LC-MS/MS using a data dependent acquisition (DDA) or shotgun approach performed in a TripleTOF 5600 (SCIEX) mass spectrometer. Proteins were identified using Protein Pilot (SCIEX) search engine.

5.2.1 LC-MS/MS ANALYSIS

5 µL of the re-suspended digestion mixture above-mentioned were loaded onto a trap column (NanoLC Column, 3µ C18-CL, 350 µm x 0.5 mm; Eksigen) and de-salted with 0.1 % TFA at 3 µL/min for 5 min. The peptides were then charged onto an analytical column (LC Column, 3 µ C18-CL, 75 µm x 12 cm, Nikkyo) equilibrated in 5 % ACN 0.1 % FA (formic acid). Elution was carried out with a linear gradient of 5 to 40 % B in A for 120 min (A: 0.1 % FA; B: ACN, 0.1 % FA) at a flow rate of 300 nl/min.

Peptides were analysed in a mass spectrometer nanoESI qQTOF (5600 TripleTOF, SCIEX). The pooled sample was ionized applying 2.8 kV to the spray emitter. The analysis was carried out in a data-dependent mode. Survey MS1 scans were acquired from 350–1250 m/z for 250 ms. The quadrupole resolution was set to 'UNIT' for MS2 experiments, which were acquired 100–1500 m/z for 50 ms in 'high sensitivity' mode. The switch criteria set up were: charge 2+ to 5+; minimum intensity; 70 counts per second (cps). Up to 50 ions were selected for fragmentation after each survey scan. Dynamic exclusion was set to 15 s. The system sensitivity was controlled by injecting 2 fmol of a commercial protein-mix (LC Packings). ProteinPilot default parameters were used to generate peak list directly from 5600 TripleTof wiff files. The Paragon algorithm (310) of ProteinPilot v 5.0 search engine (SCIEX) was applied to search against the Swissprot database (version 03-2018) with the following parameters: trypsin specificity, cys-alkylation, taxonomy restricted to human (40632 proteins searched). The protein grouping was made by Pro group algorithm: a protein group in a Pro Group Report is a set of proteins that share some physical evidence. In contrast to the sequence alignment analyses in which full-length theoretical sequences are compared, the formation of protein groups in Pro Group is guided entirely by the observed peptides. Since the observed peptides are determined from experimentally acquired spectra, the grouping process can be considered to proceed from the spectra usage. Percent confidence, expressed in ProtScore units, is reported in **Table 4**. Proteins showing unused score > 1.3 were identified with a confidence ≥ 95% according to the following equation:

$$\text{ProtScore}=-\log(1-(\text{percent confidence}/100))$$

Table 4: Percent confidence, expressed in ProtScore units.

Percent confidence	ProtScore
99%	2.0
95%	1.3
90%	1.0
66%	0.47

Finally, applying the false discovery rate (FDR), the metric for global confidence assessment of a large-scale proteomics dataset, the human salivary proteins identified to build the HNSCC spectral library were 1053.

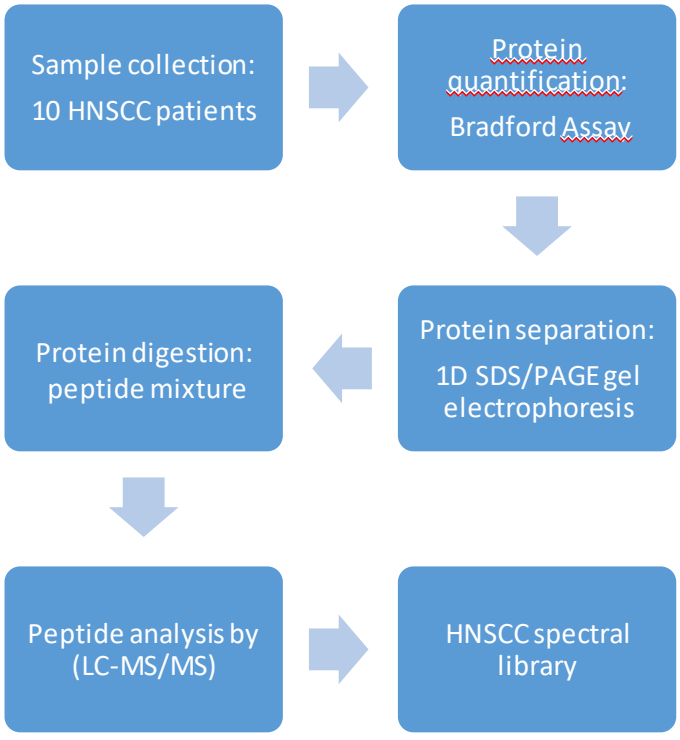

Figure 17: Workflow of the construction of the HNSCC Spectral Library. A pool of 10 specimens (selected between early and advanced stages) was used to create the HNSCC Spectral Library. Samples were processed as described in the text.

5.3 Salivary expression of individual proteome profiles

A total of 30 samples were applied to accomplish the second part of the proteomic analysis. Based on specific criteria (gender, age, clinical parameters) a selection was made between the two cohorts of the study to identify the best candidates for the investigation of salivary proteome profiles. The included subjects were divided as follows:

- GROUP 1 composed by 10 HNC patients recruited before radiotherapy (BRT)
- GROUP 2 composed by 10 HNC patients recruited after radiotherapy (ART)
- GROUP 3 consisted of 10 healthy volunteers enrolled as controls (CTRL)

Samples belonging to Group 2 were obtained from the same patients of Group 1, evaluated pre- and post-treatment, both groups were included in Cohort 1 of the study. Control subjects recruited in Group 3 were selected from Cohort 2. Saliva specimens were processed as cited previously (Section 5.1). Firstly, they were quantified by Bradford assay, subsequently, 20 µg of proteins from each sample were loaded onto a 4 – 15% acrylamide resolving gel and run through it by application of 20 mA for 20 min. To avoid the fractionation step by gel electrophoresis, gel running was stopped as soon as the proteins migrated to the resolving gel (***Figure 18***). Following the staining and de-staining process, the expressed protein bands (representing each sample loaded) were cut, processed as before. The peptides generated were analysed by LC-MS/MS using a TripleTOF 6600 (SCIEX) mass spectrometer operated in SWATH mode. SWATH-MS is a mass spectrometric technique that combines the advantages of shotgun proteomics (high throughput) with those of targeted proteomics (high specificity and quantitative accuracy). In order to accomplish the salivary proteome profiles analysis, the wiff files obtained from SWATH experiment were analysed by Peak View 2.1, using the HNSCC spectral library.

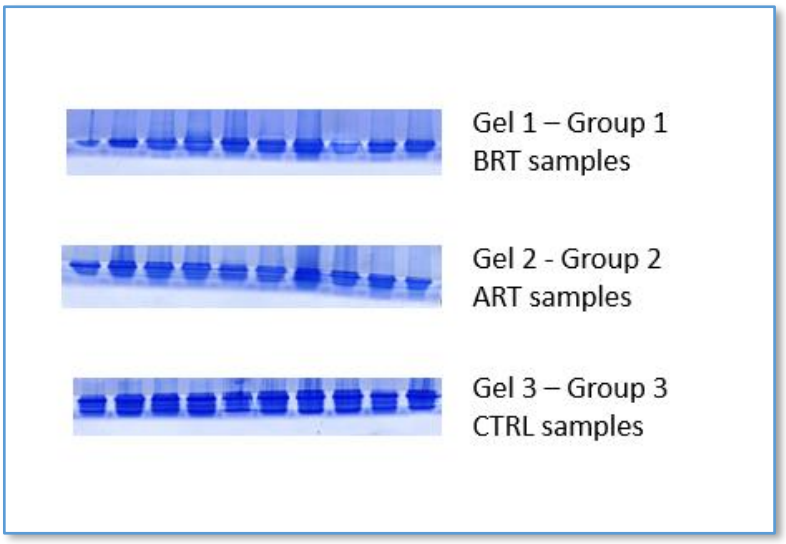

Figure 18: 1D SDS-PAGE gel running. Gels were charged with 10 stimulated saliva samples, corresponding to the different groups of the study. Protein amount loaded per each specimen: 20 µg/µL. Group1-BRT, before radiotherapy treatment; Group 2-ART, after radiotherapy treatment; Group3-CTRL, controls.

5.3.1 Protein Identification - LC-MS/MS & SWATH ANALYSIS

For the LC-MS/MS assay, 5 µL per each of the 30 samples (BRT, ART, CTRL) were loaded onto a trap column (LC Column, 12 nm, 3 µm Triart-C18, 0.5 x5.0 mm; YMC) and desalted with 0.1 % TFA at 10 µL/min during 5 min. The peptides were then loaded onto an analytical column (LC Column, Luna Omega 3 µm Polar C18, 150 x 0.3 mm, Capillary Phenomenex) equilibrated in 3 % ACN 0.1 % FA. Elution was carried out with a linear gradient of 3 to 35% B in A for 45 min (60 min in total) (A: 0.1% FA; B: ACN, 0.1% FA) at a flow rate of 300 nl/min. Peptides were analysed in a mass spectrometer qQTOF (6600plus TripleTOF, SCIEX). Samples were ionized in a Source Type: Optiflow 1-50 µL Micro applying 4.5 kV to the spray emitter. The analysis was carried out in a data-independent mode. Survey MS1 scans were acquired from 400–1250 m/z for 250 ms. A quantity of 100 variable windows from 400 to 1250 m/z were obtained throughout the experiment. The total cycle time was 2.79 sec. The quadrupole resolution was set to 'UNIT' for MS2 experiments, which were gathered 100–1500 m/z for 25 ms in 'high sensitivity' mode. Samples were introduced in a random order to avoid bias in the analysis.

5.3.2 Protein Quantitation - DATA ANALYSIS

The wiff files obtained from the SWHAT experiment were analysed by Peak View 2.1, counting the HNSCC spectral library as a reference and according to the following scheme:

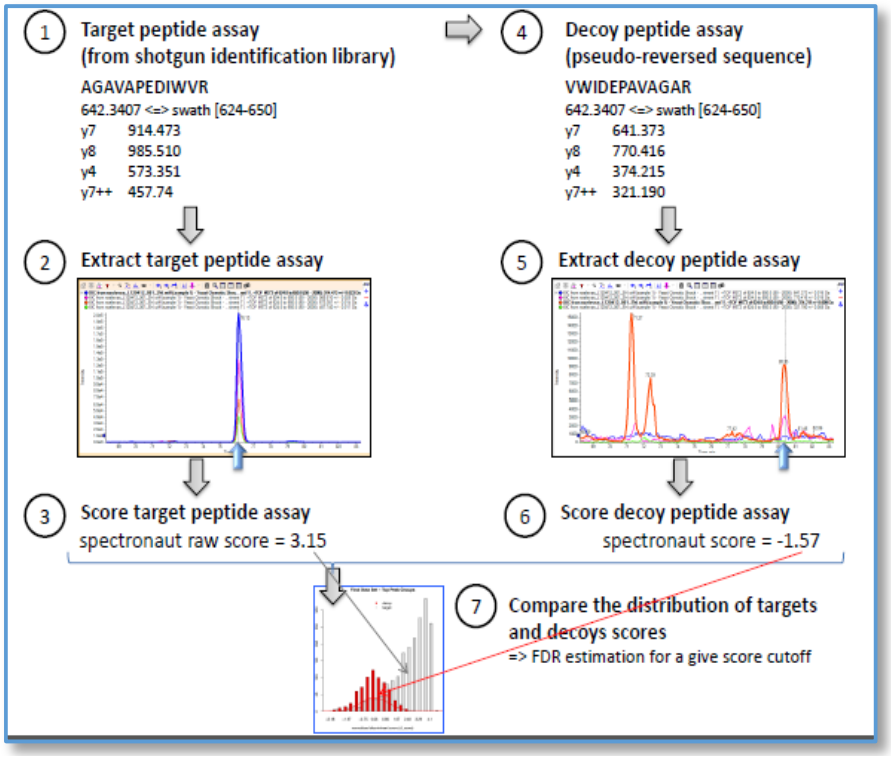

Once calibrated the retention time, the processing settings to use for peptides selection were established. The cycle time used in the tandem MS (MS/MS) acquisition allowed the quantification of each peptide area with more than 7 points. The data obtained with Peak View were analysed by Marker View (SCIEX). According to the extraction parameters used for calculating the areas, **695** proteins (FDR <1%) were quantified in 30 samples.

6 STATISTICAL ANALYSIS

Concerning the evaluation of the salivary inflammatory markers, firstly a descriptive statistical study was performed per each analyte and each group investigated. To investigate the causes of variability among the groups (CTRL, BRT, ART), principal component analysis (PCA) was performed. The R programming language, executed with STATools provided by GPRO suite, was used for both purposes.

To achieve Objective 1, the examination of salivary EGF, IL-10, IL-4, IL-6, IL-8, MCP-1, TNF-α and VEGF levels in HNC patients pre and post–RT treatment, the Wilcoxon matched-pairs test was performed.

To reach Objective 2, the analysis of salivary inflammatory markers in control subjects and HNC patients evaluated before and after the irradiation treatment, a non-parametric Mann-Whitney U test was used.

To determine how the different salivary proteins were related to the HNC cases and also to the healthy controls, a correlation analysis was carried out. To reach this purpose a Pearson's pairwise correlation test was applied, using the R programming language and the caleb function (core.test).

To accomplish Objective 3, firstly an indexation of the data regarding the significant analytes and their clinical metadata was carried out using the Bayesian network probabilistic model. Secondly, the inference of a conditional probabilistic distribution was studied among each cytokine and the treatment response, depending on the LOD (limit of detection) or LOQ (limit of quantification) values and the probabilities of the different clinical observation. The Bayesian network was constructed using directed acyclic graphing (DAG) and conditional probability methodology, to build the DAG the *bnlearn* R package and the *hill-climbing* model were used.

Finally, to achieve Objective 4 and determine if there is a salivary protein that may be considered as a predictive biological marker of the response to the treatment, the nonparametric Mann-Whitney U test was applied to plot responders versus non-

responders. Subsequently, the receiver operating characteristic (ROC) analysis was performed and the area under the curve (AUC) was measured.

The analysis of the data carried out by parametric or non-parametric analysis, as appropriate, was generated using GraphPad Prism v6.0 (GraphPad Software Inc.). Values of *p<0.05, **p<0.01 and ***p<0.001 were considered statistically significant.

Regarding the investigation of the salivary proteome, the use of penalized regression models such as Lasso or Elastic Net was preferred. To reach the first two objectives of the study, the identification of which proteins may differentiate the considered groups, cluster analysis and hierarchical classification was carried out, followed by the partial least squares-discriminant analysis (PLS-DA). Results are presented using the Heatmap graphical representation. The *glmnet* package in R was utilized to fit the regression models. Also, a different R package known as *mixOmics*, was applied for the PLS-DA classification (Partial Least Squares-Discriminant Analysis). All analyses were carried out on normalised and log2-transformed dataset values.

The classification of genes and proteins according to their roles in biological systems is also the basis for the analysis of relationships and interactions between them. Therefore, networks of the differentially expressed proteins were generated using STRING version 11.0, followed by functional enrichment analysis.

In conclusion, to accomplish the last aim of the proteomic investigation and to identify whether any of the above-mentioned differentially expressed salivary proteins may be considered as a putative biomarker of RT response, ROC analysis and AUC measurement were carried out.

IV. Results

1 EVALUATION OF SALIVARY INFLAMMATORY MARKERS LEVELS

Evaluation of salivary levels of pro-inflammatory (IL-6, IL-8, TNF-α) and anti-inflammatory cytokines (IL-4, IL-10), chemokines (MCP-1/CCL2) and growth factors (EGF, VEGF) was performed in HNC patients and age-matched controls using immunobased assay. Summary of all the subject enrolled in the study is shown in **Table 5**. Samples in which one or more proteins were below the lower limit of detection (LOD) were excluded from the statistical calculations (N=3), as well as, due to the impossibility to recover some clinicopathological characteristics, individuals with incomplete clinical data (N=12) were not considered for investigating the association of altered cytokine expression with patients' clinical variables. These reasons forced to reduce the number of subjects included in statistical analysis to 30, for the HNC patients belonging to Cohort 1, and 37 for the healthy volunteers belonging to Cohort 2.

Table 5: Resume of the subjects considered for the study. *Criteria for exclusion: not detected proteins values or incomplete clinicopathological data.

Cohort 1 _ HNC patients	N = 42	Cohort 2 _ Controls	N = 40
Excluded from statistical analysis *	**12**	Excluded from statistical analysis *	**3**
Included in statistical analysis	**30**	Included in statistical analysis	**37**

For the estimation of significant differences in the levels of the studied analytes, a non-parametric Wilcoxon signed-rank test was used to compare the HNC patients (Cohort 1) analysed before and after RT; whereas a nonparametric Mann-Whitney U test was applied to plot the cancer patients (Cohort 1) versus their healthy counterparts (Cohort 2), according to the specific objectives.

1.1 Patients characteristics

The most relevant demographic and clinicopathological characteristics of the two Groups recruited for this prospective observational study are shown in **Table 6**.

Table 6: Demographic and clinicopathological characteristics of the subjects included in the study. HNC, Head and Neck cancer; SCC, Squamous Cell Carcinoma; ACC, Adenoid Cystic carcinoma; NS, not specified; RT, Radiotherapy; CRT, Chemoradiation therapy; T=0 (RT ends); T=1 (three months after the RT).

Study population_Cohort 1		***N***		***%***
HNC patients		30		
Median age		60.5		
Gender				
Male		20		66.76
Female		10		33.33
Tumour sites				
Oral cavity		11		36.67
Pharynx		8		26.67
-Hypopharynx		(3)		
-Oropharynx		(5)		
-Nasopharynx		(0)		
Larynx		10		33.33
Salivary glands		1		3.33
Histology				
SCC		29		96.67
ACC		1		3.33
TNM classification				
T1		4		13.33
T2		8		26.67
T3		11		36.67
T4		7		23.33
Neck metastasis				
Yes		14		46.67
No		16		53.33
Treatment				
Surgery + RT		18		60.00
CRT therapy		10		33.33
RT alone		2		6.67
Development of mucositis				
Grade I		2		6.67
Grade II		12		40.00
Grade III		13		43.33
NS		3		10.00
Response to the treatment	**T=0**	**%**	**T=1**	**%**
Complete Response (CR)	29	96.67	24	80.00
Partial Response (PR)	1	3.33	1	3.33
No Response (NR)	-	-	5	16.67

Study population _ Cohort 2	*N*	*%*
Controls	37	
Median age	57	
Gender		
Male	19	51.35
Female	18	48.65

HNC patients (Cohort 1) median age was 60.5 years (SD=13.1), 66.76% were males and 33.33% were females. The tumour site with major incidence was the oral cavity (36.67%), followed by the larynx (33.33%). SCC histologic description was observed in 96.76% of the cases. Moreover, 60% of the patients were diagnosed at advanced stage of disease (T3-T4) and 46.67% presented neck metastasis as well. The majority of the HNC population received postoperative adjuvant RT (60%). Development of oral mucositis was observed in 90% of the cases. Treatment response recorded at T=0 (RT ends) showed a CR in 96.67% of the patients, albeit a slight decrease was observed at T=1 (three months after the therapy) where the percentage of CR reported was 80.0%. Control subjects (Cohort 2) included 19 healthy males (51.35%) and 18 healthy females (48.65%) with a median age of 57 years (SD=10.4).

1.2 Descriptive Statistics - Univariate analysis

A descriptive statistical study was performed per each analyte (IL-6, IL-8, TNF-α, IL-4, IL-10, MCP-1, EGF, VEGF) and each group investigated, including: mean, median, minimum and maximum values, first and third quartiles, variance and standard deviation (SD), coefficient of variation (CV). Complete data are presented in Supplemental Table 1 (Chapter VIII Appendix, SUPPLEMENTAL TABLES). The R programming language, executed with STATools provided by GPRO suite, was used for this purpose.

Starting from this moment, Cohort 1 will be differentiated into two subgroups: HNC patients evaluated before (BRT Group) and after radiotherapy (ART Group),

while the abbreviation CTRL will be always used to refer to Cohort 2 (Control subjects).

Focusing, in particular, on the coefficient of variation and considering its value (when <1 it describes low variability between the data, when >1 it reveals high variability), the eight salivary proteins analysed showed a wide variation among them and also within the groups (**Table 7**). Hence, the significant dispersion observed between samples and analytes indicated that data were heterogeneous.

Table 7: Coefficients of variation (CV) expressed per each protein analysed in each group of the study. CV <1 defines a low variability between the data, CV >1 reveals a high variability. CTRL, controls; BRT, before radiotherapy treatment; ART, after radiotherapy treatment.

Coefficient of variation (CV)	CTRL	BRT	ART
EGF	0,6025	0,8093	0,6734
IL-10	1,6565	0,3092	1,7190
IL-4	2,8538	0,9157	0,8864
IL-6	1,0837	2,0267	3,1811
IL-8	0,6986	1,1051	0,8504
MCP-1	1,5003	1,3010	0,7865
TNF-α	0,8723	1,8614	2,3958
VEGF	0,6739	0,7471	0,6538

Considering the mean concentration of pro-inflammatory (IL-6, IL-8, TNF-α) and anti-inflammatory cytokines (IL-4, IL-10), chemokines (MCP-1/CCL2) and growth factors (EGF, VEGF) in saliva samples of HNC patients, BRT and ART groups, and in control subjects as well, an increasing trend was observed (**Table 8**); firstly, to correlate with the cancer presence (BRT group) and, secondly, to link with the irradiation process (ART group). However, this tendency was not confirmed for EGF and VEGF salivary levels. These proteins showed an increment in presence of tumour (BRT group) but exhibited a decreasing pattern at the end of the irradiation treatment (ART group).

Table 8: Salivary levels of EGF, IL-10, IL-4, IL-6, IL-8, MCP-1, TNF-α and VEGF expressed as mean values and detected in control subjects (N=37) and HNC patients BRT and ART (N=30). CTRL, controls; BRT, before radiotherapy treatment; ART, after radiotherapy treatment

[Salivary mean]	CTRL	BRT	ART
EGF	1176,00	1273,80	931,50
IL-10	27,97	41,16	77,65
IL-4	41,03	51,11	47,00
IL-6	9,01	113,50	175,43
IL-8	861,60	1632,48	3076,00
MCP-1	1279,70	1118,20	3187,00
TNF-α	13,30	27,58	50,94
VEGF	421,55	519,68	471,51

1.3 Principal component analysis

In order to investigate the causes of variability among the groups (CTRL, BRT, ART), principal component analysis (PCA) was performed. The R programming language, executed with STATools provided by GPRO suite, was used for this purpose. Generally, the aim of this analysis is to graphically display the relative positions of data points in fewer dimensions while retaining as much information as possible and explore relationships between dependent variables. It allows us to summarize and to visualize the information in a data set containing individuals/observations described by multiple inter-correlated quantitative variables. Each variable could be considered as a different dimension.

PCA results showed that the variability observed between samples and groups was mainly determined by the different nature of each group (PC1 component) which

represents 33% of it, in contrast with the intra-specific variability of each individual (PC2 component) represented by 19.7% (***Figure 19***). The increment of variability was especially noticed among the three cohorts, being the CTRL group the most homogeneous and the ART the most heterogeneous. This indicates that the cancer group presents a clear dispersion with respect to normal patterns, considering both conditions (BRT and ART). Besides, within the salivary protein concentrations, a big dispersion was observed among treated HNC patients (ART group), to probably link with the irradiation process. Some outliers were recognized, two samples per each group (CTRL14 and CTRL36, BRT14 and BRT27, ART15 and ART12); although, to maintain the variability as a factor to be considered for the whole analysis they were not excluded.

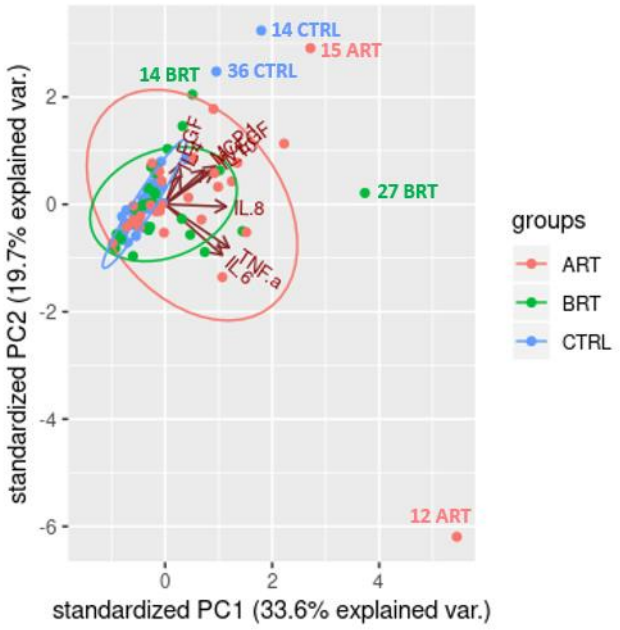

Figure 19: Principal component analysis (PCA). PC1 component is determined by the different nature of the groups (CTRL, BRT, ART), PC2 is referring to the intra-specific variability of each individual belonging to the groups. CTRL, controls; BRT, before radiotherapy treatment; ART, after radiotherapy treatment

1.4 Heatmap representation and cluster analysis

The objective of this analysis was the identification of which salivary proteins may differentiate the groups considered for the study (CTRL, BRT, ART). Results are presented using the heatmap graphical representation. Heatmaps are an efficient method of visualizing complex data sets organized as matrices. In a biological context, a typical matrix is created by arranging the results in a way that each column contains the data from a single sample and each row corresponds to a single feature (e.g., a spectrum, peptide or protein, as in this case). Proteins were represented ordered according to the result of the hierarchical classification. In particular, columns were clustered using the complete linkage method with Euclidean distance measure (311). GPRO STATools was employed, colour mapping (red, white and blue) was defined by the quartile values (0.3, 0.6 and 0.9) of the proteins analysed.

Based on cluster analysis, the level of proteins can discriminate the CTRL group from the HNC patients, BRT and ART. Salivary IL-6, IL-10, TNF-α and IL-4 showed a lower expression profile in contrast with the other proteins (VEGF, EGF, IL-8, MCP-1) characterized by higher expression profile. In general, some variability was observed within the groups (CTRL, BRT, ART) but a clear difference was noticed across the control subjects and the HNC patient profiles, referring to both conditions (pre- and post-RT). This contrast is especially evident for IL-6, IL-10 and TNF-α in case of lower concentration profiles and it is noticed for IL-8 and MCP-1 among the higher expression profiles.

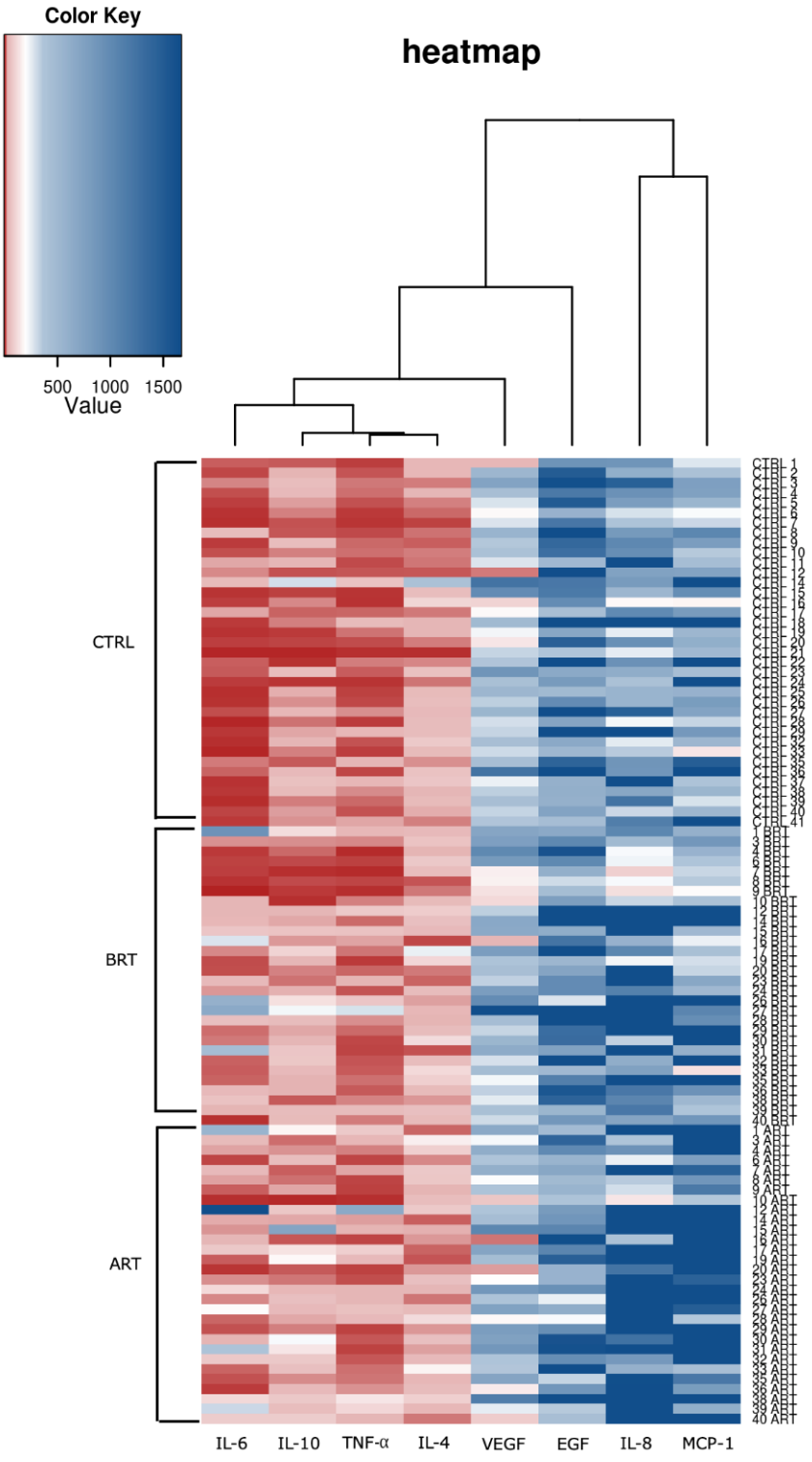

Figure 20: Heatmap representation of the salivary proteins (EGF, IL-10, IL-4, IL-6, IL-8, MCP-1, TNF-α and VEGF) and their relation with the groups of the study (CTRL, BRT, ART) according to cluster analysis. Columns correspond to each protein analysed, rows represent each sample quantified. Colour mapping is explained by the colour key on top of the graph.

1.5 Analysis of salivary inflammatory markers in HNC patient evaluated pre- and post–RT treatment (BRT vs ART)

Concerning the examination of salivary EGF, IL-10, IL-4, IL-6, IL-8, MCP-1, TNF-α and VEGF levels in HNC patients, pre and post–RT treatment, statistical analysis was performed using the Wilcoxon matched-pairs test. Typically, this nonparametric test is used to compare two paired groups, being in this case BRT and ART.

It is known from the literature that ionizing radiation increases the expression of a number of cytokines involved in inflammation and wound healing and our results seem to confirm this trend (***Figure 21***). Analysed data revealed that IL-8 and MCP-1 concentration significatively increased in saliva of HNC patients after RT, showing a *p-value* ≤ 0,001 and ≤ 0,0001, respectively. However, no notable changes were observed in the expression levels of IL-10, IL-4, IL-6, TNF-α and VEGF. Finally, an interesting decrease in EGF levels was detected, albeit without achieving statistical significance (***Figure 21***).

a)

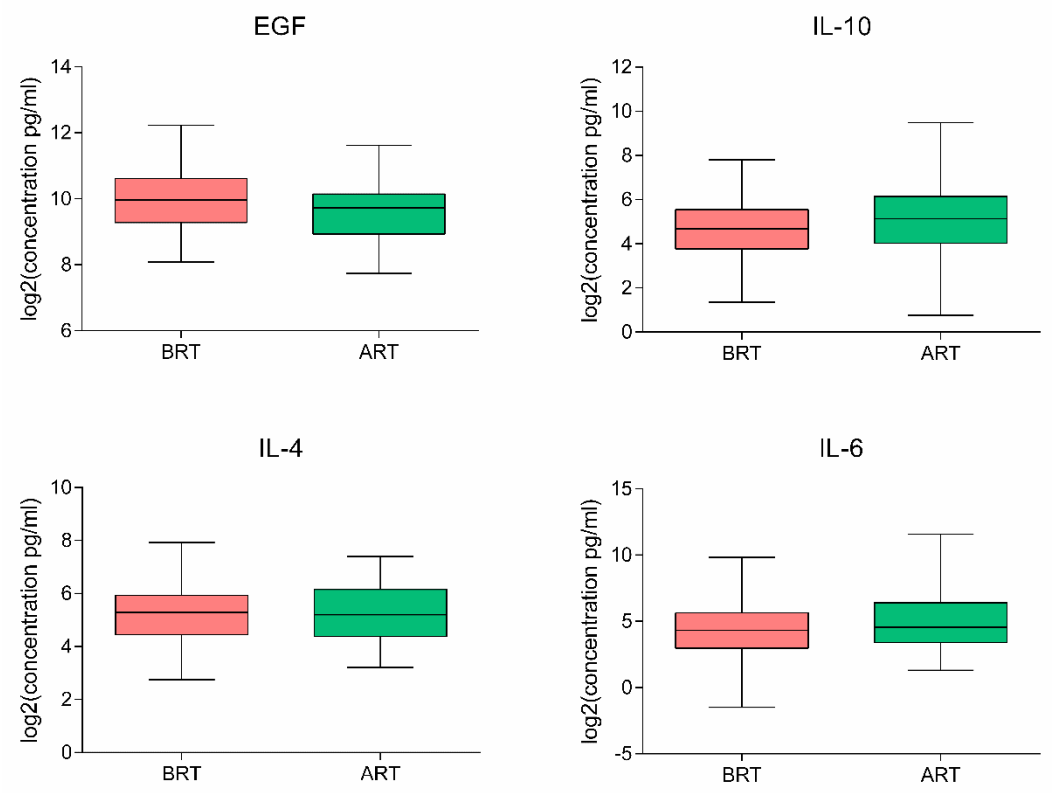

b)

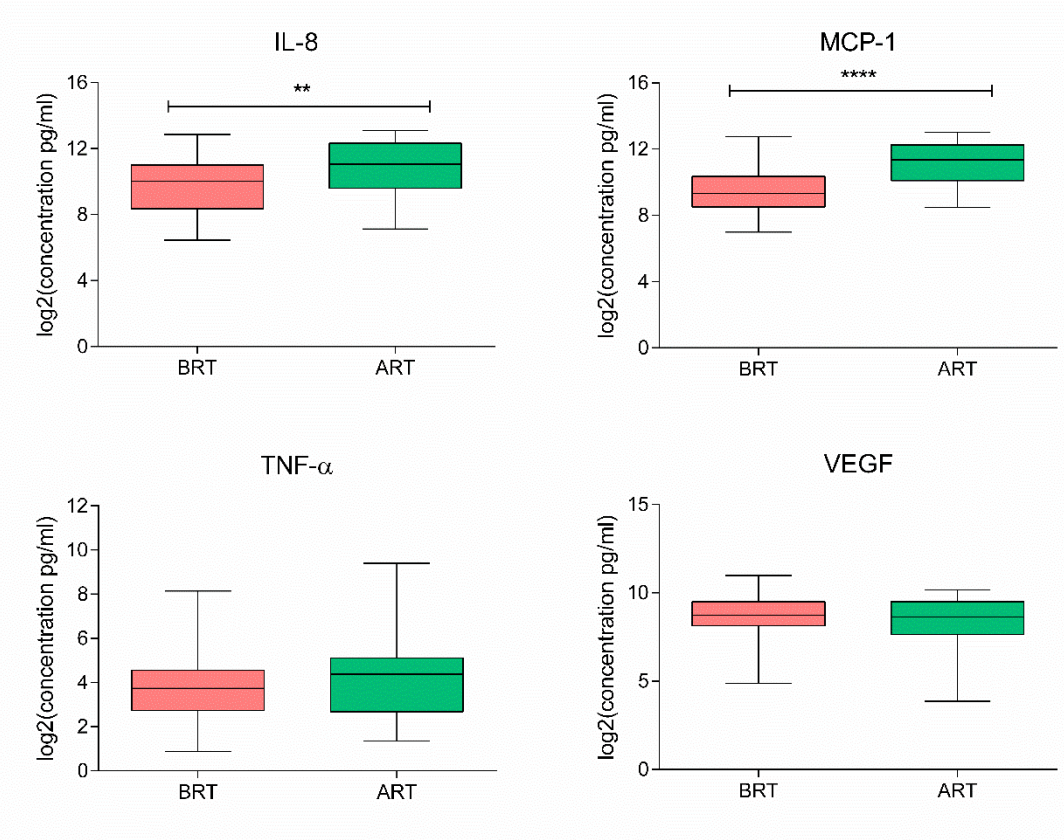

Figure 21 a) and b): Salivary levels of EGF, IL-10, IL-4, IL-6, IL-8, MCP-1, TNF-α and VEGF detected in HNC patients BRT and ART (N=30). Data are expressed as log2(mean signal ratios). Statistical analysis was performed using Wilcoxon signed-rank non-parametric test, ****p ≤ 0.0001; **p ≤ 0.01. HNC, Head and neck cancer; BRT, before radiotherapy treatment; ART, after radiotherapy treatment.

1.5.1 Analysis of salivary inflammatory markers in HNC patients pre- and post–RT treatment considering the variable "tumour site", head and neck area vs oral cavity

Before starting with the analysis, it was necessary to divide the HNC patients in two clusters, based on the site where the tumour growth. Cancers of larynx, pharynx and salivary glands were included in the head and neck district (N=19), whereas cancer of the tongue, lips, floor of the mouth, hard or soft palate, gingiva and buccal mucosa were grouped in the oral cavity region (N=11). Thus, the HNC patients were analysed to compare the levels of salivary proteins before and after the irradiation process according to the new clusters, applying the non-parametric Wilcoxon signed-rank test.

Results concerning the tumours gathered in the head and neck area, revealed that salivary levels of IL-8 and MCP-1 were differentially expressed from pre- to post-treatment, as observed in the previous analysis but with less significance, *p-value* ≤ 0.05 and ≤ 0.01, respectively (***Figure 22***).

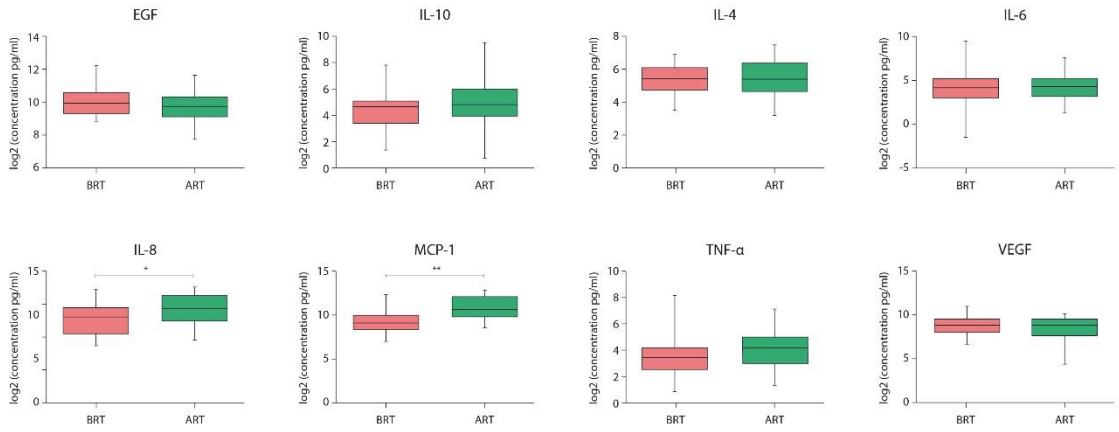

Figure 22: Salivary levels of EGF, IL-10, IL-4, IL-6, IL-8, MCP-1, TNF-α and VEGF detected in cancer patients of the head and neck area region (N=19) evaluated BRT and ART. Data are expressed as log2(mean signal ratios). Statistical analysis was performed using Wilcoxon signed-rank non-parametric test, **p ≤ 0.01; *p ≤ 0.05.

Regarding the analysis focused on the tumours of the oral cavity, it was observed that only MCP-1 levels were statistically significant in the post-treatment condition, with a *p-value* ≤ 0.01 (***Figure 23***).

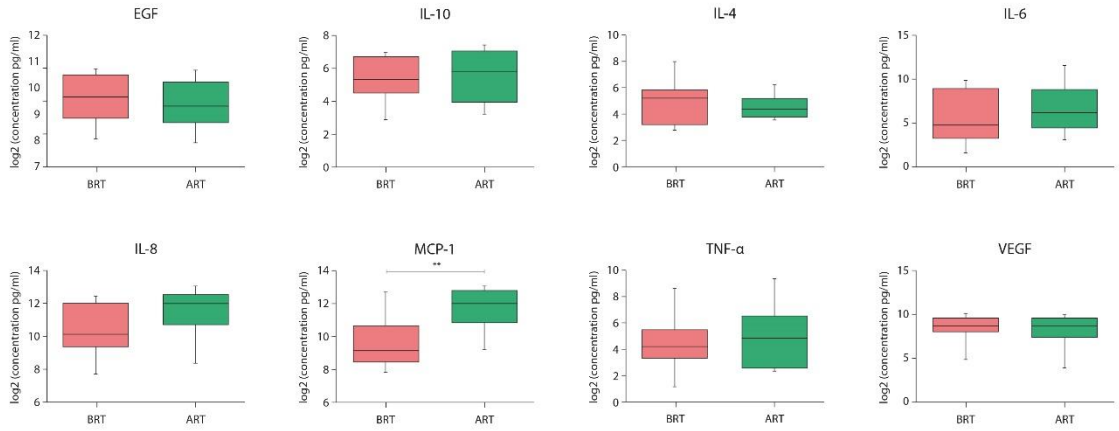

Figure 23: Salivary levels (pg/ml) of EGF, IL-10, IL-4, IL-6, IL-8, MCP-1, TNF-α and VEGF detected in patients with cancer of the oral cavity evaluated BRT and ART (N=11). Data are expressed as log2(mean signal ratios). Statistical analysis was performed using Wilcoxon signed-rank non-parametric test, **p ≤ 0.01.

1.6 Analysis of salivary inflammatory markers between HNC patient and healthy controls

Salivary levels of pro-inflammatory (IL-6, IL-8, TNF-α) and anti-inflammatory cytokines (IL-4, IL-10), chemokines (MCP-1/CCL2) and growth factors (EGF, VEGF) were firstly analysed in control subjects and HNC patients evaluated before the treatment (BRT group) and, secondly, the CTRL group was plotted against the HNC samples collected after the irradiation process (ART group). Since the two comparisons had to be made between independent groups, a non-parametric Mann-Whitney U test was used.

Results showed that various inflammatory markers increased in saliva of tumour patients (***Figure 24***). A trend towards an increment in salivary IL-10, IL-4, IL-8, MCP-1, TNF-α and VEGF levels was observed, associated to cancer disease. However, significance was confirmed only for protein concentration of IL-6, presenting a *p-value* ≤ 0,0001. Concerning the EGF levels, results showed no changes among HNC patients evaluated before RT and their healthy counterparts (CTRL group).

a)

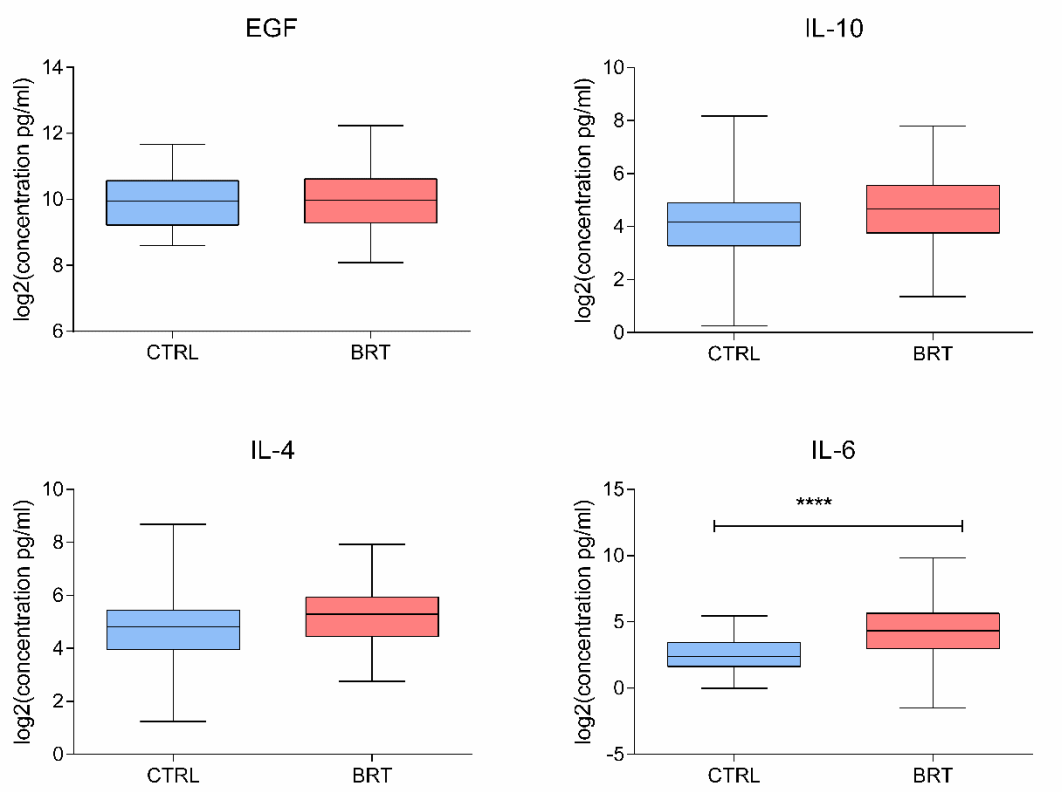

b)

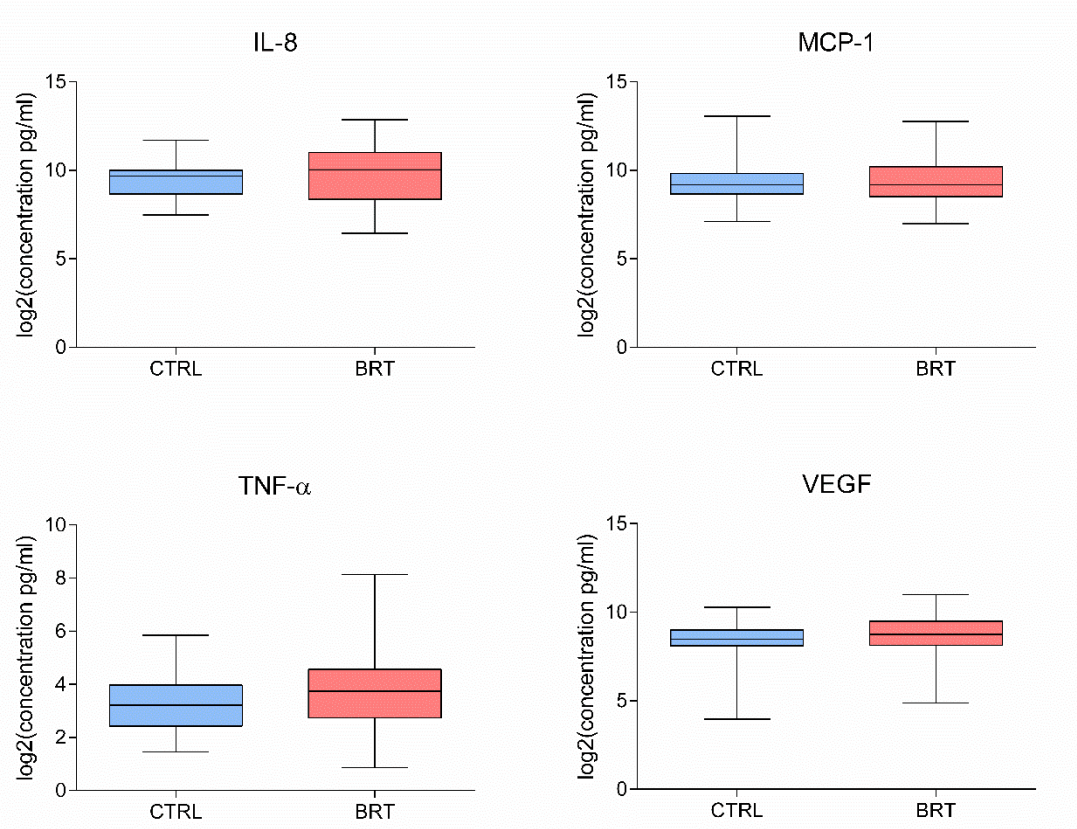

Figure 24 a) and b): Salivary levels of EGF, IL-10, IL-4, IL-6, IL-8, MCP-1, TNF-α and VEGF detected in control subjects (N=37) and HNC patients BRT (N=30). Data are expressed as log2(mean signal ratios). Statistical analysis was performed using the non-parametric Mann-Whitney U test; ****p ≤ 0.0001. HNC, Head and neck cancer; CTRL, healthy individuals; BRT, before radiotherapy treatment

Contrariwise, results obtained by matching the CTRL group with the HNC patients evaluated after the irradiation process (ART group) showed a tendency for significantly increasing protein concentration of IL-10, IL-6, IL-8, MCP-1 and TNF-α following the treatment (***Figure 25***). No changes statistically significant were observed in the expression levels of VEGF, whereas a reduction of EGF salivary levels was detected, although without being statistically significant.

a)

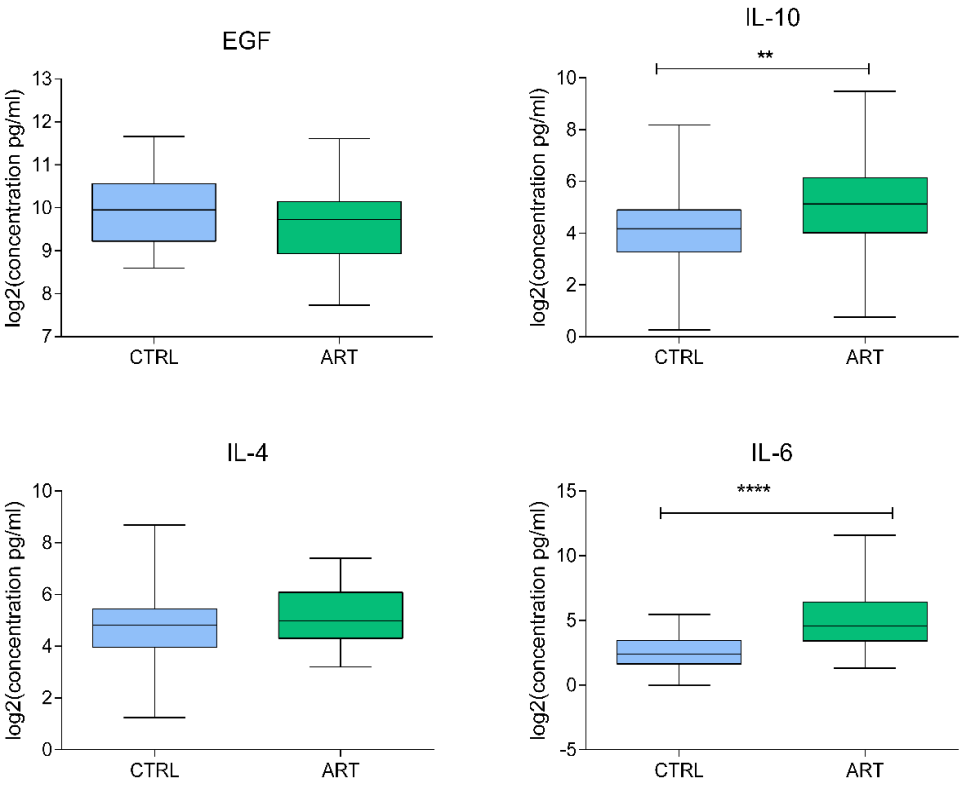

b)

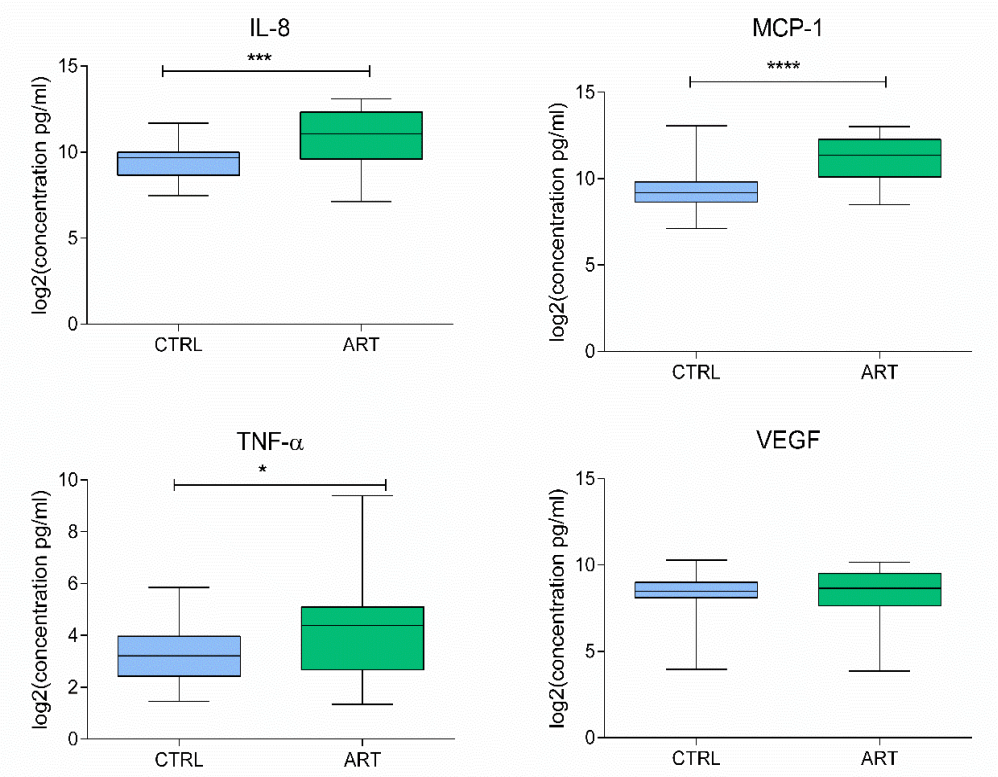

Figure 25 a) and b): Salivary levels of EGF, IL-10, IL-4, IL-6, IL-8, MCP-1, TNF-α and VEGF detected in control subjects (N=37) and HNC patients ART (N=30). Data are expressed as log2(mean signal ratios). Statistical analysis was performed using the non-parametric Mann-Whitney U test. ****p ≤ 0.0001; ***p ≤ 0.001; **p ≤ 0.01; *p ≤ 0.05.
HNC, Head and neck cancer; CTRL, healthy individuals; ART, after radiotherapy treatment.

1.6.1 Analysis of salivary inflammatory markers in HNC patients and healthy controls considering the variable "tumour site", head and neck area vs oral cavity

To study in depth if the modulation of the salivary inflammatory markers observed in the previous analysis (Section 1.6) was depending on cancer location, the two sub-groups of HNC patients (head and neck area vs oral cavity), evaluated before and after the irradiation treatment, were matched with their healthy counterparts. Firstly, we compared the HNC patients belong to the head and neck area (N=19) with the control subjects (N=37) pre- and post-treatment (BRT and ART) using a non-parametric Mann-Whitney U test; secondly, applying the same methodology, we plotted the HNC patients included in the oral cavity sub-group (N=11) against the healthy controls.

I. Results concerning the analysis of the tumours gathered in the head and neck area revealed that salivary levels of IL-4 and IL-6 were differentially expressed in HNC patients not yet treated (BRT group) in comparison with the CTRL group, presenting a *p-value* ≤ 0.05 and ≤ 0.01, respectively (***Figure 26***).

Whereas, a significant augmentation of IL-4, IL-6, IL-8 and TNF-α levels was observed when controls where matched with the HNC patients who have already been irradiated (ART group) (***Figure 27***).

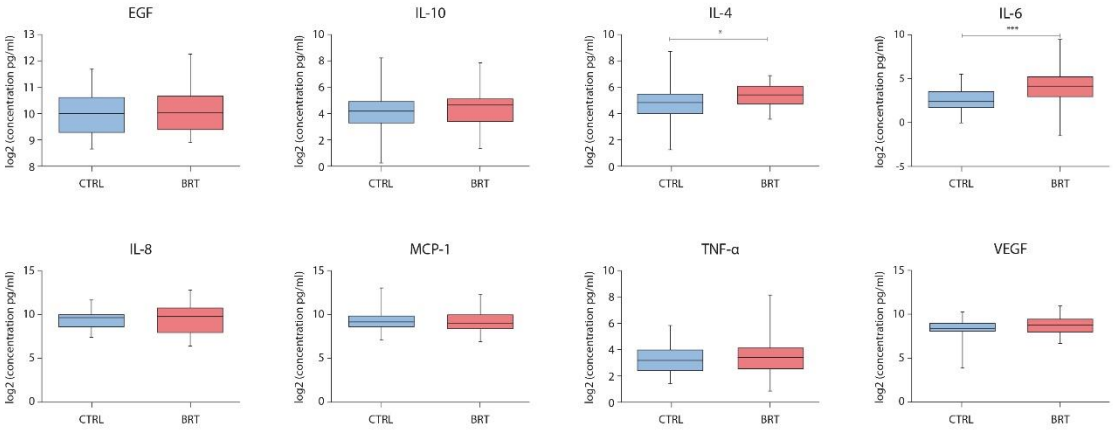

Figure 26: Salivary levels of EGF, IL-10, IL-4, IL-6, IL-8, MCP-1, TNF-α and VEGF detected in healthy subjects (N=37) and patients with cancer of the head and neck area region evaluated BRT (N=19). Data are expressed as log2(mean signal ratios). Statistical analysis was performed using the non-parametric Mann-Whitney U test; ***p ≤ 0.001; *p ≤ 0.05.

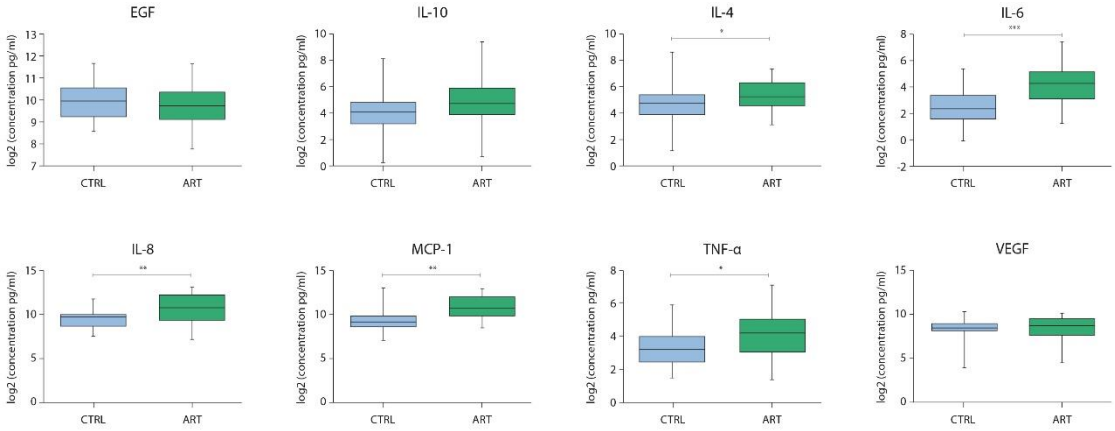

Figure 27: Salivary levels of EGF, IL-10, IL-4, IL-6, IL-8, MCP-1, TNF-α and VEGF detected in healthy subjects (N=37) and patients with cancer of the head and neck area region evaluated ART (N=19). Data are expressed as log2(mean signal ratios). Statistical analysis was performed using the non-parametric Mann-Whitney U test; ***p ≤ 0.001; **p ≤ 0.01; *p ≤ 0.05

II. When the HNC patients diagnosed with a tumour comprised in the oral cavity region (N=11) and not yet treated (BRT group) were plotted against the CTRL group (N=37) it was observed a significant increment of IL-4, IL-6, IL-8 and TNF-α levels in saliva of OSCC patients (***Figure 28***).

While, results obtained by matching the control subjects with the irradiated oral cancer patients (ART group) showed a significant augmentation of IL-10, IL-6, IL-8 y MCP-1 salivary levels, to probably link with the irradiation process (***Figure 29***).

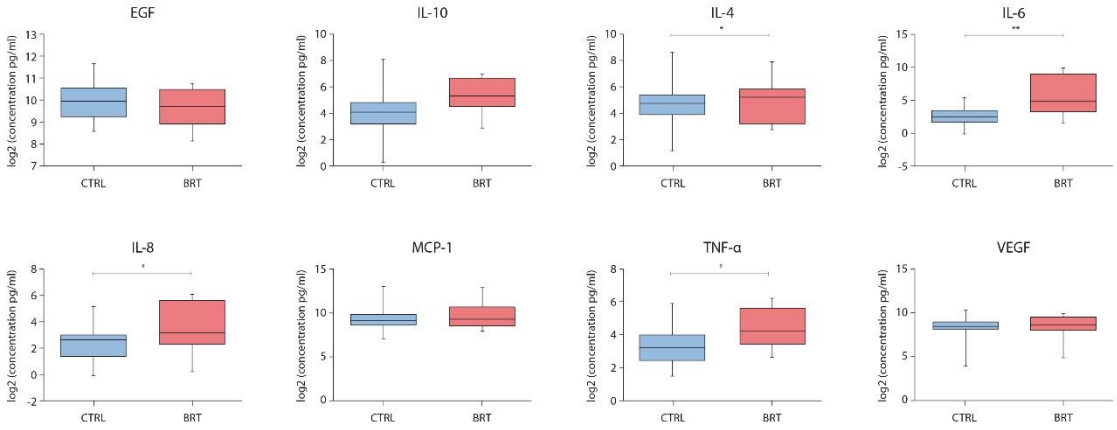

Figure 28: Salivary levels of EGF, IL-10, IL-4, IL-6, IL-8, MCP-1, TNF-α and VEGF detected in healthy subjects (N=37) and patients with cancer of the oral cavity evaluated BRT (N=11). Data are expressed as log2(mean signal ratios). Statistical analysis was performed using the non-parametric Mann-Whitney U test; **p ≤ 0.01; *p ≤ 0.05.

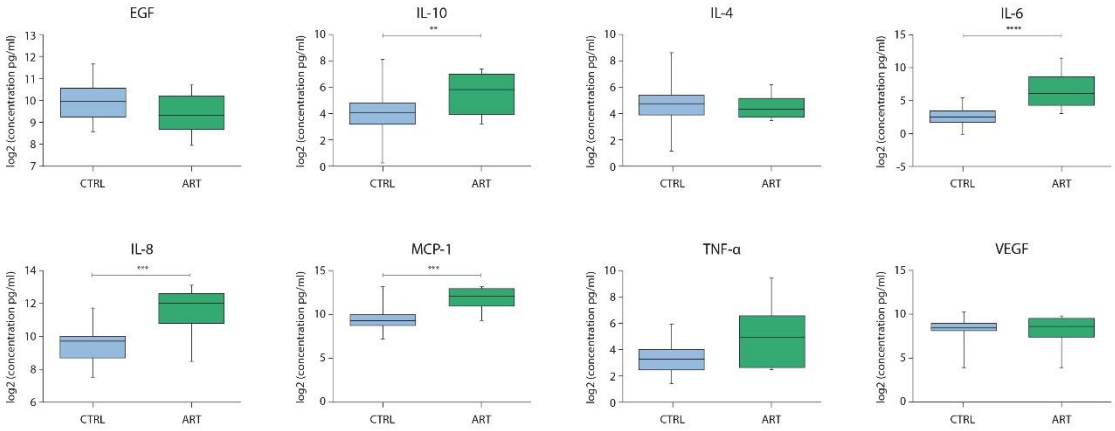

Figure 29: Salivary levels of EGF, IL-10, IL-4, IL-6, IL-8, MCP-1, TNF-α and VEGF detected in healthy subjects (N=37) and patients with cancer of the oral cavity evaluated ART (N=11). Data are expressed as log2(mean signal ratios). Statistical analysis was performed using the non-parametric Mann-Whitney U test; ****p ≤ 0.0001; ***p ≤ 0.001; **p ≤ 0.01.

1.7 Correlation analysis – Pearson's coefficient

To determine how the different salivary proteins (EGF, IL-10, IL-4, IL-6, IL-8, MCP-1, TNF-α and VEGF) were related to the HNC cases, examined before and after RT, and also to the healthy controls, a correlation analysis was carried out. The Pearson's pairwise correlation test was applied, using the R programming language and the caleb function (core.test).

The most common method of discovering whether there is a linear association among two continuous quantitative variables is the Pearson Correlation Analysis. With this method, the Pearson Correlation Coefficient is obtained, usually represented by the letter R. Two aspects of the correlation coefficient are important: strength and direction of the linear association between two continuous variables, named magnitude and sign, respectively.

Simplifying, the positive sign suggests that the values of both variables change in the same direction, while the negative sign indicates that they change in the opposite

direction. Thus, referring to the CTRL group and according to Pearson's R, a significant correlation was observed between the following analytes (***Figure 30***):

EGF <-> MCP-1

IL10 <-> IL4, IL6, TNF-α, VEGF

IL4 <-> IL6, TNF-α, VEGF

IL8 <-> TNF-α

MCP-1 <-> TNF-α, VEGF

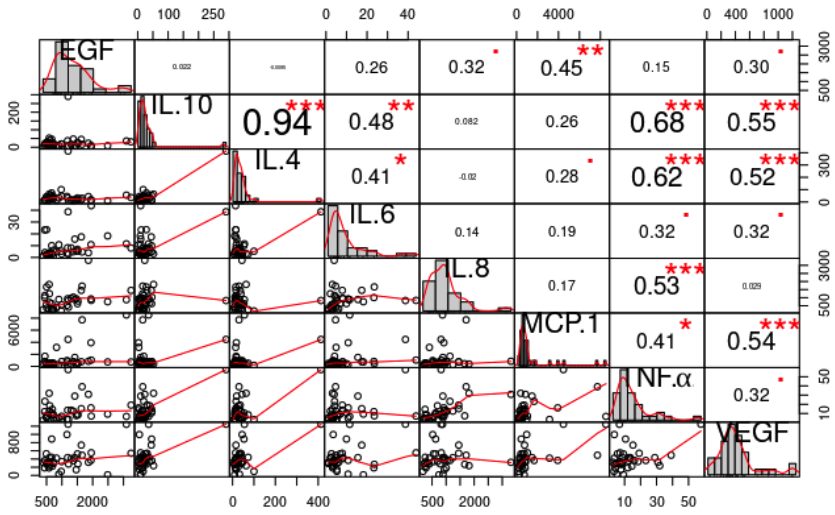

Figure 30: CTRL group R-chart. Correlation matrix plot to be read from the diagonal, where the histograms indicate the distribution. The lower panel displays bivariate scatter plots with a fitted line for every possible pairing; the upper panel gives the corresponding Pearson correlation coefficient, with text size proportional to its absolute value plus the significance level. Each significance level is associated with a different p-value: *** ≤ 0.001, ** ≤ 0.01, * ≤ 0.05

Considering the group of HNC patients evaluated before the irradiation process (BRT group), a significant correlation was observed between the following analytes (***Figure 31***):

EGF <-> MCP-1

IL10 <-> IL6, IL8, TNF-α, VEGF

IL6 <-> IL8, TNF-α, VEGF

IL8 <-> MCP-1, TNF-α, VEGF

TNF-α <-> VEGF

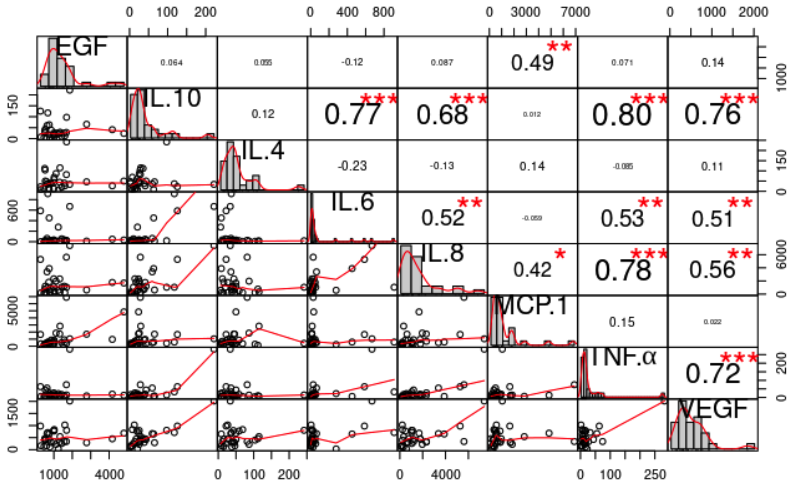

Figure 31: BRT group R-chart. Correlation matrix plot to be read from the diagonal, where the histograms indicate the distribution. The lower panel displays bivariate scatter plots with a fitted line for every possible pairing; the upper panel gives the corresponding Pearson correlation coefficient, with text size proportional to its absolute value plus the significance level. Each significance level is associated with a different p-value: *** ≤ 0.001, ** ≤ 0.01, * ≤ 0.05.

Besides, regarding the HNC patients assessed after the RT treatment (ART group) and according to Pearson's R, a significant correlation was observed within the following analytes (***Figure 32***):

EGF <-> VEGF

IL10 <-> VEGF

IL6 <-> TNF-α

IL8 <-> TNF-α, VEGF

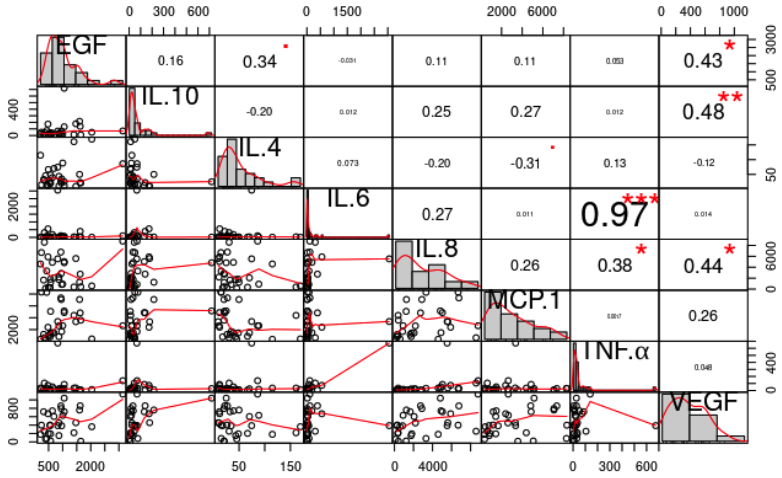

Figure 32: ART group R-chart. Correlation matrix plot to be read from the diagonal, where the histograms indicate the distribution. The lower panel displays bivariate scatter plots with a fitted line for every possible pairing; the upper panel gives the corresponding Pearson correlation coefficient, with text size proportional to its absolute value plus the significance level. Each significance level is associated with a different p-value: *** ≤ 0.001, ** ≤ 0.01, * ≤ 0.05.

Finally, comparing both groups of HNC patients estimated before and after the irradiation process (BRT and ART), a significant correlation was noticed among these salivary proteins (***Figure 33***):

IL10 <-> IL8, MCP-1, VEGF

IL6 <-> IL8, TNF-α

IL8 <-> MCP-1, TNF-α, VEGF

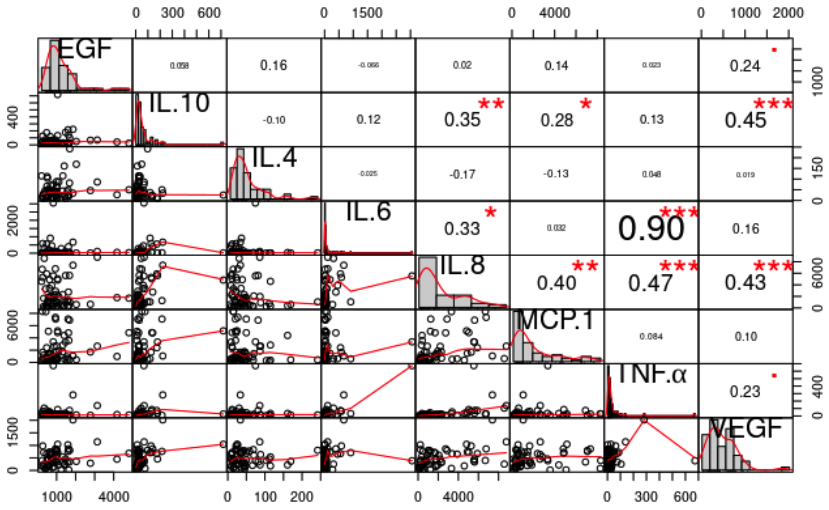

Figure 33: BRT vs. ART group R_chart. Correlation matrix plot to be read from the diagonal, where the histograms indicate the distribution. The lower panel displays bivariate scatter plots with a fitted line for every possible pairing; the upper panel gives the corresponding Pearson correlation coefficient, with text size proportional to its absolute value plus the significance level. Each significance level is associated with a different p-value: *** ≤ 0.001, ** ≤ 0.01, * ≤ 0.05.

A strong pre-treatment correlation (R ≥ 0.8) was evident between IL-10 with TNF-α (***Figure 31***). In contrast, a positive correlation such as between IL-6 and TNF-α was evident post-treatment but was not strong pre-treatment (***Figure 32***). However, there were significant correlations between changes in IL-10 with VEGF, IL-8 and MCP-1, as well as changes in IL-8 with TNF-α, VEGF and MCP-1, and among IL-6 with TNF-α and IL-8 (***Figure 33***). Together these data showed differential changes in salivary markers pre- and post-treatment, i.e., patients with increasing IL-8 also tended to have increasing MCP-1, TNF-α and VEGF levels.

1.8 Determination of likely relationships between alteration of salivary protein levels and HNC patients' clinical parameters

To accomplish this aim, a Bayesian network was constructed using directed acyclic graphing (DAG) and conditional probability methodology. The Bayesian network generally assumes that the data is normally distributed, in our case, it was not due to the small sample size. Because of it, the variables had to be simplified since they were presenting an excessive number of conditions in relation to the number of samples, for more detail refers to Supplemental Table 2 (Chapter VIII Appendix, SUPPLEMENTAL TABLES). Once reduced the variables, the dependency analysis was performed correlating:

a) the average data of EGF, IL-10, IL-4, IL-6, IL-8, MCP-1, TNF-α and VEGF obtained from the group of patients evaluated before the RT (BRT group) and the following variables: diagnosis, location, neck metastasis, primary tumour ("TNM.T") and extent of regional lymph node metastasis ("TNM.N");

b) the average data of the above-mentioned analytes resultant from the analysis of the group of HNC after the irradiation process (ART group) and the consequent variables: type of treatment, treatment response, treatment tolerance (dermatitis, mucositis, xerostomia).

Regarding the HNC cases belonging to BRT group, results revealed no relations between salivary proteins and the variable *TNM.T*, as well as for the variable *treatment* and *mucositis* concerning the ART group. It is important to underline the fact that these relationships may do not exist due to the limited number of samples used for the analysis. Considering the remaining clinical variables, various direct and indirect connections were detected (***Figure 34***) (**Table 9**). In particular, focusing on the clinical data analysed in the BRT group, the network indicated that all the analytes could present significant values applicable to diagnose HNC or OSCC pathology (variable *diagnosis*). Moreover, taking into consideration the tumour *location* variable, a direct relation was observed with IL-10 and IL-6; whereas for the *TNM.N*

parameter, a direct connection was detected only with the protein MCP-1. Besides, about the clinical variables analysed in the ART group, for the parameter *treatment response* there is a range of values per each protein that could be used as diagnostic criteria of favourable treatment outcomes in HNC patients undergoing RT, refers to Supplemental Table 3 (Chapter VIII Appendix, SUPPLEMENTAL TABLES). Finally, referring to the parameter *treatment tolerance*, in particular dermatitis and xerostomia status, results pointed out that for IL-6 and IL-10 a diagnostic range was detected, even if just to merely rule out the possible development of that side effects. Complete data are presented in Supplemental Table 3 (Chapter VIII Appendix, SUPPLEMENTAL TABLES). However, due to the small number of samples available, we have to assume that these are preliminary results and need to be validated in a large cohort of patients.

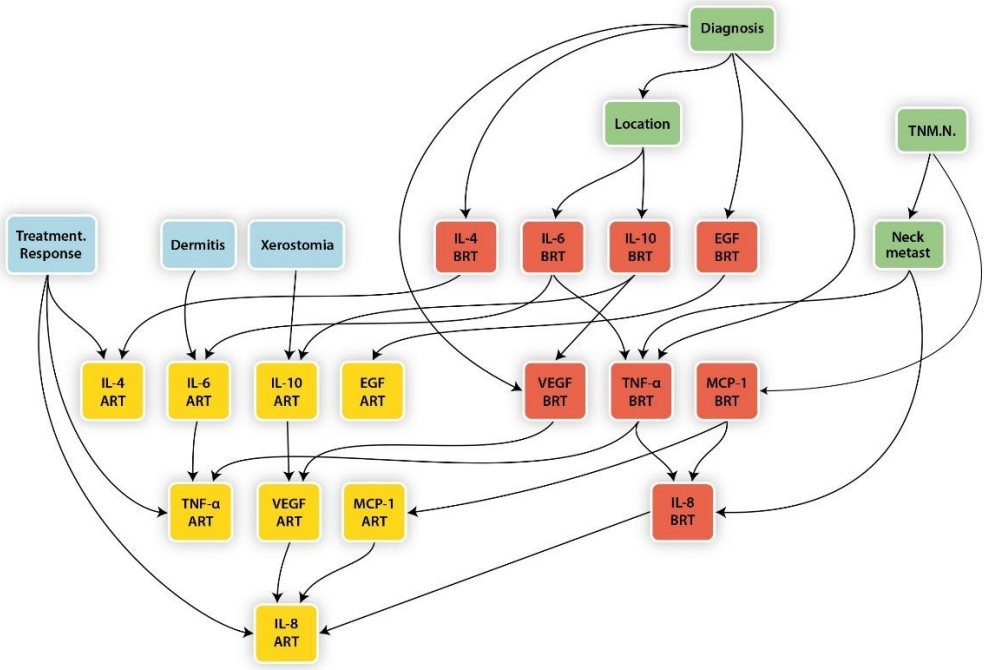

Figure 34: Graphical representation of the Bayesian network created with the HNC samples belonging to BRT and ART groups (N=30).

Table 9: Direct and indirect connections of the Bayesian network constructed using directed acyclic graphing (DAG) and conditional probability methodology. BRT, before radiotherapy treatment; ART, after radiotherapy treatment; TNM.N, regional lymph node metastasis.

BRT_Clinical variables	Direct Connection	Indirect Connection
Diagnosis (HNC or OSCC)	IL-4	-IL-4 ART
	VEGF	-VEGF ART, IL-8 ART
	EGF	-EGF ART
	TNF-α	-TNF-α ART; -IL-8 BRT, IL-8 ART
Location	IL-6	-IL-6 ART, TNF-α ART; -TNF-α BRT, TNF-α ART; -IL-8 BRT, IL-8 ART
	IL-10	-IL-10 ART, VEGF ART, IL-8 ART; -VEGF BRT, VEGF ART, IL-8 ART
TNM.N	MCP-1	-MCP-1 ART, IL-8 ART; IL-8 BRT, IL-8 ART
Neck metastasis	TNF-α	-TNF-α ART; -IL-8 BRT, IL-8 ART
	IL-8	-IL-8 ART

ART_Clinical variables	Direct Connection	Indirect Connection
Treatment response	IL-4 TNF-α IL-8	
Dermitis	IL-6	-TNF-α
Xerostomia	IL-10	-VEGF, IL-8

1.9 Salivary cytokines as putative predictive biomarkers of RT response

The aim of this section was to investigate if, using the samples obtained before the treatment (BRT group), we were able to predict the therapy outcomes of the recruited HNC patients. To find a predictive biomarker with clinical utility, specimens collected before the therapy must be considered, since there is no interest to find a marker in a sample for whom clinicians already know the treatment response. Hence, the salivary abundance of the studied analytes (EGF, IL-10, IL-4, IL-6, IL-8, MCP-1, TNF-α and VEGF) was compared among the HNC patients evaluated before receiving the irradiation therapy (BRT group), to determine if the concentration was associated with the treatment response recorded at T=1 (three months later the therapy). For this purpose, the HNC patients belonging to the BRT group were divided in two subgroups and classified as: responders, patients that achieved a complete response at the end of the treatment (N=24); non responders, patients that presented none or partial response to the therapy at T=1 (N=6). RT outcomes reported at T=0 (end of the treatment) were excluded from the analysis since the clinical data registered at T=1 were homogeneous. The nonparametric Mann-Whitney U test was applied to plot responders versus non responders. Subsequently, in order to evaluate the diagnostic ability of these putative biomarkers to predict RT response, employing the same data-set, receiver operating characteristic (ROC) curve analysis was conducted.

In a ROC curve, the true positive rate (Sensitivity) is plotted as a function of the false positive rate (100-Specificity) for different cut-off points of a parameter. Each point on the ROC curve represents a sensitivity/specificity pair corresponding to a particular decision threshold. The area under the ROC curve (AUC) is a measure of how well a parameter can distinguish between two diagnostic status (disease/ healthy or presence/absence of a specific condition). AUC is a measure of diagnostic accuracy, which incorporates sensitivity and specificity. It usually represents the overlap between the healthy and diseased population. An AUC value of 1 would represent a perfect diagnostic accuracy (no population overlap) and an AUC of 0.5 would represent no difference between groups (no diagnostic value). In our study, we considered an AUC > 0.7 as a useful discriminating biomarker.

Results revealed a trend towards an increase of IL-10, IL-4, IL-6, MCP-1 and TNF-α levels in saliva specimens of *HNC non responders* (***Figure 35***). However, significance was confirmed only for protein concentration of IL-8 (*p-value* ≤ 0.05). Contrariwise, a reduction of EGF levels was detected, even though without achieving statistical significance. Furthermore, ROC curves substantially confirmed the results obtained from the nonparametric Mann-Whitney U test, pointed out the strong potential of IL-8 as a predictive biomarker of RT outcomes (AUC= 0.84; *p-value*= 0.018) and suggesting the hypothetical role of TNF-α as well (AUC= 0.768; *p-value*=0.0623) (***Figure 36***).

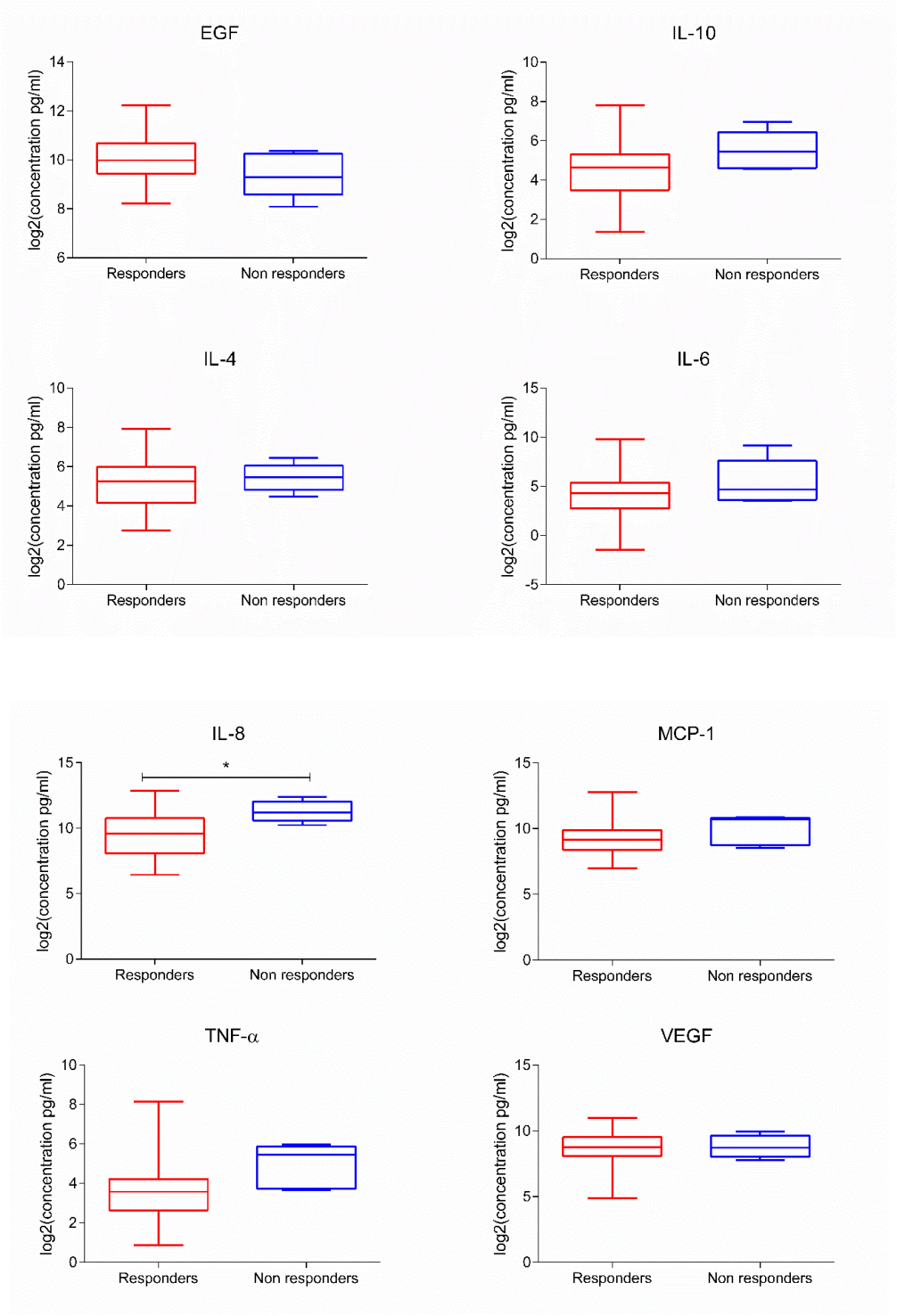

Figure 35: Protein concentration of EGF, IL-10, IL-4, IL-6, IL-8, MCP-1, TNF-α and VEGF detected in saliva of RT responders (N=24) and RT non responders (N=6), belonging to the group of HNC patients evaluated before the treatment (BRT). Data are expressed as log2(mean signal ratios). Statistical analysis was performed using the non-parametric Mann-Whitney U test, *$p \leq 0.05$.

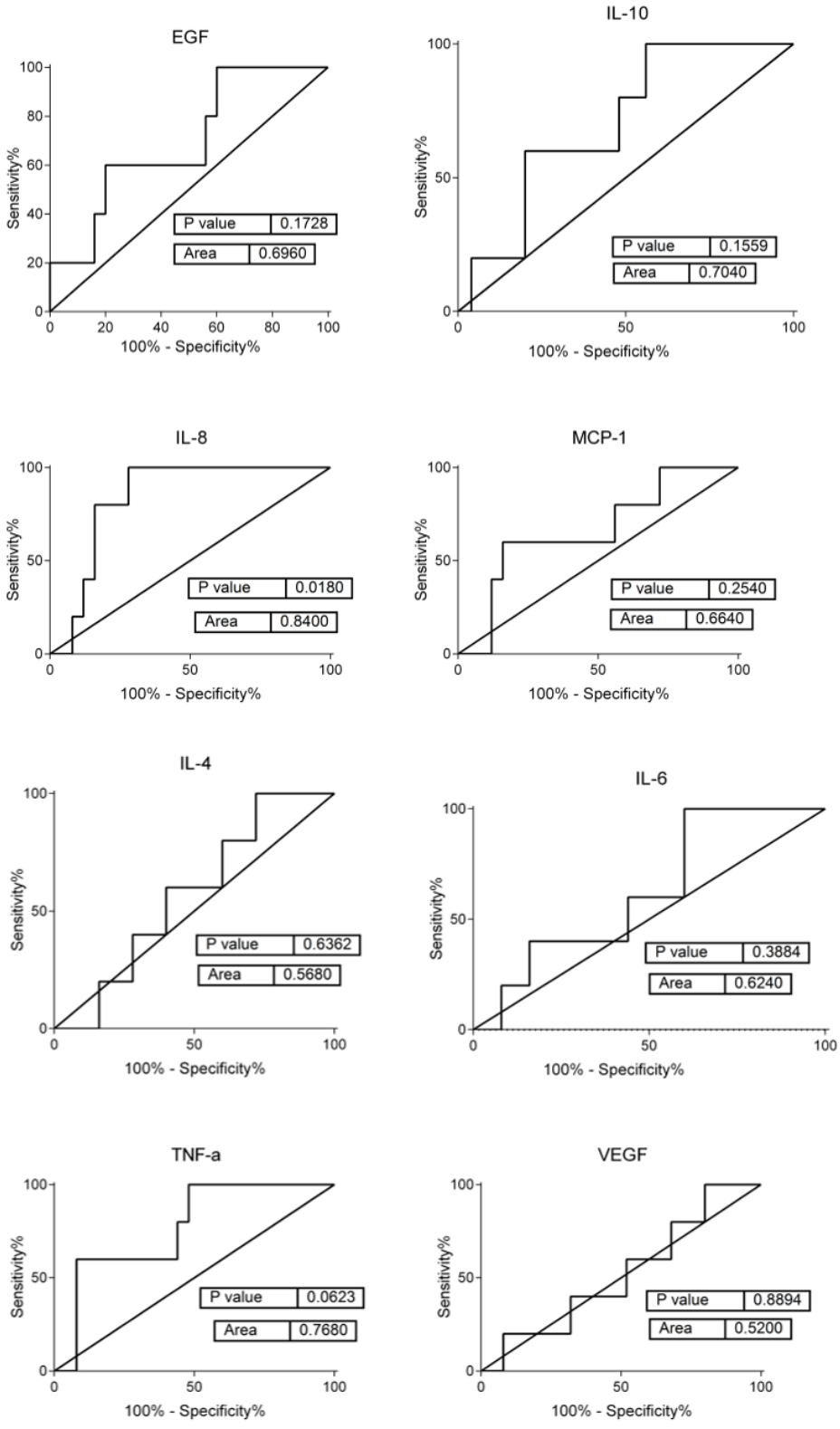

Figure 36: ROC plots of salivary EGF, IL-10, IL-4, IL-6, IL-8, MCP-1, TNF-α and VEGF. P-value and area under the ROC curve are presented. AUC value > 0.7 was considered in deciding if a given biomarker was informative in discriminating RT responders (N=24) from RT non- responders (N=6), both belonging to the group of HNC patients evaluated before RT treatment (BRT).

2 EVALUATION OF SALIVARY PROTEOME

Investigation of salivary proteome profiles in control samples and HNC specimens, gathered before and after radiotherapy treatment, was carried out using the liquid chromatography and tandem mass spectrometry technique (LC-MS/MS). The process consisted of two phases: 1) generation of a peptide spectral library from a pool of 10 HNC samples and 2) quantification of 30 individual salivary proteome profiles. Once the construction of the "HNC spectral library" using the whole saliva was accomplished, the investigation of the proteome before and after the irradiation process proceeded along with: targeted quantification of salivary proteins and comparison between patients and controls proteome profiles.

2.1 Patients characteristics

Based on specific criteria (gender, age, clinical parameters), a total of 30 samples were selected between the two cohorts of the study (Cohort 1_HNC patients; Cohort 2_Controls) in order to identify the best candidates for the investigation of the salivary proteome. The included subjects were divided as follows:

i. GROUP 1 comprised 10 HNC patients evaluated before radiotherapy (BRT)
ii. GROUP 2 composed by 10 HNC analysed after radiotherapy (ART)
iii. GROUP 3 consisted of 10 healthy volunteers enrolled as controls (CTRL)

Samples belonging to Group 2 were obtained from the same patients comprised in Group 1, evaluated pre- and post-treatment. The most relevant demographic and clinicopathological characteristics of the recruited HNC patients and controls are shown in **Table 10**.

Table 10: Demographic and clinicopathological characteristics of the subjects included in the study. HNC, Head and Neck cancer; NS, not specified; RT, Radiotherapy; CRT, Chemoradiation therapy

Group 1 (BRT) & 2 (ART)	*N*	*%*
HNC patients	10	
Median age	63.5	
Gender		
Male	8	80.0
Female	2	20.0
Tumour sites		
Oral cavity	3	30.0
Pharynx	1	10.0
Larynx	6	60.0
TNM classification		
T1	1	10.0
T2	3	30.0
T3	5	50.0
T4	1	10.0
Neck metastasis		
Yes	5	50.0
No	5	50.0
Treatment		
Surgery + RT	6	60.0
CRT therapy	4	40.0
Development of mucositis		
Grade I	1	10.0
Grade II	2	20.0
Grade III	4	40.0
NS	3	30.0
Response to the treatment **T=0**		
Complete Response (CR)	9	90.0
No Response (NR)	1	10.0
Response to the treatment **T=1**		
Complete Response (CR)	7	70.0
No Response (NR)	3	30.0

Group 3 (CTRL)	*N*	*%*
Healthy volunteers	10	
Median age	61	
Gender		
Male	5	50.0
Female	5	50.0

Group 1 (BRT) and 2 (ART) median age was 63.5 years [range: 38-85], 80.0% were male and 20.0% were female. The tumour site with major incidence was the larynx (60.0%), followed by the oral cavity (30.0%). Squamous cell carcinoma (SCC) histologic description was observed in 100% of the cases. Besides, 60% of the patients were diagnosed at advanced stage of disease (T3-T4) and presented neck metastasis

as well (50.0%). The majority of the HNC population received postoperative adjuvant RT (60.0%). Treatment response recorded at T=0 (RT ends) showed a complete response (CR) in 90.0% of the patients, albeit a slight decrease was observed at T=1 (three months after the therapy) where the percentage of CR reported was 70.0%. The control group (Group 3) included 5 healthy males (50.0%) and 5 healthy females (50.0%) with a median age of 61 years.

2.2 Salivary proteome analysis – HNC Spectral Library construction

A pool of 10 HNC saliva specimens (**Table 11**), not included in the final group of 30 samples above-mentioned, was used to build the Spectral Library. Data obtained from the LC-MS/MS assay performed were analysed using ProteinPilot default parameters. The Paragon algorithm (310) of ProteinPilot v 5.0 search engine (SCIEX) was applied to search against the Swissprot database (version 03-2018). For the construction of the library, only specimens from cancer patients were utilized, assuming that the majority of the proteins exhibited by tumour profiles were concurrently present in healthy profiles. After applying an FDR of 1.0% the number of identified proteins for the construction of the HNC Spectral Library was **1053**.

Table 11: Demographic and clinicopathological characteristics of the HNC patients (N=10) selected for the Spectral Library Cohort.

Spectral Library Cohort	*N*	*%*
HNC patients	10	
Median age	63	
Gender		
Male	4	40.0
Female	6	60.0
Tumour stage		
Early (T1-T2)	3	30.0
Advanced (T3-T4)	7	70.0

2.3 Salivary proteome profiles in HNC patients undergoing radiotherapy and healthy controls

Data resulted from the LC-MS/MS experiment performed with a TripleTOF 6600 (SCIEX) mass spectrometer operated in SWATH mode, involving the selected saliva specimens (N=30) of HNC patients undergoing radiotherapy and healthy controls, were analysed by Peak View 2.1, using the HNC spectral library as reference. The cycle time used in the tandem MS (MS/MS) acquisition allowed the quantification of each peptide area with more than 7 points. Peak View results were further analysed by Marker View (SCIEX). According to the extraction parameters used to measure the peptides areas, **695** proteins (FDR <1%) were quantified in 30 individual samples. A list of the whole 695 proteins identified is presented in Supplemental Table 4 (Chapter VIII Appendix, SUPPLEMENTAL TABLES). Therefore, the results obtained from the SWATH experiment were statistically analysed. The use of penalized regression models such as Elastic Net was preferred instead of the best-known classic models like t-test, ANOVA or chi-square, being that the number of variables of interest is much higher than the number of observations available. The objective of the analysis was to identify which proteins may differentiate the considered groups (Group1-BRT; Group2-ART; Group3-CTRL). Results are presented using the Heatmap graphical representation, followed by the partial least squares-discriminant analysis (PLS-DA).

2.3.1 Heatmap representation and cluster analysis

Figure 37 represents the 695 proteins quantified during the SWATH analysis, without performing any type of statistical analysis. Samples and proteins were both represented ordered according to the result of the hierarchical classification. Results showed that samples were not distributed according to the groups considered. However, once the Elastic Net penalized regression model was applied, some of these proteins appeared differentially expressed between the groups, classifying them properly (***Figure 38***) (**Table 12**).

This tendency also arose when the comparison was made only between two groups instead of three. In fact, results obtained by matching the samples belonging to Group 1 (BRT) with the others comprised in Group 2 (ART) revealed that a number of proteins (N=21) were differentially expressed among the proteomic profiles of the two groups of HNC patients (BRT vs ART) (***Figure 39***) (**Table 13**). The same analysis was followed to determine if there were modifications in the salivary proteome profiles between control subjects (Group 3_CTRL) and HNC patients valued before the treatment (Group 1_BRT) and after the irradiation process (Group 2_ART). When the Elastic Net penalized regression model was applied, results demonstrated that some of these proteins (N=11 for CTRL vs BRT; N=12 for CTRL vs ART) were differentially expressed between the groups, being able to classify them properly (***Figure 40 & Figure 41***) (**Table 13 & Table 14**). Furthermore, the PLS-DA analysis confirmed that the groups could be differentiated (***Figure 42, Figure 43, Figure 44***). In conclusion, data showed that the proteome varies in saliva of cancer patients undergoing radiotherapy, comparing pre- and post-treatment conditions and analysing the pattern followed by the control subjects, an altered protein profile was observed.

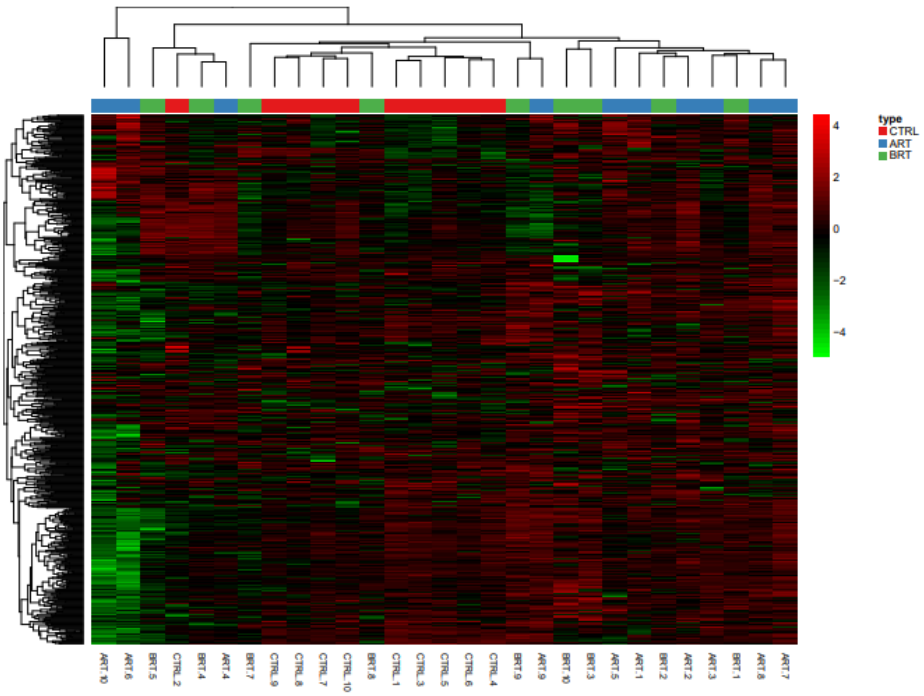

Figure 37: Heatmap representation of the whole set of proteins resulted from the SWATH analysis quantification. Columns correspond to each sample analysed, rows represent each protein quantified. Data were normalized to avoid scale problems. Colour mapping is based on the Z-score value. Groups are labelled as types in the graph legend.

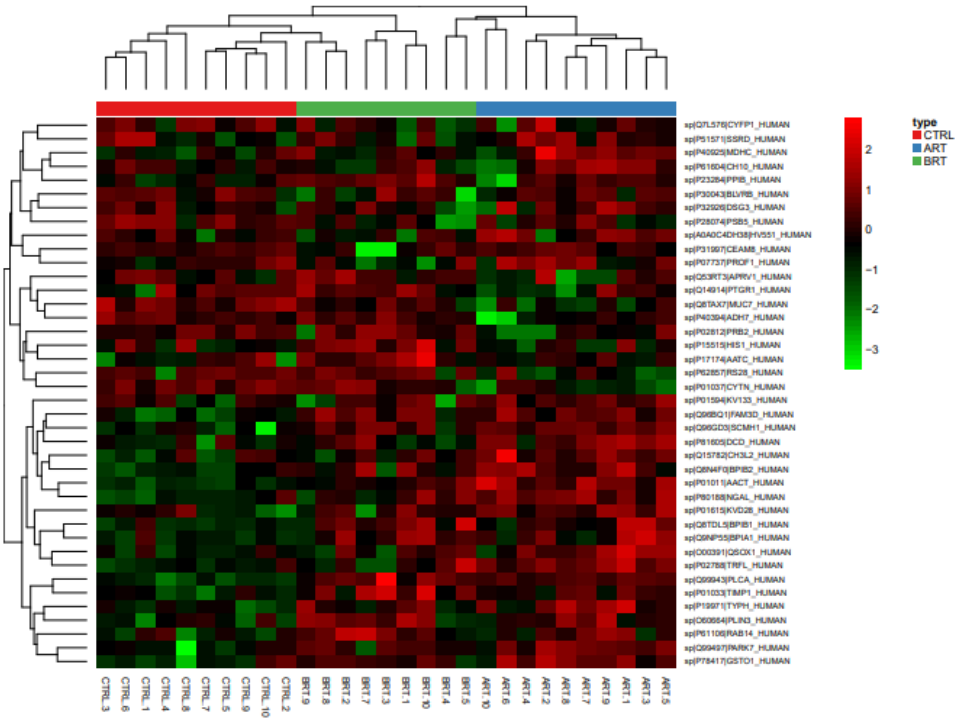

Figure 38: Heatmap representation of the differentially expressed proteins between the groups considered for the analysis (Group1-BRT; Group2-ART; Group3-CTRL) according to the Elastic Net penalized regression model (N=40). Columns correspond to each sample analysed, rows represent each protein quantified. Data were normalized to avoid scale problems. Colour mapping is based on the Z-score value. Groups are labelled as types in the graph legend.

Table 12: Proteins differentially expressed among the three groups considered for the analysis (Group1-BRT; Group2-ART; Group3-CTRL) according to the Elastic Net penalized regression model (N=40). The UniProt ID, the gene name, the protein name, the salivary protein abundance (presented as average of log2 data) is expressed per each group, according to the Red-Yellow-Green colour scale.

UniProt ID	Gene name	Proteine name	CTRL Av	BRT Av	ART AV
P02788	LTF	Lactotransferrin	7,999651	8,305077	9,349096
P01037	CST1	Cystatin-SN	6,934931	6,023205	3,874229
Q8TDL5	BPIFB1	BPI fold-containing family B member 1	3,748067	6,106249	5,733215
P80188	LCN2	Neutrophil gelatinase-associated lipocalin	4,597651	5,15634	5,963233
P01011	SERPINA3	Alpha-1-antichymotrypsin	1,234395	2,249982	3,26056
P32926	DSG3	Desmoglein-3	2,177967	1,853727	2,399825
Q8N4F0	BPIFB2	BPI fold-containing family B member 2	4,034108	4,641112	5,323648
P23284	PPIB	Peptidyl-prolyl cis-trans isomerase B	3,274448	3,760755	3,357865
P07737	PFN1	Profilin-1	2,925427	2,311059	3,159993
O00391	QSOX1	Sulfhydryl oxidase 1	-0,65091	-0,5207	0,115499
Q8TAX7	MUC7	Mucin-7	2,218732	0,907999	-0,3353
Q9NP55	BPIFA1	BPI fold-containing family A member 1	1,905932	4,501367	4,596703
P40394	ADH7	All-trans-retinol dehydrogenase	2,380762	2,227655	1,455274
O60664	PLIN3	Perilipin-3	-1,73644	-0,61259	-0,76814
P61106	RAB14	Ras-related protein Rab-14	-2,42749	-1,79417	-1,98464
P01033	TIMP1	Metalloproteinase inhibitor 1	2,400579	3,787451	3,22845
Q14914	PTGR1	Prostaglandin reductase 1	-1,41339	-1,09854	-2,3015
P19971	TYMP	Thymidine phosphorylase	-0,91732	-0,113	0,673598
P81605	DCD	Dermcidin	-3,68621	-3,48858	-2,21875
P30043	BLVRB	Flavin reductase (NADPH-flavin reductase)	-2,94249	-3,8218	-3,10396
P15515	HTN1	Histatin-1	-5,64108	-4,61797	-5,96868
P40925	MDH1	Malate dehydrogenase, cytoplasmic	0,856407	0,878665	1,274269
P61604	HSPE1	10 kDa heat shock protein, mitochondrial (Hsp10)	-0,25023	-0,60608	-0,07305
Q7L576	CYFIP1	Cytoplasmic FMR1-interacting protein 1	-2,50567	-3,36146	-2,86787
Q15782	CHI3L2	Chitinase-3-like protein 2	-2,36058	-1,93811	-0,54331
P19105	MYL12A	Myosin regulatory light chain 12A	-0,06652	0,570957	0,069557
Q14515	SPARCL1	SPARC-like protein 1	-0,25069	0,306777	0,370945
P02747	C1QC	Complement C1q	-3,18621	-4,69124	-3,61866
P01615	IGKV2D-28	Immunoglobulin kappa variable 2D-28	0,164246	0,442125	1,140375
Q9Y2V2	CARHSP1	Calcium-regulated heat-stable protein 1	-2,94409	-2,78752	-2,72419
P26599	PTBP1 PTB	Polypyrimidine tract-binding protein 1	-2,34489	-2,02849	-1,87852
P05156	CFI	Complement factor I	-3,64588	-3,40794	-2,88623
P20292	ALOX5AP	Arachidonate 5-lipoxygenase-activating protein	-0,24267	-0,49791	-0,13025
P22352	GPX3	Glutathione peroxidase 3	-2,19735	-2,24665	-1,51227
Q9UFN0	NIPSNAP3A	Protein NipSnap homolog 3A	-10,0021	-13,4601	-13,1198
P36957	DLST	Dihydrolipoyllysine-residue succinyltransferase	-1,51744	-0,55416	-0,19203
Q9UM00	TMCO1	Calcium load-activated calcium channel	-3,0139	-3,31448	-3,43108
Q99943	AGPAT1	1-acyl-sn-glycerol-3-phosphate acyltransferase alpha	-1,43934	1,793176	1,420934
Q53RT3	ASPRV1	Retroviral-like aspartic protease 1	-2,58335	-2,13797	-3,34875
P62857	RPS28	40S ribosomal protein S28	2,619035	2,963218	-0,66081

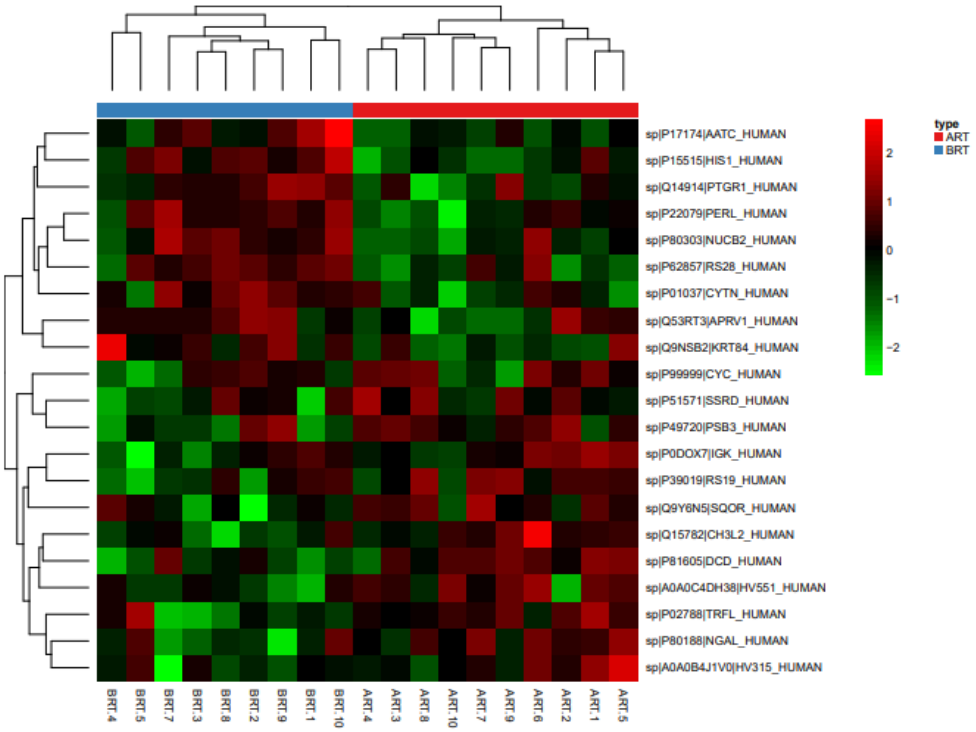

Figure 39: Heatmap representation of the proteins that differentiate Group2-ART vs Group1-BRT, according to the Elastic Net penalized regression model (N=21). Columns correspond to each sample analysed, rows represent each protein quantified. Data were normalized to avoid scale problems. Colour mapping is based on the Z-score value. Groups are labelled as types in the graph legend.

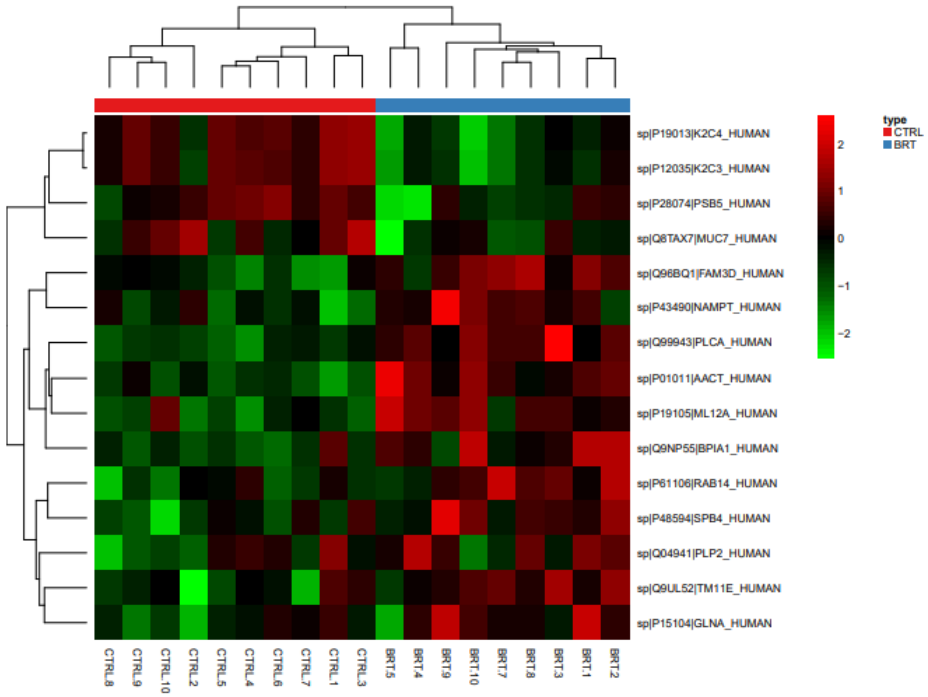

Figure 40: Heatmap representation of the proteins that differentiate Group3-CTRL vs Group1-BRT, according to the Elastic Net penalized regression model (N=11). Columns correspond to each sample analysed, rows represent each protein quantified. Data were normalized to avoid scale problems. Colour mapping is based on the Z-score value. Groups are labelled as types in the graph legend.

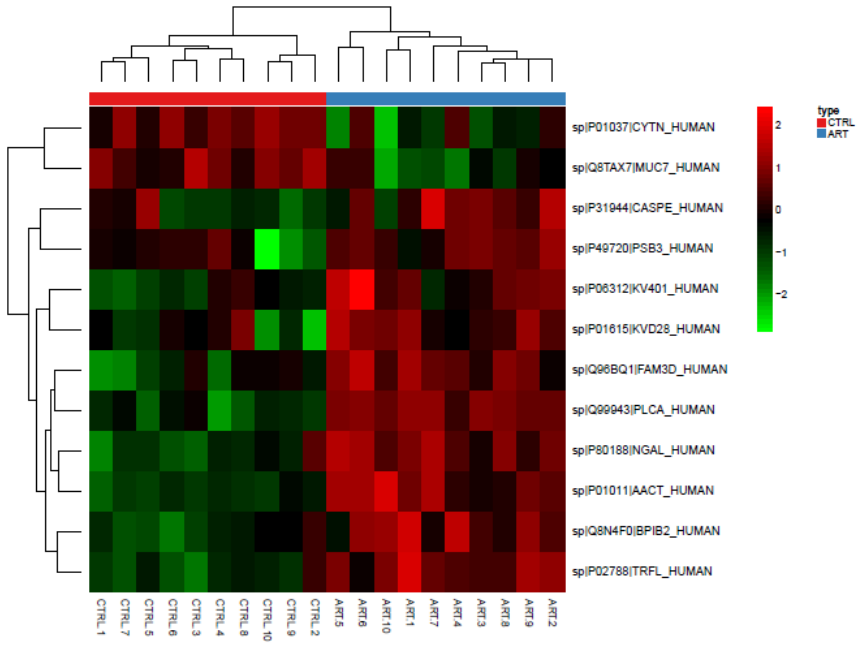

Figure 41: Heatmap representation of the proteins that differentiate Group3-CTRL vs Group2-ART, according to the Elastic Net penalized regression model (N=12). Columns correspond to each sample analysed, rows represent each protein quantified. Data were normalized to avoid scale problems. Colour mapping is based on the Z-score value. Groups are labelled as types in the graph legend.

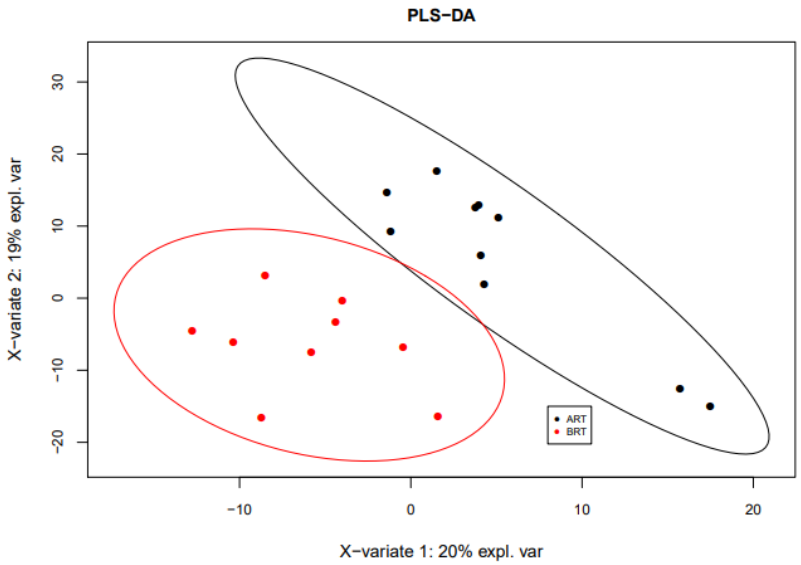

Figure 42: Classification of the salivary HNC samples belong to Group1-BRT and Group2-ART, based on the PLS-DA analysis

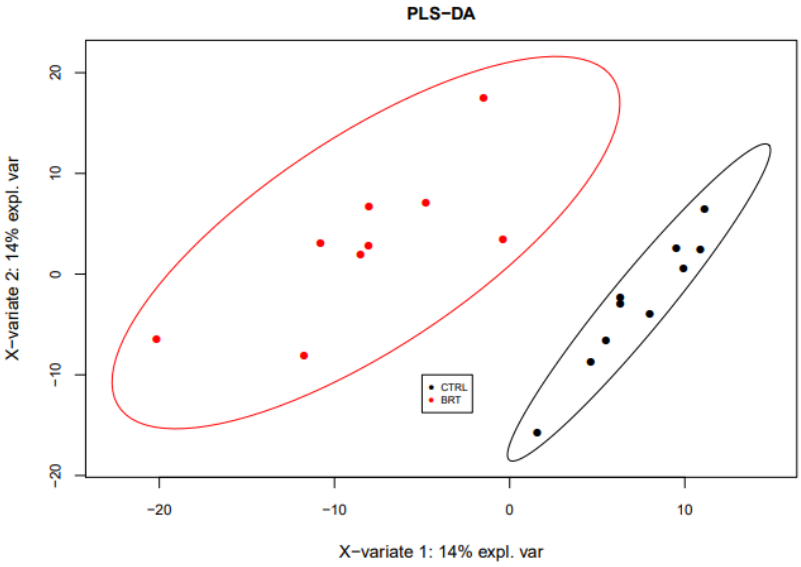

Figure 43: Classification of the salivary samples belong to Group1-BRT and Group3-CTRL, based on the PLS-DA analysis

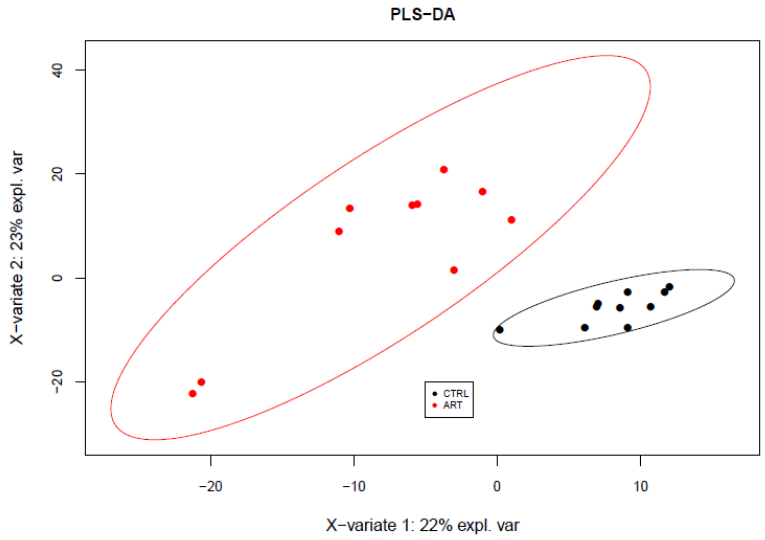

Figure 44: Classification of the salivary samples belong to Group2-ART and Group3-CTRL, based on the PLS-DA analysis

2.3.2 Proteins differentially expressed in saliva specimens

In order to investigate if the proteins differentially expressed in the salivary proteome, obtained from the SWATH experiment, would have shown statistical significance in respect of their salivary abundance, a parametric t-test was used, followed by the application of the Benjamini-Hochberg False Discovery Rate (FDR) for the adjustment of the p-value.

Table 13 represents the results of the comparison between Group2-ART and Group1-BRT. The salivary proteins differentially expressed from the Elastic Net analysis were 21, among them, 15 proteins appeared statistically significant based on the t-test, presenting a p-value < 0.05. Considering all molecules, 9 proteins resulted down-regulated and 11 were up-regulated in the group of HNC patients evaluated ART (Group2-ART).

Table 13: Proteins differentially expressed (21) in saliva of HNC patients evaluated before and after RT treatment (Group2-ART vs Group1-BRT). P-values are based on the results of the non-parametric t-test. Significantly altered proteins (p < 0.05).

UniProt ID	Gene name	Proteine name	Peptide count	p-value	↑Up-regulated ↓Down-regulated
P02788	LTF	Lactotransferrin	67	0,0263	↑
P22079	LPO	Lactoperoxidase	26	0,0280	↓
P01037	CST1	Cystatin-SN	7	0,0286	↓
P0DOX7	N/A	Immunoglobulin kappa light chain	2	0,0475	↑
Q9NSB2	KRT84	Keratin, type II cuticular Hb4 (Keratin-84)	12	0,0482	↓
P80188	LCN2	Neutrophil gelatinase-associated lipocalin	12	0,0330	↑
P80303	NUCB2	Nucleobindin-2	3	0,0489	↓
Q9Y6N5	SQOR	Sulfide:quinone oxidoreductase, mitochondrial	3	0,0596	↑
P39019	RPS19	40S ribosomal protein S19	1	0,0165	↑
Q14914	PTGR1	Prostaglandin reductase 1	2	0,0238	↓
P81605	DCD	Dermcidin	1	0,0123	↑
A0A0B4 /J1V0	IGHV3-15	Immunoglobulin heavy variable 3-15	1	0,0664	↑
P15515	HTN1	Histatin-1	2	0,0079	↓
Q15782	CHI3L2	Chitinase-3-like protein 2	2	0,0247	↑
P49720	PSMB3	Proteasome subunit beta type-3	1	0,0562	↑
P19105	MYL12A	Myosin regulatory light chain 12A	1	0,0612	↑
P35237	SERPINB6	Serpin B6	1	0,1780	↑
P22352	GPX3	Glutathione peroxidase 3	3	0,0601	↓
Q9UFN0	NIPSNAP3A	Protein NipSnap homolog 3A	1	0,0481	↑
Q53RT3	ASPRV1	Retroviral-like aspartic protease 1	1	0,0618	↓
P62857	RPS28	40S ribosomal protein S28	1	0,0146	↓

Referring to the comparison among the healthy volunteers (Group3-CTRL) and the HNC patients examined before the irradiation therapy (Group1-BRT), the Elastic net analysis determined that 11 proteins were differentially expressed (**Table 14**). Results obtained from the t-test showed that 9 proteins reached the statistical significance with a p-value < 0.05. Taking into consideration the levels of expression of the whole 11 proteins, 2 of them were down-regulated, while the remaining proteins appeared to be up-regulated in the group of healthy subjects (Group3-CTRL).

Table 14: Salivary proteins differentially expressed (11) between the healthy subjects and the HNC patients examined before RT treatment (Group3-CTRL vs Group1-BRT). P-values are based on the results of the non-parametric t-test. Significantly altered proteins (p < 0.05).

UniProt ID	Gene name	Proteine name	Peptide count	p-value	↑Up-regulated ↓Down-regulated
P19013	KRT4	Keratin, type II cytoskeletal 4	63	0,0001	↓
P12035	KRT3	Keratin, type II cytoskeletal 3	13	0,0001	↓
P01011	SERPINA3	Alpha-1-antichymotrypsin	8	0,0016	↑
P43490	NAMPT	Nicotinamide-phosphoribosyltransferase	4	0,0594	↑
P15104	GLUL	Glutamine synthetase	6	0,1252	↑
Q9NP55	BPIFA1	BPI fold-containing family A member 1	8	0,0053	↑
P61106	RAB14	Ras-related protein Rab-14	2	0,0234	↑
P48594	SERPINB4	Serpin B4	4	0,0174	↑
P21926	CD9	CD9 antigen	2	0,0064	↑
P20292	ALOX5AP	Arachidonate 5-lipoxygenase-activating protein	2	0,0029	↑
Q99943	AGPAT1	1-acyl-sn-glycerol-3-phosphate acyltransferase alpha	1	0,0002	↑

Finally, proteins identified as differentially expressed in saliva of healthy controls (Group3-CTRL) compared to the HNC patients examined after the radiotherapy (Group2-ART), are presented in **Table 15**. A total amount of 12 proteins appeared to be differential, based on the results of the t-test all of them were statistically significant, showing a *p-value* < 0.05. Concerning the levels of expression, 10 resulted up-regulated and 2 were down-regulated referring to the group of healthy volunteers (Group3-CTRL).

Table 15: Salivary proteins differentially expressed (12) among the healthy subjects and the HNC patients evaluated after RT treatment (Group3-CTRL vs Group2-ART). P-values are based on the results of the non-parametric t-test. Significantly altered proteins (p<0.05).

UniProt ID	Gene name	Proteine name	Peptide count	p-value	↑Up-regulated ↓Down-regulated
P02788	LTF	Lactotransferrin	67	4,8974E-05	↑
P01037	CST1	Cystatin-SN	7	0,0010	↓
P80188	LCN2	Neutrophil gelatinase-associated lipocalin	12	0,0003	↑
P01011	SERPINA3	Alpha-1-antichymotrypsin	8	0,0005	↑
Q8N4F0	BPIFB2	BPI fold-containing family B member 2	11	0,0043	↑
Q8TAX7	MUC7	Mucin-7	2	0,0006	↓
P06312	IGKV4-1	Immunoglobulin kappa variable 4-1	3	0,0245	↑
P31944	CASP14	Caspase-14	1	0,0045	↑
P49720	PSMB3	Proteasome subunit beta type-3	1	0,0312	↑
Q9Y2V2	CARHSP1	Calcium-regulated heat-stable protein 1	2	0,0122	↑
P20292	ALOX5AP	Arachidonate 5-lipoxygenase-activating protein	2	0,0018	↑
Q99943	AGPAT1	1-acyl-sn-glycerol-3-phosphate acyltransferase alpha	1	8,7317E-07	↑

2.4 Functional analysis of the differential salivary proteins

Proteomics experiments often generate a vast amount of data. However, the simple identification and quantification of proteins are not sufficient for the full understanding of complex mechanisms occurring in the biological systems. A functional annotation analysis of protein datasets using bioinformatics tools is essential for interpreting the results of high-throughput proteomics. The classification of genes and proteins according to their roles in biological systems is also the basis for the analysis of relationships and interactions between them. Therefore, networks of the differentially expressed proteins were generated using STRING version 11.0, followed by functional enrichment analysis. Enrichment analysis takes GO (*Gene Ontology*) terms and uses them to summarize the biological pathways and processes that are most likely related to the proteomic data. Thus, for a more detailed functional analysis of the differentially expressed proteins obtained applying the Elastic-Net penalized regression model, GO analysis was carried out; the biological process, molecular function and cellular localization were examined.

Statistical methodologies are used to compare the abundance of GO terms in the analysed network with the natural abundance in a reference dataset. Terms that are overrepresented are extracted by the calculation of a p-value, followed by the application of the FDR.

2.4.1 Functional analysis of the salivary proteins differentially expressed in the whole dataset of HNC patients and controls profiles

Proteins identified as differentially expressed (N=40) among the whole cohorts (Group1-BRT, Group2-ART, Group3-CTRL), based on the Elastic Net penalized regression model performed, were submitted to STRING for functional analysis. The network view summarizes the predicted associations for a particular set of proteins. The interaction between the above-mentioned proteins is shown in ***Figure 45***, it includes a total of 39 nodes and 27 edges, of which nodes represent the identified proteins and each edge represents the functional associations. The protein-protein interaction (PPI) enrichment p-value was 2.65E-09. Generally, a small PPI enrichment p-value indicates that the nodes are not random and that the observed number of edges is significant. Basically, if the proteins are significantly interconnected, it is reasonable to assume that the results are consistent and that they are biologically meaningful.

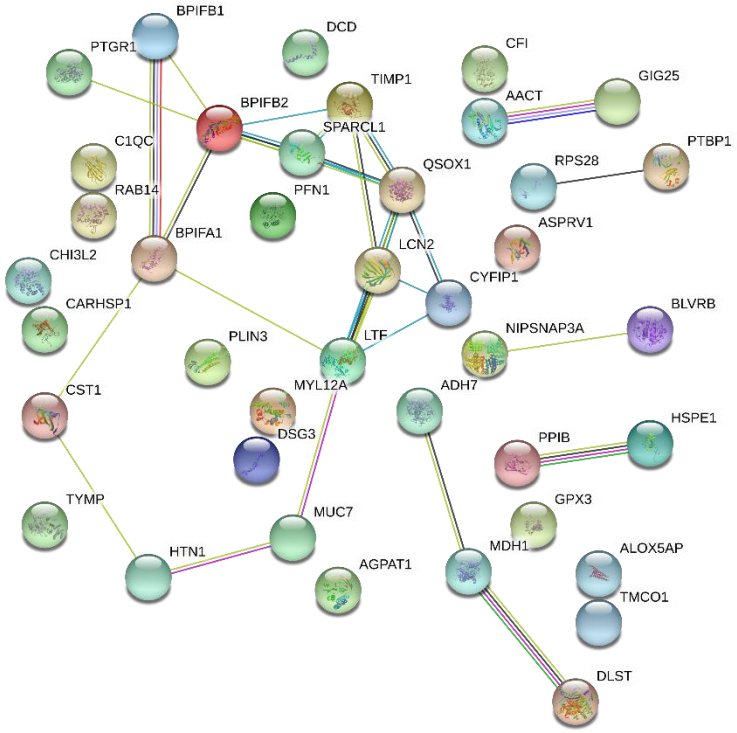

Figure 45: The protein interaction network of the salivary proteins differentially expressed between the HNC patients and controls profiles. Target proteins were displayed by STRING 11.0 using default settings and medium stringency. Each node represents a protein and the edges represent protein-protein interactions based on different levels of evidence calculated by STRING.

Afterwards, functional analysis and protein interaction network were performed per each group of proteins resulted differentially expressed from the Elastic Net analysis (**Table 13**, **Table 14**, **Table 15**/Section 2.3.2): Group2-ART vs Group1-BRT, Group3-CTRL vs Group1-BRT, Group3-CTRL vs Group2-ART.

The interaction between the salivary proteins differentially expressed (N=21) between the two groups of HNC patients evaluated before and after RT treatment (Group2-ART vs Group1-BRT) is shown in **Figure *46***. It includes a total of 18 nodes and 9 edges. The PPI enrichment p-value was 0.000263, which indicates that the proteins were partially biologically connected as a group and that the network showed significantly more interactions than expected. The results of the functional enrichment analysis indicate that the identified target proteins were biologically related to defence response to other organisms, such as bacterium or fungus, hence

to the antimicrobial humoral immune response. Concerning the cellular component analysis, some proteins belong to the endoplasmic reticulum membrane but the majority are located in the extracellular space, secreted outside the cell membrane.

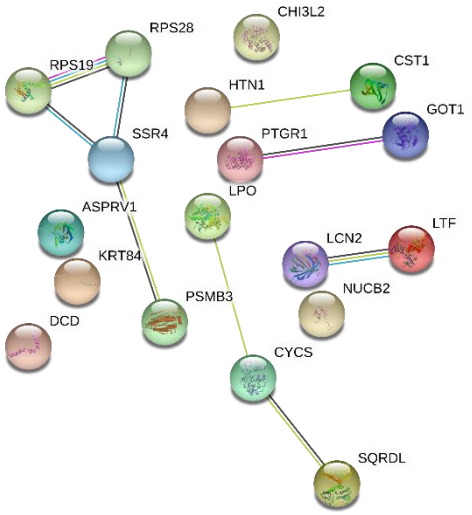

Figure 46: The protein interaction network of the salivary proteins differentially expressed among the HNC patients analysed pre- and post-Rt treatment (Group2-ART vs Group1-BRT) Target proteins were displayed by STRING 11.0 using default settings and medium stringency. Each node represents a protein and the edges represent protein-protein interactions based on different levels of evidence calculated by STRING.

According to the Elastic Net analysis, 11 proteins were differentially expressed between the salivary proteome profiles of healthy controls and HNC patients not yet treated with RT (Group3-CTRL vs Group1-BRT). The network between them did not showed significant. Nevertheless, the network generated among the 12 proteins differentially expressed in salivary proteome profiles of HNC patients after RT treatment and the group of healthy volunteers (Group3-CTRL vs Group2-ART) showed significantly more interactions than expected (***Figure 47***).

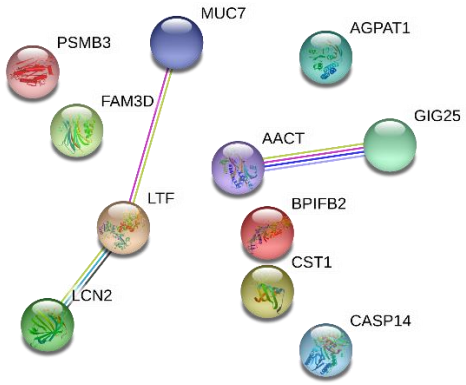

Figure 47: The protein interaction network of the salivary proteins differentially expressed among the HNC patients analysed pre- and post-RT treatment (Group3-CTRL vs Group2-ART). Target proteins were displayed by STRING 11.0 using default settings and medium stringency. Each node represents a protein and the edges represent protein-protein interactions based on different levels of evidence calculated by STRING.

Furthermore, GO enrichment analysis was performed per each group of proteins analysed and the top GO entries were selected based on false discovery rate (FDR < 0.05). Data in details are presented in Supplemental Table 5 (Chapter VIII Appendix, SUPPLEMENTAL TABLES).

In general, the results of the enrichment functional analysis showed that the identified target proteins were biologically related immune response, in particular humoral and antimicrobial, and stress response. Concerning the cellular component analysis, proteins were mainly secreted, located outside the cell membrane in the extracellular space.

2.5 Determination of altered salivary proteins linked to wound healing, tumour control and response to the therapy

Our study is based on two-stages approach for the discovery of HNC-specific salivary biomarker candidates. Among the 695 proteins identified from the 30 salivary samples, only 59 resulted differentially expressed according to the Elastic Net penalized regression model; between them, based on the patterns observed from the results of the t-test previously performed (Section 2.3.2), it was possible to differentiate four classes of proteins:

1) CTRL vs Cancer → altered proteins in salivary profiles of HNC patients with respect to healthy controls (N=10);

2) Reversed → proteins differentially expressed in cancer patients not yet treated (BRT group) that return to their normal state (control status) after the irradiation therapy (N=3);

3) Treatment → proteins mainly altered after the RT treatment, probably as a consequence of it (N=12);

4) Progress → proteins differentially expressed in HNC patients evaluated before RT but even more representative after the treatment (N=3).

The remaining proteins that did not follow a particular trend were classified as non-specific (N=31).

In order to observe the specific trend characteristic of these molecules, we considered the average values among the groups (Group1-BRT, Group2-ART, Group-3) and, afterwards, we examined the p-values and the FDR obtained from the t-test performed between them (BRTvsART, CTRLvsBRT, CTRLvsART). Per each class of proteins detected, a table containing all the statistical information was created (**Table 16**, **Table 17**, **Table 18**, **Table 19**).

Table 16: List of proteins classified as "CTRL vs Cancer" (N=10). The UniProt ID, the gene name and the number of unique peptides is presented. P-values are based on the results of the non-parametric t-test. Av= average

CTRL vs Cancer (N=10)			CTRL	BRT	ART	CTRL/BRT	CTRL/ ART	BRT/ART
UniProt ID	Gene name	Peptide count	Av	Av	Av	p-value	p-value	p-value
Q99943	AGPAT1	1	-1,4393	1,7932	1,4209	0,0002	8,7317E-07	0,5336
P12035	KRT3	13	8,6909	7,1519	5,8442	0,0001	0,0007	0,0601
Q96GD3	SCMH1	1	-3,8936	-1,8748	-1,1076	0,0110	0,0007	0,1304
P19971	TYMP	4	-0,9173	-0,1130	0,6736	0,0287	0,0010	0,0699
Q96BQ1	FAM3D	2	-1,0680	-0,0503	0,1342	0,0029	0,0018	0,5895
Q8TDL5	BPIFB1	24	3,7481	6,1062	5,7332	0,0044	0,0044	0,6436
Q9NP55	BPIFA1	8	1,9059	4,5014	4,5967	0,0053	0,0100	0,9280
P01033	TIMP1	5	2,4006	3,7875	3,2285	0,0058	0,0131	0,2034
P48594	SERPINB4	4	-0,0301	0,5383	1,3821	0,0174	0,0059	0,0645
O60664	PLIN3	3	-1,7364	-0,6126	-0,7681	0,0148	0,0149	0,6956

Table 17: List of proteins classified as "Reversed" (N=3). The UniProt ID, the gene name and the number of unique peptides is presented. P-values are based on the results of the non-parametric t-test. Av= average

Reversed (N=3)			CTRL	BRT	ART	CTRL/BRT	CTRL/ ART	BRT/ART
UniProt ID	Gene name	Peptide count	Av	Av	Av	p-value	p-value	p-value
P23284	PPIB	6	3,2744	3,7608	3,3579	0,0036	0,5845	0,0027
P61604	HSPE1	2	-0,2502	-0,6061	-0,0730	0,0316	0,1983	0,0030
P80303	NUCB2	3	0,8850	1,9536	1,0652	0,0126	0,6858	0,0489

Table 18: List of proteins classified as "Treatment" (N=12). The UniProt ID, the gene name and the number of unique peptides is presented. P-values are based on the results of the non-parametric t-test. Av= average

Treatment (N=12)			CTRL	BRT	ART	CTRL/BRT	CTRL/ ART	BRT/ART
UniProt ID	**Gene name**	**Peptide count**	**Av**	**Av**	**Av**	**p-value**	**p-value**	**p-value**
P02788	LTF	67	7,9997	8,3051	9,3491	0,4533	4,9E-05	0,0263
P80188	LCN2	12	4,5977	5,1563	5,9632	0,0987	0,0003	0,0330
P40394	ADH7	9	2,3808	2,2277	1,4553	0,3494	0,0003	0,0014
P01037	CST1	7	6,9349	6,0232	3,8742	0,2086	0,0010	0,0286
O00391	QSOX1	4	-0,6509	-0,5207	0,1155	0,6292	0,0014	0,0396
P81605	DCD	1	-3,6862	-3,4886	-2,2187	0,6525	0,0027	0,0123
Q99497	PARK7	1	-2,0766	-1,4842	-0,9590	0,0779	0,0029	0,0327
Q15782	CHI3L2	2	-2,3606	-1,9381	-0,5433	0,4106	0,0056	0,0247
P40925	MDH1	4	0,8564	0,8787	1,2743	0,8739	0,0107	0,0086
P62857	RPS28	1	2,6190	2,9632	-0,6608	0,7824	0,0317	0,0146
P0DOX7	N/A	2	-1,9353	-1,5009	-0,6977	0,3636	0,0171	0,0475
Q9NSB2	KRT84	12	1,6169	1,0094	0,1285	0,3021	0,0176	0,0482

Table 19: List of proteins classified as "Progress" (N=3). The UniProt ID, the gene name and the number of unique peptides is presented. P-values are based on the results of the non-parametric t-test. Av= average

Progress (N=3)			CTRL	BRT	ART	CTRL/BRT	CTRL/ART	BRT/ART
UniProt ID	**Gene name**	**Peptide count**	**Av**	**Av**	**Av**	**p-value**	**p-value**	**p-value**
P19013	KRT4	63	10,7770	9,3177	7,9647	0,0001	0,0007	0,0491
P01011	SERPINA3	8	1,2344	2,2500	3,2606	0,0016	0,0005	0,0408
Q8TAX7	MUC7	2	2,2187	0,9080	-0,3353	0,0082	0,0006	0,0454

Subsequently, the four classes of proteins were submitted to STRING analysis and functional enrichment analysis to investigate the possible presence of biological processes related to them. The network generated by the proteins included in the categories "CTRL vs Cancer" and "Progress" did not show significant interactions, this does not necessarily mean that it is not a biologically meaningful selection of proteins, it could be that their interactions might not yet be known to STRING.

Figure 48 **a)** shows the protein interaction network created with the group of proteins classified as "Reversed", while ***Figure 48*** **b)** represents the network constructed with the group of proteins belonging to the class "Treatment".

The salivary proteins renamed “Reversed” are partially biologically connected (PPI enrichment p-value was 0.0359). The enrichment analysis revealed that two of the target proteins, in particular PPBI and HSPE1, were related to the chaperone-mediated protein folding biological process (GO term: 0061077, 2 of 63 counts in the gene set, FDR=0.0036) and to the unfolded protein binding concerning the molecular function (GO term: 0051082, 2 of 106 counts in the gene set, FDR=0.0032).

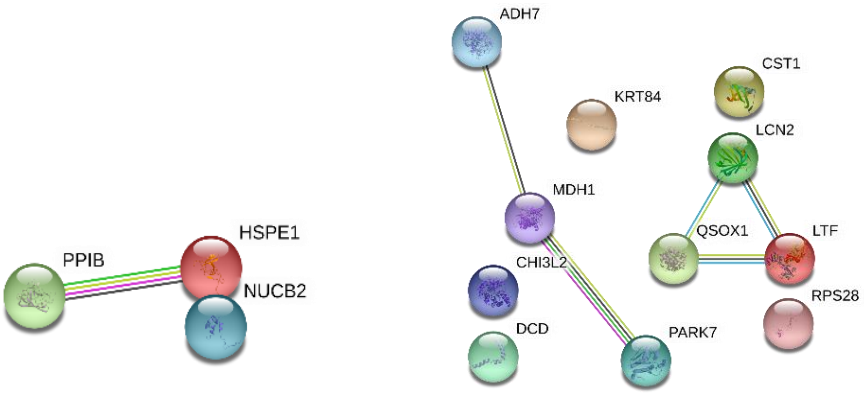

a) b)

Figure 48 a) & b): The protein interaction network of the salivary proteins included in the classes named “Reversed” (a) and “Treatment” (b). Target proteins were displayed by STRING 11.0 using default settings and medium stringency. Each node represents a protein and the edges represent protein-protein interactions based on different levels of evidence calculated by STRING.

The other group of proteins renamed “Treatment” were significantly interconnected as well (PPI enrichment p-value was 0.00122). The enrichment analysis indicated that the proteins were biologically related to antimicrobial humoral response, antibiotic metabolic process and defence response to other organisms, i.e., fungus or Gram-negative bacterium. Regarding the cellular component analysis, the majority were located in the extracellular region, secreted outside the cell membrane.

2.6 Identification of putative proteomic biomarkers for HNC

Proteomic discovery experiments are rapidly generating lists of putative biomarkers for diseases and pathologies. To identify the salivary proteins that could be used to distinguish HNC cases from controls, and cancer patients who have not yet been treated from those who have already been treated with radiotherapy, ROC analysis for individual markers was carried out. ROC curves analysis was performed to assess the biomarker potential of the differentially expressed proteins obtained from the comparisons between the groups (ARTvsBRT, CTRLvsBRT, CTRLvsART). Frequently, there are more than two states to be differentiated. However, the clinical question can often (but not always) be dichotomized where the objective is to separate patients into two groups based on the presence or absence of a certain disease or condition.

Among the salivary proteins differentially expressed in saliva of HNC patients evaluated before and after RT treatment (Group2-ART vs Group1-BRT) (**Table 20**), there are two proteins with a good predictive potential. The highest predictive value was reached by Lactotransferrin (gene LTF product) with an AUC of 0.86 (***Figure 49 a***), followed by Nucleobindin-2 (gene NUCB2 product) with an AUC of 0.83 (***Figure 49 b***). Although, it is important to underline that the majority of the proteins showed an AUC > 0.7.

Table 20: AUC values of the proteins differentially expressed (N=21) in saliva of HNC patients evaluated before and after RT treatment (Group2-ART vs Group1-BRT). The UniProt ID, the gene name, the protein name and the number of unique peptides is presented. To determine if a given biomarker was informative in discriminating compared groups from each other we considered an AUC > 0.7.

UniProt ID	Gene name	Proteine name	Peptide count	AUC ARTvsBRT
P02788	LTF	Lactotransferrin	67	0,86
P22079	LPO	Lactoperoxidase	26	0,70
P01037	CST1	Cystatin-SN	7	0,68
P0DOX7	N/A	Immunoglobulin kappa light chain	2	0,74
Q9NSB2	KRT84	Keratin, type II cuticular Hb4 (Keratin-84)	12	0,76
P80188	LCN2	Neutrophil gelatinase-associated lipocalin	12	0,78
P80303	NUCB2	Nucleobindin-2	3	0,83
Q9Y6N5	SQOR	Sulfide quinone oxidoreductase, mitochondrial	3	0,74
P39019	RPS19	40S ribosomal protein S19	1	0,84
Q14914	PTGR1	Prostaglandin reductase 1	2	0,81
P81605	DCD	Dermcidin	1	0,81
A0A0B4 /J1V0	IGHV3-15	Immunoglobulin heavy variable 3-15	1	0,74
P15515	HTN1	Histatin-1	2	0,72
Q15782	CHI3L2	Chitinase-3-like protein 2	2	0,79
P49720	PSMB3	Proteasome subunit beta type-3	1	0,72
P19105	MYL12A	Myosin regulatory light chain 12A	1	0,76
P35237	SERPINB6	Serpin B6	1	0,69
P22352	GPX3	Glutathione peroxidase 3	3	0,64
Q9UFN0	NIPSNAP3A	Protein NipSnap homolog 3A	1	0,78
Q53RT3	ASPRV1	Retroviral-like aspartic protease 1	1	0,74
P62857	RPS28	40S ribosomal protein S28	1	0,81

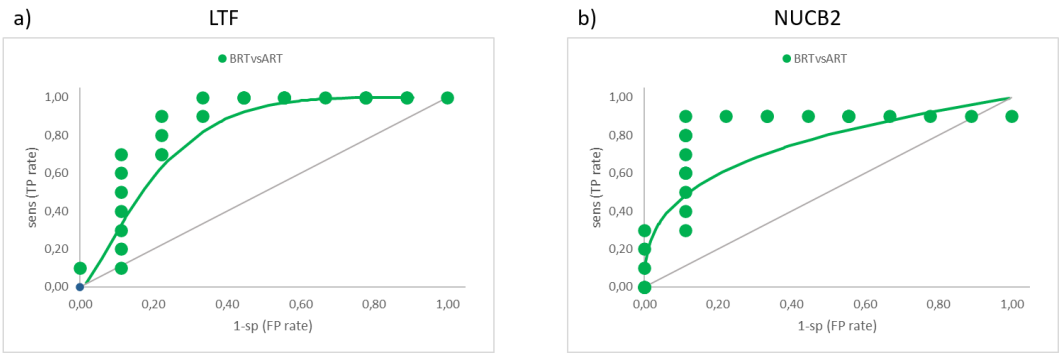

Figure 49: ROC curve analysis of a) LTF (AUC-value = 0.86) and b) NUCB2 (AUC-value = 0.83). Both salivary proteins were differentially expressed in saliva of HNC patients evaluated before and after RT treatment (BRT vs ART).

Regarding the proteins differentially expressed obtained by matching the healthy subjects with the HNC patients examined before RT treatment (Group3-CTRL vs Group1-BRT) (**Table 21**), gene AGAPAT1 product had the best predictive accuracy (AUC-value = 1, ***Figure 50 a***) but also gene SERPINA3 product (AUC-value = 0.93, ***Figure 50 b***) and gene BPIFA1 product (AUC-value = 0.88, ***Figure 50 c***) showed important predictive values. In this case, none of the proteins identified exhibited an AUC < 0.7.

Table 21: AUC values of the salivary proteins differentially expressed (N=11) between the healthy subjects and the HNC patients examined before RT treatment (Group3-CTRL vs Group1-BRT). The UniProt ID, the gene name, the protein name and the number of unique peptides is presented. To determine if a given biomarker was informative in discriminating compared groups from each other we considered an AUC > 0.7.

UniProt ID	Gene name	Protein name	Peptide count	AUC CTRLvsBRT
P19013	KRT4	Keratin, type II cytoskeletal 4	6	0,87
P12035	KRT3	Keratin, type II cytoskeletal 3	3	0,87
P01011	SERPINA3	Alpha-1-antichymotrypsin	1	0,93
P43490	NAMPT	Nicotinamide-phosphoribosyltransferase	3	0,76
P15104	GLUL	Glutamine synthetase	8	0,71
Q9NP55	BPIFA1	BPI fold-containing family A member 1	4	0,88
P61106	RAB14	Ras-related protein Rab-14	6	0,79
P48594	SERPINB4	Serpin B4	8	0,80
P21926	CD9	CD9 antigen	2	0,88
P20292	ALOX5AP	Arachidonate 5-lipoxygenase-activating protein	4	0,88
Q99943	AGPAT1	1-acyl-sn-glycerol-3-phosphate acyltransferase alpha	2	1,00

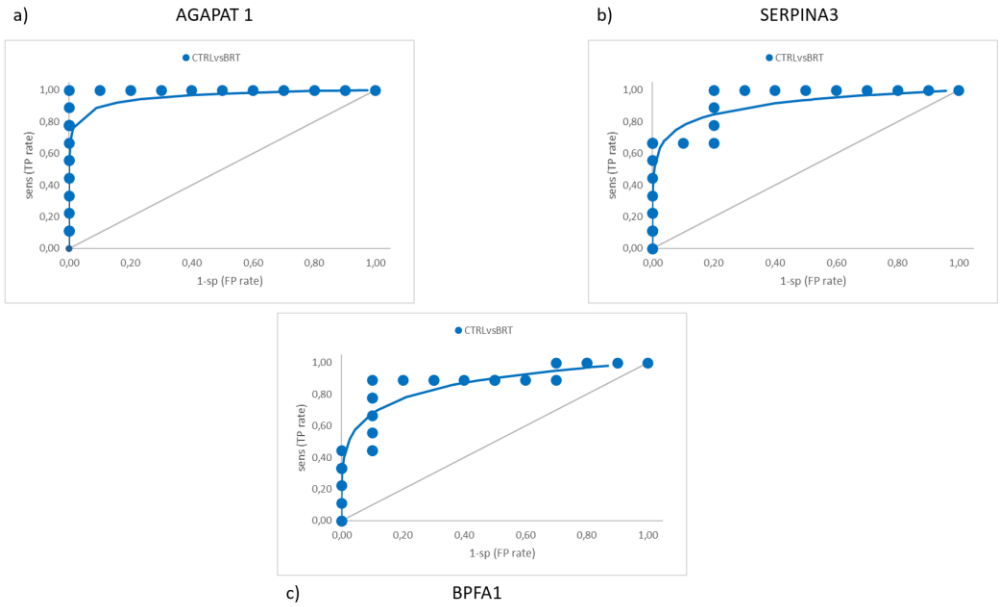

Figure 50: ROC curve analysis of salivary a) AGAPAT1 (AUC-value = 1), b) SERPINA3 (AUC-value = 0.93), c) BPFA1 (AUC-value = 0.88). Proteins analysed were differentially expressed within the healthy subjects and the HNC patients examined before the irradiation treatment (CTRL vs BRT).

Finally, concerning the salivary proteins differentially expressed between the healthy subjects and the HNC patients examined after RT treatment (Group3-CTRL vs Group2-ART) (**Table 22**), gene SERPINA3 product and gene AGPAT1 product had the best predictive accuracy (AUC-value = 1, ***Figure 51 a & b***), followed by gene LTF product (AUC-value = 0.97, ***Figure 51 c***) and gene LCN2 product (AUC-value = 0.93, ***Figure 51 d***). Of note, SERPINA3 and AGPAT1 were also the top proteins identified for discriminating the control group from the HNC patients evaluated before RT (**Table 21**), while LTF was the protein with the highest predictive value for discriminating HNC patients who have not yet been treated from those who have already been treated with radiotherapy (**Table 20**).

.

Table 22: List of the AUC values of the salivary proteins differentially expressed (N=12) between the healthy subjects and the HNC patients examined after RT treatment (Group3-CTRL vs Group2-ART). The UniProt ID, the gene name, the protein name and the number of unique peptides is presented. To determine if a given biomarker was informative in discriminating compared groups from each other we considered an AUC > 0.7.

UniProt ID	Gene name	Protein name	Peptide count	AUC CTRLvsART
P02788	LTF	Lactotransferrin	67	0,97
P01037	CST1	Cystatin-SN	7	0,90
P80188	LCN2	Neutrophil gelatinase-associated lipocalin	12	0,93
P01011	SERPINA3	Alpha-1-antichymotrypsin	8	1,00
Q8N4F0	BPIFB2	BPI fold-containing family B member 2	11	0,88
Q8TAX7	MUC7	Mucin-7	2	0,81
P06312	IGKV4-1	Immunoglobulin kappa variable 4-1	3	0,86
P31944	CASP14	Caspase-14	1	0,86
P49720	PSMB3	Proteasome subunit beta type-3	1	0,81
Q9Y2V2	CARHSP1	Calcium-regulated heat-stable protein 1	2	0,80
P20292	ALOX5AP	Arachidonate 5-lipoxygenase-activating protein	2	0,90
Q99943	AGPAT1	1-acyl-sn-glycerol-3-phosphateacyltransferase alpha	1	1,00

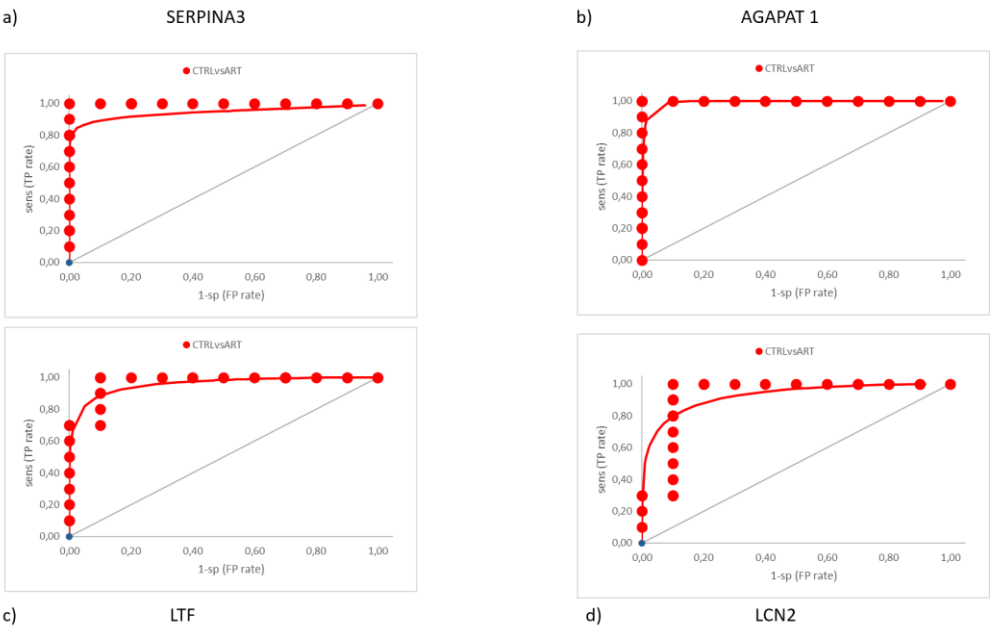

Figure 51: ROC curve analysis of salivary a) SERPINA3 (AUC-value = 1), b) AGAPAT1 (AUC-value = 1), c) LTF (AUC-value = 0.97), d) LCN2 (AUC-value = 0.93). Proteins analysed showed a differential expression comparing the healthy subjects with the HNC patients examined post-RT treatment (CTRL vs ART).

Overall, results from the ROC curves analysis showed that gene SERPINA3 product and gene AGPAT1 product exhibited potentiality to serve as HNC biomarkers, being able to discriminate healthy controls from cancer patients. In addition, gene LTF product and gene NUCB2 product could help to discriminate between HNC cases pre- and post-RT treatment. In particular, NUCB2 together with HSPE1 and PPIB, the three proteins that are part of the class called “Reverted”, may be considered as putative predictive biomarkers of response to the treatment, considering the fact that the level of salivary abundance returns to their normal statement (control status) after the irradiation process. Although, no cross-validation or validation on external data was performed to support our results.

V. Discussion

1 EVALUATION OF SALIVARY INFLAMMATORY MARKERS

Nowadays many scientists emphasize the utility of salivary biomarkers in identifying and managing various diseases. In the cancer field, a series of biomolecules have been studied; among them, markers of inflammation have attracted attention given the role of inflammation in tumorigenesis (312). The tumour microenvironment consists of cancer, immune, stromal, and inflammatory cells, all of which produce cytokines, growth factors, and adhesion molecules that may promote cancer progression and metastases (268). Inflammatory responses and alterations in the immune system, play a critical role in disease progression and aggressiveness in HNC, particularly in OSCC patients (282,285,313). Since OSCC has been found to be associated with chronic inflammation, it has been shown that there is an imbalance in local and systemic immunomodulatory cytokine levels (251,272,314), leading to increased growth and proliferation of tumours and a significant reduction in tumour immunosurveillance program (315).

Our data show that cytokine levels are increased in saliva of tumour patients, which confirm previous reports from the literature. The levels of pro-inflammatory (IL-6, IL-8, TNF-α) and anti-inflammatory cytokines (IL-4, IL-10), together with the salivary chemokine MCP-1 and the vascular endothelial growth factor (VEGF) followed a similar trend, displaying an increment comparing cancer patients and controls. Although, statistical significance was confirmed only for protein concentration of IL-6. All these inflammatory markers were elevated in saliva of HNC patients evaluated before undergoing the RT treatment, indicating that may potentially be involved in disease progression and severity.

Furthermore, other investigations have described increases in salivary levels of IL-8, TNF-α and IL-6 (252,316–318) in HNSCC compared to control subjects, but did not quantify changes from pre- to post-treatment, as the present study has done. Among the studied analytes (EGF, IL-10, IL-4, IL-6, IL-8, MCP-1, TNF-α and VEGF), IL-8 and MCP-1 showed significant levels of augmentation after the ionizing radiation process,

while IL-10, IL-6 and TNF-α were also detected in higher concentration post-RT, albeit without achieving statistical significance.

Concerning the role of pro-inflammatory cytokines (IL-6, IL-8, TNF-α), there is evidence that these proteins are produced in dysregulated fashion in oropharyngeal SCC and that they have roles in growth, invasion, interruption of tumour suppression, immune status and even survival (319). IL-6 is a multifunctional cytokine that was originally characterized as a regulator of immune and inflammatory responses (320); however, under certain conditions, high levels of this molecule may lead to perturb the immune reaction (321–323). Elevated expression of IL-6 has been detected in multiple epithelial tumours (324). Many studies have documented high IL-6 levels in serum of patients with lymphoma and breast or lung carcinomas, and have correlated it with a poor clinical prognosis (319). Also, IL-6 can induce the transition from acute to chronic inflammation by recruiting monocytes to the site of inflammation through monocyte chemoattractant protein-1 (MCP-1) secretion (325), which may explain the increment of that marker levels as well. On the other hand, IL-8 plays also an important role in the acute inflammatory response and persists for a relatively long time at the site of inflammation (326). Moreover, its expression is modulated by other various stimuli such as hypoxia or steroid hormones. It binds to CRCX-1 and CRCX-2 receptors which have been identified both on inflammatory cells from the tumour-associated infiltrate and tumour cells (267,327). Besides, the pathological activity of TNF-α is a key mediator in inflammation. TNF-α is important in early events of tumours, regulating a cascade of cytokines, chemokines, adhesions, matrix metalloproteinases (MMPs) and pro-angiogenic activities (328). Thus, it may be one of the ways in which inflammation acts as a tumour promoter. There is evidence that high levels of this pro-inflammatory cytokine correlate with increased risk of mortality (319). The concurrent increase of IL-6 and IL-8 levels in post-treatment samples suggests a common regulatory mechanism, such as NF-κB, which plays an important role in development and progression of HNSCC (329). NF-κB-regulated cytokines are upregulated in saliva of HNSCC patients (252). The pattern of change evaluated in traditional pro-inflammatory cytokines may provide evidence of acute inflammation after the radiotherapy treatment (273). Both MCP-1 and IL-8 result in

inflammatory cell recruitment and may reflect local inflammation (273). This growth may be related to RT response but other factors to consider are post-radiation complications, as mucositis, which correlates with an increment in cytokines levels (330). However, in our study, there was no relation between the levels of salivary proteins and the clinical parameters regarding the treatment tolerance, especially for the variable mucositis, estimated in the group of HNC patients evaluated after the radiotherapy. Moreover, as described by *Russo et al.* (329), IL-6 levels were increased in HNSCC patients who received surgery alone suggesting that this increment could be related to an inflammatory response following the invasive procedure and not being radiation-induced.

The majority of the studies concerning cytokine imbalance in HNC and OSCC have been focused on serum and salivary pro-inflammatory molecules. Data regarding anti-inflammatory immunosuppressive cytokine levels in systemic fluids are still scarce (268). In our study, results showed a slight augmentation in the salivary expression of IL-10 and IL-4 in HNC patients not yet treated compared to healthy individuals. However, it is interesting to point out that, at the end of RT, IL-10 was found to be significantly elevated and IL-4 exhibited a minor increase in its expression, being both immunosuppressive cytokines. IL-10 works as a double-edged sword, where, on one hand, it antagonizes the tumour-promoting effects of pro-inflammatory cytokines, while, on the other hand, increase tumour growth by allowing the escape of tumour cells from immune surveillance through inhibition of lymphocytes and macrophages (314,315,331). The latter leads to immune deviation from TH1 to TH2 responses, thus preventing tumour rejection (268). Among the TH2 cytokines, IL-4 has been demonstrated to be the most critical cytokine to induce TH2 cells (332). It presents anti-angiogenic properties, which could inhibit tumour progression (333). However, IL-4 can enhance tumour growth due to its anti-apoptotic property, which helps increase tumour survival (334). The fact that this anti-inflammatory protein was found statistically significant in HNC patients, independently from the tumour site, compared to control subjects may reflect towards the fact that there is an inhibitory effect on tumour growth, while an increased tumour survival due to its anti-apoptotic property. Contrariwise, our

results concerning the IL-10 status after RT are not comparable with other investigations, since data regarding its modulation and association with treatment outcomes are not present. To date, literature available reports that high levels of salivary IL-10 are related to higher grades of mucositis in HNC patients treated with ionizing radiation (273), and that advanced stages of HNSCC presented significantly higher serum levels of this molecule, except for oral cavity tumours (335). Our findings regarding IL-10 levels in HNC patients diagnosed with a tumour located in the oral cavity region are contrary to the above-mentioned study, which may be explained by the fact that we used saliva instead of serum.

Nevertheless, is it known that ionizing radiation increases the expression of inflammatory cytokines and our results appear to be consistent with other studies supporting this statement (190,273). Finally, to determine the discriminatory efficacy and estimate the potential of the inflammatory proteins as predictive biomarkers of RT outcomes, ROC analyses were performed. Among the studied molecules, IL-8 presented an AUC value higher than 0.8, being the only salivary marker, whose *p-value* resulted statistically significant. This finding suggests that IL-8 showed a great capability to distinguish between two diagnostic status, being in our case radiotherapy responders versus non-responders. HNC patients with higher levels of IL-8 in pre-treatment samples presented a worse response to the therapy, whereas patients with decreased levels of IL-8 were associated with a better outcome. To our knowledge, the potential role of salivary IL-8 as a predictive biomarker of RT response in HNC was assessed in the present study for the first time.

HNSCC patients may develop recurrent or second primary tumours (6) highlighting the importance of permanently monitoring patients after treatment (329). Radiation, delivered alone or with chemotherapy, is frequently used in the definitive management of this kind of malignancy, being the primary treatment for advanced HNC cases. Due to concerns for healing during and after the delivery of the ionizing radiation, assessment of tumour and healthy tissue in the radiated field through biopsies or invasive techniques for correlative assays may be limited. A minimally invasive technique for sampling local effects of radiation on tumour and surrounding area may provide a method to predict which patients will develop severe toxicity or

allow earlier prognostication in the treatment course (273). When applied to a high-risk population such as HNSCC survivors, a saliva-based test utilizing a panel of biomarkers for HNSCC could provide an accurate, non-invasive and relatively inexpensive monitoring method (329). The initial step in developing such a test is characterizing changes in saliva post-treatment. Unfortunately, this has been a challenge likely due to unavailability of saliva. This xerostomia (perception of dry mouth) or salivary hypofunction (decreased salivary flow) due to destruction of salivary glands is the most common long-term complication of conventional radiation (329). The impact is usually permanent. Consequently, information about post-treatment salivary changes is sparse. IMRT minimizes normal organ exposure while delivering high-dose RT to a target volume, it spares salivary glands and is associated with preferential recovery of stimulated saliva whereas unstimulated volumes remain depressed (14,329). Thus, to maximize the likelihood of detecting changes from pre- to post-treatment, we used stimulated saliva. Certainly, a significant advantage of the current study was the longitudinal design, i.e., pre- and post-treatment comparison of the same patient. Most investigations of cancer biomarkers in saliva used a cross-sectional design, making pre-treatment comparisons only to healthy controls. While a limitation of this research was the timing of the post-treatment specimen's collection, the salivary markers were measured in a range of 4/8 weeks after the irradiation process due to the expected inflammatory sequels subsequent the therapy. The period was arbitrary chosen to avoid those side effects, even so, we can't be fully confident on the fact that all the patients were at the same health status at the time of collection. Given the small sample size, we have to assume that these are preliminary results and need to be validated in a large cohort of patients. Although saliva exhibits protein changes in response to HNC (336) and RT treatment (190,273), the mechanism needs to be further evaluated. Our data do not provide definitive conclusions but evidence about whether the significant changes reported are worthy of further exploration.

2 EVALUATION OF THE SALIVARY PROTEOME

Proteins are attractive as potential biomarkers due to the fact that they participate more arguably in cellular activities than DNA and RNA. In particular, proteins which are regulatory molecules in relevant cellular pathways have more chances to be considered as ideal biomarkers (249). Saliva contains more than 2000 proteins that are involved in many biological functions to maintain oral homeostasis (292). The evaluation of salivary biomarkers alterations can be applied to the early detection, risk assessment, diagnosis, prognosis and monitoring of the progress of a variety of diseases, including cancers, infectious and immune pathologies (292). A number of studies have been carried out using various proteomic approaches to identify potential biomarkers for OSCC (249,287,288), although comparative proteomic analysis of HNC patients evaluated pre- and post-oncologic treatment have not been deeply investigated, literature available is still scarce. In our study, human whole saliva was analysed with the primary aim to recognise putative markers associated with RT response and also proteins with the capability to distinguish between healthy controls and HNC patient's proteome profiles. Results confirmed the possibility of utilizing the salivary proteome for the discovery of HNC potential biomarkers, but cross-validation or validation on external data needs to be performed to support our conclusions.

Regarding the investigation of potentially predictive biomarkers of RT outcomes, this study showed that 21 proteins were differentially expressed between the salivary proteome profiles of the HNC patients evaluated before and after the RT, demonstrating their ability to discriminate between pre- and post-treatment status. Among them, gene NUCB2 product (Nucleobindin-2) attracted much attention due to the specific trend followed. This molecule was not only able to distinguish the HNC patients who have already been irradiated from those who not, but also the control subjects from the cancer patients. Together with other two proteins, Peptidyl-prolyl cis-trans isomerase B (gene PPIB product) and 10 kDa heat shock protein (gene HSPE1 product), these molecules, classified as "Reversed", shared the same pattern, being differentially expressed in cancer patients not yet treated (BRT group) and returning to their normal condition (control status) after the RT. Taking into consideration these

findings, we postulated that this class of proteins may be potentially correlated with a favourable RT response. NUCB2 was previously identified in saliva of OSCC patients (288,337) and the salivary levels of HSPE1 were found statistically significant in HNC patients who developed oral mucositis after receiving primary or adjuvant radiochemotherapy (185). No data were found on the presence of PPIB in HNC; however, results from the enrichment analysis revealed that PPBI and HSPE1 partake in the same biological process and the same molecular function, being related to the chaperone-mediated protein folding.

Concerning the investigation of the salivary proteome profiles between control subjects and HNC patients, significant differences were detected among them. Results obtained from the comparison between the control group and the cancer patients not yet treated revealed a differential expression of 11 proteins. Among the proteins significantly overrepresented in those patients, gene AGPAT1 product (1-acyl-sn-glycerol-3-phosphate acyltransferase Alpha), gene SERPINA3 product (Alpha-1-antichymotrypsin) and gene BIPIFA1 product (BPI fold-containing family A member 1) presented the best diagnostic accuracy in discriminating between cancer patients and healthy controls. Gene SERPINA3 product, a protease inhibitor, and gene BIPIFA2 product, another protein from the same family member connected to immune response and defence, were already identified in saliva of OSCC samples by *Csősz et al.* (288). Concerning AGPAT1, the first of 11 human AGPAT isoforms acting as intermediate enzymes in the pathway for the biosynthesis of glycerophospholipids (GPL) and triacylglycerol (TAG), no association with HNC was found so far. In particular, gene AGPAT1 product encodes an enzyme that converts lysophosphatidic acid (LPA) into phosphatidic acid (PA), phospholipids involved in signal transduction and lipid biosynthesis. Metabolic reprogramming is firmly established as a hallmark of cancer (7) and lipid metabolism plays an essential role in carcinogenesis due to the requirements of tumoral cells to sustain increased structural, energetic and biosynthetic precursor demands for cell proliferation (338). These findings may help to explain the increased levels of this protein in saliva of cancer patients.

Afterwards, we focused on the differences in the salivary proteome findings among the HNC patients analysed post-RT treatment and the control subjects. The

comparison between the groups showed that 12 proteins appeared differentially expressed, 10 resulted up-regulated and 2 down-regulated referring to the group of healthy volunteers, in particular Cystatin-SN (gene CST1 product) and Mucin-7 (gene MUC7 product). Cystatins constitute a large group of related proteins with diverse biological activities. Initially, they were characterized as inhibitors of lysosomal cysteine proteases – cathepsins. Cathepsins are involved in processing and presentation of antigens, as well as several pathological conditions such as inflammation and cancer (339). Human saliva appears to contain several cysteine proteinase inhibitors that are immunologically related to cystatin S but that differ in their specificity due to amino acid sequence differences. Salivary cystatin S is a defence protein mainly produced by submandibular glands and involved in innate oral immunity (340). Recently, this molecule appeared significantly decreased in primary Sjogren's syndrome (pSS) and positively correlated with unstimulated salivary flow rate (340). Since pSS is characterized by chronic inflammation and dysfunction of salivary and lacrimal glands and taking into consideration the ionizing radiation sequels on the oral cavity and particularly on the salivary glands, we may postulate that the down-regulation of CST1 in HNC patients after RT could be related to them. However, our results differ from the investigation of *Ohshiro et al.* (341) where cystatin S was detected in saliva of healthy donors and not in HNC patients.

Mucins are one of the major components of saliva, comprising nearly 20% of the whole proteins (342). They are high-molecular weight glycoproteins secreted from sublingual, submandibular and minor salivary glands, acting like potent lubricants and providing an effective barrier against oral dryness. Currently, a heterogeneous group of 20 structurally-unique human mucins has been distinguished, from which the presence of MUC5B, MUC7, MUC19, MUC1 and MUC4 has been demonstrated in sputum (343). MUC5B, MUC7 and MUC19 represent a subgroup of secreted mucins, while MUC1 and MUC4 represent membrane-associated mucins. Over the past decade, much attention has been focused on the involvement of these molecules in tumour carcinogenesis and metastasis. Mucins play an important role in cell-cell adhesion, immune response and alteration of intracellular signalling. However, the tightly regulated homeostatic expression may be disrupted by various factors such as

cancer cells. Results from the meta-analysis conducted by *Lu et al.* (344) suggested that aberrant MUC expression may be predictive biomarkers in HNC. In particular, the elevated expression of MUC1 and MUC4 was significantly associated with worse prognosis and more detrimental clinicopathological outcomes (344). No data were found on the salivary expression of MUC7 in HNC patients, even though, we may hypothesize that the decrement observed after the irradiation therapy may be involved in the presence of one of the sequels associated to the treatment, knowing that reduced concentrations of MUC5B and MUC7 are linked to development of dental caries (343). Besides, Mucin-7 is part of the group of proteins classified as "Progress", together with gene KRT4 product (Keratin, type II cytoskeletal 4) and gene SERPINA3 product, being differentially expressed in HNC patients evaluated before RT but even more representative after the treatment. Gene KRT4 product was already identified as a protein expressed in saliva samples of HNSCC patients (234). KRT4 is a member of the keratin gene family, this type II cytokeratin is specifically expressed in differentiated layers of the mucosal and oesophageal epithelia with family member KRT13 (345). These two molecules, KRT4 and MUC7, were able to discriminate 1) controls from HNC patients before and after the irradiation process, and 2) cancer patients not yet treated from those who have already been submitted to RT, even though with less diagnostic accuracy than gene SERPINA3 product.

SERPINA3 (Serpin peptidase inhibitor, clade A member 3), is a member of the serpin superfamily of protease inhibitors and was previously known as α1-antichymotrypsin (346). It is a secreted serine protease inhibitor normally produced by the liver, which proteolytically inhibits the activation of several serine proteases including chymotrypsin and cathepsin G (347). Also, this acute phase reactant protein is involved in cytokinesis, proliferation, apoptosis and tumour metastasis (348). Its aberrant expression has been observed in various tumours but not yet in HNC. Specifically, an overexpression of gene SERPINA3 product is documented in melanoma (347), endometrial cancer (349), lung cancer (350), colon cancer (351), breast cancer(352) and hepatocellular carcinoma (348). In our study, its expression appeared up-regulated in HNC patients evaluated before RT treatment, which may explain an important role in cancer progression, but its overexpression was observed

also after the irradiation therapy, suggesting a probable association with inflammatory and immune response.

Furthermore, in the class of molecules named “Treatment”, there were two proteins, gene LTF product (Lactotransferrin) and gene LCN2 product (Neutrophil gelatinase-associated lipocalin), that were differentially expressed in saliva of HNC patients before the irradiation therapy but appeared even more expressed after it. This observation suggests that the upregulation of these molecules was mainly caused by ionizing radiation and not only from the cancer presence.

Among the salivary proteins, Lactotransferrin is the most important factor of natural immunity (353). It is an iron-binding glycoprotein belonging to the transferrin family, a component of human secretions particularly expressed in exocrine fluids as tears or saliva (354), and it is synthesized by exocrine glands and neutrophils in infection/inflammation sites. The first function attributed to Lactotransferrin was antibacterial activity depending on its ability to sequester iron necessary for bacterial growth and survival but it has a wide variety of physiological functions including, antioxidant activities, neuroprotective properties, regulation of the immune response, anti-inflammatory and anti-carcinogenic potential (354,355). Its concentration in oral cavity is influenced by different factors but it mainly depends on the amount of the excreted fluid, which, in turn, depends on the physiological or pathological status of the subject (353). Thus, Lactotransferrin concentration in human exocrine secretions may increase in infection and/or inflammation sites due to the recruitment of neutrophils.

Gene LCN2 product (Neutrophil gelatinase-associated lipocalin also known as Lipocalin-2) is a protein that belongs to the lipocalin family and their members transport small hydrophobic molecules such as lipids, steroid hormones and retinoids. It plays a role in innate immunity by limiting bacterial growth as a result of sequestering iron-containing siderophores (345). Lipocalins are upregulated in a number of pathological conditions and may function as transporters of essential factors and regulators of cell homoeostasis and the modulation of the immune response (356). They affect cellular proliferation and differentiation, and may be involved in the development of tumours (357). In the literature is described that in

different cancer high expression of Lipocalin-2 was observed, including breast, colorectal, pancreatic and ovarian carcinomas (358,359). In head and neck tumours, *Hiromoto et al.* (360) found that LCN2 expression was strongly upregulated in well-differentiated OSCC tissues and slightly to weakly upregulated in moderately to poorly differentiated OSCC tissues, while its expression was weak or very weak in normal mucosa and leukoplakia. In our case, the salivary expression of Lipocalin-2 increased from controls to cancer patients, to reach the overexpression in the HNC patients after the RT treatment. To date, the functional role of LCN2 in the progression of OSCC, which accounts for most head and neck cancers, remains poorly understood. However, considering that Lipocalin-2 is also an iron-binding protein involved in the innate immune system and is particularly responsible for the activation of neutrophils (361), our results regarding the upregulation of this protein together with the above-mentioned Lactotransferrin, may have the same hypothetical explanation. Our data showed that both salivary protein profiles after the RT changed even more respect to the pattern observed in presence of the tumour, exhibiting an increase in its expression that may be putatively correlated to the presence of inflammatory processes or abnormal activity of polymorphonuclear leukocytes in the tumour microenvironment after the irradiation process.

The potential of differently expressed saliva proteins as useful complementary biomarkers for the early detection and/or monitoring of OSCC has already been studied extensively *Yakob et al.* (362) provide a survey of numerous studies which observed differences in the salivary proteome profile of OSCC patients and OSCC-free controls (362), also emphasizing a potential role of matrix metalloproteinases (MMPs). In our study, not the matrix metalloproteinase family but one of the natural inhibitors of the MMPs, namely tissue inhibitors of metalloproteinases (TIMPs) was identified as a protein displaying significantly different levels in HNC patients when compared with healthy controls. MMPs are involved in the breakdown of extracellular matrix such as embryonic development and tissue remodelling, as well as in disease processes, like arthritis and metastasis (363). In 2011, *Stott-Miller et al.* (364) tested MMP1 and MMP3 levels in saliva samples of 100 subjects (60 primary OSCC cases, 15 dysplasia cases, and 25 controls) and the results showed that the

salivary concentration of both proteins was higher in saliva of OSCC patients compared to the healthy subjects. In our study MMPs were not detected, but TIMP1 was found to be present at increased levels in the HNC group evaluated before the treatment. The activities of MMPs in body tissues, such as the periodontium, are regulated by TIMPs (363). TIMP-1 is the most common inhibitor, which is secreted by the regional cells of the periodontium (fibroblasts, keratinocytes and endothelial cells) and by the migratory cells of the inflammatory infiltrate (monocytes/macrophages) (363). The balance between activated MMPs and TIMPs controls the extent of extracellular matrix (ECM) remodelling. As consequence, an imbalance between them may lead to excessive degradation of ECM proteins (365) and abnormal ECM dynamics are linked to tissue fibrosis of many organs, chronic inflammation and are a hallmark of cancer (366).

Another important point of this discussion is that the salivary protein profiles may also reflect the presence of other oral pathologies after the ionizing radiation, such as periodontitis or dental caries. Since poor oral hygiene is a common factor in HNC patients (234), concomitant pathological processes may modify the protein levels in saliva of these subjects. In our study, this finding may be confirmed by the presence, in the salivary proteome profiles of the HNC patients post-RT, of specific molecules like mucins, cystatins and lactoferrin, all involved in dental pathologies and already identified by previous studies (367). Furthermore, the investigation of *Jehmlich et al.* (185) regarding the changes between the salivary proteome profiles of HNC patients undergoing radiotherapy, showed that there are other proteins linked to the side effects of the treatment, in particular related to the development of oral mucositis (OM). Among them, the proteins overexpressed in saliva of HNC patients with OM included proteinase 3 (PRTN3), fibrinogen beta chain (FGB), matrix metalloproteinases 8 and 9 (MMP-8 and MMP-9), ceruloplasmin (CP) and complement C3 (C3), whereas the proteins that displayed lower levels of expression in patients later or not developing OM included 60S ribosomal protein L18a (RPL18A), metalloproteinase inhibitor 1 (TIMP1) and prostaglandin reductase 1 (PTGR1) (185). Interestingly, none of the upregulated proteins was detected in our study, but two of

the downregulated proteins, TIMP1 and PTGR1, were also differentially expressed in our group of HNC patients evaluated before the RT.

In conclusion, in the present study, we comparatively analysed the salivary proteome profiles of healthy volunteers and HNC patients evaluated pre- and post-RT treatment to determine possible modifications between them. To the best of our knowledge, this is one of the few investigations on the discovery of HNC biomarkers in which profiling of salivary proteome aims to prioritize predictive instead of diagnostic or prognostic candidates, that are worthy to be further evaluated and validated.

VI. Conclusions

Based on the results obtained from the investigation of the salivary inflammatory markers and the evaluation of the salivary proteome, we can conclude that:

I. The ionizing radiation affects the salivary expression of pro-inflammatory and anti-inflammatory cytokines, chemokines and growth factors. The levels of IL-8 and MCP-1 significatively increase in saliva of HNC patients analysed after the radiotherapy treatment.

II. In saliva of HNC patients evaluated before the irradiation therapy, there is a significant augmentation of IL-6 levels and a general increase of all the salivary inflammatory markers. The increment can be associated with the presence of the tumour lesion.

III. No relation was found between the altered salivary inflammatory markers and the development of oral mucositis in the cohort of HNC patients already treated with RT. Although, this relationship may do not exist due to the limited number of samples used for the analysis.

IV. IL-8 has a strong potential as salivary predictive biomarker of RT outcomes in HNC patients. Decreased levels of this molecule in saliva of cancer patients before receiving the irradiation therapy are linked to positive treatment response.

V. Differences are observed in the salivary proteome of HNC patients undergoing radiotherapy, before and after the treatment, as well as when comparing them with the control group.

VI. Among the salivary proteome profiles of the HNC patients analysed pre- and post-RT, a total of 21 proteins results differentially expressed. The majority of these target proteins are biologically related to immune response and inflammation.

VII. Between the salivary markers identified, gene NUCB2 product, gene PPIB product and gene HSPE1 product are associated with favourable RT outcomes and may be considered as potential predictive biomarkers of response to the treatment. Gene LTF product is able to discriminate between HNC cases pre- and post-irradiation therapy, while gene SERPINA3 product and gene AGPAT1 product are related to the presence of HNC.

VII. References

1. Zou H, Hastie T. Regularization and variable selection via the elastic net. J R Stat Soc Ser B (statistical Methodol. 2005);67(2):301–20.

2. Benjamini Y, Drai D, Elmer G, Kafkafi N, Golani I. Controlling the false discovery rate in behavior genetics research. Behav Brain Res. 2001;125(1–2):279–84.

3. Ferris RL. Immunology and immunotherapy of head and neck cancer. J Clin Oncol. 2015;33(29):3293–304.

4. Bray F, Ferlay J, Soerjomataram I, Siegel RL, Torre LA, Jemal A. Global cancer statistics 2018: GLOBOCAN estimates of incidence and mortality worldwide for 36 cancers in 185 countries. CA Cancer J Clin. 2018;68(6):394–424.

5. Hanahan D, Weinberg RA. The Hallmarks of Cancer. Cell. 2000;100(1):57–70.

6. Leemans CR, Braakhuis BJM, Brakenhoff RH. The molecular biology of head and neck cancer. Nat Rev Cancer. 2011;11(1):9–22.

7. Hanahan D, Weinberg RA. Hallmarks of cancer: The next generation. Cell 2011;144(5):646–74.

8. Burkhart DL, Sage J. Cellular mechanisms of tumour suppression by the retinoblastoma gene. Nat Rev Cancer. 2008;8(9):671–82.

9. Hayflick L. Mortality and immortality at the cellular level. A review. Biochem. 1997;

10. Shay JW, Bacchetti S. A survey of telomerase activity in human cancer. Eur J Cancer Part A. 1997;

11. J. F. Fundamental concepts of the angiogenic process. Curr Mol Med. 2003;

12. Talmadge JE, Fidler IJ. AACR centennial series: the biology of cancer metastasis:

historical perspective. Cancer Res. 2010;70(14):5649–69.

13. Grivennikov SI, Greten FR, Karin M. Immunity, Inflammation, and Cancer. Cell. 2010.

14. Lo Nigro C, Denaro N, Merlotti A, Merlano M. Head and neck cancer: Improving outcomes with a multidisciplinary approach. Cancer Manag Res. 2017;9:363–71.

15. Warnakulasuriya S. Global epidemiology of oral and oropharyngeal cancer. Oral Oncol. 2009 Apr 1;45(4–5):309–16.

16. Vigneswaran N, Williams MD. Epidemiologic trends in head and neck cancer and aids in diagnosis. Oral and Maxillofacial Surgery Clinics of North America. 2014.

17. Pulte D, Brenner H. Changes in survival in head and neck cancers in the late 20th and early 21st century: a period analysis. Oncologist 2010;15(9):994–1001.

18. Ferlay J, Steliarova-Foucher E, Lortet-Tieulent J, Rosso S, Coebergh J-WW, Comber H, et al. Cancer incidence and mortality patterns in Europe: estimates for 40 countries in 2012. Eur J Cancer. 2013;49(6):1374–403.

19. Gupta N, Gupta R, Acharya AK, Patthi B, Goud V, Reddy S, et al. Changing Trends in oral cancer – a global scenario. Nepal J Epidemiol. 2017 May 1;6(4):613–9.

20. Siegel R, Naishadham D, Jemal A. Cancer statistics, 2013. CA Cancer J Clin [Internet]. 2013/01/17. 2013 Jan;63(1):11–30.

21. Sturgis EM, Cinciripini PM. Trends in head and neck cancer incidence in relation to smoking prevalence: An emerging epidemic of human papillomavirus-associated cancers? Cancer. 2007.

22. Ramqvist T, Dalianis T. Oropharyngeal cancer epidemic and human papillomavirus. Emerg Infect Dis. 2010;

23. Heroiu Cataloiu A-D, Danciu CE, Popescu CR. Multiple cancers of the head and neck. Maedica (Buchar) 2013;8(1):80–5.

24. Pai SI, Westra WH. Molecular pathology of head and neck cancer: implications for diagnosis, prognosis, and treatment. Annu Rev Pathol 2009;4:49–70.

25. Cantu G, Solero CL, Mariani L, Lo Vullo S, Riccio S, Colombo S, et al. Intestinal type adenocarcinoma of the ethmoid sinus in wood and leather workers: a retrospective study of 153 cases. Head Neck 2011 Apr;33(4):535–42.

26. Cyprian FS, Al-Farsi HF, Vranic S, Akhtar S, Al Moustafa AE. Epstein-Barr virus and human papillomaviruses interactions and their roles in the initiation of epithelial-mesenchymal transition and cancer progression. Front Oncol. 2018;8(MAY).

27. Jethwa AR, Khariwala SS. Tobacco-related carcinogenesis in head and neck cancer. Cancer Metastasis Rev. 2017;

28. Hashibe M, Brennan P, Chuang SC, Boccia S, Castellsague X, Chen C, et al. Intera1. Hashibe M, Brennan P, Chuang SC, Boccia S, Castellsague X, Chen C, et al. Interaction between tobacco and alcohol use and the risk of head and neck cancer: Pooled analysis in the international head and neck cancer Epidemiology consortium. Cancer . Cancer Epidemiol Biomarkers Prev. 2009;

29. Hashibe M, Brennan P, Benhamou S, Castellsague X, Chen C, Curado MP, et al. Alcohol drinking in never users of tobacco, cigarette smoking in never drinkers, and the risk of head and neck cancer: pooled analysis in the International Head and Neck Cancer Epidemiology Consortium. J Natl Cancer Inst 2007 May 16;99(10):777–89.

30. Boing AF, Antunes JLF, de Carvalho MB, de Góis Filho JF, Kowalski LP, Michaluart Jr P, et al. How much do smoking and alcohol consumption explain socioeconomic inequalities in head and neck cancer risk? J Epidemiol Community Health 2011 Aug;65(8):709–14.

31. Dhull AK, Atri R, Dhankhar R, Chauhan AK, Kaushal V. Major Risk Factors in Head and Neck Cancer: A Retrospective Analysis of 12-Year Experiences. World J Oncol. 2018;9(3):80–4.

32. D'Souza G, Kreimer AR, Viscidi R, Pawlita M, Fakhry C, Koch WM, et al. Case–Control Study of Human Papillomavirus and Oropharyngeal Cancer. N Engl J Med 2007 May 10;356(19):1944–56.

33. Gillison ML, D'Souza G, Westra W, Sugar E, Xiao W, Begum S, et al. Distinct Risk Factor Profiles for Human Papillomavirus Type 16–Positive and Human Papillomavirus Type 16–Negative Head and Neck Cancers. JNCI J Natl Cancer Inst 2008 Mar 19;100(6):407–20.

34. Tian S, Switchenko JM, Jhaveri J, Cassidy RJ, Ferris MJ, Press RH, et al. Survival outcomes by HPV status in non-oropharyngeal head and neck cancers: A propensity score matched analysis of population level data. J Clin Oncol 2018 May 20;36(15_suppl):6005.

35. Young LS, Dawson CW. Epstein-Barr virus and nasopharyngeal carcinoma. Chin J Cancer 2014 Dec;33(12):581–90.

36. Alter BP, Joenje H, Oostra AB, Pals G. Fanconi Anemia: Adult Head and Neck Cancer and Hematopoietic Mosaicism. Arch Otolaryngol Neck Surg 2005 Jul 1;131(7):635–9.

37. Powles T, Powles J, Nelson M, Sandison A, Peston D, Buchannan J, et al. Head and neck cancer in patients with human immunodeficiency virus-1 infection: incidence, outcome and association with Epstein-Barr virus. J Laryngol Otol. 2004;118(3):207–12.

38. Purgina B, Pantanowitz L, Seethala R. A Review of Carcinomas Arising in the Head and Neck Region in HIV-Positive Patients. Patholog Res Int. 2011 May 10;2011:469150.

39. Siddiqui F, Gwede CK. Head and Neck Cancer in the Elderly Population. Semin Radiat Oncol 2012;22(4):321–33.

40. Ng J, Shuryak I. Minimizing second cancer risk following radiotherapy: current perspectives. Cancer Manag Res. 2014 Dec 17;7:1–11.

41. Bugter O, van Iwaarden DLP, Dronkers EAC, de Herdt MJ, Wieringa MH, Verduijn GM, et al. Survival of patients with head and neck cancer with metachronous multiple primary tumors is surprisingly favorable. Head Neck 2019 Jun;41(6):1648–55.

42. Chernock RD, Lewis JS. Approach to metastatic carcinoma of unknown primary in the head and neck: squamous cell carcinoma and beyond. Head Neck Pathol 2015 Mar;9(1):6–15.

43. Elrefaey S, Massaro MA, Chiocca S, Chiesa F, Ansarin M. HPV in oropharyngeal cancer: the basics to know in clinical practice. Acta Otorhinolaryngol Ital 2014;34(5):299–309.

44. El-Naggar AK. What Is New in the World Health Organization 2017 Histopathology Classification? Curr Treat Options Oncol 2017 Jul;18(7):43.

45. Müller S. Update from the 4th Edition of the World Health Organization of Head and Neck Tumours: Tumours of the Oral Cavity and Mobile Tongue. Head Neck Pathol 2017 Mar;11(1):33–40.

46. Haines GK. Pathology of Head and Neck Cancer I: Epithelial and Related Tumors BT - Head & Neck Cancer: Current Perspectives, Advances, and Challenges. In: Radosevich JA, editor. Dordrecht: Springer Netherlands; 2013. p. 257–87.

47. Reagan JW, Hamonic MJ. Dysplasia of the uterine cervix. Ann N Y Acad Sci. 1956;63(6):1236–44.

48. Robbins SL, Cotran RS, Kumar V. Pathological basis of disease. WB Saunder Company, London. 1979;1009.

49. Izumo T. Oral premalignant lesions: from the pathological viewpoint. Int J Clin Oncol 2011;16(1):15–26.

50. Fleskens S, Slootweg P. Grading systems in head and neck dysplasia: their prognostic value, weaknesses and utility. Head Neck Oncol 2009 May 11;1:11.

51. Gale N, Pilch BZ, Sidransky D, Westra W, Califano J, Barnes L, et al. World Health Organization Classification of Tumours Pathology & genetics Head and neck tumours International Agency for Research on Cancer (IARC). 2005;

52. Warnakulasuriya S, Reibel J, Bouquot J, Dabelsteen E. Oral epithelial dysplasia classification systems: predictive value, utility, weaknesses and scope for improvement. J Oral Pathol Med. 2008;37(3):127–33.

53. Speight PM. Update on oral epithelial dysplasia and progression to cancer. Head Neck Pathol 2007 Sep;1(1):61–6.

54. Califano J, Van Der Riet P, Westra W, Nawroz H, Clayman G, Piantadosi S, et al. Genetic progression model for head and neck cancer: Implications for field cancerization. Cancer Res. 1996;56(11):2488–92.

55. Perez-Ordoñez B, Beauchemin M, Jordan RCK. Molecular biology of squamous cell carcinoma of the head and neck. J Clin Pathol. 2006;59(5):445–53.

56. Tabor MP, Brakenhoff RH, Ruijter-Schippers HJ, Van Der Wal JE, Snow GB, Leemans CR, et al. Multiple head and neck tumors frequently originate from a single preneoplastic lesion. Am J Pathol 2002 Sep;161(3):1051–60.

57. Amagasa T, Yamashiro M, Ishikawa H. Oral Leukoplakia Related to Malignant Transformation. Oral Sci Int 2006;3(2):45–55.

58. Braakhuis BJM, Tabor MP, Leemans CR, van der Waal I, Snow GB, Brakenhoff RH. Second primary tumors and field cancerization in oral and oropharyngeal cancer: molecular techniques provide new insights and definitions. Head Neck 2002 Feb;24(2):198–206.

59. Braakhuis BJM, Brakenhoff RH, René Leemans C. Treatment choice for locally advanced head and neck cancers on the basis of risk factors: biological risk factors. Ann Oncol 2012 Sep 1;23:x173–7.

60. Argiris A, Karamouzis M V., Raben D, Ferris RL. Head and neck cancer. The Lancet. 2008.

61. Sankaranarayanan R, Ramadas K, Thomas G, Muwonge R, Thara S, Mathew B, et al. Effect of screening on oral cancer mortality in Kerala, India: a cluster-randomised controlled trial. Lancet. 2005;365(9475):1927–33.

62. Warnakulasuriya S, Johnson NW, Van Der Waal I. Nomenclature and classification of potentially malignant disorders of the oral mucosa. J Oral Pathol Med. 2007;36(10):575–80.

63. Witcher TP, Williams MD, Howlett DC. “One-stop” clinics in the investigation and diagnosis of head and neck lumps. Br J Oral Maxillofac Surg. 2007;45(1):19–22.

64. Branstetter IV BF, Blodgett TM, Zimmer LA, Snyderman CH, Johnson JT, Raman S, et al. Head and neck malignancy: is PET/CT more accurate than PET or CT alone? Radiology. 2005;235(2):580–6.

65. Argiris A, Smith SM, Stenson K, Mittal BB, Pelzer HJ, Kies MS, et al. Concurrent chemoradiotherapy for N2 or N3 squamous cell carcinoma of the head and neck from an occult primary. Ann Oncol. 2003;

66. Wittekindt C, Wagner S, Mayer CS, Klussmann JP. Basics of tumor development and importance of human papilloma virus (HPV) for head and neck cancer. GMS

Curr Top Otorhinolaryngol Head Neck Surg [Internet]. 2012/12/20. 2012;11:Doc09–Doc09.

67. Zhang J, Shu C, Song Y, Li Q, Huang J, Ma X. Epstein-Barr virus DNA level as a novel prognostic factor in nasopharyngeal carcinoma: A meta-analysis. Medicine (Baltimore) 2016 Oct;95(40):e5130–e5130.

68. Vatca M, Lucas JT, Laudadio J, D'Agostino RB, Waltonen JD, Sullivan CA, et al. Retrospective analysis of the impact of HPV status and smoking on mucositis in patients with oropharyngeal squamous cell carcinoma treated with concurrent chemotherapy and radiotherapy. Oral Oncol 2014 Sep 1;50(9):869–76.

69. Fakhry C, Zhang Q, Nguyen-Tan PF, Rosenthal D, El-Naggar A, Garden AS, et al. Human papillomavirus and overall survival after progression of oropharyngeal squamous cell carcinoma. J Clin Oncol. 2014;32(30):3365.

70. Ang KK, Harris J, Wheeler R, Weber R, Rosenthal DI, Nguyen-Tân PF, et al. Human papillomavirus and survival of patients with oropharyngeal cancer. N Engl J Med. 2010;363(1):24–35.

71. Poeta ML, Manola J, Goldwasser MA, Forastiere A, Benoit N, Califano JA, et al. TP53 mutations and survival in squamous-cell carcinoma of the head and neck. N Engl J Med. 2007;357(25):2552–61.

72. Bertero L, Massa F, Metovic J, Zanetti R, Castellano I, Ricardi U, et al. Eighth Edition of the UICC Classification of Malignant Tumours: an overview of the changes in the pathological TNM classification criteria—What has changed and why? Virchows Arch. 2018;472(4):519–31.

73. Cancer TIC for OR (ICOR) in H and N. Primary Tumor Staging for Oral Cancer and a Proposed Modification Incorporating Depth of Invasion: An International Multicenter Retrospective Study. JAMA Otolaryngol Neck Surg 2014 Dec 1;140(12):1138–48.

74. Matos LL, Dedivitis RA, Kulcsar MAV, de Mello ES, Alves VAF, Cernea CR. External validation of the AJCC Cancer Staging Manual, 8th edition, in an independent cohort of oral cancer patients. Oral Oncol 2017;71:47–53.

75. Huang SH, Xu W, Waldron J, Siu L, Shen X, Tong L, et al. Refining American Joint Committee on Cancer/Union for International Cancer Control TNM Stage and Prognostic Groups for Human Papillomavirus–Related Oropharyngeal Carcinomas. J Clin Oncol 2015 Feb 9;33(8):836–45.

76. El-Naggar AK, Westra WH. p16 expression as a surrogate marker for HPV-related oropharyngeal carcinoma: a guide for interpretative relevance and consistency. Head Neck. 2012;34(4):459–61.

77. Chen M-Y, Jiang R, Guo L, Zou X, Liu Q, Sun R, et al. Locoregional radiotherapy in patients with distant metastases of nasopharyngeal carcinoma at diagnosis. Chin J Cancer 2013 Nov;32(11):604–13.

78. Teymoortash A, Werner JA. Current advances in diagnosis and surgical treatment of lymph node metastasis in head and neck cancer. GMS Curr Top Otorhinolaryngol Head Neck Surg. 2012;11:Doc04–Doc04.

79. Huang SH, Hwang D, Lockwood G, Goldstein DP, O'Sullivan B. Predictive value of tumor thickness for cervical lymph-node involvement in squamous cell carcinoma of the oral cavity: a meta-analysis of reported studies. Cancer 2009 Apr 1;115(7):1489–97.

80. Huang S-H, O'Sullivan B. Oral cancer: Current role of radiotherapy and chemotherapy. Med Oral Patol Oral Cir Bucal 2013;18(2):e233-40.

81. Marur S, Forastiere AA. Head and Neck Squamous Cell Carcinoma: Update on Epidemiology, Diagnosis, and Treatment. Mayo Clin Proc 2016;91(3):386–96.

82. DG P, SA L, GS W, WM M, DJ A, KK A, et al. American Society of Clinical Oncology

clinical practice guideline for the use of larynx-preservation strategies in the treatment of laryngeal cancer. J Clin Oncol. 2006;

83. Argiris A, Stenson KM, Brockstein BE, Mittal BB, Pelzer H, Kies MS, et al. Neck dissection in the combined-modality therapy of patients with locoregionally advanced head and neck cancer. Head Neck. 2004;

84. Greenberg JS, El Naggar AK, Mo V, Roberts D, Myers JN. Disparity in pathologic and clinical lymph node staging in oral tongue carcinoma: Implications for therapeutic decision making. Cancer. 2003;

85. Simental AA, Duvvuri U, Johnson JT, Myers EN. Selective neck dissection in patients with upper aerodigestive tract cancer with clinically positive nodal disease. Annals of Otology, Rhinology and Laryngology. 2006.

86. Ferris RL, Xi L, Raja S, Hunt JL, Wang J, Gooding WE, et al. Molecular staging of cervical lymph nodes in squamous cell carcinoma of the head and neck. Cancer Res. 2005;

87. Kofler B, Laban S, Busch CJ, Lörincz B, Knecht R. New treatment strategies for HPV-positive head and neck cancer. European Archives of Oto-Rhino-Laryngology. 2014.

88. M.A. C, G.S. W, B.W. OJ, M. F, H. Q. Transoral robotic surgery and human papillomavirus status: Oncologic results. Head Neck. 2011;

89. S. M, A.A. F. Head and neck cancer: Changing epidemiology, diagnosis, and treatment. Mayo Clin Proc. 2008;

90. Pfister DG, Ang K-K, Brizel DM, Burtness BA, Busse PM, Caudell JJ, et al. Head and neck cancers, version 2.2013. Featured updates to the NCCN guidelines. J Natl Compr Canc Netw 2013 Aug;11(8):917–23.

91. Langendijk JA, Doornaert P, Verdonck-de Leeuw IM, Leemans CR, Aaronson NK, Slotman BJ. Impact of late treatment-related toxicity on quality of life among patients with head and neck cancer treated with radiotherapy. J Clin Oncol 2008 Aug 1;26(22):3770–6.

92. Cohen EEW, Lingen MW, Vokes EE. The expanding role of systemic therapy in head and neck cancer. Journal of Clinical Oncology. 2004.

93. Colevas AD. Chemotherapy options for patients with metastatic or recurrent squamous cell carcinoma of the head and neck. Journal of Clinical Oncology. 2006.

94. Blanchard P, Baujat B, Holostenco V, Bourredjem A, Baey C, Bourhis J, et al. Meta-analysis of radiotherapy in HNSCC Meta-analysis of chemotherapy in head and neck cancer (MACH-NC): A comprehensive analysis by tumour site , on behalf of the MACH-CH Collaborative group. Radiother Oncol. 2011;

95. Pignon JP, Bourhis J, Domenge C, Designé L. Chemotherapy added to locoregional treatment for head and neck squamous-cell carcinoma: Three meta-analyses of updated individual data. Lancet. 2000;

96. J.A. B, P.M. H, J. G, R.B. C, C.U. J, R.K. S, et al. Radiotherapy plus cetuximab for locoregionally advanced head and neck cancer: 5-year survival data from a phase 3 randomised trial, and relation between cetuximab-induced rash and survival. Lancet Oncol. 2010;

97. Brockstein B, Haraf DJ, Rademaker AW, Kies MS, Stenson KM, Rosen F, et al. Patterns of failure, prognostic factors and survival in locoregionally advanced head and neck cancer treated with concomitant chemoradiotherapy: A 9-year, 337-patient, multi-institutional experience. Ann Oncol. 2004;

98. Argiris A. Induction chemotherapy for head and neck cancer: Will history repeat itself? JNCCN J Natl Compr Cancer Netw. 2005;

99. Blanchard P, Bourhis J, Lacas B, Posner MR, Vermorken JB, Hernandez JJC, et al. Taxane-cisplatin-fluorouracil as induction chemotherapy in locally advanced head and neck cancers: An individual patient data meta-analysis of the meta-analysis of chemotherapy in head and neck cancer group. In: Journal of Clinical Oncology. 2013.

100. M. B. Induction chemotherapy for squamous cell head and neck cancer: A neverending story? Oral Oncol. 2013;

101. Budach W, Bölke E, Kammers K, Gerber PA, Orth K, Gripp S, et al. Induction chemotherapy followed by concurrent radio-chemotherapy versus concurrent radio-chemotherapy alone as treatment of locally advanced squamous cell carcinoma of the head and neck (HNSCC): A meta-analysis of randomized trials. In: Radiotherapy and Oncology. 2016.

102. Dietz A, Wiegand S, Kuhnt T, Wichmann G. Laryngeal Preservation Approaches: Considerations for New Selection Criteria Based on the DeLOS-II Trial. Front Oncol 2019 Jul 10;9:625.

103. J.-J. M, J.-M. A, C. H-M, G. K, P. L, D. P, et al. GEC-ESTRO recommendations for brachytherapy for head and neck squamous cell carcinomas. Radiother Oncol. 2009;

104. Mellman I, Coukos G, Dranoff G. Cancer immunotherapy comes of age. Nature. 2011.

105. Economopoulou P, Perisanidis C, Giotakis EI, Psyrri A. The emerging role of immunotherapy in head and neck squamous cell carcinoma (HNSCC): anti-tumor immunity and clinical applications. Ann Transl Med2016 May;4(9):173.

106. Pai SI, Zandberg DP, Strome SE. The role of antagonists of the PD-1:PD-L1/PD-L2 axis in head and neck cancer treatment. Oral Oncol 2016 Oct;61:152–8.

107. Chen DS, Mellman I. Oncology meets immunology: The cancer-immunity cycle. Immunity. 2013.

108. Seiwert TY, Burtness B, Mehra R, Weiss J, Berger R, Eder JP, et al. Safety and clinical activity of pembrolizumab for treatment of recurrent or metastatic squamous cell carcinoma of the head and neck (KEYNOTE-012): an open-label, multicentre, phase 1b trial. Lancet Oncol. 2016;

109. Ferris RL, Blumenschein G, Fayette J, Guigay J, Colevas AD, Licitra L, et al. Nivolumab for recurrent squamous-cell carcinoma of the head and neck. N Engl J Med. 2016;

110. Wei WI, Kwong DLW. Current management strategy of nasopharyngeal carcinoma. Clinical and Experimental Otorhinolaryngology. 2010.

111. Duvvuri U, Simental AA, D'Angelo G, Johnson JT, Ferris RL, Gooding W, et al. Elective neck dissection and survival in patients with squamous cell carcinoma of the oral cavity and oropharynx. Laryngoscope. 2004;

112. Jones AS, Fish B, Fenton JE, Husband DJ. The treatment of early laryngeal cancers (T1-T2 N0): surgery or irradiation? Head Neck 2004 Feb;26(2):127–35.

113. Mendenhall WM, Werning JW, Hinerman RW, Amdur RJ, Villaret DB. Management of T1-T2 Glottic Carcinomas. Cancer. 2004.

114. Steuer CE, El-Deiry M, Parks JR, Higgins KA, Saba NF. An update on larynx cancer. CA Cancer J Clin. 2017;

115. Corvò R. Evidence-based radiation oncology in head and neck squamous cell carcinoma. Radiother Oncol 2007 Oct 1;85(1):156–70.

116. Forastiere AA, Zhang Q, Weber RS, Maor MH, Goepfert H, Pajak TF, et al. Long-term results of RTOG 91-11: A comparison of three nonsurgical treatment

strategies to preserve the larynx in patients with locally advanced larynx cancer. J Clin Oncol. 2013;

117. Pignon J-P, Maître A le, Maillard E, Bourhis J. Meta-analysis of chemotherapy in head and neck cancer (MACH-NC): An update on 93 randomised trials and 17,346 patients. Radiother Oncol 2009 Jul 1;92(1):4–14.

118. Pignon J-P, le Maître A, Bourhis J. Meta-Analyses of Chemotherapy in Head and Neck Cancer (MACH-NC): An Update. Int J Radiat Oncol 2007 Oct 1;69(2):S112–4.

119. Bahig H, Fortin B, Alizadeh M, Lambert L, Filion E, Guertin L, et al. Predictive factors of survival and treatment tolerance in older patients treated with chemotherapy and radiotherapy for locally advanced head and neck cancer. Oral Oncol 2015 May 1;51(5):521–8.

120. Naidu MUR, Ramana GV, Rani PU, Mohan IK, Suman A, Roy P. Chemotherapy-induced and/or radiation therapy-induced oral mucositis--complicating the treatment of cancer. Neoplasia 2004;6(5):423–31.

121. Lalla R V, Sonis ST, Peterson DE. Management of oral mucositis in patients who have cancer. Dent Clin North Am 2008 Jan;52(1):61–viii.

122. Duncan W, MacDougall RH, Kerr GR, Downing D. Adverse effect of treatment gaps in the outcome of radiotherapy for laryngeal cancer. Radiother Oncol. 1996;

123. Robertson C, Robertson AG, Hendry JH, Roberts SA, Slevin NJ, Duncan WB, et al. Similar decreases in local tumor control are calculated for treatment protraction and for interruptions in the radiotherapy of carcinoma of the larynx in four centers. Int J Radiat Oncol Biol Phys. 1998;

124. Murphy CT, Galloway TJ, Handorf EA, Egleston BL, Wang LS, Mehra R, et al. Survival impact of increasing time to treatment initiation for patients with head and neck cancer in the United States. J Clin Oncol. 2016;

125. R.S. W, B.A. B, A. F, J. C, M. M, H. G, et al. Outcome of salvage total laryngectomy following organ preservation therapy: The Radiation Therapy Oncology Group Trial 91-11. Arch Otolaryngol - Head Neck Surg. 2003;

126. Janot F, de Raucourt D, Castaing M, Giger R, Babin E, Ferron C, et al. Randomised trial of re-irradiation combined with chemotherapy after salvage surgery in head and neck carcinoma: Carcinologic and quality of life results gettec and gortec groups. Radiother Oncol. 2007;

127. Bossi P, Alfieri S. Investigational drugs for head and neck cancer. Expert Opinion on Investigational Drugs. 2016.

128. Jang DW, Teng MS, Ojo B, Genden EM. Palliative surgery for head and neck cancer with extensive skin involvement. In: Laryngoscope. 2013.

129. Slotman BJ, Cottier B, Bentzen SM, Heeren G, Lievens Y, van den Bogaert W. Overview of national guidelines for infrastructure and staffing of radiotherapy. ESTRO-QUARTS: Work package 1. Radiother Oncol 2005 Jun 1;75(3):349.E1-349.E6.

130. Begg AC, Stewart FA, Vens C. Strategies to improve radiotherapy with targeted drugs. Nature Reviews Cancer. 2011.

131. Delaney G, Jacob S, Featherstone C, Barton M. The role of radiotherapy in cancer treatment: Estimating optimal utilization from a review of evidence-based clinical guidelines. Cancer. 2005.

132. Barnett GC, West CML, Dunning AM, Elliott RM, Coles CE, Pharoah PDP, et al. Normal tissue reactions to radiotherapy: Towards tailoring treatment dose by genotype. Nature Reviews Cancer. 2009.

133. Bernier J, Hall EJ, Giaccia A. Radiation oncology: A century of achievements. Nature Reviews Cancer. 2004.

134. Baskar R, Lee KA, Yeo R, Yeoh KW. Cancer and radiation therapy: Current advances and future directions. Int J Med Sci. 2012;9(3):193–9.

135. Jackson SP, Bartek J. The DNA-damage response in human biology and disease. Nature. 2009.

136. van der Kogel A. Basic Clinical Radiobiology Fourth Edition. Basic Clinical Radiobiology Fourth Edition. 2009.

137. O'Donovan A, Leech M, Gillham C. Assessment and management of radiotherapy induced toxicity in older patients. J Geriatr Oncol. 2017;8(6):421–7.

138. Scherer E, Streffer C, Trott K-R. Radiopathology of organs and tissues. Springer; 1991.

139. Rodney Withers H, Taylor JMG, Maciejewski B. Treatment volume and tissue tolerance. Int J Radiat Oncol Biol Phys. 1988;

140. Marks LB, Yorke ED, Jackson A, Ten Haken RK, Constine LS, Eisbruch A, et al. Use of Normal Tissue Complication Probability Models in the Clinic. Int J Radiat Oncol Biol Phys. 2010;

141. Baskar R. Emerging role of radiation induced bystander effects: Cell communications and carcinogenesis. Genome Integrity. 2010.

142. Hall EJ. Cancer caused by x-rays-a random event? Lancet Oncology. 2007.

143. Fabbrizi MR, Warshowsky KE, Zobel CL, Hallahan DE, Sharma GG. Molecular and epigenetic regulatory mechanisms of normal stem cell radiosensitivity. Cell Death Discov 2018;4(1):117.

144. Verheij M. Clinical biomarkers and imaging for radiotherapy-induced cell death. Cancer and Metastasis Reviews. 2008.

145. Fogg VC, Lanning NJ, MacKeigan JP. Mitochondria in cancer: At the crossroads of life and death. Chinese Journal of Cancer. 2011.

146. Eriksson D, Stigbrand T. Radiation-induced cell death mechanisms. Tumor Biology. 2010.

147. Vakifahmetoglu H, Olsson M, Zhivotovsky B. Death through a tragedy: Mitotic catastrophe. Cell Death and Differentiation. 2008.

148. Hotchkiss RS, Strasser A, McDunn JE, Swanson PE. Cell death in Disease: Mechanisms and Emerging Therapeutic Concepts. N Engl J Med. 2009;

149. Roninson IB. Tumor cell senescence in cancer treatment. Cancer Research. 2003.

150. Schmitt CA. Cellular senescence and cancer treatment. Biochimica et Biophysica Acta - Reviews on Cancer. 2007.

151. Fukumoto M, Kuwahara Y, Oikawa T, Ochiai Y, Roudkenar MH, Fukamoto M, et al. Enhancement of autophagy is a potential modality for tumors refractory to radiotherapy. Cell Death Dis. 2011;

152. Kirthi Koushik AS, Harish K, Avinash HU. Principles of radiation oncology: a beams eye view for a surgeon. Indian J Surg Oncol 2013 Sep;4(3):255–62.

153. Clark CH, Bidmead AM, Mubata CD, Harrington KJ, Nutting CM. Intensity-modulated radiotherapy improves target coverage, spinal cord sparing and allows dose escalation in patients with locally advanced cancer of the larynx. In: Radiotherapy and Oncology. 2004.

154. Teoh M, Clark CH, Wood K, Whitaker S, Nisbet A. Volumetric modulated arc therapy: A review of current literature and clinical use in practice. British Journal of Radiology. 2011.

155. Mallick S, Benson R, Julka PK, Rath GK. Altered fractionation radiotherapy in head and neck squamous cell carcinoma. J Egypt Natl Canc Inst 2016 Jun 1;28(2):73–80.

156. Skladowski K, Maciejewski B, Golen M, Tarnawski R, Slosarek K, Suwinski R, et al. Continuous accelerated 7-days-a-week radiotherapy for head-and-neck cancer: Long-term results of Phase III clinical trial. Int J Radiat Oncol Biol Phys. 2006;

157. Le QTX, Fu KK, Kroll S, Ryu JK, Quivey JM, Meyler TS, et al. Influence of fraction size, total dose, and overall time on local control of T1-T2 glottic carcinoma. Int J Radiat Oncol Biol Phys. 1997;

158. Bernier J. Alteration of radiotherapy fractionation and concurrent chemotherapy: A new frontier in head and neck oncology? Nature Clinical Practice Oncology. 2005.

159. Nguyen LN, Ang KK. Radiotherapy for cancer of the head and neck: Altered fractionation regimens. Lancet Oncology. 2002.

160. Fu KK, Pajak TF, Trotti A, Jones CU, Spencer SA, Phillips TL, et al. A radiation therapy oncology group (RTOG) phase III randomized study to compare hyperfractionation and two variants of accelerated fractionation to standard fractionation radiotherapy for head and neck squamous cell carcinomas: First report of RTOG 9003. Int J Radiat Oncol Biol Phys. 2000;

161. Bourhis J, Overgaard J, Audry H, Ang KK, Saunders M, Bernier J, et al. Hyperfractionated or accelerated radiotherapy in head and neck cancer: a meta-analysis. [reprint in Clin Otolaryngol. 2007 Apr;32(2):119; PMID: 17403229]. [Review] Lancet. 2006;

162. Basch E, Reeve BB, Mitchell SA, Clauser SB, Minasian LM, Dueck AC, et al. Development of the National Cancer Institute's patient-reported outcomes version of the common terminology criteria for adverse events (PRO-CTCAE). J

Natl Cancer Inst. 2014;106(9):dju244.

163. Ojo B, Genden EM, Teng MS, Milbury K, Misiukiewicz KJ, Badr H. A systematic review of head and neck cancer quality of life assessment instruments. Oral Oncology. 2012.

164. Rogers SN, Semple C, Babb M, Humphris G. Quality of life considerations in head and neck cancer: United Kingdom National Multidisciplinary Guidelines. J Laryngol Otol 2016 May;130(S2):S49–52.

165. Brady LW, Perez CA, Wazer DE. Perez & Brady's principles and practice of radiation oncology. Lippincott Williams & Wilkins; 2013.

166. Hall EJ, Giaccia AJ. Radiobiology for the radiologist: Seventh edition. Radiobiology for the Radiologist: Seventh Edition. 2012.

167. Kim JH, Jenrow KA, Brown SL. Mechanisms of radiation-induced normal tissue toxicity and implications for future clinical trials. Radiation Oncology Journal. 2014.

168. Brush J, Lipnick SL, Phillips T, Sitko J, McDonald JT, McBride WH. Molecular Mechanisms of Late Normal Tissue Injury. Semin Radiat Oncol. 2007;

169. Lalla R V., Saunders DP, Peterson DE. Chemotherapy or Radiation-Induced Oral Mucositis. Dent Clin North Am 2014 Apr 1;58(2):341–9.

170. Villa A, Sonis S. Toxicities associated with head and neck cancer treatment and oncology-related clinical trials. Curr Probl Cancer 2016;40(5–6):244–57.

171. Trotti A, Bellm LA, Epstein JB, Frame D, Fuchs HJ, Gwede CK, et al. Mucositis incidence, severity and associated outcomes in patients with head and neck cancer receiving radiotherapy with or without chemotherapy: a systematic literature review. Radiother Oncol 2003 Mar 1;66(3):253–62.

172. Rosenthal DI, Lewin JS, Eisbruch A. Prevention and treatment of dysphagia and aspiration after chemoradiation for head and neck cancer. Journal of Clinical Oncology. 2006.

173. Bonner JA, Harari PM, Giralt J, Azarnia N, Shin DM, Cohen RB, et al. Radiotherapy plus cetuximab for squamous-cell carcinoma of the head and neck. N Engl J Med. 2006;

174. Machtay M, Moughan J, Trotti A, Garden AS, Weber RS, Cooper JS, et al. Factors associated with severe late toxicity after concurrent chemoradiation for locally advanced head and neck cancer: An RTOG analysis. J Clin Oncol. 2008;

175. Yeh S-A. Radiotherapy for head and neck cancer. Semin Plast Surg 2010 May;24(2):127–36.

176. Bensinger W, Schubert M, Ang KK, Brizel D, Brown E, Eilers JG, et al. NCCN task force report: Prevention and management of mucositis in cancer care. JNCCN Journal of the National Comprehensive Cancer Network. 2008.

177. Epstein JB, Thariat J, Bensadoun RJ, Barasch A, Murphy BA, Kolnick L, et al. Oral complications of cancer and cancer therapy: From cancer treatment to survivorship. CA Cancer J Clin. 2012;

178. Buglione M, Cavagnini R, Di Rosario F, Sottocornola L, Maddalo M, Vassalli L, et al. Oral toxicity management in head and neck cancer patients treated with chemotherapy and radiation: Dental pathologies and osteoradionecrosis (Part 1) literature review and consensus statement. Critical Reviews in Oncology/Hematology. 2016.

179. Rosenthal DI, Trotti A. Strategies for Managing Radiation-Induced Mucositis in Head and Neck Cancer. Seminars in Radiation Oncology. 2009.

180. Russo G, Haddad R, Posner M, Machtay M. Radiation Treatment Breaks and

Ulcerative Mucositis in Head and Neck Cancer. Oncologist. 2008;

181. Rose-Ped AM, Bellm LA, Epstein JB, Trotti A, Gwede C, Fuchs HJ. Complications of radiation therapy for head and neck cancers: The patient's perspective. Cancer Nurs. 2002;

182. Sonis ST, Elting LS, Bekele BN, Keefe D, Peterson DE, Schubert M, et al. Perspectives on Cancer Therapy-Induced Mucosal Injury: Pathogenesis, Measurement, Epidemiology, and Consequences for Patients. Cancer. 2004;

183. De Sanctis V, Bossi P, Sanguineti G, Trippa F, Ferrari D, Bacigalupo A, et al. Mucositis in head and neck cancer patients treated with radiotherapy and systemic therapies: Literature review and consensus statements. Crit Rev Oncol Hematol 2016;100:147–66.

184. Vera-Llonch M, Oster G, Hagiwara M, Sonis S. Oral mucositis in patients undergoing radiation treatment for head and neck carcinoma. Cancer. 2006;

185. Jehmlich N, Stegmaier P, Golatowski C, Salazar MG, Rischke C, Henke M, et al. Differences in the whole saliva baseline proteome profile associated with development of oral mucositis in head and neck cancer patients undergoing radiotherapy. J Proteomics [Internet]. 2015 Jul 1;125:98–103.

186. Rosenthal DI, Mendoza TR, Chambers MS, Burkett VS, Garden AS, Hessell AC, et al. The MD Anderson symptom inventory–head and neck module, a patient-reported outcome instrument, accurately predicts the severity of radiation-induced mucositis. Int J Radiat Oncol Biol Phys. 2008;72(5):1355–61.

187. Elting LS, Cooksley CD, Chambers MS, Garden AS. Risk, Outcomes, and Costs of Radiation-Induced Oral Mucositis Among Patients With Head-and-Neck Malignancies. Int J Radiat Oncol Biol Phys. 2007;

188. Santos RCS, Dias RS, Giordani AJ, Segreto RA, Segreto HRC. Mucositis in head and

neck cancer patients undergoing radiochemotherapy. Rev da Esc Enferm. 2011;45(6):1338–44.

189. Villa A, Sonis ST. Mucositis: pathobiology and management. Curr Opin Oncol. 2015;27(3):159–64.

190. Bossi P, Bergamini C, Miceli R, Cova A, Orlandi E, Resteghini C, et al. Salivary Cytokine Levels and Oral Mucositis in Head and Neck Cancer Patients Treated With Chemotherapy and Radiation Therapy. Int J Radiat Oncol Biol Phys 2016;96(5):959–66.

191. Kaae JK, Stenfeldt L, Eriksen JG. Xerostomia after Radiotherapy for Oral and Oropharyngeal Cancer: Increasing Salivary Flow with Tasteless Sugar-free Chewing Gum. Front Oncol 2016 May 3;6:111.

192. Jensen SB, Pedersen AML, Vissink A, Andersen E, Brown CG, Davies AN, et al. A systematic review of salivary gland hypofunction and xerostomia induced by cancer therapies: Management strategies and economic impact. Supportive Care in Cancer. 2010.

193. Amerongen AN, Veerman E. Current therapies for xerostomia and salivary gland hypofunction associated with cancer therapies. Support care cancer. 2003;11(4):226–31.

194. Dirix P, Nuyts S, Van Den Bogaert W. Radiation-induced xerostomia in patients with head and neck cancer: A literature review. Cancer. 2006.

195. Zeilstra LJW, Vissink A, Konings AWT, Coppes RP. Radiation induced cell loss in rat submandibular gland and its relation to gland function. Int J Radiat Biol. 2000;

196. Eisbruch A. Radiotherapy: IMRT reduces xerostomia and potentially improves QoL. Nat Rev Clin Oncol. 2009;

197. Gupta T, Agarwal J, Jain S, Phurailatpam R, Kannan S, Ghosh-Laskar S, et al. Three-dimensional conformal radiotherapy (3D-CRT) versus intensity modulated radiation therapy (IMRT) in squamous cell carcinoma of the head and neck: a randomized controlled trial. Radiother Oncol. 2012;104(3):343–8.

198. Cox JD, Stetz JA, Pajak TF. Toxicity criteria of the Radiation Therapy Oncology Group (RTOG) and the European organization for research and treatment of cancer (EORTC). Int J Radiat Oncol Biol Phys. 1995;31(5):1341–6.

199. Jha N, Seikaly H, Harris J, Williams D, Liu R, McGaw T, et al. Prevention of radiation induced xerostomia by surgical transfer of submandibular salivary gland into the submental space. Radiother Oncol. 2003;

200. Brizel DM, Wasserman TH, Henke M, Strnad V, Rudat V, Monnier A, et al. Phase III randomized trial of amifostine as a radioprotector in head and neck cancer. J Clin Oncol. 2000;

201. Schwartz DL, Garden AS. Radiotherapy for Head and Neck Cancer. Hematol Oncol Clin North Am 2006;20(2):259–85.

202. Irune E, Dwivedi RC, Nutting CM, Harrington KJ. Treatment-related dysgeusia in head and neck cancer patients. Cancer Treatment Reviews. 2014.

203. Mirza N, Machtay M, Devine PA, Troxel A, Abboud SK, Doty RL. Gustatory impairment in patients undergoing head and neck irradiation. Laryngoscope. 2008;

204. Matsuo R. Role of saliva in the maintenance of taste sensitivity. Crit Rev Oral Biol Med 2000;11(2):216–29.

205. Vissink A, Jansma J, Spijkervet FKL, Burlage FR, Coppes RP. Oral sequelae of head and neck radiotherapy. Critical Reviews in Oral Biology and Medicine. 2003.

206. Nadella KR, Kodali RM, Guttikonda LK, Jonnalagadda A. Osteoradionecrosis of the Jaws: Clinico-Therapeutic Management: A Literature Review and Update. J Maxillofac Oral Surg 2015 Dec;14(4):891–901.

207. Silvestre-Rangil J, Silvestre FJ. Clinico-therapeutic management of osteoradionecrosis: A literature review and update. Medicina Oral, Patologia Oral y Cirugia Bucal. 2011.

208. McLeod NMH, Bater MC, Brennan PA. Management of patients at risk of osteoradionecrosis: results of survey of dentists and oral & maxillofacial surgery units in the United Kingdom, and suggestions for best practice. Br J Oral Maxillofac Surg. 2010;

209. Pitak-Arnnop P, Sader R, Dhanuthai K, Masaratana P, Bertolus C, Chaine A, et al. Management of osteoradionecrosis of the jaws: An analysis of evidence. European Journal of Surgical Oncology. 2008.

210. Nabil S, Samman N. Incidence and prevention of osteoradionecrosis after dental extraction in irradiated patients: A systematic review. International Journal of Oral and Maxillofacial Surgery. 2011.

211. Mordente A, Meucci E, Martorana GE, Silvestrini A. Cancer Biomarkers Discovery and Validation: State of the Art, Problems and Future Perspectives BT - Advances in Cancer Biomarkers: From biochemistry to clinic for a critical revision. In: Scatena R, editor. Dordrecht: Springer Netherlands; 2015. p. 9–26.

212. Atkinson AJ, Colburn WA, DeGruttola VG, DeMets DL, Downing GJ, Hoth DF, et al. Biomarkers and surrogate endpoints: Preferred definitions and conceptual framework. Clin Pharmacol Ther. 2001;69(3):89–95.

213. Issaq HJ, Waybright TJ, Veenstra TD. Cancer biomarker discovery: Opportunities and pitfalls in analytical methods. Electrophoresis. 2011;32(9):967–75.

214. Drucker E, Krapfenbauer K. Pitfalls and limitations in translation from biomarker discovery to clinical utility in predictive and personalised medicine. Vol. 4, EPMA Journal. Springer International Publishing; 2013.

215. Sidransky D. Emerging molecular markers of cancer. Nature Reviews Cancer. 2002.

216. Ray P, Le Manach Y, Riou B, Houle TT. Statistical evaluation of a biomarker. Anesthesiol J Am Soc Anesthesiol. 2010;112(4):1023–40.

217. Fathi E, Mesbah-namin SA. Biomarkers in Medicine: An Overview. Br J Med Med Res. 2013;4(8):1701–18.

218. Mazzone PJ, Sears CR, Arenberg DA, Gaga M, Gould MK, Massion PP, et al. Evaluating molecular biomarkers for the early detection of lung cancer: When is a biomarker ready for clinical use? An official American Thoracic Society Policy Statement. American Journal of Respiratory and Critical Care Medicine. 2017.

219. Henry NL, Hayes DF. Cancer biomarkers. Mol Oncol. 2012;6(2):140–6.

220. Kim KY, McShane LM, Conley BA. Designing biomarker studies for head and neck cancer. Head Neck 2014 Jul;36(7):1069–75.

221. Goossens N, Nakagawa S, Sun X, Hoshida Y. Cancer biomarker discovery and validation. Transl Cancer Res 2015 Jun;4(3):256–69.

222. Nalejska E, Mączyńska E, Lewandowska MA. Prognostic and Predictive Biomarkers: Tools in Personalized Oncology. Mol Diagn Ther 2014;18(3):273–84.

223. Duffy MJ, Crown J. A Personalized Approach to Cancer Treatment: How Biomarkers Can Help. Clin Chem 2008 Nov 1;54(11):1770–9.

224. Allegra CJ, Jessup JM, Somerfield MR, Hamilton SR, Hammond EH, Hayes DF, et

al. American society of clinical oncology provisional clinical opinion: Testing for KRAS gene mutations in patients with metastatic colorectal carcinoma to predict response to anti-epidermal growth factor receptor monoclonal antibody therapy. Journal of Clinical Oncology. 2009.

225. Slamon DJ, Leyland-Jones B, Shak S, Fuchs H, Paton V, Bajamonde A, et al. Use of chemotherapy plus a monoclonal antibody against her2 for metastatic breast cancer that overexpresses HER2. N Engl J Med. 2001;

226. Piccart-Gebhart MJ, Procter M, Leyland-Jones B, Goldhirsch A, Untch M, Smith I, et al. Trastuzumab after adjuvant chemotherapy in HER2-positive breast cancer. N Engl J Med. 2005;

227. Romond EH, Perez EA, Bryant J, Suman VJ, Geyer CE, Davidson NE, et al. Trastuzumab plus adjuvant chemotherapy for operable HER2-positive breast cancer. N Engl J Med. 2005;

228. Van De Vijver MJ, He YD, Van 'T Veer LJ, Dai H, Hart AAM, Voskuil DW, et al. A gene-expression signature as a predictor of survival in breast cancer. N Engl J Med. 2002;

229. Nguyen HG, Welty CJ, Cooperberg MR. Diagnostic associations of gene expression signatures in prostate cancer tissue. Current Opinion in Urology. 2015.

230. Hoshida Y, Villanueva A, Kobayashi M, Peix J, Chiang DY, Camargo A, et al. Gene expression in fixed tissues and outcome in hepatocellular carcinoma. N Engl J Med. 2008;

231. Hoshida Y, Villanueva A, Sangiovanni A, Sole M, Hur C, Andersson KL, et al. Prognostic gene expression signature for patients with hepatitis C-related early-stage cirrhosis. Gastroenterology. 2013;

232. Genzen JR. Regulation of Laboratory-Developed Tests. Am J Clin Pathol 2019 Jul

5;152(2):122–31.

233. Kulasingam V, Diamandis EP. Strategies for discovering novel cancer biomarkers through utilization of emerging technologies. Nature Clinical Practice Oncology. 2008.

234. Vidotto A, Henrique T, Raposo LS, Maniglia JV, Tajara EH. Salivary and serum proteomics in head and neck carcinomas: Before and after surgery and radiotherapy. Cancer Biomarkers. 2010;8(2):95–107.

235. Zelles T, Purushotham KR, Macauley SP, Oxford GE, Humphreys-Beher MG. Concise Review: Saliva and Growth Factors: The Fountain of Youth Resides in Us All. Journal of Dental Research. 1995.

236. Tiwari M. Science behind human saliva. Journal of Natural Science, Biology and Medicine. 2011.

237. Humphrey SP, Williamson RT. A review of saliva Normal composition, flow, and function. Humphrey, Williamson. 2001. Journal of Prosthetic Dentistry.pdf. J Prosthet Dent. 2001;

238. Wang A, Wang CP, Tu M, Wong DTW. Oral biofluid biomarker research: Current status and emerging frontiers. Diagnostics. 2016;6(4).

239. Yoshizawa JM, Schafer CA, Schafer JJ, Farrell JJ, Paster BJ, Wong DTW. Salivary biomarkers: Toward future clinical and diagnostic utilities. Clinical Microbiology Reviews. 2013.

240. Schafer CA, Schafer JJ, Yakob M, Lima P, Camargo P, Wong DTW. Saliva diagnostics: Utilizing oral fluids to determine health status. Monogr Oral Sci. 2014;

241. Haeckel R, Petra H. Application of Saliva for Drug Monitoring an in Vivo Model for

Transmembrane Transport. Clin Chem Lab Med. 1996;

242. Lew KH, Jusko WJ. Pharmacodynamic modeling of cortisol suppression from fluocortolone. Eur J Clin Pharmacol. 1993;

243. Jehmlich N, Stegmaier P, Golatowski C, Salazar MG, Rischke C, Henke M, et al. Proteome data of whole saliva which are associated with development of oral mucositis in head and neck cancer patients undergoing radiotherapy. Data Br. 2016;

244. Zhang Q, Fillmore TL, Schepmoes AA, Clauss TRW, Gritsenko MA, Mueller PW, et al. Serum proteomics reveals systemic dysregulation of innate immunity in type 1 diabetes. J Exp Med. 2013;

245. Hu S, Wang J, Meijer J, Ieong S, Xie Y, Yu T, et al. Salivary proteomic and genomic biomarkers for primary Sjögren's syndrome. Arthritis Rheum. 2007;

246. Rao P V., Reddy AP, Lu X, Dasari S, Krishnaprasad A, Biggs E, et al. Proteomic identification of salivary biomarkers of type-2 diabetes. J Proteome Res. 2009;

247. Salazar MG, Jehmlich N, Murr A, Dhople VM, Holtfreter B, Hammer E, et al. Identification of periodontitis associated changes in the proteome of whole human saliva by mass spectrometric analysis. J Clin Periodontol. 2013;

248. Jarai T, Maasz G, Burian A, Bona A, Jambor E, Gerlinger I, et al. Mass Spectrometry-Based Salivary Proteomics for the Discovery of Head and Neck Squamous Cell Carcinoma. Pathol Oncol Res 2012;18(3):623–8.

249. Malik UU, Zarina S, Pennington SR. Oral squamous cell carcinoma: Key clinical questions, biomarker discovery, and the role of proteomics. Arch Oral Biol 2016 Mar 1;63:53–65.

250. Khan RS, Khurshid Z, Akhbar S, Moin SF. Advances of salivary proteomics in oral

squamous cell carcinoma (OSCC) detection: An update. Proteomes. 2016;4(4):1–11.

251. Schapher M, Wendler O, Gröschl M. Salivary cytokines in cell proliferation and cancer. Clin Chim Acta 2011;412(19–20):1740–8.

252. Rhodus NL, Cheng B, Myers S, Miller L, Ho V, Ondrey F. The feasibility of monitoring NF-κB associated cytokines: TNF-α, IL-1α, IL-6, and IL-8 in whole saliva for the malignant transformation of oral lichen planus. Mol Carcinog. 2005;

253. Dumbrigue HB, Sandow PL, Nguyen K-HT, Humphreys-Beher MG. Salivary epidermal growth factor levels decrease in patients receiving radiation therapy to the head and neck. Oral Surgery, Oral Med Oral Pathol Oral Radiol Endodontology 2000;89(6):710–6.

254. Principe S, Dikova V, Bagán J. Salivary Cytokines in patients with Head and Neck Cancer (HNC) treated with Radiotherapy. J Clin Exp Dent 2019 Nov 1;11(11):e1072–7.

255. Ohshima M, Sato M, Ishikawa M, Maeno M, Otsuka K. Physiologic levels of epidermal growth factor in saliva stimulate cell migration of an oral epithelial cell line, HO-1-N-1. Eur J Oral Sci. 2002;

256. Fischgrabe J, Wulfing P. Targeted therapies in breast cancer: established drugs and recent developments. Curr Clin Pharmacol. 2008;3(2):85–98.

257. Ramos M, Benavente S, Giralt J. Management of squamous cell carcinoma of the head and neck: updated European treatment recommendations. Expert Rev Anticancer Ther. 2010;10(3):339–44.

258. Domingo G, Perez CA, Velez M, Cudris J, Raez LE, Santos ES. EGF receptor in lung cancer: a successful story of targeted therapy. Expert Rev Anticancer Ther. 2010;10(10):1577–87.

259. Cohen DJ, Hochster HS. Update on clinical data with regimens inhibiting angiogenesis and epidermal growth factor receptor for patients with newly diagnosed metastatic colorectal cancer. Clin Colorectal Cancer. 2007;7:S21–7.

260. Kamatani T, Shiogama S, Yoshihama Y, Kondo S, Shirota T, Shintani S. Interleukin-1 beta in unstimulated whole saliva is a potential biomarker for oral squamous cell carcinoma. Cytokine. 2013;

261. Guerra ENS, Rêgo DF, Elias ST, Coletta RD, Mezzomo LAM, Gozal D, et al. Diagnostic accuracy of serum biomarkers for head and neck cancer: A systematic review and meta-analysis. Crit Rev Oncol Hematol. 2016;101(March):93–118.

262. Stenken JA, Poschenrieder AJ. Bioanalytical chemistry of cytokines - A review. Anal Chim Acta 2015;853(1):95–115.

263. Lackie J. A dictionary of biomedicine. Oxford University Press; 2010.

264. Younger P. Stedman's Medical Dictionary, 28th ed.200734 Stedman's Medical Dictionary, 28th ed. . Philadelphia, PA: Lippincott Williams and Wilkins 2006.

265. Ferrari SM, Ruffilli I, Elia G, Ragusa F, Paparo SR, Patrizio A, et al. Chemokines in hyperthyroidism. J Clin Transl Endocrinol 2019 May 17;16:100196.

266. Schetter AJ, Heegaard NHH, Harris CC. Inflammation and cancer: interweaving microRNA, free radical, cytokine and p53 pathways. Carcinogenesis 2009 Dec 2;31(1):37–49.

267. Waugh DJJ, Wilson C. The interleukin-8 pathway in cancer. Clinical Cancer Research. 2008.

268. Aziz S, Ahmed SS, Ali A, Khan FA, Zulfiqar G, Iqbal J, et al. Salivary immunosuppressive cytokines IL-10 and IL-13 are significantly elevated in oral squamous cell carcinoma patients. Cancer Invest. 2015;33(7):318–28.

269. Balkwill F. Tumour necrosis factor and cancer. Nature Reviews Cancer. 2009.

270. Dinarello CA. Proinflammatory cytokines. Chest. 2000;

271. Bienvenu J, Monneret G, Fabien N, Revillard JP. The clinical usefulness of the measurement of cytokines. Clinical Chemistry and Laboratory Medicine. 2000.

272. Pries R, Wollenberg B. Cytokines in head and neck cancer. Cytokine and Growth Factor Reviews Pergamon; Jun 1, 2006 p. 141–6.

273. Citrin DE, Hitchcock YJ, Chung EJ, Frandsen J, Urick ME, Shield W, et al. Determination of cytokine protein levels in oral secretions in patients undergoing radiotherapy for head and neck malignancies. Radiat Oncol 2012;7:64.

274. Tozzoli R, D';Aurizio F, Falcomer F, M.M. Basso S, Lumachi F. Serum Tumor Markers in Stage I-II Breast Cancer. Med Chem (Los Angeles). 2016;

275. McGrath S, Christidis D, Perera M, Hong SK, Manning T, Vela I, et al. Prostate cancer biomarkers: Are we hitting the mark? Prostate International. 2016.

276. Gyoba J, Shan S, Roa W, Bédard ELR. Diagnosing lung cancers through examination of micro-RNA biomarkers in blood, plasma, serum and sputum: A review and summary of current literature. International Journal of Molecular Sciences. 2016.

277. Flower L, Ahuja RH, Humphries SE, Mohamed-Ali V. Effects of sample handling on the stability of interleukin 6, tumour necrosis factor-α and leptin. Cytokine. 2000;

278. Jackman RP, Utter GH, Heitman JW, Hirschkorn DF, Law JP, Gefter N, et al. Effects of blood sample age at time of separation on measured cytokine concentrations in human plasma. Clin Vaccine Immunol. 2011;

279. Brailo V, Vucicevic-Boras V, Lukac J, Biocina-Lukenda D, Zilic-Alajbeg I, Milenovic

A, et al. Salivary and serum interleukin 1 beta, interleukin 6 and tumor necrosis factor alpha in patients with leukoplakia and oral cancer. Med Oral Patol Oral Cir Bucal. 2012;

280. Khandavilli SD, Ceallaigh PÓ, Lloyd CJ, Whitaker R. Serum C-reactive protein as a prognostic indicator in patients with oral squamous cell carcinoma. Oral Oncol. 2009;

281. Czerninski R, Basile JR, Kartin-Gabay T, Laviv A, Barak V. Cytokines and tumor markers in potentially malignant disorders and oral squamous cell carcinoma: A pilot study. Oral Dis. 2014;

282. Chang KP, Wu CC, Fang KH, Tsai CY, Chang YL, Liu SC, et al. Serum levels of chemokine (C-X-C motif) ligand 9 (CXCL9) are associated with tumor progression and treatment outcome in patients with oral cavity squamous cell carcinoma. Oral Oncol. 2013;

283. Elashoff D, Zhou H, Reiss J, Wang J, Xiao H, Henson B, et al. Prevalidation of salivary biomarkers for oral cancer detection. Cancer Epidemiol Biomarkers Prev. 2012;

284. Arellano-Garcia ME, Hu S, Wang J, Henson B, Zhou H, Chia D, et al. Multiplexed immunobead-based assay for detection of oral cancer protein biomarkers in saliva. Oral Dis 2008 Nov;14(8):705–12.

285. Korostoff A, Reder L, Masood R, Sinha UK. The role of salivary cytokine biomarkers in tongue cancer invasion and mortality. Oral Oncol. 2011;

286. Schaaij-Visser TBM, Brakenhoff RH, Leemans CR, Heck AJR, Slijper M. Protein biomarker discovery for head and neck cancer. Journal of Proteomics. 2010.

287. Kawahara R, Bollinger JG, Rivera C, Ribeiro ACP, Brandão TB, Leme AFP, et al. A targeted proteomic strategy for the measurement of oral cancer candidate

biomarkers in human saliva. Proteomics. 2016 Jan 1;16(1):159–73.

288. Csősz É, Márkus B, Darula Z, Medzihradszky KF, Nemes J, Szabó E, et al. Salivary proteome profiling of oral squamous cell carcinoma in a Hungarian population. FEBS Open Bio. 2018 Apr 1;8(4):556–69.

289. Hu S, Loo JA, Wong DT. Human saliva proteome analysis. In: Annals of the New York Academy of Sciences. 2007.

290. Hu S, Xie Y, Ramachandran P, Loo RRO, Li Y, Loo JA, et al. Large-scale identification of proteins in human salivary proteome by liquid chromatography/mass spectrometry and two-dimensional gel electrophoresis-mass spectrometry. Proteomics. 2005;

291. Schulz BL, Cooper-White J, Punyadeera CK. Saliva proteome research: Current status and future outlook. Critical Reviews in Biotechnology. 2013.

292. Zhang Y, Sun J, Lin CC, Abemayor E, Wang MB, Wong DTW. The emerging landscape of salivary diagnostics. Periodontol 2000. 2016;70(1):38–52.

293. Choudhary C, Mann M. Decoding signalling networks by mass spectrometry-based proteomics. Nature Reviews Molecular Cell Biology. 2010.

294. Chen G, Pramanik BN. Application of LC/MS to proteomics studies: current status and future prospects. Drug Discov Today. 2009;14(9–10):465–71.

295. Pitt JJ. Principles and applications of liquid chromatography-mass spectrometry in clinical biochemistry. Clin Biochem Rev. 2009;

296. Aebersold R, Mann M. Mass spectrometry-based proteomics. Nature. 2003.

297. Domon B, Aebersold R. Options and considerations when selecting a quantitative proteomics strategy. Nat Biotechnol. 2010;28(7):710–21.

298. Neilson KA, Ali NA, Muralidharan S, Mirzaei M, Mariani M, Assadourian G, et al. Less label, more free: Approaches in label-free quantitative mass spectrometry. Proteomics. 2011.

299. Picotti P, Rinner O, Stallmach R, Dautel F, Farrah T, Domon B, et al. High-throughput generation of selected reaction-monitoring assays for proteins and proteomes. Nat Methods. 2010;

300. Lange V, Picotti P, Domon B, Aebersold R. Selected reaction monitoring for quantitative proteomics: A tutorial. Molecular Systems Biology. 2008.

301. Navazesh M, Kumar SKS. Measuring salivary flow. J Am Dent Assoc 2008;139(May):35S-40S.

302. NOVAK KF. Chapter 5 - Periodontal Disease and Associated Risk Factors. In: CAPPELLI DP, MOBLEY CCBT-P in COHC, editors. Saint Louis: Mosby; 2008. p. 56–67.

303. Gulabivala K, Ng Y-L. 4 - Diagnosis of endodontic problems. In: Gulabivala K, Ng Y-LBT-E (Fourth E, editors. Mosby; 2014. p. 93–119).

304. Lee LT, Wong YK, Hsiao HY, Wang YW, Chan MY, Chang KW. Evaluation of saliva and plasma cytokine biomarkers in patients with oral squamous cell carcinoma. Int J Oral Maxillofac Surg 2018;47(6):699–707.

305. Zhang Y, Birru R, Di YP. Analysis of Clinical and Biological Samples Using Microsphere-Based Multiplexing Luminex System BT - Molecular Toxicology Protocols. In: Keohavong P, Grant SG, editors. Totowa, NJ: Humana Press; 2014. p. 43–57.

306. Tighe P, Negm O, Todd I, Fairclough L. Utility, reliability and reproducibility of immunoassay multiplex kits. Methods 2013;61(1):23–9.

307. Timms JF, Hale OJ, Cramer R. Advances in mass spectrometry-based cancer research and analysis: from cancer proteomics to clinical diagnostics. Expert Rev Proteomics. 2016;13(6):593–607.

308. Zor T, Selinger Z. Linearization of the Bradford protein assay increases its sensitivity: theoretical and experimental studies. Anal Biochem. 1996;236(2):302–8.

309. Shevchenko A, Jensen ON, Podtelejnikov A V., Sagliocco F, Wilm M, Vorm O, et al. Linking genome and proteome by mass spectrometry: Large-scale identification of yeast proteins from two dimensional gels. Proc Natl Acad Sci U S A. 1996;93(25):14440–5.

310. Shilov I V., Seymourt SL, Patel AA, Loboda A, Tang WH, Keating SP, et al. The paragon algorithm, a next generation search engine that uses sequence temperature values sequence temperature values and feature probabilities to identify peptides from tandem mass spectra. Mol Cell Proteomics. 2007;6(9):1638–55.

311. Everitt BS, Landau SL. M. 2001. Cluster Analysis. Arnold, London. 2001;

312. SahebJamee M, Eslami M, AtarbashiMoghadam F, Sarafnejad A. Salivary concentration of TNFalpha, IL1 alpha, IL6, and IL8 in oral squamous cell carcinoma. Med Oral Patol Oral Cir Bucal. 2008;13(5):E292–5.

313. Zhang X, Junior CR, Liu M, Li F, D'Silva NJ, Kirkwood KL. Oral squamous carcinoma cells secrete RANKL directly supporting osteolytic bone loss. Oral Oncol. 2013;

314. Ben-Baruch A. Inflammation-associated immune suppression in cancer: The roles played by cytokines, chemokines and additional mediators. Seminars in Cancer Biology. 2006.

315. M T, JM P, JA B. Role of IL-13 in regulation of anti-tumor immunity and tumor

growth. Cancer Immunol Immunother. 2004;

316. Cheng Y-S, Rees T, Wright J. A review of research on salivary biomarkers for oral cancer detection. Clin Transl Med. 2014;

317. John MARS, Li Y, Zhou X, Denny P, Ho C-M, Montemagno C, et al. Interleukin 6 and interleukin 8 as potential biomarkers for oral cavity and oropharyngeal squamous cell carcinoma. Arch Otolaryngol Neck Surg. 2004;130(8):929–35.

318. Katakura A, Kamiyama I, Takano N, Shibahara T, Muramatsu T, Ishihara K, et al. Comparison of salivary cytokine levels in oral cancer patients and healthy subjects. Bull Tokyo Dent Coll. 2007;

319. Cerovic R, Belusic-Gobic M, Brekalo Prso I, Kqiku L, Spalj S, Pezelj-Ribaric S. Salivary levels of TNF-alpha and IL-6 in patients with oral premalignant and malignant lesions. Folia Biol (Praha). 2013;59(2):99–102.

320. Tampa M, Mitran MI, Mitran CI, Sarbu MI, Matei C, Nicolae I, et al. Mediators of inflammation – A potential source of biomarkers in oral squamous cell carcinoma. J Immunol Res. 2018;

321. Chen Z, Malhotra PS, Thomas GR, Ondrey FG, Duffey DC, Smith CW, et al. Expression of proinflammatory and proangiogenic cytokines in patients with head and neck cancer. Clin Cancer Res. 1999;

322. Choudhary MM, France TJ, Teknos TN, Kumar P. Interleukin-6 role in head and neck squamous cell carcinoma progression Production and Hosting by Elsevier on behalf of KeAi. World J Otorhinolaryngol Neck Surg. 2016;

323. Tanaka T, Narazaki M, Kishimoto T. Il-6 in inflammation, Immunity, And disease. Cold Spring Harb Perspect Biol. 2014;

324. Kishimoto T. Interleukin-6: from basic science to medicine—40 years in

immunology. Annu Rev Immunol. 2005;23:1–21.

325. Gabay C. Interleukin-6 and chronic inflammation. Arthritis Res Ther. 2006;

326. Remick DG. Interleukin-8. Crit Care Med. 2005;

327. Sahibzada HA, Khurshid Z, Khan RS, Naseem M, Siddique KM, Mali M, et al. Salivary IL-8, IL-6 and TNF-α as Potential Diagnostic Biomarkers for Oral Cancer. Diagnostics 2017;7(2):21.

328. Murata M. Inflammation and cancer. Environ Health Prev Med. 2018;23(1).

329. Russo N, Bellile E, Murdoch-Kinch CA, Liu M, Eisbruch A, Wolf GT, et al. Cytokines in saliva increase in head and neck cancer patients after treatment. In: Oral Surgery, Oral Medicine, Oral Pathology and Oral Radiology. 2016.

330. Epstein JB, Gorsky M, Guglietta A, Le N, Sonis ST. The Correlation between Epidermal Growth Factor Levels in Saliva and the Severity of Oral Mucositis during Oropharyngeal Radiation Therapy.

331. Costa NL, Valadares MC, Souza PPC, Mendonça EF, Oliveira JC, Silva TA, et al. Tumor-associated macrophages and the profile of inflammatory cytokines in oral squamous cell carcinoma. Oral Oncol. 2013;

332. Fallon PG, Jolin HE, Smith P, Emson CL, Townsend MJ, Fallon R, et al. IL-4 induces characteristic Th2 responses even in the combined absence of IL-5, IL-9, and IL-13. Immunity. 2002;

333. Volpert O V., Fong T, Koch AE, Peterson JD, Waltenbaugh C, Tepper RI, et al. Inhibition of angiogenesis by interleukin 4. J Exp Med. 1998;

334. Conticello C, Pedini F, Zeuner A, Patti M, Zerilli M, Stassi G, et al. IL-4 Protects Tumor Cells from Anti-CD95 and Chemotherapeutic Agents via Up-Regulation of

Antiapoptotic Proteins. J Immunol. 2004;

335. Alhamarneh O, Agada F, Madden L, Stafford N, Greenman J. Serum IL10 and circulating CD4+ CD25high regulatory T cell numbers as predictors of clinical outcome and survival in patients with head and neck squamous cell carcinoma. Head Neck. 2011;33(3):415–23.

336. Hu S, Wong DT. Oral cancer proteomics. Current Opinion in Molecular Therapeutics. 2007.

337. Wu C, Chu H, Hsu C, Chang K, Liu H. Saliva proteome profiling reveals potential salivary biomarkers for detection of oral cavity squamous cell carcinoma. 2015;3394–404.

338. Vargas T, Moreno-Rubio J, Herranz J, Cejas P, Molina S, González-Vallinas M, et al. ColoLipidGene: signature of lipid metabolism-related genes to predict prognosis in stage-II colon cancer patients. Oncotarget 2015 Mar 30;6(9):7348–63.

339. Letters F, Biology M, Received J, Miyasaka M. The role of cystatins in cells of the immune system. 2006;580:6295–301.

340. Martini D, Gallo A, Vella S, Sernissi F, Cecchettini A, Luciano N, et al. Cystatin S—a candidate biomarker for severity of submandibular gland involvement in Sjögren's syndrome. Rheumatology 2017 Jun 1;56(6):1031–8.

341. Ohshiro K, Rosenthal DI, Koomen JM, Streckfus CF, Chambers M, Kobayashi R, et al. Pre-analytic saliva processing affect proteomic results and biomarker screening of head and neck squamous carcinoma. Int J Oncol. 2007;30(3):743–9.

342. Takehara S, Yanagishita M, Podyma-Inoue KA, Kawaguchi Y. Degradation of MUC7 and MUC5B in human saliva. PLoS One 2013 Jul 18;8(7):e69059–e69059.

343. Szkaradkiewicz-Karpińska AK, Ronij A, Goślińska-Kuźniarek O, Przybyłek I,

Szkaradkiewicz A. MUC7 Level As A New Saliva Risk Factor For Dental Caries In Adult Patients. Int J Med Sci 2019 Jan 1;16(2):241–6.

344. Lu H, Liang D, Zhu Y, Xu W, Zhou K, Liu L, et al. Prognostic and clinicopathological significance of MUC expression in head and neck cancer: A systematic review and meta-analysis. Oncotarget. 2017;8(56):96359–72.

345. O'Leary NA, Wright MW, Brister JR, Ciufo S, Haddad D, McVeigh R, et al. Reference sequence (RefSeq) database at NCBI: current status, taxonomic expansion, and functional annotation. Nucleic Acids Res 2016 Jan 4;44(D1):D733–45.

346. Luo D, Chen W, Tian Y, Li J, Xu X, Chen C, et al. Serpin peptidase inhibitor, clade A member 3 (SERPINA3), is overexpressed in glioma and associated with poor prognosis in glioma patients. Onco Targets Ther 2017 Apr 18;10:2173–81.

347. Zhou J, Cheng Y, Tang L, Martinka M, Kalia S. Up-regulation of SERPINA3 correlates with high mortality of melanoma patients and increased migration and invasion of cancer cells. Oncotarget 2017 Mar 21;8(12):18712–25.

348. Santamaria M, Pardo–Saganta A, Alvarez–Asiain L, Di Scala M, Qian C, Prieto J, et al. Nuclear α1-antichymotrypsin promotes chromatin condensation and inhibits proliferation of human hepatocellular carcinoma cells. Gastroenterology. 2013;144(4):818–28.

349. Yang G-D, Yang X-M, Lu H, Ren Y, Ma M-Z, Zhu L-Y, et al. SERPINA3 promotes endometrial cancer cells growth by regulating G2/M cell cycle checkpoint and apoptosis. Int J Clin Exp Pathol. 2014;7(4):1348.

350. Jin Y, Wang J, Ye X, Su Y, Yu G, Yang Q, et al. Identification of GlcNAcylated alpha-1-antichymotrypsin as an early biomarker in human non-small-cell lung cancer by quantitative proteomic analysis with two lectins. Br J Cancer. 2016;114(5):532–44.

351. Karashima S, Kataoka H, Itoh H, Maruyama R, Koono M. Prognostic significance of alpha-1-antitrypsin in early stage of colorectal carcinomas. Int J cancer. 1990;45(2):244–50.

352. Yamamura J, Miyoshi Y, Tamaki Y, Taguchi T, Iwao K, Monden M, et al. mRNA expression level of estrogen-inducible gene, α1-antichymotrypsin, is a predictor of early tumor recurrence in patients with invasive breast cancers. Cancer Sci. 2004;95(11):887–92.

353. Berlutti F, Pilloni A, Pietropaoli M, Polimeni A, Valenti P. Lactoferrin and oral diseases: current status and perspective in periodontitis. Ann Stomatol (Roma) [Internet]. 2011 Mar;2(3–4):10–8.

354. González-Sánchez M, Bartolome F, Antequera D, Puertas-Martín V, González P, Gómez-Grande A, et al. Decreased salivary lactoferrin levels are specific to Alzheimer's disease. EBioMedicine 2020 Jul;57:102834.

355. Baker EN. Lactoferrin: A multi-tasking protein par excellence. Cell Mol Life Sci. 2005;62(22):2529–30.

356. Shiiba M, Saito K, Fushimi K, Ishigami T, Shinozuka K, Nakashima D, et al. Lipocalin-2 is associated with radioresistance in oral cancer and lung cancer cells. Int J Oncol 2013;42(4):1197–204.

357. Bratt T. Lipocalins and cancer. Biochim Biophys Acta - Protein Struct Mol Enzymol 2000;1482(1):318–26.

358. Candido S, Maestro R, Polesel J, Catania A, Maira F, Signorelli SS, et al. Roles of neutrophil gelatinase-associated lipocalin (NGAL) in human cancer. Oncotarget. 2014;5(6):1576.

359. Yang J, Moses MA. Lipocalin 2: A multifaceted modulator of human cancer. Cell Cycle. 2009;8(15):2347–52.

360. Hiromoto T, Noguchi K, Yamamura M, Zushi Y, Segawa E, Takaoka K, et al. Up-regulation of neutrophil gelatinase-associated lipocalin in oral squamous cell carcinoma: Relation to cell differentiation. Oncol Rep 2011;26(6):1415–21.

361. Aqrawi LA, Galtung HK, Vestad B, Øvstebø R, Thiede B, Rusthen S, et al. Identification of potential saliva and tear biomarkers in primary Sjögren's syndrome, utilising the extraction of extracellular vesicles and proteomics analysis. Arthritis Res Ther 2017;19(1):14.

362. Yakob M, Fuentes L, Wang MB, Abemayor E, Wong DTW. Salivary Biomarkers for Detection of Oral Squamous Cell Carcinoma: Current State and Recent Advances. Curr Oral Heal Reports. 2014;1(2):133–41.

363. Miller CS, Foley JD, Bailey AL, Campell CL, Humphries RL, Christodoulides N, et al. Current developments in salivary diagnostics. Biomark Med 2010 Feb;4(1):171–89.

364. Stott-Miller M, Houck JR, Lohavanichbutr P, Méndez E, Upton MP, Futran ND, et al. Tumor and salivary matrix metalloproteinase levels are strong diagnostic markers of oral squamous cell carcinoma. Cancer Epidemiol Biomarkers Prev 2011 Dec;20(12):2628–36.

365. Burduk PK, Bodnar M, Sawicki P, Szylberg Ł, Wiśniewska E, Kaźmierczak W, et al. Expression of metalloproteinases 2 and 9 and tissue inhibitors 1 and 2 as predictors of lymph node metastases in oropharyngeal squamous cell carcinoma. Head Neck. 2015;

366. Byron A, Humphries JD, Humphries MJ. Defining the extracellular matrix using proteomics. Int J Exp Pathol 2013 Apr;94(2):75–92.

367. Castagnola M, Picciotti PM, Messana I, Fanali C, Fiorita A, Cabras T, et al. Potential applications of human saliva as diagnostic fluid. Acta Otorhinolaryngol Ital 2011 Dec;31(6):347–57.

VIII. Appendix

1 SUPPLEMENTAL TABLES

Supplemental Table 1: Univariate analysis performed per each analyte (IL-6, IL-8, TNF-α, IL-4, IL-10, MCP-1, EGF, VEGF) and each group investigated (CTRL, BRT, ART). Data include: first and third quartiles, median, minimum and maximum values, variance and standard deviation (SD).

CTRL Group	1st Qu	3rd Qu	Median	Min	Max	Variance	SD
EGF	604,40	1504,40	990,90	387,80	3245,20	501997,20	708,52
IL-10	9,92	28,61	18,05	1,20	290,22	2146,14	46,33
IL-4	15,83	43,34	28,05	2,37	413,05	4364,12	66,06
IL-6	3,12	10,78	5,27	0,98	43,86	95,31	9,76
IL-8	404,80	1002,90	821,20	178,40	3309,60	362349,20	601,95
MCP-1	416,00	849,40	581,50	138,20	8530,90	3685936,00	1919,88
TNF-α	5,55	15,26	9,29	2,73	57,75	134,65	11,60
VEGF	277,65	492,55	358,17	15,69	1248,43	80698,40	284,07

BRT Group	1st Qu	3rd Qu	Median	Min	Max	Variance	SD
EGF	639,40	1528,50	1003,90	272,70	4799,80	1062606,00	1030,83
IL-10	14,73	42,69	25,53	2,55	221,75	2161,96	46,50
IL-4	23,26	56,43	39,10	6,75	241,98	2190,61	46,80
IL-6	8,56	45,11	20,04	0,36	911,23	52915,64	230,03
IL-8	370,01	1927,29	1046,76	86,97	7389,83	3254481,00	1804,02
MCP-1	368,00	1029,30	578,50	127,00	6893,60	2116288,00	1454,75
TNF-α	7,32	21,81	13,35	1,83	282,07	2636,36	51,35
VEGF	291,13	702,10	429,33	29,25	2014,64	150758,90	388,28

ART Group	1st Qu	3rd Qu	Median	Min	Max	Variance	SD
EGF	506,30	1055,60	846,60	213,40	3137,10	393464,60	627,27
IL-10	17,03	68,86	35,08	1,70	718,75	17817,08	133,48
IL-4	20,68	62,38	31,53	9,23	169,46	1735,24	41,66
IL-6	10,96	75,80	23,49	2,48	3052,01	311418,20	558,05
IL-8	865,00	5002,90	2132,80	139,90	8777,30	6842415,00	2615,80
MCP-1	1185,00	4853,00	2635,00	359,00	8320,00	6282871,00	2506,57
TNF-α	6,76	33,99	20,90	2,54	674,09	14892,93	122,04
VEGF	206,40	718,81	399,72	14,63	1138,85	95032,70	308,27

Supplemental Table 2: Simplified clinical variables applied for the construction of the Bayesian network, using directed acyclic graphing (DAG) and conditional probability methodology.

Clinical variables:	***Simplified parameters***			
Diagnosis	HNC	OSCC		
Tumour Location	Oral cavity	Larynx area	Pharynx area	
Neck metastasis	Yes	No		
TNM.T	T1	T2	T3	T4
TNM.N	N0	N1	N2	N3
Type of treatment	Adjuvant RT	RT+QT	Radical RT	
Treatment response	Responders	Non-responders		
Mucositis	NO (absence)	G1	G2	G3
Xerostomia	NO (absence)	G1	G2	
Dermitis	NO (absence)	G1	G2	

Supplemental Table 3: Every table (3.1; 3.2; 3.3; 3.4; 3.5; 3.6; 3.7) represents the answer of a query regarding the simplified clinical parameters above-mentioned (Supplemental Table 2). For example, Table 3.1 presents the results regarding the variable "Diagnosis" when its condition is "HNC" or "OSCC". In particular, what we have done is to infer a range of values per each analyte investigated (EGF, IL -10, IL-4, IL-6, IL-8, MCP-1, TNF-α and VEGF), that can be associated with a given probability to belong to one of the possible states of the variable. In this case, Table 3.1, the variable "Diagnosis" has two states HNC or OSCC, hence for every analyte, there will be a range of values and its probability to be associated with HNC or OSCC. Regarding the HNC cases belonging to the BRT group, results revealed no relations between salivary proteins and the variable "TNM.T", as well as for the variable "type of treatment" and "mucositis" concerning the ART group, thus results are not shown.

Per each query concerning the clinic parameters analysed and its relative group (BRT or ART), the mean value, the lower (L) and upper values (U) of each analyte is expressed. The other two columns represent the probability (P) of the variable to belong to one of the possible states of the clinical parameter. In case of EGF, in Table 3.1, P is 0.746 (with a standard error of 0.0696) if the value of EGF is in the range [1419:1430]; whereas the probability that the diagnosis will be OSCC is 0.257, according to the same EGF range of values.

Table 3.1: Results regarding the clinical variable "Diagnosis". Per each clinic parameters analysed and its relative group (BRT or ART), the mean value, the lower (L) and upper values (U) of every analyte are expressed, plus the probability (P) and the standard error [ ] to belong to one of the possible states of the variable.

Diagnosis = 'HNC'					
BRT Group	**mean**	**L**	**U**	**P(Diagnosis = 'HNC')**	**P(Diagnosis = 'OSCC')**
EGF	1.424	1.419	1.430	0.746 [+0.0696]	0.257 [+0.0698]
IL-10	36	35	36	0.666 [+0.0547]	0.338 [+0.0603]
IL-4	51	51	51	0.77 [+0.0643]	0.218 [+0.0645]
IL-6	172	140	203	0.349 [+0.0302]	0.65 [+0.0293]
IL-8	2.656	2.302	3.011	0.559 [+0.0219]	0.439 [+0.0183]
MCP-1	1.186	1.175	1.198	0.664 [+0.0646]	0.342 [+0.0607]
TNF-a	43	37	48	0.49 [+0.0263]	0.509 [+0.0216]
VEGF	567	565	570	0.79 [+0.0639]	0.217 [+0.0636]
Diagnosis = 'OSCC'					
BRT Group	**mean**	**L**	**U**	**P(Diagnosis = 'HNC')**	**P(Diagnosis = 'OSCC')**
EGF	973	968	979	0.671 [+0.0536]	0.341 [+0.0619]
IL-10	72	71	73	0.541 [+0.0721]	0.471 [+0.0758]
IL-4	57	56	57	0.781 [+0.0434]	0.225 [+0.044]
IL-6	782	728	836	0.254 [+0.0633]	0.738 [+0.0698]
IL-8	2.377	2.349	2.405	0.572 [+0.0631]	0.429 [+0.0627]
MCP-1	1.186	1.169	1.203	0.669 [+0.0467]	0.33 [+0.0457]
TNF-a	35	35	35	0.529 [+0.0805]	0.479 [+0.0713]
VEGF	647	638	656	0.782 [+0.0373]	0.223 [+0.0398]

Table 3.2: Results regarding the clinical variable "Location". Per each clinic parameters analysed and its relative group (BRT or ART), the mean value, the lower (L) and upper values (U) of every analyte are expressed, plus the probability (P) and the standard error [ ] to belong to one of the possible states of the variable.

Location ='Oral cavity'						
BRT Group	**mean**	**L**	**U**	**P(Location = ' Oral cavity')**	**P(Location = 'Larynx area')**	**P(Location = 'Pharynx area')**
EGF	1.082	1.076	1.088	0.381 [+0.0578]	0.424 [+0.0648]	0.201 [+0.0469]
IL-10	77	76	78	0.633 [+0.0677]	0.272 [+0.072]	0.106 [+0.0441]
IL-4	55	55	56	0.318 [+0.053]	0.472 [+0.0517]	0.221 [+0.0436]
IL-6	903	834	972	0.997 [+0.0071]	0 [+0]	0.003 [+0.0073]
IL-8	4.476	3.886	5.066	0.595 [+0.0253]	0.246 [+0.0243]	0.16 [+0.0202]
MCP-1	1.178	1.163	1.192	0.403 [+0.0506]	0.398 [+0.0503]	0.188 [+0.0418]
TNF-a	76	66	85	0.739 [+0.0257]	0.132 [+0.023]	0.134 [+0.0239]
VEGF	705	697	713	0.337 [+0.055]	0.41 [+0.0543]	0.25 [+0.0454]

Location = 'Larynx area'						
BRT Group	**mean**	**L**	**U**	**P(Location = 'Oral cavity')**	**P(Location = 'Larynx area')**	**P(Location = 'Pharynx area')**
EGF	1.427	1.419	1.434	0.344 [+0.0642]	0.442 [+0.0715]	0.202 [+0.0561]
IL-10	28	28	28	0.325 [+0.0493]	0.337 [+0.0513]	0.35 [+0.0576]
IL-4	51	51	51	0.308 [+0.0638]	0.469 [+0.0708]	0.221 [+0.0651]
IL-6	21	21	21	0.199 [+0.0625]	0.564 [+0.0734]	0.232 [+0.0683]
IL-8	1.208	1.196	1.219	0.384 [+0.0658]	0.409 [+0.0679]	0.21 [+0.0488]
MCP-1	1.195	1.180	1.210	0.399 [+0.0582]	0.403 [+0.0523]	0.207 [+0.0481]
TNF-a	15	15	15	0.336 [+0.0605]	0.438 [+0.0639]	0.219 [+0.0564]
VEGF	512	509	515	0.309 [+0.0732]	0.444 [+0.0741]	0.249 [+0.0628]

Location = 'Pharynx area'						
BRT Group	**mean**	**L**	**U**	**P(Location = 'Oral cavity')**	**P(Location = 'Larynx area')**	**P(Location = 'Pharynx area')**
EGF	1.350	1.340	1.361	0.348 [+0.0568]	0.434 [+0.059]	0.211 [+0.0472]
IL-10	29	29	29	0.322 [+0.0723]	0.324 [+0.0676]	0.347 [+0.0717]
IL-4	52	51	52	0.321 [+0.0439]	0.459 [+0.0515]	0.223 [+0.0445]
IL-6	30	29	30	0.253 [+0.0468]	0.508 [+0.0531]	0.235 [+0.049]
IL-8	1.445	1.423	1.467	0.408 [+0.0528]	0.387 [+0.0509]	0.2 [+0.0422]
MCP-1	1.186	1.164	1.209	0.398 [+0.0415]	0.4 [+0.0403]	0.199 [+0.0347]
TNF-a	19	19	20	0.391 [+0.0539]	0.393 [+0.0508]	0.204 [+0.04]
VEGF	535	531	539	0.312 [+0.059]	0.429 [+0.0605]	0.258 [+0.0541]

Table 3.3: Results regarding the clinical variable "Neck metastasis". Per each clinic parameters analysed and its relative group (BRT or ART), the mean value, the lower (L) and upper values (U) of every analyte are expressed, plus the probability (P) and the standard error [ ] to belong to one of the possible states of the variable.

Neck_metastasis = 'no'					
BRT Group	**mean**	**L**	**U**	**P(Neck_metastasis = 'yes')**	**P(Neck_metastastasis = 'no')**
EGF	1.277	1.271	1.283	0.473 [+0.0639]	0.542 [+0.0771]
IL-10	48	47	49	0.458 [+0.0613]	0.529 [+0.0651]
IL-4	53	52	53	0.465 [+0.0652]	0.531 [+0.066]
IL-6	367	332	402	0.461 [+0.051]	0.535 [+0.0546]
IL-8	1.438	1.420	1.455	0.493 [+0.057]	0.516 [+0.0603]
MCP-1	885	878	892	0.422 [+0.061]	0.588 [+0.0608]
TNF-a	30	30	31	0.441 [+0.0476]	0.564 [+0.0478]
VEGF	597	592	602	0.473 [+0.0608]	0.535 [+0.0601]

Neck_metastasis = 'yes'					
BRT Group	**mean**	**L**	**U**	**P(Neck_metastasis = 'yes')**	**P(Neck_metastasis = 'no')**
EGF	1.270	1.264	1.276	0.469 [+0.0704]	0.542 [+0.0749]
IL-10	47	47	48	0.466 [+0.0609]	0.533 [+0.057]
IL-4	53	53	53	0.474 [+0.0612]	0.538 [+0.0603]
IL-6	385	341	429	0.462 [+0.0445]	0.541 [+0.0443]
IL-8	3.845	3.341	4.350	0.588 [+0.0235]	0.413 [+0.0267]
MCP-1	1.530	1.511	1.548	0.507 [+0.0598]	0.492 [+0.0613]
TNF-a	51	44	59	0.453 [+0.0248]	0.547 [+0.0243]
VEGF	590	585	595	0.469 [+0.0545]	0.546 [+0.0589]

Table 3.4: Results regarding the clinical variable "TNM.N". Per each clinic parameters analysed and its relative group (BRT or ART), the mean value, the lower (L) and upper values (U) of every analyte are expressed, plus the probability (P) and the standard error [ ] to belong to one of the possible states of the variable.

TNM.N.only = 'N0'							
BRT Group	mean	L	U	P(TNM.N.only == 'N0')	P(TNM.N.only == 'N1')	P(TNM.N.only == 'N2')	P(TNM.N.only == 'N3')
EGF	1.274	1.268	1.281	0.466 [+0.0672]	0.168 [+0.0556]	0.268 [+0.0607]	0.093 [+0.0391]
IL-10	48	48	49	0.458 [+0.0603]	0.162 [+0.0481]	0.265 [+0.0503]	0.1 [+0.0342]
IL-4	53	52	53	0.468 [+0.0629]	0.165 [+0.0468]	0.262 [+0.0517]	0.1 [+0.036]
IL-6	387	348	426	0.463 [+0.0476]	0.166 [+0.0386]	0.272 [+0.0478]	0.102 [+0.0328]
IL-8	1.390	1.374	1.406	0.44 [+0.0627]	0.171 [+0.0438]	0.27 [+0.0532]	0.102 [+0.0318]
MCP-1	795	791	800	0.535 [+0.0795]	0.149 [+0.0473]	0.205 [+0.0542]	0.113 [+0.0439]
TNF-a	30	29	31	0.486 [+0.0466]	0.154 [+0.0359]	0.253 [+0.0422]	0.101 [+0.0286]
VEGF	600	595	606	0.46 [+0.0553]	0.164 [+0.038]	0.272 [+0.0552]	0.1 [+0.0333]

TNM.N.only = 'N1'							
BRT Group	mean	L	U	P(TNM.N.only = 'N0')	P(TNM.N.only = 'N1')	P(TNM.N.only = 'N2')	P(TNM.N.only = 'N3')
EGF	1.275	1.265	1.286	0.465 [+0.053]	0.164 [+0.0394]	0.267 [+0.0463]	0.099 [+0.0305]
IL-10	47	46	48	0.465 [+0.0447]	0.166 [+0.0366]	0.268 [+0.039]	0.101 [+0.0313]
IL-4	53	52	53	0.47 [+0.0504]	0.171 [+0.0348]	0.265 [+0.0433]	0.1 [+0.0272]
IL-6	403	337	469	0.473 [+0.0386]	0.162 [+0.0299]	0.263 [+0.0366]	0.099 [+0.0239]
IL-8	3.438	3.161	3.716	0.36 [+0.0289]	0.195 [+0.0257]	0.335 [+0.0288]	0.106 [+0.019]
MCP-1	981	968	995	0.507 [+0.0502]	0.148 [+0.0357]	0.224 [+0.0375]	0.119 [+0.0272]
TNF-a	54	44	64	0.475 [+0.0193]	0.162 [+0.0156]	0.263 [+0.0181]	0.097 [+0.0122]
VEGF	592	583	600	0.472 [+0.0491]	0.164 [+0.0335]	0.27 [+0.0406]	0.103 [+0.0278]

TNM.N.only = 'N2'							
BRT Group	mean	L	U	P(TNM.N.only = 'N0')	P(TNM.N.only = 'N1')	P(TNM.N.only = 'N2')	P(TNM.N.only = 'N3')
EGF	1.275	1.267	1.283	0.477 [+0.0661]	0.171 [+0.0447]	0.271 [+0.0516]	0.098 [+0.0414]
IL-10	47	46	48	0.461 [+0.0468]	0.168 [+0.0355]	0.27 [+0.0448]	0.1 [+0.0329]
IL-4	53	52	53	0.465 [+0.0534]	0.165 [+0.0379]	0.266 [+0.0389]	0.098 [+0.0302]
IL-6	444	358	529	0.466 [+0.0371]	0.169 [+0.0263]	0.267 [+0.0283]	0.096 [+0.0228]
IL-8	3.702	3.402	4.001	0.351 [+0.03]	0.197 [+0.0256]	0.336 [+0.0304]	0.11 [+0.0208]
MCP-1	2.104	2.071	2.136	0.339 [+0.0683]	0.157 [+0.0501]	0.387 [+0.0612]	0.099 [+0.037]
TNF-a	50	42	58	0.479 [+0.022]	0.163 [+0.0171]	0.26 [+0.0203]	0.1 [+0.0138]
VEGF	593	586	599	0.458 [+0.0535]	0.169 [+0.038]	0.267 [+0.0401]	0.098 [+0.0335]

TNM.N.only = 'N3'							
BRT Group	mean	L	U	P(TNM.N.only = 'N0')	P(TNM.N.only = 'N1')	P(TNM.N.only = 'N2')	P(TNM.N.only = 'N3')
EGF	1.280	1.267	1.294	0.465 [+0.0498]	0.166 [+0.0361]	0.259 [+0.0396]	0.099 [+0.0263]
IL-10	47	46	48	0.473 [+0.0384]	0.165 [+0.0253]	0.265 [+0.0359]	0.099 [+0.0259]
IL-4	53	52	54	0.467 [+0.0389]	0.17 [+0.0339]	0.265 [+0.0361]	0.101 [+0.0256]
IL-6	399	324	474	0.47 [+0.0356]	0.167 [+0.0271]	0.266 [+0.0347]	0.101 [+0.0213]
IL-8	2.621	2.436	2.806	0.386 [+0.0279]	0.192 [+0.0246]	0.315 [+0.026]	0.106 [+0.0158]
MCP-1	927	915	939	0.514 [+0.0452]	0.154 [+0.0376]	0.221 [+0.0409]	0.11 [+0.0306]
TNF-a	38	35	41	0.489 [+0.0276]	0.154 [+0.019]	0.256 [+0.0212]	0.097 [+0.0154]
VEGF	588	579	598	0.476 [+0.0418]	0.168 [+0.0311]	0.268 [+0.0353]	0.099 [+0.0248]

Table 3.5: Results regarding the clinical variable "Treatment Response". Per each clinic parameters analysed and its relative group (BRT or ART), the mean value, the lower (L) and upper values (U) of every analyte are expressed, plus the probability (P) and the standard error [ ] to belong to one of the possible states of the variable.

Treatment.Response = 'Non responders'					
ART Group	mean	L	U	P(Treatment.Response = 'Non responders')	P(Treatment.Response = 'Responders')
EGF	944	937	951	0.163 [+0.038]	0.834 [+0.039]
IL-10	125	115	134	0.169 [+0.0232]	0.833 [+0.0213]
IL-4	25	25	25	0.281 [+0.0551]	0.719 [+0.0597]
IL-6	137	130	145	0.168 [+0.03]	0.832 [+0.0276]
IL-8	14.761	14.421	15.101	0.453 [+0.0846]	0.543 [+0.0798]
MCP-1	3.517	3.469	3.565	0.168 [+0.0396]	0.831 [+0.0395]
TNF-α	42	40	43	0.168 [+0.0262]	0.832 [+0.0272]
VEGF	633	621	645	0.171 [+0.0328]	0.823 [+0.0363]

Treatment.Response = 'Responders'					
ART Group	mean	L	U	P(Treatment.Response = 'Non responders')	P(Treatment.Response = 'Responders')
EGF	949	946	952	0.16 [+0.06]	0.834 [+0.0572]
IL-10	120	116	124	0.166 [+0.032]	0.829 [+0.0339]
IL-4	53	53	54	0.068 [+0.0434]	0.938 [+0.0453]
IL-6	140	136	144	0.171 [+0.0392]	0.832 [+0.0423]
IL-8	3.404	3.372	3.436	0.165 [+0.0554]	0.839 [+0.0494]
MCP-1	3.531	3.510	3.553	0.169 [+0.059]	0.842 [+0.0574]
TNF-α	44	43	44	0.168 [+0.0533]	0.829 [+0.0507]
VEGF	631	626	636	0.165 [+0.0548]	0.836 [+0.054]

Table 3.6: Results regarding the clinical variable "Dermatitis". Per each clinic parameters analysed and its relative group (BRT or ART), the mean value, the lower (L) and upper values (U) of every analyte are expressed, plus the probability (P) and the standard error [ ] to belong to one of the possible states of the variable.

Dermatitis = 'Dermatitis G1'						
ART Group	**mean**	**L**	**U**	**P(Dermatitis = 'Dermatitis G1')**	**P(Dermatitis = 'Dermatitis G2')**	**P(Dermatitis = 'Dermatitis NO')**
EGF	951	944	959	0.172 [+0.0361]	0.263 [+0.049]	0.563 [+0.0495]
IL-10	124	117	131	0.166 [+0.0262]	0.269 [+0.0317]	0.567 [+0.0341]
IL-4	48	48	49	0.168 [+0.04]	0.266 [+0.0477]	0.571 [+0.0537]
IL-6	141	126	156	0.142 [+0.0204]	0.274 [+0.0224]	0.58 [+0.0251]
IL-8	5.227	5.085	5.368	0.165 [+0.0335]	0.265 [+0.038]	0.57 [+0.0451]
MCP-1	3.516	3.469	3.564	0.163 [+0.0363]	0.27 [+0.0463]	0.565 [+0.055]
TNF-α	46	44	47	0.166 [+0.0254]	0.268 [+0.035]	0.575 [+0.0398]
VEGF	637	625	650	0.17 [+0.0369]	0.269 [+0.0402]	0.568 [+0.048]

Dermatitis = 'Dermatitis G2'						
ART Group	**mean**	**L**	**U**	**P(Dermatitis = 'Dermatitis NO')**	**P(Dermatitis = 'Dermatitis G1')**	**P(Dermatitis = 'Dermatitis G2')**
EGF	945	939	951	0.564 [+0.0566]	0.16 [+0.0468]	0.272 [+0.052]
IL-10	120	113	128	0.565 [+0.0318]	0.164 [+0.0231]	0.264 [+0.0313]
IL-4	48	48	49	0.572 [+0.0617]	0.164 [+0.0414]	0.266 [+0.0556]
IL-6	151	145	157	0.584 [+0.0419]	0.139 [+0.0325]	0.274 [+0.0428]
IL-8	5.406	5.278	5.533	0.573 [+0.0491]	0.171 [+0.0362]	0.266 [+0.0436]
MCP-1	3.543	3.505	3.581	0.562 [+0.0554]	0.169 [+0.0429]	0.263 [+0.0496]
TNF-α	46	46	47	0.581 [+0.0481]	0.156 [+0.0342]	0.266 [+0.0395]
VEGF	635	626	645	0.571 [+0.057]	0.167 [+0.0384]	0.264 [+0.046]

Dermatitis = 'Dermatitis NO'						
ART Group	**mean**	**L**	**U**	**P(Dermatitis = 'Dermatitis NO')**	**P(Dermatitis = 'Dermatitis G1')**	**P(Dermatitis = 'Dermatitis G2')**
EGF	949	945	953	0.567 [+0.0699]	0.165 [+0.0538]	0.261 [+0.0617]
IL-10	120	116	125	0.571 [+0.0432]	0.159 [+0.0301]	0.266 [+0.0336]
IL-4	49	48	49	0.579 [+0.0637]	0.164 [+0.0573]	0.261 [+0.0636]
IL-6	133	130	136	0.576 [+0.0616]	0.148 [+0.0397]	0.276 [+0.0547]
IL-8	5.282	5.193	5.372	0.563 [+0.0628]	0.167 [+0.0426]	0.262 [+0.051]
MCP-1	3.526	3.500	3.552	0.566 [+0.0621]	0.166 [+0.0502]	0.271 [+0.0659]
TNF-α	41	41	42	0.58 [+0.0644]	0.161 [+0.0505]	0.259 [+0.0523]
VEGF	628	622	634	0.565 [+0.0689]	0.171 [+0.0488]	0.267 [+0.057]

Table 3.7: Results regarding the clinical variable "Xerostomia". Per each clinic parameters analysed and its relative group (BRT or ART), the mean value, the lower (L) and upper values (U) of every analyte are expressed, plus the probability (P) and the standard error [ ] to belong to one of the possible states of the variable.

Xerostomia = 'Xerostomia G1'						
ART Group	**mean**	**L**	**U**	**P(Xerostomia = 'Xerostomia NO')**	**P(Xerostomia = 'Xerostomia G1')**	**P(Xerostomia = 'Xerostomia G2')**
EGF	948	942	955	0.67 [+0.0522]	0.2 [+0.0436]	0.13 [+0.0361]
IL-10	50	50	51	0.676 [+0.0605]	0.247 [+0.0525]	0.086 [+0.0312]
IL-4	49	48	49	0.671 [+0.0515]	0.204 [+0.0417]	0.131 [+0.034]
IL-6	135	130	140	0.666 [+0.0411]	0.204 [+0.0369]	0.133 [+0.0346]
IL-8	5,328	5,157	5,499	0.663 [+0.0444]	0.203 [+0.0334]	0.132 [+0.0316]
MCP-1	3,500	3,457	3,542	0.663 [+0.0508]	0.191 [+0.039]	0.136 [+0.0383]
TNF-α	43	42	44	0.662 [+0.0472]	0.201 [+0.037]	0.137 [+0.033]
VEGF	555	546	563	0.667 [+0.0525]	0.204 [+0.0406]	0.13 [+0.0337]

Xerostomia = 'Xerostomia G2'						
ART Group	**mean**	**L**	**U**	**P(Xerostomia = 'Xerostomia NO')**	**P(Xerostomia = 'Xerostomia G1')**	**P(Xerostomia = 'Xerostomia G2')**
EGF	949	941	957	0.67 [+0.0457]	0.199 [+0.0382]	0.134 [+0.0377]
IL-10	378	354	403	0.69 [+0.0555]	0.044 [+0.0227]	0.267 [+0.0527]
IL-4	48	48	49	0.666 [+0.0445]	0.199 [+0.0411]	0.13 [+0.0339]
IL-6	140	133	147	0.672 [+0.037]	0.201 [+0.0323]	0.133 [+0.0274]
IL-8	5,352	5,185	5,518	0.669 [+0.0385]	0.196 [+0.0346]	0.131 [+0.0318]
MCP-1	3,547	3,492	3,602	0.661 [+0.0406]	0.195 [+0.0384]	0.133 [+0.0333]
TNF-α	43	42	44	0.668 [+0.0487]	0.201 [+0.0377]	0.133 [+0.0307]
VEGF	738	722	753	0.667 [+0.0432]	0.203 [+0.0372]	0.134 [+0.0305]

Xerostomia = 'Xerostomia _NO'						
ART Group	mean	L	U	P(Xerostomia = 'Xerostomia NO')	P(Xerostomia = 'Xerostomia G1')	P(Xerostomia = 'Xerostomia G2')
EGF	948	945	952	0.662 [+0.0642]	0.198 [+0.0589]	0.134 [+0.0538]
IL-10	90	89	91	0.7 [+0.065]	0.199 [+0.0525]	0.106 [+0.042]
IL-4	49	48	49	0.67 [+0.0788]	0.199 [+0.0578]	0.139 [+0.0455]
IL-6	140	136	145	0.667 [+0.0395]	0.2 [+0.0424]	0.131 [+0.0352]
IL-8	5,290	5,214	5,367	0.655 [+0.0606]	0.197 [+0.0515]	0.134 [+0.0429]
MCP-1	3,534	3,510	3,558	0.662 [+0.0694]	0.199 [+0.06]	0.129 [+0.0447]
TNF-α	44	43	44	0.66 [+0.0533]	0.204 [+0.0487]	0.127 [+0.0387]
VEGF	633	628	639	0.664 [+0.0623]	0.2 [+0.0589]	0.129 [+0.0469]

Supplemental Table 4: List of salivary proteins (N=695) quantified by the LC-MS/MS analysis operated in SWATH mode, identified in 30 individual samples. UniProt ID, gene and protein name, number of unique peptides and the subcellular location are presented. The average (Av) value obtained from the normalised and log2-transformed dataset is expressed per each group investigated. In addition, the salivary proteins resulted differentially expressed according to the Elastic Net penalized regression model (N=59) are shown (1= significant; 0= not significant).

List #	UniProt ID	Gene names	Protein names	CTRL Av	BRT Av	ART Av	Peptides #	Significance Elastic Net analysis	Subcellular location
1	Q99943	AGPAT1 G15	1-acyl-sn-glycerol-3-phosphate acyltransferase alpha	-1.4393	1.7932	1.4209	1	1	Endoplasmic reticulum membrane
2	P02788	LTF GIG12 LF	Lactotransferrin (Lactoferrin)	7.9997	8.3051	9.3491	67	1	Secreted, Cytoplasmic granule
3	P19013	KRT4 CYK4	Keratin, type II cytoskeletal 4 (Cytokeratin-4)	10.7770	9.3177	7.9647	63	1	
4	P12035	KRT3	Keratin, type II cytoskeletal 3 (Cytokeratin-3)	8.6909	7.1519	5.8442	13	1	
5	P80188	LCN2 HNL NGAL	Neutrophil gelatinase-associated lipocalin (NGAL)	4.5977	5.1563	5.9632	12	1	Secreted
6	P40394	ADH7	All-trans-retinol dehydrogenase [NAD(+)] ADH7	2.3808	2.2277	1.4553	9	1	Cytoplasm
7	P01011	SERPINA3 AACT GIG24 GIG25	Alpha-1-antichymotrypsin (ACT)	1.2344	2.2500	3.2606	8	1	Secreted
8	Q8TAX7	MUC7 MG2	Mucin-7	2.2187	0.9080	-0.3353	2	1	Secreted
9	Q96GD3	SCMH1	Polycomb protein SCMH1	-3.8936	-1.8748	-1.1076	1	1	Nucleus
10	P19971	TYMP ECGF1	Thymidine phosphorylase (TP)	-0.9173	-0.1130	0.6736	4	1	
11	P01037	CST1	Cystatin-SN (Cystatin-1)	6.9349	6.0232	3.8742	7	1	Secreted
12	O00391	QSOX1 QSCN6 UNQ2520/PRO6013	Sulfhydryl oxidase 1	-0.6509	-0.5207	0.1155	4	1	Golgi apparatus membrane
13	Q96BQ1	FAM3D UNQ567 / PRO1130	Protein FAM3D	-1.0680	-0.0503	0.1342	2	1	Secreted
14	P81605	DCD AIDD DSEP	Dermcidin	-3.6862	-3.4886	-2.2187	1	1	Secreted
15	P23284	PPIB CYPB	Peptidyl-prolyl cis-trans isomerase B (PPIase B)	3.2744	3.7608	3.3579	6	1	Virion (Note=Microbial infection)
16	Q99497	PARK7	Protein/nucleic acid deglycase DJ-1	-2.0766	-1.4842	-0.9590	1	1	Cell membrane
17	P61604	HSPE1	10 kDa heat shock protein, mitochondrial (Hsp10)	-0.2502	-0.6061	-0.0730	2	1	Mitochondrion matrix
18	Q8N4F0	BPIFB2	BPI fold-containing family B member 2	4.0341	4.6411	5.3236	11	1	Secreted

List #	UniProt ID	Gene names	Protein names	CTRL Av	BRT Av	ART Av	Peptides #	Significance Elastic Net analysis	Subcellular location
19	Q8TDL5	BPIFB1	BPI fold-containing family B member 1	3.7481	6.1062	5.7332	24	1	Secreted
20	P31944	CASP14	Caspase-14 (CASP-14)	-4.6363	-3.4568	-3.0262	1	1	Cytoplasm
21	Q9NP55	BPIFA1	BPI fold-containing family A member 1	1.9059	4.5014	4.5967	8	1	Secreted
22	Q15782	CHI3L2	Chitinase-3-like protein 2 (Chondrocyte protein 39)	-2.3606	-1.9381	-0.5433	2	1	Secreted
23	P01033	TIMP1 CLGI TIMP	Metalloproteinase inhibitor 1	2.4006	3.7875	3.2285	5	1	Secreted
24	P48594	SERPINB4	Serpin B4	-0.0301	0.5383	1.3821	4	1	Cytoplasm
25	P28074	PSMB5 LMPX MB1X	Proteasome subunit beta type-5	-2.9121	-4.5262	-3.7768	1	1	Cytoplasm
26	P19105	MYL12A MLCB MRLC3 RLC	Myosin regulatory light chain 12A	-0.0665	0.5710	0.0696	2	1	
27	P15515	HTN1 HIS1	Histatin-1 (Histidine-rich protein 1)	-5.6411	-4.6180	-5.9687	2	1	Secreted
28	P40925	MDH1 MDHA	Malate dehydrogenase	0.8564	0.8787	1.2743	4	1	Cytoplasm
29	P78417	GSTO1 GSTTLP28	Glutathione S-transferase omega-1 (GSTO-1)	0.0746	0.4140	0.8122	1	1	Cytoplasm, cytosol
30	P01615	IGKV2D-28	Immunoglobulin kappa variable 2D-28 (Ig kappa chain V-II region FR)	0.1642	0.4421	1.1404	2	1	Secreted
31	P80303	NUCB2	Nucleobindin-2	0.8850	1.9536	1.0652	3	1	Golgi apparatus
32	P02812	PRB2	Basic salivary proline-rich protein 2 (Salivary proline-rich protein)	-2.3473	-2.7225	-7.7225	1	1	Secreted
33	P62857	RPS28	40S ribosomal protein S28	2.6190	2.9632	-0.6608	1	1	Cytoplasm, cytosol
34	O60664	PLIN3	Perilipin-3	-1.7364	-0.6126	-0.7681	3	1	Cytoplasm
35	P39019	RPS19	40S ribosomal protein S19	-3.2237	-3.0676	-2.0451	1	1	Nucleus
36	P0DOX7		Immunoglobulin kappa light chain	-1.9353	-1.5009	-0.6977	2	1	Secreted
37	Q9NSB2	KRT84 KRTHB4	Keratin, type II cuticular Hb4 (Keratin-84)	1.6169	1.0094	0.1285	12	1	
38	P17174	GOT1	Aspartate aminotransferase, cytoplasmic (cAspAT)	-1.1249	-0.2971	-0.8749	3	1	Cytoplasm
39	P61106	RAB14	Ras-related protein Rab-14	-2.4275	-1.7942	-1.9846	2	1	Recycling endosome

List #	UniProt ID	Gene names	Protein names	CTRL Av	BRT Av	ART Av	Peptides #	Significance Elastic Net analysis	Subcellular location
40	Q14914	PTGR1 LTB4DH	Prostaglandin reductase 1 (PRG-1)	-1.4134	-1.0985	-2.3015	2	1	Cytoplasm
41	P06312	IGKV4-1	Immunoglobulin kappa variable 4-1 (Ig kappa chain V-IV region B17)	2.4749	2.8466	3.3830	3	1	Secreted
42	P22079	LPO SAPX	Lactoperoxidase (LPO)	5.5840	6.1730	5.3708	26	1	Secreted
43	P49720	PSMB3	Proteasome subunit beta type-3	-3.7061	-3.4300	-2.6884	1	1	Cytoplasm
44	Q7L576	CYFIP1	Cytoplasmic FMR1-interacting protein 1	-2.5057	-3.3615	-2.8679	1	1	Cytoplasm
45	P07737	PFN1	Profilin-1	2.9254	2.3111	3.1600	7	1	Cytoplasm, cytoskeleton
46	A0A0C4DH38	IGHV5-51	Immunoglobulin heavy variable 5-51	-3.4747	-4.1791	-2.5482	1	1	Secreted
47	P31997	CEACAM8 CGM6	Carcinoembryonic antigen-related cell adhesion molecule 8 (CD67 antigen)	-3.8608	-6.7382	-3.8682	1	1	Cell membrane
48	P43490	NAMPT PBEF PBEF1	Nicotinamide phosphoribosyltransferase (NAmPRTase)	1.2956	1.6089	1.5976	4	1	Nucleus
49	Q9Y6N5	SQOR SQRDL CGI-44	Sulfide:quinone oxidoreductase, mitochondrial (SQOR)	-0.6570	-1.2773	-0.4041	3	1	Mitochondrion
50	P51571	SSR4 TRAPD	Translocon-associated protein subunit delta (TRAP-delta)	-4.4957	-4.8099	-3.7807	1	1	Endoplasmic reticulum membrane
51	Q53RT3	ASPRV1 SASP	Retroviral-like aspartic protease 1	-2.5833	-2.1380	-3.3487	1	1	Membrane
52	A0A0B4J1V0	IGHV3-15	Immunoglobulin heavy variable 3-15	-0.8720	-0.9206	-0.0450	1	1	Secreted
53	P01594	IGKV1-33	Immunoglobulin kappa variable 1-33 (Ig kappa chain V-I region AU)	-2.1640	-2.4645	-1.2635	1	1	Secreted
54	Q04941	PLP2 A4	Proteolipid protein 2	-2.2665	-2.0556	-1.8568	1	1	Membrane
55	P30043	BLVRB FLR	Flavin reductase (NADPH)	-2.9425	-3.8218	-3.1040	1	1	Cytoplasm
56	O95147	DUSP14 MKP6	Dual specificity protein phosphatase 14	-5.5493	-4.7380	-5.2598	1	1	
57	P15104	GLUL GLNS	Glutamine synthetase (GS)	1.4997	1.9793	2.0357	6	1	Cytoplasm, cytosol
58	P32926	DSG3 CDHF6	Desmoglein-3	2.1780	1.8537	2.3998	10	1	Cell membrane
59	P99999	CYCS CYC	Cytochrome c	-3.6765	-3.8626	-3.3497	1	1	Mitochondrion intermembrane space
60	Q9UBD6	RHCG	Ammonium transporter Rh type C (Rh glycoprotein kidney)	1.4969	0.5216	0.2517	4	0	Apical cell membrane

List #	UniProt ID	Gene names	Protein names	CTRL Av	BRT Av	ART Av	Peptides #	Significance Elastic Net analysis	Subcellular location
61	Q8N1N4	KRT78 K5B KB40	Keratin, type II cytoskeletal 78 (Cytokeratin-78)	6.3726	5.3584	4.5306	31	0	
62	P11021	HSPA5 GRP78	Endoplasmic reticulum chaperone BiP	2.2650	2.6316	2.7965	14	0	Endoplasmic reticulum lumen
63	P30044	PRDX5 ACR1 SBBI10	Peroxiredoxin-5, mitochondrial	2.0341	1.7168	1.4056	5	0	Mitochondrion
64	A8K2U0	A2ML1 CPAMD9	Alpha-2-macroglobulin-like protein 1	5.6206	4.9561	4.9750	31	0	Secreted
65	P06702	S100A9	Protein S100-A9 (Calgranulin-B)	4.7503	4.2781	3.6505	7	0	Secreted, Cytoplasm
66	P23141	CES1 CES2 SES1	Liver carboxylesterase 1	-2.3052	-2.5193	-3.5571	2	0	Endoplasmic reticulum lumen
67	Q8N3Y7	SDR16C5 RDHE2	Epidermal retinol dehydrogenase 2 (EPHD-2)	0.4466	-0.5652	-0.1002	2	0	Endoplasmic reticulum membrane
68	P02750	LRG1 LRG	Leucine-rich alpha-2-glycoprotein (LRG)	-0.0369	1.2317	1.6014	2	0	Secreted
69	Q16610	ECM1	Extracellular matrix protein 1 (Secretory component p85)	1.4080	1.0096	0.7333	7	0	Secreted, extracellular space and matrix
70	P46779	RPL28	60S ribosomal protein L28 (Large ribosomal subunit protein eL28)	0.7028	-0.2919	-0.2487	2	0	
71	P36957	DLST DLTS	Dihydrolipoyllysine-residue succinyltransferase component of 2-oxoglutarate dehydrogenase complex, mitochondrial	-1.5174	-0.5542	-0.1920	1	0	Mitochondrion matrix
72	P11142	HSPA8 HSC70 HSP73 HSPA10	Heat shock cognate 71 kDa protein (Heat shock 70 kDa protein 8)	3.0853	3.2715	3.4294	12	0	Cytoplasm
73	Q96G03	PGM2 MSTP006	Phosphoglucomutase-2 (PGM 2)	-2.4116	-1.7250	-0.6172	2	0	Cytoplasm
74	O14880	MGST3	Microsomal glutathione S-transferase 3 (Microsomal GST-3)	-1.5011	-2.3008	-2.6802	1	0	Endoplasmic reticulum membrane
75	P09429	HMGB1 HMG1	High mobility group protein B1	-2.4961	-2.8654	-4.1627	1	0	Nucleus
76	P45880	VDAC2	Voltage-dependent anion-selective channel protein 2 (VDAC-2)	1.7619	1.0842	0.7349	2	0	Mitochondrion outer membrane
77	P07237	P4HB ERBA2L PDI PDIA1 PO4DB	Protein disulfide-isomerase (PDI)	4.3247	4.6631	4.6241	26	0	Endoplasmic reticulum
78	Q969Q0	RPL36AL	60S ribosomal protein L36a-like	-1.4011	-2.6234	-2.4762	1	0	Cytoplasm
79	Q02543	RPL18A	60S ribosomal protein L18a	-0.3347	-1.1207	-1.3499	2	0	
80	Q9UBG3	CRNN	Cornulin (53 kDa putative calcium-binding protein)	5.1092	4.9300	4.1081	23	0	Cytoplasm

List #	UniProt ID	Gene names	Protein names	CTRL Av	BRT Av	ART Av	Peptides #	Significance Elastic Net analysis	Subcellular location
81	P05141	SLC25A5 ANT2	ADP/ATP translocase 2 (ADP, ATP carrier protein 2)	1.3809	0.6608	0.6546	2	0	Mitochondrion inner membrane
82	P20061	TCN1 TC1	Transcobalamin-1 (TC-1)	3.1479	3.9875	4.1262	10	0	Secreted
83	P13646	KRT13	Keratin, type I cytoskeletal 13 (Cytokeratin-13)	8.4278	7.4589	6.7864	35	0	
84	P12236	SLC25A6 ANT3 CDABP0051	ADP/ATP translocase 3 (ADP, ATP carrier protein 3)	-1.1372	-2.2172	-2.0991	1	0	Mitochondrion inner membrane
85	P00338	LDHA PIG19	L-lactate dehydrogenase A chain (LDH-A)	4.2951	4.4494	4.7063	9	0	Cytoplasm
86	P09228	CST2	Cystatin-SA (Cystatin-2)	4.5383	3.6405	2.3437	8	0	Secreted
87	P61313	RPL15 EC45 TCBAP0781	60S ribosomal protein L15	-1.0612	-3.2519	-2.7987	1	0	Membrane
88	P07305	H1-0 H1F0 H1FV	Histone H1.0 (Histone H1')	-0.5467	-1.5194	-1.3233	3	0	Nucleus
89	P31930	UQCRC1	Cytochrome b-c1 complex subunit 1, mitochondrial (Complex III subunit 1)	-1.4966	-2.1707	-1.9791	2	0	Mitochondrion inner membrane
90	P62266	RPS23	40S ribosomal protein S23 (Small ribosomal subunit protein uS12)	0.2323	-0.7138	-0.5281	2	0	Cytoplasm, cytosol
91	P50914	RPL14	60S ribosomal protein L14 (CAG-ISL 7)	0.4066	-0.2168	-0.1847	2	0	
92	P01591	JCHAIN IGCJ IGJ	Immunoglobulin J chain (Joining chain of multimeric IgA and IgM)	4.9019	5.7194	5.5338	7	0	Secreted
93	P17655	CAPN2 CANPL2	Calpain-2 catalytic subunit	-0.1977	-0.6111	-0.8291	3	0	Cytoplasm, Cell membrane
94	P10909	CLU APOJ CLI KUB1 AAG4	Clusterin (Aging-associated gene 4 protein) (Apolipoprotein J)	1.3626	2.1653	2.7293	5	0	Secreted
95	Q9UBX7	KLK11	Kallikrein-11 (hK11)	-0.2998	0.3162	0.4874	1	0	[Isoform 1]: Secreted; [Isoform 2]: Golgi apparatus.
96	P31025	LCN1	Lipocalin-1 (Tear lipocalin)	3.4941	5.0693	4.7666	12	0	Secreted
97	Q9UKR3	KLK13	Kallikrein-13	1.3354	1.9189	2.2010	5	0	Secreted
98	P00367	GLUD1 GLUD	Glutamate dehydrogenase 1, mitochondrial (GDH 1)	-1.4358	-1.8274	-2.4568	1	0	Mitochondrion
99	P60981	DSTN ACTDP DSN	Destrin (Actin-depolymerizing factor) (ADF)	-0.5798	-1.3180	-1.5486	1	0	
100	P15924	DSP	Desmoplakin (DP) (250/210 kDa paraneoplastic pemphigus antigen)	3.8460	3.4716	3.2582	28	0	Cell junction, desmosome

List #	UniProt ID	Gene names	Protein names	CTRL Av	BRT Av	ART Av	Peptides #	Significance Elastic Net analysis	Subcellular location
101	P36578	RPL4 RPL1	60S ribosomal protein L4	0.8914	0.1524	0.2521	3	0	
102	P00491	PNP NP	Purine nucleoside phosphorylase (PNP)	-0.4907	-0.0773	0.0409	3	0	Cytoplasm, cytoskeleton
103	P13639	EEF2 EF2	Elongation factor 2 (EF-2)	3.4103	3.0960	3.0245	14	0	Cytoplasm
104	Q9NRJ3	CCL28 SCYA28	C-C motif chemokine 28 (Mucosae-associated epithelial chemokine)	-1.4851	-0.7817	-2.1955	1	0	Secreted
105	Q00610	CLTC CLH17 CLTCL2 KIAA0034	Clathrin heavy chain 1	0.7878	-0.0586	-0.0319	7	0	Cytoplasmic vesicle membrane
106	Q9UJ70	NAGK	N-acetyl-D-glucosamine kinase (N-acetylglucosamine kinase)	1.8610	1.4902	1.2037	8	0	
107	P29508	SERPINB3	Serpin B3	2.2715	2.5401	2.9683	10	0	Cytoplasm
108	P43304	GPD2	Glycerol-3-phosphate dehydrogenase, mitochondrial	-2.6920	-3.5465	-3.4749	1	0	Mitochondrion
109	P25311	AZGP1 ZAG ZNGP1	Zinc-alpha-2-glycoprotein	5.9351	6.9102	6.4608	20	0	Secreted.
110	O15231	ZNF185	Zinc finger protein 185	-2.0147	-2.8883	-2.9457	1	0	Cytoplasm, cytoskeleton
111	P13647	KRT5	Keratin, type II cytoskeletal 5 (Cytokeratin-5)	6.9530	6.2020	6.0406	23	0	
112	P01036	CST4	Cystatin-S (Cystatin-4)	0.2503	-0.4239	-2.4290	2	0	Secreted
113	P02743	APCS PTX2	Serum amyloid P-component (SAP)	-1.7665	-0.9976	-0.5679	4	0	Secreted
114	P18621	RPL17	60S ribosomal protein L17	-2.0358	-2.7978	-2.9750	1	0	
115	P27797	CALR CRTC	Calreticulin	1.8908	1.9255	2.1765	11	0	Endoplasmic reticulum lumen
116	Q99536	VAT1	Synaptic vesicle membrane protein VAT-1 homolog	-4.6791	-3.4148	-3.8571	1	0	Cytoplasm, Mitochondrion outer membrane
117	P30041	PRDX6 AOP2	Peroxiredoxin-6	3.5042	3.4701	2.8987	11	0	Cytoplasm
118	P11216	PYGB	Glycogen phosphorylase, brain form	-0.8430	-2.5049	-3.0187	1	0	
119	P00738	HP	Haptoglobin	3.4580	4.4373	5.0998	24	0	Secreted
120	P21926	CD9	CD9 antigen (5H9 antigen)	-0.1318	-1.1969	-0.5286	2	0	Cell membrane
121	P49755	TMED10 TMP21	Transmembrane emp24 domain-containing protein 10	-1.1380	-2.4082	-1.6624	1	0	Endoplasmic reticulum membrane

List #	UniProt ID	Gene names	Protein names	CTRL Av	BRT Av	ART Av	Peptides #	Significance Elastic Net analysis	Subcellular location
122	P35754	GLRX GRX	Glutaredoxin-1 (Thioltransferase-1) (TTase-1)	-6.5509	-4.5712	-4.6832	1	0	Cytoplasm
123	P28325	CST5	Cystatin-D (Cystatin-5)	5.9161	4.4166	4.1209	14	0	Secreted
124	P01009	SERPINA1	Alpha-1-antitrypsin (Alpha-1 protease inhibitor)	4.5630	5.3309	6.1177	26	0	Secreted, Endoplasmic reticulum
125	P07339	CTSD CPSD	Cathepsin D	1.3782	1.8628	2.1600	3	0	Lysosome, Melanosome, Secreted
126	P04406	GAPDH	Glyceraldehyde-3-phosphate dehydrogenase (GAPDH)	4.9234	4.6143	4.9756	18	0	Cytoplasm, cytosol
127	Q9UL52	TMPRSS11E DESC1	Transmembrane protease serine 11E	-0.3030	0.5351	-0.3411	5	0	Cell membrane
128	Q07065	CKAP4	Cytoskeleton-associated protein 4	-1.6932	-0.7013	-0.8866	3	0	Endoplasmic reticulum membrane region.
129	P61026	RAB10	Ras-related protein Rab-10	2.1558	1.2628	1.5613	5	0	Cytoplasmic vesicle membrane
130	P09758	TACSTD2 GA733-1 M1S1 TROP2	Tumor-associated calcium signal transducer 2 (Cell surface glycoprotein Trop-2)	-0.3591	-0.6803	-0.9313	2	0	Membrane
131	P30086	PEBP1 PBP PEBP	Phosphatidylethanolamine-binding protein 1 (PEBP-1)	0.0247	0.6041	0.6241	4	0	Cytoplasm
132	P46777	RPL5 MSTP030	60S ribosomal protein L5	-0.6444	-1.1753	-1.1938	1	0	Cytoplasm
133	Q9Y446	PKP3	Plakophilin-3	-0.6674	-1.3087	-0.7290	3	0	Nucleus, cell junction, desmosome.
134	P05109	S100A8 CAGA CFAG MRP8	Protein S100-A8 (Calgranulin-A)	8.8929	8.6237	8.0457	19	0	Secreted
135	P06748	NPM1 NPM	Nucleophosmin (NPM)	-5.3994	-4.8498	-4.3804	1	0	Nucleus, nucleolus
136	Q9BRA2	TXNDC17 TXNL5	Thioredoxin domain-containing protein 17 (14 kDa thioredoxin-related protein)	-0.8468	-0.4321	-0.2768	1	0	Cytoplasm
137	Q99685	MGLL	Monoglyceride lipase (MGL)	-1.0074	-1.6046	-1.7890	2	0	Cytoplasm, cytosol
138	P68366	TUBA4A TUBA1	Tubulin alpha-4A chain (Alpha-tubulin 1)	1.6586	1.3077	0.9345	4	0	Cytoplasm, cytoskeleton
139	Q08188	TGM3	Protein-glutamine gamma-glutamyltransferase E (Transglutaminase E)	5.8769	5.3476	5.1353	31	0	Cytoplasm
140	Q6KB66	KRT80 KB20	Keratin, type II cytoskeletal 80 (Cytokeratin-80)	-0.6588	-1.2112	-1.4053	4	0	
141	P55084	HADHB MSTP029	Trifunctional enzyme subunit beta, mitochondrial (TP-beta)	0.0804	-1.2003	-0.5070	1	0	Mitochondrion

List #	UniProt ID	Gene names	Protein names	CTRL Av	BRT Av	ART Av	Peptides #	Significance Elastic Net analysis	Subcellular location
142	Q9HCY8	S100A14 S100A15	Protein S100-A14 (S100 calcium-binding protein A14) (S114)	3.7604	3.5201	2.7568	8	0	Cytoplasm
143	P29373	CRABP2	Cellular retinoic acid-binding protein 2	0.5493	0.5662	1.0305	3	0	Cytoplasm, Endoplasmic reticulum, Nucleus.
144	O76013	KRT36 HHA6 HKA6 KRTHA6	Keratin, type I cuticular Ha6 (Keratin-36)	0.6481	0.7849	-0.6272	5	0	
145	Q96FQ6	S100A16 S100F AAG13	Protein S100-A16 (Aging-associated gene 13 protein)	2.1761	1.8951	1.3009	5	0	Nucleus, nucleolus
146	O00303	EIF3F EIF3S5	Eukaryotic translation initiation factor 3 subunit F (eIF3f) (Deubiquitinating enzyme eIF3f)	-3.2890	-3.9759	-3.2873	1	0	Cytoplasm
147	P17858	PFKL	ATP-dependent 6-phosphofructokinase, liver type (ATP-PFK)	-4.8816	-4.0200	-4.0850	1	0	Cytoplasm
148	P61981	YWHAG	14-3-3 protein gamma (Protein kinase C inhibitor protein 1)	-0.2366	0.0287	0.1057	4	0	Cytoplasm
149	Q6ZN66	GBP6	Guanylate-binding protein 6 (GTP-binding protein 6)	2.2669	2.1765	1.6406	8	0	
150	P25398	RPS12	40S ribosomal protein S12	-0.5561	-0.8371	-1.1519	2	0	Cytoplasm
151	P14923	JUP CTNNG DP3	Junction plakoglobin (Catenin gamma)	4.7302	4.3674	3.8376	25	0	Cell junction
152	P15814	IGLL1 IGL1	Immunoglobulin lambda-like polypeptide 1	-4.1304	-3.2107	-2.7139	1	0	Endoplasmic reticulum
153	P02763	ORM1 AGP1	Alpha-1-acid glycoprotein 1 (AGP 1)	1.6434	2.5663	3.0360	3	0	Secreted
154	Q5VTE0	EEF1A1P5 EEF1AL3	Putative elongation factor 1-alpha-like 3 (EF-1-alpha-like 3)	4.9914	4.4182	4.3121	14	0	Cytoplasm
155	P26373	RPL13 BBC1	60S ribosomal protein L13	0.1979	-0.5480	-0.4367	3	0	Cytoplasm
156	Q14134	TRIM29 ATDC	Tripartite motif-containing protein 29	1.6736	0.4922	0.9354	4	0	Cytoplasm
157	P30740	SERPINB1	Leukocyte elastase inhibitor (LEI)	4.8470	5.0137	5.1650	18	0	Secreted
158	P19367	HK1	Hexokinase-1	-0.7470	-1.2659	-1.2399	2	0	Mitochondrion outer membrane
159	P61916	NPC2 HE1	NPC intracellular cholesterol transporter 2 (Epididymal secretory protein E1)	-2.9889	-2.5571	-1.6053	1	0	Secreted
160	Q6P4A8	PLBD1	Phospholipase B-like 1	-0.6188	-0.5829	-0.1055	2	0	Lysosome
161	P04844	RPN2	Ribophorin-2	-1.2930	-1.9257	-1.7891	2	0	Endoplasmic reticulum

List #	UniProt ID	Gene names	Protein names	CTRL Av	BRT Av	ART Av	Peptides #	Significance Elastic Net analysis	Subcellular location
162	P01031	C5 CPAMD4	Complement C5	-4.4328	-3.3966	-2.9508	1	0	Secreted
163	P04259	KRT6B K6B KRTL1	Keratin, type II cytoskeletal 6B (Cytokeratin-6B)	2.7468	1.6129	2.0950	2	0	
164	Q6P5S2	LEG1 C6orf58	Protein LEG1 homolog	3.5521	4.4450	4.0816	10	0	Secreted
165	Q6MZM9	PRR27 C4orf40	Proline-rich protein 27	1.6011	1.6092	0.3697	1	0	Secreted
166	Q01546	KRT76 KRT2B KRT2P	Keratin, type II cytoskeletal 2 oral (Cytokeratin-2P)	3.4087	2.4675	1.8557	9	0	
167	P21128	ENDOU	Poly(U)-specific endoribonuclease	-1.0710	-1.4641	-1.8014	1	0	Secreted
168	P11279	LAMP1	Lysosome-associated membrane glycoprotein 1 (LAMP-1)	-0.4447	-1.1542	-0.8793	2	0	Cell membrane
169	P61353	RPL27	60S ribosomal protein L27	0.6205	0.0085	0.0854	1	0	Cytoplasm, cytosol
170	P0DJI8	SAA1	Serum amyloid A-1 protein (SAA)	-1.9728	-0.9023	-1.2714	2	0	Secreted
171	P13489	RNH1 PRI RNH	Ribonuclease inhibitor	1.1569	0.8670	0.5588	6	0	Cytoplasm
172	P22735	TGM1 KTG	Protein-glutamine gamma-glutamyltransferase K (Transglutaminase K)	3.6373	2.9695	2.9934	20	0	Cell membrane
173	P46776	RPL27A	60S ribosomal protein L27a	0.3611	-0.7220	-0.4799	1	0	
174	P62701	RPS4X CCG2 RPS4 SCAR	40S ribosomal protein S4, X isoform (SCR10)	1.7196	1.2381	1.1489	6	0	Cytoplasm
175	Q00325	SLC25A3 PHC	Phosphate carrier protein, mitochondrial	0.4277	-0.3324	-0.2578	2	0	Mitochondrion inner membrane
176	Q14624	ITIH4 IHRP ITIHL1 PK120 PRO1851	Inter-alpha-trypsin inhibitor heavy chain H4 (ITI heavy chain H4)	-0.3168	0.4835	0.6918	7	0	Secreted
177	P30101	PDIA3 ERP57 ERP60 GRP58	Protein disulfide-isomerase A3	1.4821	1.7499	1.6639	9	0	Endoplasmic reticulum
178	P07355	ANXA2 ANX2 ANX2L4 CAL1H LPC2D	Annexin A2	3.5114	3.1950	2.7431	6	0	Secreted
179	P22307	SCP2	Non-specific lipid-transfer protein (NSL-TP)	-2.1473	-2.3802	-1.7436	1	0	Cytoplasm
180	P08571	CD14	Monocyte differentiation antigen CD14 (CD antigen CD14)	-1.5843	-0.5302	-0.4219	3	0	Cell membrane
181	P62888	RPL30	60S ribosomal protein L30	0.8967	0.4017	0.8537	3	0	
182	Q9H0U4	RAB1B	Ras-related protein Rab-1B	-4.3126	-7.5743	-5.9538	1	0	Cytoplasm

List #	UniProt ID	Gene names	Protein names	CTRL Av	BRT Av	ART Av	Peptides #	Significance Elastic Net analysis	Subcellular location
183	Q99714	HSD17B10	3-hydroxyacyl-CoA dehydrogenase type-2	0.1149	-0.1031	-0.5669	2	0	Mitochondrion
184	P35268	RPL22	60S ribosomal protein L22 (Epstein-Barr virus small RNA-associated protein)	0.7555	0.2281	0.2572	2	0	
185	Q16851	UGP2 UGP1	UTP--glucose-1-phosphate uridylyltransferase (UGPase)	-3.5294	-3.0718	-2.4510	2	0	Cytoplasm
186	P07384	CAPN1 CANPL1 PIG30	Calpain-1 catalytic subunit	2.6858	2.4020	2.2710	11	0	Cytoplasm
187	Q96DR5	BPIFA2	BPI fold-containing family A member 2 (Parotid secretory protein)	6.3578	6.7749	5.6440	21	0	Secreted
188	Q04828	AKR1C1	Aldo-keto reductase family 1 member C1	0.0041	-0.3649	-1.0753	1	0	Cytoplasm
189	P50395	GDI2 RABGDIB	Rab GDP dissociation inhibitor beta	1.0611	1.0626	1.4080	6	0	Cytoplasm
190	O95867	LY6G6C	Lymphocyte antigen 6 complex locus protein G6c	0.4402	-0.5267	-0.8435	2	0	Cell membrane
191	P06703	S100A6 CACY	Protein S100-A6 (Calcyclin)	-3.6066	-6.2607	-4.4002	1	0	Nucleus envelope, Cytoplasm, Cell membrane
192	P51572	BCAP31 BAP31 DXS1357E	B-cell receptor-associated protein 31	-0.5083	-0.6542	-0.9590	4	0	Endoplasmic reticulum membrane
193	P06310	IGKV2-30	Immunoglobulin kappa variable 2-30 (Ig kappa chain V-II region RPMI 6410)	-1.2263	-0.7288	-0.0865	2	0	Secreted
194	P02652	APOA2	Apolipoprotein A-II (Apo-AII)	-3.1815	-1.6398	-2.5352	1	0	Secreted
195	P14550	AKR1A1 ALDR1 ALR	Aldo-keto reductase family 1 member A1	0.3167	0.3237	-0.0554	3	0	Cytoplasm, cytosol
196	P35237	SERPINB6 PI6 PTI	Serpin B6	-0.1093	0.1763	0.2667	2	0	Cytoplasm
197	P10809	HSPD1 HSP60	60 kDa heat shock protein, mitochondrial	-1.5477	-1.0012	-1.3373	3	0	Mitochondrion matrix
198	P02753	RBP4 PRO2222	Retinol-binding protein 4	-2.7915	-2.1440	-1.7669	2	0	Secreted
199	P62249	RPS16	40S ribosomal protein S16	1.4172	0.8505	1.0554	5	0	
200	P25705	ATP5F1A ATP5A	ATP synthase subunit alpha, mitochondrial	3.3960	3.5129	3.7416	12	0	Mitochondrion
201	P37837	TALDO1 TAL TALDO TALDOR	Transaldolase	3.5375	3.5238	3.9044	9	0	Cytoplasm
202	P12830	CDH1 CDHE UVO	Cadherin-1	-0.5631	-1.1962	-0.9566	2	0	Cell junction

List #	UniProt ID	Gene names	Protein names	CTRL Av	BRT Av	ART Av	Peptides #	Significance Elastic Net analysis	Subcellular location
203	Q9UFN0	NIPSNAP3A NIPSNAP4 HSPC299	Protein NipSnap homolog 3A (NipSnap3A)	-10.0021	-13.4601	-13.1198	1	0	Cytoplasm, cytosol
204	P30838	ALDH3A1 ALDH3	Aldehyde dehydrogenase, dimeric NADP-preferring (Aldehyde dehydrogenase family 3 member A1)	2.9545	2.7530	2.3514	8	0	Cytoplasm
205	P60842	EIF4A1 DDX2A EIF4A	Eukaryotic initiation factor 4A-I (eIF-4A-I)	1.9975	1.5371	1.5630	5	0	
206	P00505	GOT2	Aspartate aminotransferase, mitochondrial (mAspAT)	-4.8058	-4.2788	-4.1451	1	0	Mitochondrion matrix
207	P62879	GNB2	Guanine nucleotide-binding protein	-0.0589	-0.9889	-0.7677	2	0	Cytoplasm, perinuclear region
208	P49902	NT5C2 NT5B NT5CP PNT5	Cytosolic purine 5'-nucleotidase	-3.6971	-3.1480	-3.1504	1	0	Cytoplasm
209	P09960	LTA4H LTA4	Leukotriene A-4 hydrolase (LTA-4 hydrolase)	1.2258	0.8672	1.3883	8	0	Cytoplasm
210	P29475	NOS1	Nitric oxide synthase, brain	-3.1405	-3.7398	-5.0253	1	0	Cell membrane, sarcolemma
211	P04217	A1BG	Alpha-1B-glycoprotein (Alpha-1-B glycoprotein)	0.8074	1.4023	1.6799	7	0	Secreted
212	Q5SSG8	MUC21	Mucin-21	-1.4577	-2.6069	-2.6118	1	0	Cell membrane
213	Q96QR1	SCGB3A1	Secretoglobin family 3A member 1 (Cytokine HIN-1)	-3.6635	-2.0458	-3.2879	1	0	Secreted
214	P0DMV9	HSPA1B HSP72	Heat shock 70 kDa protein 1B (Heat shock 70 kDa protein 2)	3.7799	3.6351	3.9318	13	0	Cytoplasm
215	Q8WVV4	POF1B	Protein POF1B (Premature ovarian failure protein 1B)	-1.7600	-1.5475	-2.7377	1	0	Cell junction, tight junction
216	P12273	PIP GCDFP15 GPIP4	Prolactin-inducible protein	7.8769	7.6534	7.1587	7	0	Secreted
217	P08758	ANXA5 ANX5 ENX2 PP4	Annexin A5	1.6957	2.2595	2.1263	6	0	
218	P0DP03	IGHV3-30-5	Immunoglobulin heavy variable 3-30-5	0.2697	0.4934	0.8651	1	0	Secreted
219	P63167	DYNLL1 DLC1 DNCL1 DNCLC1 HDLC1	Dynein light chain 1, cytoplasmic (8 kDa dynein light chain)	1.3480	1.2016	0.7808	3	0	Cytoplasm, cytoskeleton, microtubule organizing center, centrosome
220	P62913	RPL11	60S ribosomal protein L11	0.2594	-0.4069	-0.2514	1	0	Nucleus, nucleolus
221	P61247	RPS3A FTE1 MFTL	40S ribosomal protein S3a	1.2206	0.8656	0.8090	4	0	Cytoplasm
222	O95197	RTN3 ASYIP NSPL2	Reticulon-3	-0.9445	-2.2567	-1.6221	1	0	Endoplasmic reticulum membrane

List #	UniProt ID	Gene names	Protein names	CTRL Av	BRT Av	ART Av	Peptides #	Significance Elastic Net analysis	Subcellular location
223	P19652	ORM2 AGP2	Alpha-1-acid glycoprotein 2 (AGP 2)	-0.3295	0.0013	0.5448	2	0	Secreted
224	P00352	ALDH1A1 ALDC ALDH1 PUMB1	Retinal dehydrogenase 1 (RALDH 1)	-3.3497	-2.7791	-3.9695	1	0	Cytoplasm, cytosol
225	P62241	RPS8	40S ribosomal protein S8	0.5787	0.0283	-0.0530	4	0	Cytoplasm
226	P62277	RPS13	40S ribosomal protein S13	-0.9812	-1.4067	-0.7965	2	0	
227	P04433	IGKV3-11	Immunoglobulin kappa variable 3-11 (Ig kappa chain V-III region VG)	2.5794	2.9955	3.3012	2	0	Secreted
228	A0A0C4DH68	IGKV2-24	Immunoglobulin kappa variable 2-24	-0.2607	0.4079	0.4468	2	0	Secreted
229	P0C0L4	C4A CO4 CPAMD2	Complement C4-A (Acidic complement C4)	2.2369	2.4001	2.9714	22	0	Secreted
230	Q96HE7	ERO1A	ERO1-like protein alpha (ERO1-L)	3.1275	3.4221	3.2666	13	0	Endoplasmic reticulum membrane
231	P02790	HPX	Hemopexin (Beta-1B-glycoprotein)	2.9635	3.2696	4.0854	14	0	Secreted
232	Q06830	PRDX1 PAGA	Peroxiredoxin-1	2.5327	2.6240	2.0280	6	0	Cytoplasm
233	P02774	GC	Vitamin D-binding protein (DBP)	1.8848	2.3338	2.9307	16	0	Secreted
234	P02511	CRYAB CRYA2 HSPB5	Alpha-crystallin B chain (Heat shock protein beta-5)	1.6048	1.0994	1.1239	6	0	Cytoplasm
235	E9PAV3	NACA	Nascent polypeptide-associated complex subunit alpha, muscle-specific form (Alpha-NAC, muscle-specific form)	-1.3340	-1.9477	-1.9387	2	0	Cytoplasm
236	P67775	PPP2CA	Serine/threonine-protein phosphatase 2A catalytic subunit alpha isoform (PP2A-alpha)	-1.0866	-1.0568	-1.4286	2	0	Cytoplasm
237	P04179	SOD2	Superoxide dismutase [Mn], mitochondrial	-0.5828	-0.1178	0.3027	3	0	Mitochondrion matrix
238	Q13885	TUBB2A TUBB2	Tubulin beta-2A chain (Tubulin beta class IIa)	-0.8403	-1.5233	-1.4400	1	0	Cytoplasm, cytoskeleton
239	P06753	TPM3	Tropomyosin alpha-3 chain (Gamma-tropomyosin)	0.7312	0.3953	0.3023	3	0	Cytoplasm, cytoskeleton
240	P13533	MYH6 MYHCA	Myosin-6 (Myosin heavy chain 6)	-2.7951	-2.1656	-3.1938	1	0	Cytoplasm, myofibril
241	Q16658	FSCN1 FAN1 HSN SNL	Fascin (55 kDa actin-bundling protein)	-1.2263	-1.6452	-0.8271	2	0	Cytoplasm, cytosol
242	P02538	KRT6A K6A KRT6D	Keratin, type II cytoskeletal 6A (Cytokeratin-6A)	6.8798	6.0101	6.1661	7	0	

List #	UniProt ID	Gene names	Protein names	CTRL Av	BRT Av	ART Av	Peptides #	Significance Elastic Net analysis	Subcellular location
243	P23396	RPS3	40S ribosomal protein S3	1.8576	1.4590	1.5197	5	0	Cytoplasm
244	P61254	RPL26	60S ribosomal protein L26	-0.5799	-1.4084	-0.7506	2	0	
245	P60660	MYL6	Myosin light polypeptide 6 (17 kDa myosin light chain)	1.8322	2.0445	1.5419	5	0	
246	O00571	DDX3X	ATP-dependent RNA helicase DDX3X	-1.4316	-2.0308	-1.9562	3	0	Cell membrane
247	P07195	LDHB	L-lactate dehydrogenase B chain (LDH-B)	-1.2867	-1.4968	-0.9184	3	0	Cytoplasm
248	P0DP25	CALM3	Calmodulin-3	-1.4182	-1.0801	-1.8332	1	0	Cytoplasm, cytoskeleton, spindle
249	P01624	IGKV3-15	Immunoglobulin kappa variable 3-15 (Ig kappa chain V-III region CLL)	3.1936	3.5363	4.0984	1	0	Secreted
250	Q9UM00	TMCO1	Calcium load-activated calcium channel (CLAC channel)	-3.0139	-3.3145	-3.4311	1	0	Endoplasmic reticulum membrane
251	P40926	MDH2	Malate dehydrogenase, mitochondrial	2.5378	2.7263	2.7742	8	0	Mitochondrion matrix
252	P24534	EEF1B2 EEF1B EF1B	Elongation factor 1-beta (EF-1-beta)	-2.9552	-2.0411	-2.3597	1	0	
253	O43707	ACTN4	Alpha-actinin-4 (Non-muscle alpha-actinin 4)	2.5826	2.4273	2.3307	15	0	Nucleus
254	P60174	TPI1 TPI	Triosephosphate isomerase (TIM)	4.1584	4.4039	4.5145	14	0	Cytoplasm
255	Q6UX06	OLFM4	Olfactomedin-4 (OLM4)	-0.2070	0.4336	0.8234	5	0	Secreted, extracellular space. Mitochondrion
256	Q96FX8	PERP KCP1 KRTCAP1 PIGPC1 THW	p53 apoptosis effector related to PMP-22 (Keratinocyte-associated protein 1)	-0.9787	-1.9022	-1.7005	1	0	Cell junction, desmosome
257	P22352	GPX3 GPXP	Glutathione peroxidase 3 (GPx-3)	-2.1973	-2.2466	-1.5123	1	0	Secreted
258	P49207	RPL34	60S ribosomal protein L34	0.5552	-0.3179	0.0175	2	0	Cytoplasm, cytosol
259	P06733	ENO1	Alpha-enolase	4.7538	4.8359	4.9942	27	0	Cytoplasm
260	O15144	ARPC2 ARC34 PRO2446	Actin-related protein 2/3 complex subunit 2	0.4458	0.0635	0.0089	3	0	Cytoplasm, cytoskeleton
261	Q5VT79	ANXA8L1 ANXA8L2	Annexin A8-like protein 1	2.4068	2.3114	1.9645	7	0	
262	P31151	S100A7 PSOR1 S100A7C	Protein S100-A7 (Psoriasin) (S100 calcium-binding protein A7)	1.3287	2.4851	2.1511	7	0	Cytoplasm

List #	UniProt ID	Gene names	Protein names	CTRL Av	BRT Av	ART Av	Peptides #	Significance Elastic Net analysis	Subcellular location
263	A0A0C4DH31	IGHV1-18	Immunoglobulin heavy variable 1-18	1.8649	2.1108	2.3452	1	0	Secreted
264	P06396	GSN	Gelsolin (AGEL) (Actin-depolymerizing factor) (ADF) (Brevin)	4.0122	3.8697	4.3514	18	0	[Isoform 2]: Cytoplasm, cytoskeleton; [Isoform 1]: Secreted
265	P51659	HSD17B4 EDH17B4 SDR8C1	Peroxisomal multifunctional enzyme type 2 (MFE-2)	-0.9737	-1.3913	-1.3766	3	0	Peroxisome
266	O75608	LYPLA1 APT1 LPL1	Acyl-protein thioesterase 1 (APT-1)	-2.8664	-2.5453	-2.3355	1	0	Cytoplasm
267	P49862	KLK7 PRSS6 SCCE	Kallikrein-7 (hK7)	-1.0590	-1.2339	-0.3125	2	0	Secreted
268	O75368	SH3BGRL	SH3 domain-binding glutamic acid-rich-like protein	-0.6280	-0.7214	-1.2488	2	0	
269	P61204	ARF3	ADP-ribosylation factor 3	-1.1937	-1.9231	-0.8890	1	0	Golgi apparatus
270	P59998	ARPC4 ARC20	Actin-related protein 2/3 complex subunit 4 (Arp2/3 complex 20 kDa subunit) (p20-ARC)	2.9285	2.6376	2.7237	6	0	Cytoplasm, cytoskeleton
271	P28066	PSMA5	Proteasome subunit alpha type-5	-1.3371	-1.6642	-1.2823	2	0	Cytoplasm
272	P00441	SOD1	Superoxide dismutase [Cu-Zn]	-4.0443	-4.5580	-3.0919	1	0	Cytoplasm
273	P07910	HNRNPC HNRPC	Heterogeneous nuclear ribonucleoproteins C1/C2 (hnRNP C1/C2)	-1.7107	-2.5833	-2.2434	1	0	Nucleus
274	P04632	CAPNS1 CAPN4 CAPNS	Calpain small subunit 1 (CSS1)	1.6546	1.7570	1.2517	4	0	Cytoplasm
275	P63244	RACK1 GNB2L1 HLC7 PIG21	Receptor of activated protein C kinase 1 (Cell proliferation-inducing gene 21 protein)	1.0426	0.5351	0.5567	4	0	Cell membrane
276	P06732	CKM CKMM	Creatine kinase M-type	-3.0662	-4.5002	-5.3535	1	0	Cytoplasm
277	P09972	ALDOC ALDC	Fructose-bisphosphate aldolase C (Brain-type aldolase)	-2.5041	-1.5332	-2.4617	1	0	
278	P62829	RPL23	60S ribosomal protein L23	1.1340	0.6713	0.9602	3	0	
279	P68032	ACTC1 ACTC	Actin, alpha cardiac muscle 1 (Alpha-cardiac actin)	4.4361	4.0366	4.3055	4	0	Cytoplasm, cytoskeleton
280	P62854	RPS26	40S ribosomal protein S26	-1.4584	-1.7547	-1.9723	2	0	Cytoplasm, cytosol
281	O15145	ARPC3 ARC21	Actin-related protein 2/3 complex subunit 3 (Arp2/3 complex 21 kDa subunit) (p21-ARC)	-2.4155	-1.3366	-0.7276	1	0	Cytoplasm, cytoskeleton
282	P20073	ANXA7 ANX7 SNX	Annexin A7 (Annexin VII)	-2.3671	-3.1524	-2.9120	1	0	

List #	UniProt ID	Gene names	Protein names	CTRL Av	BRT Av	ART Av	Peptides #	Significance Elastic Net analysis	Subcellular location
283	Q07020	RPL18	60S ribosomal protein L18	1.0235	0.5331	0.5444	4	0	Cytoplasm, cytosol
284	P00450	CP	Ceruloplasmin	1.2051	1.2131	1.8791	10	0	Secreted
285	P62263	RPS14 PRO2640	40S ribosomal protein S14	-1.9392	-2.1115	-2.5255	1	0	
286	O95274	LYPD3	Ly6/PLAUR domain-containing protein 3 (GPI-anchored metastasis-associated protein C4.4A homolog)	1.2881	0.8374	0.9880	5	0	Cell membrane
287	P62330	ARF6	ADP-ribosylation factor 6	0.9179	0.7404	0.3341	3	0	Cytoplasm, cytosol
288	P12724	RNASE3 ECP RNS3	Eosinophil cationic protein (ECP)	1.7422	0.4050	0.8563	4	0	Secreted
289	Q9BYD5	CNFN	Cornifelin	-0.5047	-0.7795	-1.4344	1	0	Cytoplasm
290	P38646	HSPA9	Stress-70 protein, mitochondrial (75 kDa glucose-regulated protein)	-1.8052	-1.4117	-1.3617	2	0	Mitochondrion
291	P01019	AGT SERPINA8	Angiotensinogen (Serpin A8)	-1.7173	-1.2337	-0.6992	4	0	Secreted
292	Q15008	PSMD6 KIAA0107 PFAAP4	26S proteasome non-ATPase regulatory subunit 6 (26S proteasome regulatory subunit RPN7)	-2.2488	-2.8829	-2.9545	1	0	
293	P01619	IGKV3-20	Immunoglobulin kappa variable 3-20 (Ig kappa chain V-III region B6)	1.0952	1.3790	1.8182	1	0	Secreted
294	P62753	RPS6	40S ribosomal protein S6	0.3404	-0.3598	0.1361	2	0	
295	P05155	SERPING1 C1IN C1NH	Plasma protease C1 inhibitor	0.8152	1.1636	1.7619	5	0	Secreted
296	P13797	PLS3	Plastin-3 (T-plastin)	1.2179	1.2587	0.8677	6	0	Cytoplasm
297	P00403	MT-CO2 COII COX2 COXII MTCO2	Cytochrome c oxidase subunit 2	0.8142	0.6621	-0.0726	1	0	Mitochondrion inner membrane
298	Q9NVJ2	ARL8B ARL10C GIE1	ADP-ribosylation factor-like protein 8B (ADP-ribosylation factor-like protein 10C)	-3.0691	-2.4618	-2.3348	1	0	Late endosome membrane
299	Q99460	PSMD1	26S proteasome non-ATPase regulatory subunit 1	-2.5923	-4.1602	-3.1119	1	0	
300	Q8WUM4	PDCD6IP AIP1 ALIX KIAA1375	Programmed cell death 6-interacting protein (PDCD6-interacting protein)	0.6354	0.4661	0.4391	4	0	Cytoplasm, cytosol
301	P07099	EPHX1 EPHX EPOX	Epoxide hydrolase 1	-0.1656	-0.4722	-0.6393	3	0	Microsome membrane
302	Q15907	RAB11B YPT3	Ras-related protein Rab-11B (GTP-binding protein YPT3)	2.2911	2.2100	2.3798	6	0	Recycling endosome membrane

List #	UniProt ID	Gene names	Protein names	CTRL Av	BRT Av	ART Av	Peptides #	Significance Elastic Net analysis	Subcellular location
303	O75874	IDH1 PICD	Isocitrate dehydrogenase [NADP] cytoplasmic (IDH)	-1.4448	-1.7061	-2.2068	1	0	Cytoplasm, cytosol
304	P04839	CYBB NOX2	Cytochrome b-245 heavy chain	0.2797	-0.5330	-0.5427	4	0	Cell membrane
305	P29401	TKT	Transketolase (TK)	4.1017	3.5619	4.0334	14	0	
306	P01717	IGLV3-25	Immunoglobulin lambda variable 3-25 (Ig lambda chain V-IV region Hil)	0.0069	0.5427	0.7462	2	0	Secreted
307	P02760	AMBP HCP ITIL	Protein AMBP	-1.1445	-0.5316	-0.2937	3	0	Secreted
308	P0DOY3	IGLC3	Immunoglobulin lambda constant 3 (Ig lambda chain C region DOT)	-9.5811	-11.4523	-12.3322	1	0	Secreted
309	P31946	YWHAB	14-3-3 protein beta/alpha (Protein 1054) (Protein kinase C inhibitor protein 1)	0.4071	0.5921	0.5914	2	0	Cytoplasm
310	P34096	RNASE4 RNS4	Ribonuclease 4 (RNase 4)	-1.1803	-0.6311	-1.3266	2	0	Secreted
311	P21796	VDAC1 VDAC	Voltage-dependent anion-selective channel protein 1 (VDAC-1)	1.3416	1.0000	0.9292	5	0	Mitochondrion outer membrane
312	P48735	IDH2	Isocitrate dehydrogenase [NADP], mitochondrial (IDH)	-1.8138	-1.6235	-2.2052	1	0	Mitochondrion
313	P01780	IGHV3-7	Immunoglobulin heavy variable 3-7 (Ig heavy chain V-III region GAL)	0.8252	0.8932	1.3996	1	0	Secreted
314	Q9HD89	RETN	Resistin (Adipose tissue-specific secretory factor) (ADSF)	-0.0658	-1.1757	-0.4542	2	0	Secreted
315	A0A0B4J1X5	IGHV3-74	Immunoglobulin heavy variable 3-74	2.1316	2.5929	2.9480	1	0	Secreted
316	P17693	HLA-G HLA-6.0 HLAG	HLA class I histocompatibility antigen, alpha chain G (HLA G antigen)	-3.2259	-2.5404	-2.2864	1	0	Cell membrane
317	P01743	IGHV1-46	Immunoglobulin heavy variable 1-46 (Ig heavy chain V-I region DOT)	-0.0516	0.0668	0.6706	1	0	Secreted
318	P46778	RPL21	60S ribosomal protein L21	-1.8086	-2.2450	-2.4835	1	0	Cytoplasm, cytosol
319	P01700	IGLV1-47	Immunoglobulin lambda variable 1-47 (Ig lambda chain V-I region HA)	1.5030	1.7470	2.1772	2	0	Secreted
320	O14983	ATP2A1	Sarcoplasmic/endoplasmic reticulum calcium ATPase 1 (SERCA1)	-4.7140	-6.9581	-5.6704	1	0	Endoplasmic reticulum membrane
321	P23381	WARS1 IFI53 WARS WRS	Tryptophan-tRNA ligase, cytoplasmic	-4.0976	-3.8161	-2.9440	1	0	Cytoplasm
322	P19012	KRT15 KRTB	Keratin, type I cytoskeletal 15 (Cytokeratin-15)	-0.1839	-0.5669	-0.6520	4	0	
323	Q08380	LGALS3BP M2BP	Galectin-3-binding protein (Basement membrane autoantigen p105)	2.8320	3.2183	3.3032	8	0	Secreted

List #	UniProt ID	Gene names	Protein names	CTRL Av	BRT Av	ART Av	Peptides #	Significance Elastic Net analysis	Subcellular location
324	Q86YZ3	HRNR S100A18	Hornerin	-5.6763	-8.1208	-6.7058	1	0	Cytoplasmic granule
325	Q5TH69	ARFGEF3	Brefeldin A-inhibited guanine nucleotide-exchange protein 3 (ARFGEF family member 3)	-0.0311	0.5064	0.2761	1	0	Cytoplasm
326	O00299	CLIC1 G6 NCC27	Chloride intracellular channel protein 1 (Chloride channel ABP)	1.8662	2.0606	1.9540	7	0	Nucleus
327	O14818	PSMA7 HSPC	Proteasome subunit alpha type-7	-3.9261	-3.5858	-3.1148	1	0	Cytoplasm
328	Q9UJC5	SH3BGRL2 FASH3	SH3 domain-binding glutamic acid-rich-like protein 2 (Fovea-associated SH3 domain-binding protein)	-1.9761	-2.4389	-2.3629	1	0	Nucleus
329	P60866	RPS20	40S ribosomal protein S20	0.9468	0.3476	0.7474	2	0	Cytoplasm
330	O00748	CES2 ICE	Cocaine esterase	-2.1257	-1.7427	-2.8778	1	0	Endoplasmic reticulum lumen
331	P80748	IGLV3-21	Immunoglobulin lambda variable 3-21 (Ig lambda chain V-III region LOI)	-0.0678	0.1034	0.6218	2	0	Secreted
332	Q14697	GANAB G2AN KIAA0088	Neutral alpha-glucosidase AB (EC 3.2.1.207) (Alpha-glucosidase 2) (Glucosidase II subunit alpha)	-1.0581	-1.2781	-1.7768	2	0	Endoplasmic reticulum
333	Q13404	UBE2V1	Ubiquitin-conjugating enzyme E2 variant 1 (UEV-1)	0.5332	0.1426	-0.2434	1	0	Nucleus
334	O15143	ARPC1B ARC41	Actin-related protein 2/3 complex subunit 1B (Arp2/3 complex 41 kDa subunit) (p41-ARC)	-1.1697	-0.9126	-0.1586	2	0	Cytoplasm, cytoskeleton
335	P04083	ANXA1 ANX1 LPC1	Annexin A1 (Annexin I)	8.2707	8.1325	7.6075	28	0	Nucleus
336	P62081	RPS7	40S ribosomal protein S7	0.3859	-0.0374	-0.2333	2	0	Cytoplasm, cytoskeleton, microtubule organizing center, centrosome
337	P01861	IGHG4	Immunoglobulin heavy constant gamma 4 (Ig gamma-4 chain C region)	-1.9974	-2.6556	-1.1860	1	0	Secreted
338	P53004	BLVRA BLVR BVR	Biliverdin reductase A (BVR A)	-1.0862	-1.7241	-1.4426	2	0	Cytoplasm
339	P60903	S100A10 ANX2LG CAL1L CLP11	Protein S100-A10 (Calpactin I light chain)	1.2440	0.9366	0.7202	3	0	
340	O75131	CPNE3 CPN3	Copine-3 (Copine III)	0.1648	-0.4652	-0.3688	3	0	Nucleus
341	P06576	ATP5F1B ATP5B ATPMB ATPSB	ATP synthase subunit beta, mitochondrial	2.8462	3.0571	2.8851	13	0	Mitochondrion inner membrane
342	P15880	RPS2 RPS4	40S ribosomal protein S2	1.2579	0.8209	0.9279	5	0	
343	P00751	CFB BF BFD	Complement factor B	0.9082	1.2092	1.6121	12	0	Secreted

List #	UniProt ID	Gene names	Protein names	CTRL Av	BRT Av	ART Av	Peptides #	Significance Elastic Net analysis	Subcellular location
344	P80511	S100A12	Protein S100-A12 (CGRP) (Calcium-binding protein in amniotic fluid 1)	2.1712	1.6590	1.5337	6	0	Secreted
345	P01024	C3 CPAMD1	Complement C3	4.7258	4.7280	5.4506	65	0	Secreted
346	P18054	ALOX12 12LO LOG12	Arachidonate 12-lipoxygenase, 12S-type (12S-LOX)	-2.1059	-2.4431	-2.7964	2	0	Cytoplasm, cytosol
347	P06870	KLK1	Kallikrein-1	2.4003	2.6434	3.0190	9	0	
348	P02749	APOH B2G1	Beta-2-glycoprotein 1	0.7097	0.7352	1.5410	6	0	Secreted
349	P62851	RPS25	40S ribosomal protein S25	1.0400	0.8744	0.7389	2	0	
350	P02545	LMNA LMN1	Prelamin-A/C	3.1503	3.0230	2.7848	17	0	Nucleus
351	P05091	ALDH2 ALDM	Aldehyde dehydrogenase, mitochondrial	-2.1547	-2.4993	-3.0464	1	0	Mitochondrion matrix
352	Q92747	ARPC1A SOP2L	Actin-related protein 2/3 complex subunit 1A (SOP2-like protein)	-2.3973	-3.0949	-2.6291	1	0	Cytoplasm, cytoskeleton
353	Q53GQ0	HSD17B12 SDR12C1	Very-long-chain 3-oxoacyl-CoA reductase	-3.5246	-3.7913	-2.8671	1	0	Endoplasmic reticulum membrane
354	P14555	PLA2G2A	Phospholipase A2, membrane associated	-2.1330	-2.7267	-1.3714	1	0	Secreted
355	P07858	CTSB CPSB	Cathepsin B	-0.2792	0.2898	0.3188	2	0	Lysosome
356	P02679	FGG PRO2061	Fibrinogen gamma chain	2.6913	2.8014	3.3408	14	0	Secreted
357	P30050	RPL12	60S ribosomal protein L12 (Large ribosomal subunit protein uL11)	0.5963	0.2871	0.2897	2	0	
358	O95833	CLIC3	Chloride intracellular channel protein 3	0.1037	-0.0347	-0.3415	3	0	Nucleus, Membrane
359	Q9ULV4	CORO1C CRN2 CRNN4	Coronin-1C (Coronin-3) (hCRNN4)	-2.8765	-2.2058	-2.7298	1	0	Cell membrane
360	P25787	PSMA2 HC3 PSC3	Proteasome subunit alpha type-2	-2.3797	-2.6368	-1.9983	1	0	Cytoplasm
361	Q99832	CCT7 CCTH NIP7-1	T-complex protein 1 subunit eta (TCP-1-eta)	-1.5427	-0.8722	-0.6691	1	0	Cytoplasm
362	Q01518	CAP1 CAP	Adenylyl cyclase-associated protein 1 (CAP 1)	2.0241	1.6953	1.8825	12	0	Cell membrane
363	P18124	RPL7	60S ribosomal protein L7	0.6301	0.3060	0.1913	2	0	
364	P08246	ELANE ELA2	Neutrophil elastase	5.8978	4.8341	5.0187	14	0	Cytoplasmic vesicle, phagosome

List #	UniProt ID	Gene names	Protein names	CTRL Av	BRT Av	ART Av	Peptides #	Significance Elastic Net analysis	Subcellular location
365	P23526	AHCY SAHH	Adenosylhomocysteinase (AdoHcyase) (EC 3.3.1.1) (S-adenosyl-L-homocysteine hydrolase)	-1.1011	-1.3818	-1.3236	2	0	Cytoplasm
366	P69905	HBA1; HBA2	Hemoglobin subunit alpha (Alpha-globin) (Hemoglobin alpha chain)	1.6500	2.5473	2.9419	10	0	
367	Q13838	DDX39B	Spliceosome RNA helicase DDX39B	-0.6026	-0.3489	-0.6069	2	0	Nucleus
368	Q14210	LY6D E48	Lymphocyte antigen 6D (Ly-6D) (E48 antigen)	-0.4964	-0.7450	-0.9236	1	0	Cell membrane
369	O00764	PDXK	Pyridoxal kinase	-3.9533	-5.1288	-3.5301	1	0	Cytoplasm, cytosol
370	Q96QK1	VPS35	Vacuolar protein sorting-associated protein 35 (hVPS35)	-1.4771	-1.7705	-0.9962	2	0	Cytoplasm, Membrane, Endosome
371	Q96DA0	ZG16B	Zymogen granule protein 16 homolog B	9.3354	9.0679	8.8611	10	0	Secreted
372	P46782	RPS5	40S ribosomal protein S5	-0.6047	-0.3799	-0.2910	2	0	
373	P09525	ANXA4 ANX4	Annexin A4 (35-beta calcimedin)	0.4287	0.7819	0.6676	5	0	
374	P02675	FGB	Fibrinogen beta chain	2.8523	3.2019	3.5267	18	0	Secreted
375	P63000	RAC1 TC25 MIG5	Ras-related C3 botulinum toxin substrate 1	-0.9169	-1.3029	-1.5711	1	0	Cell membrane
376	P14625	HSP90B1 GRP94 TRA1	Endoplasmin (94 kDa glucose-regulated protein)	0.0081	0.2529	0.0917	3	0	Endoplasmic reticulum lumen
377	Q02487	DSC2 CDHF2 DSC3	Desmocollin-2 (Cadherin family member 2)	1.6827	1.3073	1.7597	5	0	Cell membrane
378	Q14019	COTL1 CLP	Coactosin-like protein	-0.8502	-1.5598	-0.8266	2	0	Cytoplasm
379	Q9ULZ3	PYCARD ASC CARD5 TMS1	Apoptosis-associated speck-like protein containing a CARD (hASC)	-3.1772	-3.5696	-2.9300	1	0	Cytoplasm, Endoplasmic reticulum, Mitochondrion, Nucleus
380	P61769	B2M	Beta-2-microglobulin	1.6950	2.1799	2.0922	5	0	Secreted
381	P41218	MNDA	Myeloid cell nuclear differentiation antigen	1.7154	0.8981	0.9750	5	0	Nucleus, Cytoplasm
382	P04280	PRB1	Basic salivary proline-rich protein 1 (Salivary proline-rich protein)	-5.4754	-7.9665	-7.1798	1	0	Secreted
383	P53634	CTSC CPPI	Dipeptidyl peptidase 1 (Cathepsin C)	-2.6710	-2.2064	-1.9377	1	0	Lysosome
384	O75340	PDCD6 ALG2	Programmed cell death protein 6 (Apoptosis-linked gene 2 protein homolog)	-0.6976	-0.6283	-0.8609	2	0	Endoplasmic reticulum membrane

List #	UniProt ID	Gene names	Protein names	CTRL Av	BRT Av	ART Av	Peptides #	Significance Elastic Net analysis	Subcellular location
385	Q96LJ7	DHRS1 SDR19C1	Dehydrogenase/reductase SDR family member 1	-1.0631	-2.0069	-1.5630	1	0	
386	P49368	CCT3 CCTG TRIC5	T-complex protein 1 subunit gamma (TCP-1-gamma)	-2.1859	-1.5044	-2.0661	1	0	Cytoplasm
387	P08727	KRT19	Keratin, type I cytoskeletal 19 (Cytokeratin-19)	1.9340	1.7500	1.4904	10	0	
388	O60506	SYNCRIP HNRPQ NSAP1	Heterogeneous nuclear ribonucleoprotein Q (hnRNP Q)	-1.6401	-1.6449	-2.4193	1	0	Cytoplasm
389	P24158	PRTN3 MBN	Myeloblastin	5.6403	4.7134	5.2444	9	0	Cytoplasmic granule
390	P19827	ITIH1	Inter-alpha-trypsin inhibitor heavy chain H1 (ITI heavy chain H1)	-2.0578	-1.5327	-2.0233	2	0	Secreted
391	P52209	PGD PGDH	6-phosphogluconate dehydrogenase, decarboxylating	4.4465	4.3654	4.2959	18	0	Cytoplasm
392	P02768	ALB GIG20 GIG42	Serum albumin	9.1007	9.4128	9.9969	84	0	Secreted
393	P28065	PSMB9 LMP2 PSMB6i RING12	Proteasome subunit beta type-9	-2.8868	-2.1328	-3.0182	1	0	Cytoplasm
394	P02042	HBD	Hemoglobin subunit delta (Delta-globin) (Hemoglobin delta chain)	-1.3012	-1.3291	-0.7168	3	0	
395	P61163	ACTR1A CTRN1	Alpha-centractin (Centractin) (ARP1) (Actin-RPV) (Centrosome-associated actin homolog)	-2.6413	-2.3596	-2.6984	2	0	Cytoplasm, cytoskeleton
396	P28072	PSMB6 LMPY Y	Proteasome subunit beta type-6	-0.8229	-1.6144	-0.8971	1	0	Cytoplasm
397	P62424	RPL7A	60S ribosomal protein L7a	0.2751	-0.2250	-0.2432	3	0	
398	P0DOX5		Immunoglobulin gamma-1 heavy chain (Immunoglobulin gamma-1 heavy chain NIE)	3.6592	3.2077	4.0846	7	0	Secreted
399	P03973	SLPI_HUMAN	Antileukoproteinase (ALP)	1.4284	1.8582	1.7072	4	0	Secreted
400	P04004	VTN	Vitronectin (VN) (S-protein) (Serum-spreading factor)	-1.4624	-1.7002	-0.8527	1	0	Secreted, extracellular space.
401	Q14515	SPARCL1	SPARC-like protein 1 (High endothelial venule protein)	-0.2507	0.3068	0.3709	3	0	Secreted, extracellular space and matrix
402	P20160	AZU1	Azurocidin (Cationic antimicrobial protein CAP37) (Heparin-binding protein)	5.0205	4.1341	4.4639	11	0	Cytoplasmic granule membrane
403	Q02413	DSG1 CDHF4	Desmoglein-1 (Cadherin family member 4)	-0.8211	-1.3978	-0.8359	2	0	Cell membrane
404	P07437	TUBB TUBB5 OK/SW-cl.56	Tubulin beta chain (Tubulin beta-5 chain)	-1.7788	-1.8195	-1.3504	1	0	Cytoplasm, cytoskeleton

List #	UniProt ID	Gene names	Protein names	CTRL Av	BRT Av	ART Av	Peptides #	Significance Elastic Net analysis	Subcellular location
405	P01008	SERPINC1 AT3 PRO0309	Antithrombin-III (ATIII) (Serpin C1)	0.7067	0.7112	1.3300	6	0	Secreted, extracellular space.
406	Q16563	SYPL1 SYPL	Synaptophysin-like protein 1 (Pantophysin)	0.0444	-0.0243	-0.4414	1	0	Cytoplasmic vesicle membrane
407	P62805	H4C1 H4/A H4FA HIST1H4A	Histone H4	7.9753	7.3856	7.5504	11	0	Nucleus, Chromosome
408	Q6UWP8	SBSN	Suprabasin	-2.3946	-2.7671	-2.3928	2	0	Secreted
409	P51648	ALDH3A2 ALDH10 FALDH	Aldehyde dehydrogenase family 3 member A2	-1.0644	-1.8019	-1.6238	1	0	Microsome membrane
410	P27105	STOM BND7 EPB72	Erythrocyte band 7 integral membrane protein (Protein 7.2b) (Stomatin)	0.8390	0.0006	0.5091	3	0	Cell membrane
411	P35232	PHB PHB1	Prohibitin	-1.6608	-2.0483	-1.5737	1	0	Mitochondrion inner membrane
412	P02647	APOA1	Apolipoprotein A-I (Apo-AI)	3.4581	3.8537	4.3809	23	0	Secreted
413	Q9UM07	PADI4 PAD4 PADI5 PDI5	Protein-arginine deiminase type-4	-0.2697	-0.5824	0.0815	3	0	Cytoplasm, Nucleus
414	P46940	IQGAP1 KIAA0051	Ras GTPase-activating-like protein IQGAP1 (p195)	1.3123	1.0521	1.1999	9	0	Cell membrane
415	P05156	CFI IF	Complement factor I	-3.6459	-3.4079	-2.8862	2	0	Secreted, extracellular space
416	Q13835	PKP1	Plakophilin-1 (Band 6 protein) (B6P)	1.7613	1.3771	1.4513	6	0	Nucleus
417	P02747	C1QC C1QG	Complement C1q subcomponent subunit C	-3.1862	-4.6912	-3.6187	1	0	Secreted
418	A0A0C4DH69	IGKV1-9	Immunoglobulin kappa variable 1-9	-1.2617	-1.6085	-0.9609	1	0	Secreted
419	P49189	ALDH9A1 ALDH4 ALDH7 ALDH9	4-trimethylaminobutyraldehyde dehydrogenase (TMABA-DH)	0.2416	-0.0653	0.0755	3	0	Cytoplasm, cytosol
420	P08603	CFH HF HF1 HF2	Complement factor H (H factor 1)	-0.2647	-0.7012	-0.3198	5	0	Secreted
421	P52907	CAPZA1	F-actin-capping protein subunit alpha-1 (CapZ alpha-1)	-0.0622	-0.2456	0.0436	2	0	Cytoplasm, cytoskeleton
422	P02671	FGA	Fibrinogen alpha chain [Cleaved into: Fibrinopeptide A; Fibrinogen alpha chain]	0.7919	1.3116	1.2273	6	0	Secreted
423	O75594	PGLYRP1	Peptidoglycan recognition protein 1 (Peptidoglycan recognition protein short) (PGRP-S)	0.4865	0.1793	0.9237	3	0	Secreted
424	P52566	ARHGDIB GDIA2 GDID4 RAP1GN1	Rho GDP-dissociation inhibitor 2 (Rho GDI 2) (Ly-GDI) (Rho-GDI beta)	2.0483	1.6477	2.4123	4	0	Cytoplasm, cytosol

List #	UniProt ID	Gene names	Protein names	CTRL Av	BRT Av	ART Av	Peptides #	Significance Elastic Net analysis	Subcellular location
425	P63104	YWHAZ	14-3-3 protein zeta/delta (Protein kinase C inhibitor protein 1) (KCIP-1)	4.8552	5.0774	4.7991	10	0	Cytoplasm
426	P27482	CALML3	Calmodulin-like protein 3 (CaM-like protein) (CLP) (Calmodulin-related protein NB-1)	1.2301	1.5179	1.1737	3	0	
427	P02810	PRH1; PRH2	Salivary acidic proline-rich phosphoprotein 1/2 (Db-s) (PRP-1/PRP-2) (Parotid acidic protein)	1.2172	2.3812	0.9405	5	0	Secreted
428	P61019	RAB2A RAB2	Ras-related protein Rab-2A	-0.4490	-0.4540	-0.8389	3	0	Endoplasmic reticulum-Golgi
429	P31947	SFN HME1	14-3-3 protein sigma (Epithelial cell marker protein 1) (Stratifin)	4.2804	4.6320	4.5890	12	0	Cytoplasm
430	Q6ZVX7	NCCRP1 FBXO50	F-box only protein 50 (NCC receptor protein 1 homolog)	1.1343	1.2780	1.0324	5	0	Cytoplasm
431	P19823	ITIH2 IGHEP2	Inter-alpha-trypsin inhibitor heavy chain H2 (ITI heavy chain H2)	-3.8599	-3.3728	-3.2018	1	0	Secreted
432	P11215	ITGAM CD11B CR3A	Integrin alpha-M (CD11 antigen-like family member B)	2.4646	1.7644	2.1245	14	0	Cell membrane
433	P01040	CSTA STF1 STFA	Cystatin-A (Cystatin-AS) (Stefin-A)	2.3302	2.6776	2.5030	7	0	Cytoplasm
434	P08708	RPS17 RPS17L	40S ribosomal protein S17	-2.3698	-2.6949	-3.0286	1	0	
435	Q86T26	TMPRSS11B HATL5	Transmembrane protease serine 11B	0.1516	0.0077	-0.2294	3	0	Cell membrane
436	P01042	KNG1 BDK KNG	Kininogen-1 (Alpha-2-thiol proteinase inhibitor) (Fitzgerald factor)	-2.3688	-2.8685	-1.9661	3	0	Secreted, extracellular space
437	P17900	GM2A	Ganglioside GM2 activator (Cerebroside sulfate activator protein)	-1.3832	-0.9892	-0.9842	2	0	Lysosome
438	P26639	TARS1 TARS	Threonine--tRNA ligase 1, cytoplasmic	-2.2551	-2.8806	-2.6239	1	0	Cytoplasm
439	P0DOX8		Immunoglobulin lambda-1 light chain (Immunoglobulin lambda-1 light chain MCG)	-0.2830	-0.0215	0.1901	2	0	Secreted
440	P12532	CKMT1A CKMT; CKMT1B CKMT	Creatine kinase U-type, mitochondrial	-0.5014	-0.7496	-1.0903	2	0	Mitochondrion inner membrane
441	Q9UGM3	DMBT1 GP340	Deleted in malignant brain tumors 1 protein (Glycoprotein 340)	4.7392	4.2812	4.0831	19	0	Secreted
442	O15511	ARPC5 ARC16	Actin-related protein 2/3 complex subunit 5 (Arp2/3 complex 16 kDa subunit) (p16-ARC)	0.5700	0.4554	0.4003	1	0	Cytoplasm, cytoskeleton
443	Q71U36	TUBA1A TUBA3	Tubulin alpha-1A chain (Alpha-tubulin 3)	-0.8059	-1.1274	-1.0779	2	0	Cytoplasm, cytoskeleton
444	Q9UBC9	SPRR3 SPRC	Small proline-rich protein 3 (22 kDa pancornulin) (Cornifin beta) (Esophagin)	5.6809	5.9717	5.4882	12	0	Cytoplasm

List #	UniProt ID	Gene names	Protein names	CTRL Av	BRT Av	ART Av	Peptides #	Significance Elastic Net analysis	Subcellular location
445	P02787	TF PRO1400	Serotransferrin (Transferrin) (Beta-1 metal-binding globulin) (Siderophilin)	5.3093	5.3514	5.9871	58	0	Secreted
446	P13073	COX4I1 COX4	Cytochrome c oxidase subunit 4 isoform 1, mitochondrial	-0.6557	-0.7556	-0.9920	1	0	Mitochondrion inner membrane
447	O00151	PDLIM1 CLIM1 CLP36	PDZ and LIM domain protein 1 (C-terminal LIM domain protein 1) (Elfin) (LIM domain protein CLP-36)	-2.6709	-3.3056	-2.9392	1	0	Cytoplasm
448	P26038	MSN	Moesin (Membrane-organizing extension spike protein)	0.6195	0.6657	1.0434	8	0	Cell membrane
449	P55786	NPEPPS PSA	Puromycin-sensitive aminopeptidase (PSA)	0.9003	0.7618	1.0582	4	0	Cytoplasm, cytosol
450	P62834	RAP1A KREV1	Ras-related protein Rap-1A (C21KG) (G-22K) (GTP-binding protein smg p21A) (Ras-related protein Krev-1)	1.2304	0.7634	1.1809	3	0	Cell membrane
451	P13693	TPT1	Translationally-controlled tumor protein (TCTP) (Fortilin) (Histamine-releasing factor) (HRF) (p23)	0.4239	0.5617	0.6809	3	0	Cytoplasm
452	P04745	AMY1B AMY1	Alpha-amylase 1	8.7571	9.4163	9.3506	19	0	Cytoplasm, Nucleus, Mitochondrion
453	P60900	PSMA6 PROS27	Proteasome subunit alpha type-6	-0.3197	-0.3340	-0.0310	3	0	Cytoplasm
454	P18510	IL1RN IL1F3 IL1RA	Interleukin-1 receptor antagonist protein (IL-1RN) (IL-1ra)	2.8043	3.0354	2.8314	6	0	[Isoform 1]: Secreted; [Isoform 2,3,4]: Cytoplasm
455	P13807	GYS1 GYS	Glycogen [starch] synthase, muscle	-2.8958	-3.1007	-3.6156	1	0	
456	P29692	EEF1D EF1D	Elongation factor 1-delta (EF-1-delta) (Antigen NY-CO-4)	-1.3385	-1.0897	-0.9065	2	0	Nucleus
457	P48668	KRT6C KRT6E	Keratin, type II cytoskeletal 6C (Cytokeratin-6C)	-1.5744	-1.9801	-2.0260	1	0	
458	P40199	CEACAM6 NCA	Carcinoembryonic antigen-related cell adhesion molecule 6 (Non-specific crossreacting antigen)	-0.2529	-0.6866	-0.3444	2	0	Cell membrane
459	O75083	WDR1	WD repeat-containing protein 1 (Actin-interacting protein 1) (AIP1) (NORI-1)	1.7734	1.6318	1.8100	6	0	Cytoplasm, cytoskeleton
460	O14773	TPP1 CLN2 GIG1 UNQ267/PRO304	Tripeptidyl-peptidase 1 (TPP-1)	-1.3429	-1.1115	-1.0698	1	0	Lysosome
461	O43240	KLK10 NES1 PRSSL1	Kallikrein-10	0.6477	0.3278	0.1044	2	0	Secreted
462	P01860	IGHG3	Immunoglobulin heavy constant gamma 3 (HDC)	0.1149	0.2272	0.9598	3	0	Secreted
463	P31943	HNRNPH1 HNRPH HNRPH1	Heterogeneous nuclear ribonucleoprotein H (hnRNP H)	-1.5581	-1.8013	-1.9346	2	0	Nucleus
464	Q9NZT1	CALML5 CLSP	Calmodulin-like protein 5 (Calmodulin-like skin protein)	-1.3160	-2.3418	-2.2905	1	0	

List #	UniProt ID	Gene names	Protein names	CTRL Av	BRT Av	ART Av	Peptides #	Significance Elastic Net analysis	Subcellular location
465	P38606	ATP6V1A ATP6A1 ATP6V1A1 VPP2	V-type proton ATPase catalytic subunit A (V-ATPase subunit A)	-2.8195	-3.3880	-2.8616	1	0	Cytoplasm
466	P35527	KRT9	Keratin, type I cytoskeletal 9 (Cytokeratin-9)	2.2475	2.7744	2.6580	10	0	
467	P10412	H1-4 H1F4 HIST1H1E	Histone H1.4 (Histone H1b) (Histone H1s-4)	0.6706	0.0228	0.5215	3	0	Nucleus, Chromosome
468	P51149	RAB7A RAB7	Ras-related protein Rab-7a	0.1176	0.8001	0.8424	1	0	Cytoplasmic vesicle, phagosome membrane
469	O95171	SCEL	Sciellin	-2.2658	-1.7491	-2.1561	1	0	Cytoplasm. Membrane
470	P35579	MYH9	Myosin-9 (Cellular myosin heavy chain, type A)	2.7514	2.5452	2.3846	17	0	Cytoplasm, cytoskeleton
471	P32119	PRDX2 NKEFB TDPX1	Peroxiredoxin-2	2.4340	2.5820	2.5143	7	0	Cytoplasm
472	Q15181	PPA1 IOPPP PP	Inorganic pyrophosphatase	-3.4698	-4.0850	-3.8180	1	0	Cytoplasm
473	A0A0A0MS15	IGHV3-49	Immunoglobulin heavy variable 3-49	0.2589	0.4212	0.8100	1	0	Secreted
474	P05090	APOD	Apolipoprotein D (Apo-D) (ApoD)	-2.0154	-1.5390	-1.7196	2	0	Secreted
475	P14618	PKM OIP3 PK2 PK3 PKM2	Pyruvate kinase PKM	3.0592	2.8214	3.0615	16	0	Cytoplasm
476	P09211	GSTP1 FAEES3 GST3	Glutathione S-transferase P	4.1796	4.3160	4.2882	8	0	Cytoplasm
477	Q9UL46	PSME2	Proteasome activator complex subunit 2 (11S regulator complex subunit beta)	0.1225	-0.3269	0.1376	3	0	
478	P14780	MMP9 CLG4B	Matrix metalloproteinase-9 (MMP-9)	2.6702	2.0719	2.8864	10	0	Secreted, extracellular space and matrix
479	P02766	TTR PALB	Transthyretin (ATTR) (Prealbumin) (TBPA)	1.6638	1.8532	2.2799	9	0	Secreted, Cytoplasm
480	Q9Y5Z4	HEBP2 C6orf34 SOUL	Heme-binding protein 2 (Placental protein 23) (PP23) (Protein SOUL)	-2.1596	-1.9163	-1.9881	1	0	Cytoplasm
481	P46783	RPS10	40S ribosomal protein S10	0.4222	0.1545	0.0179	3	0	Nucleus
482	P01871	IGHM	Immunoglobulin heavy constant mu (Ig mu chain C region)	-2.8991	-3.0409	-2.3586	1	0	[Isoform 1]: Secreted; [Isoform 2]: Cell membrane
483	Q07960	ARHGAP1 CDC42GAP RHOGAP1	Rho GTPase-activating protein 1 (CDC42 GTPase-activating protein)	-1.2669	-1.1894	-1.0229	2	0	Cytoplasm
484	P08311	CTSG	Cathepsin G (CG)	5.3658	4.5932	4.6907	13	0	Cell surface

List #	UniProt ID	Gene names	Protein names	CTRL Av	BRT Av	ART Av	Peptides #	Significance Elastic Net analysis	Subcellular location
485	P08238	HSP90AB1 HSP90B HSPC2 HSPCB	Heat shock protein HSP 90-beta (HSP 90) (Heat shock 84 kDa) (HSP 84) (HSP84)	1.7715	1.6354	1.8277	6	0	Cytoplasm
486	P07108	DBI	Acyl-CoA-binding protein (ACBP) (Diazepam-binding inhibitor) (DBI) (Endozepine) (EP)	-2.8475	-2.2857	-2.3131	2	0	Endoplasmic reticulum
487	P07477	PRSS1 TRP1 TRY1 TRYP1	Trypsin-1	4.2662	4.6861	3.1432	1	0	Secreted, extracellular space
488	P15311	EZR VIL2	Ezrin (Cytovillin) (Villin-2) (p81)	1.3911	1.6056	1.3988	4	0	Apical cell membrane
489	P0DOX2		Immunoglobulin alpha-2 heavy chain (Immunoglobulin alpha-2 heavy chain BUT)	4.4211	4.5890	5.0564	10	0	Secreted
490	P36542	ATP5F1C ATP5C ATP5C1 ATP5CL1	ATP synthase subunit gamma, mitochondrial	-1.2638	-1.4868	-1.5091	2	0	Mitochondrion inner membrane
491	Q9HC84	MUC5B MUC5	Mucin-5B	4.4278	4.0800	4.6208	37	0	Secreted
492	Q9H299	SH3BGRL3 P1725	SH3 domain-binding glutamic acid-rich-like protein 3 (SH3 domain-binding protein 1)	-0.9654	-0.6213	-0.4573	1	0	Cytoplasm. Nucleus
493	Q7L5L3	GDPD3 GDE7	Lysophospholipase D GDPD3	-1.9088	-2.0992	-1.8075	2	0	Membrane
494	P17213	BPI	Bactericidal permeability-increasing protein (BPI) (CAP 57)	0.2102	-0.3889	0.0123	4	0	Secreted
495	P11678	EPX EPER EPO EPP	Eosinophil peroxidase (EPO)	-3.9415	-3.4123	-3.2932	2	0	Cytoplasmic granule
496	P68871	HBB	Hemoglobin subunit beta (Beta-globin)	2.4475	3.0507	3.4639	10	0	
497	P00747	PLG	Plasminogen	-1.5279	-1.1571	-1.1085	2	0	Secreted
498	P22894	MMP8 CLG1	Neutrophil collagenase	0.3499	0.2552	0.8591	5	0	Cytoplasmic granule. Secreted, extracellular space, extracellular matrix
499	P01023	A2M CPAMD5 FWP007	Alpha-2-macroglobulin (Alpha-2-M)	3.9796	3.4754	4.0031	40	0	Secreted
500	P01859	IGHG2	Immunoglobulin heavy constant gamma 2 (Ig gamma-2 chain C region)	4.2554	4.3288	4.9001	6	0	Secreted
501	P27824	CANX	Calnexin (IP90) (Major histocompatibility complex class I antigen-binding protein p88) (p90)	0.7900	0.9800	0.6660	5	0	Endoplasmic reticulum membrane
502	O15254	ACOX3 BRCOX PRCOX	Peroxisomal acyl-coenzyme A oxidase 3	-4.1674	-3.9487	-4.4518	1	0	Peroxisome
503	P0DOX6		Immunoglobulin mu heavy chain (Immunoglobulin mu heavy chain OU)	-1.8569	-1.5069	-1.9697	1	0	Secreted

List #	UniProt ID	Gene names	Protein names	CTRL Av	BRT Av	ART Av	Peptides #	Significance Elastic Net analysis	Subcellular location
504	Q13155	AIMP2 JTV1 PRO0992	Aminoacyl tRNA synthase complex-interacting multifunctional protein 2	-3.4612	-4.0105	-3.4949	1	0	Cytoplasm, cytosol
505	Q8IUE6	H2AC21 HIST2H2AB	Histone H2A type 2-B	0.1311	-0.2682	-0.3667	2	0	Nucleus
506	Q14116	IL18 IGIF IL1F4	Interleukin-18 (IL-18)	-0.3234	-0.2645	-0.5124	2	0	Cytoplasm
507	P31949	S100A11 MLN70 S100C	Protein S100-A11 (Calgizzarin) (Metastatic lymph node gene 70 protein)	3.0052	3.1040	2.8578	5	0	Cytoplasm
508	Q9NUQ9	CYRIB CYRI FAM49B BM-009	Protein FAM49B (L1)	-2.3886	-2.1712	-2.0490	2	0	Membrane
509	P23280	CA6	Carbonic anhydrase 6	6.3993	7.1220	7.0364	18	0	Secreted
510	P30153	PPP2R1A	Serine/threonine-protein phosphatase 2A 65 kDa regulatory subunit A alpha isoform (Medium tumor antigen-associated 61 kDa protein)	-3.2028	-3.4707	-3.5195	2	0	Cytoplasm
511	Q9Y6B6	SAR1B SARA2 SARB	GTP-binding protein SAR1b (GTP-binding protein B) (GTBPB)	-0.9265	-1.4662	-0.8283	1	0	Endoplasmic reticulum membrane
512	Q99623	PHB2 BAP REA	Prohibitin-2	-0.1488	-0.0268	0.1098	4	0	Mitochondrion inner membrane
513	Q05315	CLC LGALS10 LGALS10A	Galectin-10	-0.7209	-0.8258	-0.1832	2	0	Cytoplasm, cytosol
514	P16615	ATP2A2 ATP2B	Sarcoplasmic/endoplasmic reticulum calcium ATPase 2 (SERCA2)	-3.8417	-3.4027	-4.0129	1	0	Endoplasmic reticulum membrane
515	P51665	PSMD7 MOV34L	26S proteasome non-ATPase regulatory subunit 7 (26S proteasome regulatory subunit RPN8)	-3.1701	-3.2441	-3.4425	1	0	
516	P40121	CAPG AFCP MCP	Macrophage-capping protein (Actin regulatory protein CAP-G)	0.5847	0.4056	0.5796	4	0	Nucleus
517	P50995	ANXA11 ANX11	Annexin A11	0.2069	0.3941	0.0812	4	0	Cytoplasm
518	P40939	HADHA HADH	Trifunctional enzyme subunit alpha, mitochondrial (78 kDa gastrin-binding protein)	-2.6115	-3.1113	-2.6964	1	0	Mitochondrion
519	P06744	GPI	Glucose-6-phosphate isomerase (GPI)	2.8154	2.7427	2.9424	10	0	Cytoplasm
520	P55072	VCP	Transitional endoplasmic reticulum ATPase (TER ATPase)	1.4131	1.5877	1.4329	7	0	Cytoplasm, cytosol
521	Q9UBH0	IL36RN	Interleukin-36 receptor antagonist protein (IL-36Ra)	-2.1803	-2.3013	-1.5323	1	0	Cytoplasm
522	P06331	IGHV4-34	Immunoglobulin heavy variable 4-34 (Ig heavy chain V-II region ARH-77)	2.5746	2.5448	2.9183	2	0	Secreted
523	P26599	PTBP1 PTB	Polypyrimidine tract-binding protein 1 (PTB) (57 kDa RNA-binding protein PPTB-1)	-2.3449	-2.0285	-1.8785	2	0	Nucleus

List #	UniProt ID	Gene names	Protein names	CTRL Av	BRT Av	ART Av	Peptides #	Significance Elastic Net analysis	Subcellular location
524	P54920	NAPA SNAPA	Alpha-soluble NSF attachment protein (SNAP-alpha)	-0.2845	-0.4087	-0.7616	3	0	Cell membrane
525	Q14739	LBR	Delta (14)-sterol reductase LBR (Delta-14-SR)	-2.6836	-2.8614	-2.0230	1	0	Nucleus inner membrane
526	P62273	RPS29	40S ribosomal protein S29	-1.5259	-1.7713	-1.4077	1	0	Cytoplasm, cytosol
527	O95336	PGLS	6-phosphogluconolactonase (6PGL)	-0.5298	-0.2993	-0.3460	3	0	Cytoplasm
528	P13987	CD59	CD59 glycoprotein (1F5 antigen)	-1.4437	-1.4329	-1.2755	2	0	Cell membrane
529	P05107	ITGB2 CD18 MFI7	Integrin beta-2	1.7336	1.2208	1.2820	7	0	Cell membrane
530	O75964	ATP5MG ATP5L	ATP synthase subunit g, mitochondrial (ATPase subunit g)	-0.1054	-0.0660	-0.3376	3	0	Mitochondrion. Mitochondrion inner membrane
531	P05120	SERPINB2 PAI2 PLANH2	Plasminogen activator inhibitor 2 (PAI-2)	-1.7657	-2.2444	-2.0889	1	0	Cytoplasm, Secreted, extracellular space
532	P48047	ATP5PO ATP5O ATPO	ATP synthase subunit O, mitochondrial (ATP synthase peripheral stalk subunit OSCP)	-0.1493	-0.1930	-0.4586	2	0	Mitochondrion
533	P98088	MUC5AC MUC5	Mucin-5AC	-1.1332	-0.8365	-1.0637	6	0	Secreted
534	Q92882	OSTF1	Osteoclast-stimulating factor 1	-3.2321	-3.5400	-3.4808	1	0	Cytoplasm
535	Q9BW30	TPPP3 CGI-38	Tubulin polymerization-promoting protein family member 3 (TPPP/p20)	-2.7939	-3.0217	-2.5145	1	0	Cytoplasm
536	P54108	CRISP3	Cysteine-rich secretory protein 3 (CRISP-3) (Specific granule protein of 28 kDa) (SGP28)	3.7951	3.7557	3.4606	8	0	Secreted
537	P07476	IVL	Involucrin	-2.0612	-2.5100	-2.3218	4	0	Cytoplasm
538	P24539	ATP5PB ATP5F1	ATP synthase F(0) complex subunit B1, mitochondrial (ATP synthase peripheral stalk-membrane subunit b)	-4.4318	-4.1696	-4.0261	1	0	Mitochondrion
539	P25685	DNAJB1 DNAJ1 HDJ1 HSPF1	DnaJ homolog subfamily B member 1 (Heat shock 40 kDa protein 1)	-1.5314	-1.5173	-1.8428	1	0	Cytoplasm
540	P62269	RPS18 D6S218E	40S ribosomal protein S18	1.3981	1.1633	1.2772	5	0	Cytoplasm
541	Q9HDC9	APMAP	Adipocyte plasma membrane-associated protein (Protein BSCv)	-1.0107	-1.5633	-1.4025	1	0	Membrane
542	Q9NP72	RAB18	Ras-related protein Rab-18	-2.9365	-2.8026	-2.3710	1	0	Apical cell membrane
543	P41240	CSK	Tyrosine-protein kinase CSK	-3.7636	-4.2282	-4.0442	1	0	Cytoplasm

List #	UniProt ID	Gene names	Protein names	CTRL Av	BRT Av	ART Av	Peptides #	Significance Elastic Net analysis	Subcellular location
544	P02751	FN1 FN	Fibronectin (FN) (Cold-insoluble globulin)	-1.3461	-0.9979	-1.1771	4	0	Secreted, extracellular space and matrix
545	Q9UIV8	SERPINB13 PI13	Serpin B13	3.4961	3.5778	3.6984	11	0	Cytoplasm
546	P11413	G6PD	Glucose-6-phosphate 1-dehydrogenase (G6PD)	1.9980	1.6700	1.9125	7	0	Cytoplasm, cytosol
547	P20930	FLG	Filaggrin	-1.2458	-1.3187	-1.5184	8	0	Cytoplasmic granule
548	O60218	AKR1B10 AKR1B11	Aldo-keto reductase family 1 member B10	1.3199	1.2193	1.6397	7	0	Lysosome
549	Q92820	GGH	Gamma-glutamyl hydrolase	-1.8569	-1.5754	-1.5753	2	0	Secreted, extracellular space
550	P07900	HSP90AA1 HSP90A HSPC1 HSPCA	Heat shock protein HSP 90-alpha (Heat shock 86 kDa)	1.8006	1.7161	1.8551	6	0	Nucleus
551	P62826	RAN ARA24 OK/SW-cl.81	GTP-binding nuclear protein Ran (Androgen receptor-associated protein 24)	-0.5571	-0.6259	-0.9105	2	0	Nucleus
552	P29034	S100A2 S100L	Protein S100-A2 (S100 calcium-binding protein A2)	2.4499	2.5250	2.2687	4	0	
553	P62937	PPIA CYPA	Peptidyl-prolyl cis-trans isomerase A (PPIase A)	3.3620	3.4585	3.3127	8	0	Cytoplasm
554	O00204	SULT2B1 HSST2	Sulfotransferase 2B1 (Alcohol sulfotransferase)	0.7323	0.6322	0.5514	4	0	Cytoplasm, cytosol
555	P30040	ERP29 C12orf8 ERP28	Endoplasmic reticulum resident protein 29 (ERp29) (Endoplasmic reticulum resident protein 28)	-1.8277	-2.2371	-1.8096	1	0	Endoplasmic reticulum lumen, Melanosome
556	P00492	HPRT1 HPRT	Hypoxanthine-guanine phosphoribosyltransferase (HGPRT)	-3.2961	-4.2804	-3.3125	1	0	Cytoplasm
557	Q04837	SSBP1 SSBP	Single-stranded DNA-binding protein, mitochondrial (Mt-SSB)	-4.6678	-5.5080	-4.8532	1	0	Mitochondrion
558	P63241	EIF5A	Eukaryotic translation initiation factor 5A-1 (eIF-5A-1)	1.1119	1.1007	0.9347	4	0	Cytoplasm,
559	P36952	SERPINB5	Serpin B5	2.8805	3.0566	2.8911	6	0	Secreted, extracellular space
560	P49721	PSMB2	Proteasome subunit beta type-2	-0.4608	-0.6000	-0.5653	2	0	Cytoplasm
561	Q92817	EVPL	Envoplakin (210 kDa cornified envelope precursor protein)	-0.9750	-1.2191	-1.0893	3	0	Cell junction, desmosome
562	P04080	CSTB CST6 STFB	Cystatin-B (CPI-B) (Liver thiol proteinase inhibitor) (Stefin-B)	5.1579	5.0162	4.9378	10	0	Cytoplasm
563	O60235	TMPRSS11D	Transmembrane protease serine 11D	1.6276	1.4454	1.5895	3	0	Cell membrane

List #	UniProt ID	Gene names	Protein names	CTRL Av	BRT Av	ART Av	Peptides #	Significance Elastic Net analysis	Subcellular location
564	P00558	PGK1 PGKA	Phosphoglycerate kinase 1	2.5823	2.5622	2.7383	9	0	Cytoplasm
565	P05089	ARG1	Arginase-1	-2.3862	-2.4135	-2.0630	2	0	Cytoplasm
566	P08670	VIM	Vimentin	1.2312	1.1505	1.5944	6	0	Cytoplasm
567	P35908	KRT2 KRT2A KRT2E	Keratin, type II cytoskeletal 2 epidermal (Cytokeratin-2e)	2.6878	2.9638	2.9035	12	0	
568	Q7L7L0	H2AW HIST3H2A	Histone H2A type 3	-1.8536	-2.2584	-1.7731	1	0	Nucleus
569	P68371	TUBB4B TUBB2C	Tubulin beta-4B chain (Tubulin beta-2 chain)	0.0611	0.0808	-0.0967	2	0	Cytoplasm, cytoskeleton
570	P61586	RHOA ARH12 ARHA RHO12	Transforming protein RhoA	0.7791	0.6366	0.6981	3	0	Cell membrane
571	P62942	FKBP1A FKBP1 FKBP12	Peptidyl-prolyl cis-trans isomerase FKBP1A (PPIase FKBP1A)	-0.7714	-0.8358	-0.6035	1	0	Cytoplasm, cytosol
572	Q96TA1	NIBAN2	Protein Niban 2 (Meg-3)	-0.6359	-0.8431	-0.7835	2	0	Cytoplasm, cytosol
573	P01111	NRAS HRAS1	GTPase NRas (Transforming protein N-Ras)	-1.1436	-0.9671	-1.2881	1	0	Cell membrane
574	P13796	LCP1 PLS2	Plastin-2 (L-plastin)	3.4016	3.0528	3.5685	16	0	Cytoplasm, cytoskeleton
575	P18206	VCL	Vinculin (Metavinculin) (MV)	-1.1853	-0.8408	-0.9631	3	0	Cell membrane
576	P08493	MGP MGLAP GIG36	Matrix Gla protein (MGP) (Cell growth-inhibiting gene 36 protein)	-6.1843	-7.1038	-7.4428	1	0	Secreted
577	P31146	CORO1A CORO1	Coronin-1A (Coronin-like protein A)	1.9128	1.4910	1.9982	9	0	Cytoplasm, cytoskeleton
578	P27348	YWHAQ	14-3-3 protein theta (14-3-3 protein T-cell)	-0.4280	-0.2882	-0.4577	3	0	Cytoplasm
579	P08779	KRT16 KRT16A	Keratin, type I cytoskeletal 16 (Cytokeratin-16)	6.7203	6.3907	6.3926	18	0	
580	Q02878	RPL6 TXREB1	60S ribosomal protein L6	-1.2147	-1.8159	-1.6034	1	0	Cytoplasm, cytosol
581	P61626	LYZ LZM	Lysozyme C	6.3119	6.3743	6.0311	8	0	Secreted
582	P26583	HMGB2 HMG2	High mobility group protein B2 (High mobility group protein 2) (HMG-2)	-1.4139	-1.6161	-1.1721	2	0	Nucleus
583	P37802	TAGLN2 KIAA0120 CDABP0035	Transgelin-2 (Epididymis tissue protein Li 7e) (SM22-alpha homolog)	0.9591	0.7561	0.8276	5	0	
584	P40429	RPL13A	60S ribosomal protein L13a	-0.7713	-0.9463	-1.1269	1	0	Cytoplasm

List #	UniProt ID	Gene names	Protein names	CTRL Av	BRT Av	ART Av	Peptides #	Significance Elastic Net analysis	Subcellular location
585	P25788	PSMA3 HC8 PSC8	Proteasome subunit alpha type-3	-4.5419	-5.2846	-4.6965	1	0	Cytoplasm
586	P04899	GNAI2 GNAI2B	Guanine nucleotide-binding protein G(i) subunit alpha-2 (Adenylate cyclase-inhibiting G alpha protein)	-1.1670	-1.4422	-1.1077	2	0	Cytoplasm
587	Q9UHA7	IL36A FIL1E IL1E IL1F6	Interleukin-36 alpha (FIL1 epsilon) (Interleukin-1 epsilon)	0.6085	0.6591	0.4286	3	0	Cytoplasm
588	P04264	KRT1 KRTA	Keratin, type II cytoskeletal 1 (67 kDa cytokeratin) (Cytokeratin-1)	5.2451	5.2638	5.0544	14	0	Cell membrane
589	Q99877	H2BC15 H2BFD HIST1H2BN	Histone H2B type 1-N (Histone H2B.d) (H2B/d)	3.2339	3.0338	2.9380	2	0	Nucleus
590	P50991	CCT4 CCTD SRB	T-complex protein 1 subunit delta (TCP-1-delta)	-0.4358	-0.5356	-0.5652	3	0	Cytoplasm
591	Q08AI8	MAB21L4 C2orf54	Protein mab-21-like 4	-0.9211	-1.0475	-1.2127	2	0	
592	P62244	RPS15A OK/SW-cl.82	40S ribosomal protein S15a	0.7468	0.5535	0.6445	3	0	
593	P06727	APOA4	Apolipoprotein A-IV (Apo-AIV) (ApoA-IV) (Apolipoprotein A4)	-1.8347	-1.6469	-1.2939	2	0	Secreted
594	P62140	PPP1CB	Serine/threonine-protein phosphatase PP1-beta catalytic subunit (PP-1B)	-2.4800	-2.3472	-2.5005	2	0	Cytoplasm
595	P01833	PIGR	Polymeric immunoglobulin receptor (PIgR) (Poly-Ig receptor)	7.4854	7.5498	7.7534	35	0	Cell membrane
596	P06899	H2BC11 H2BFR HIST1H2BJ	Histone H2B type 1-J (Histone H2B.1) (Histone H2B.r) (H2B/r)	0.6404	0.3835	0.3780	1	0	Nucleus
597	P39023	RPL3 OK/SW-cl.32	60S ribosomal protein L3	-2.7965	-3.2225	-2.8599	1	0	Nucleus
598	Q13510	ASAH1 ASAH HSD-33 HSD33	Acid ceramidase (AC)	-1.8344	-1.6464	-2.1561	1	0	Lysosome
599	P52790	HK3	Hexokinase-3	-2.1653	-1.8835	-1.8953	2	0	
600	P22392	NME2 NM23B	Nucleoside diphosphate kinase B (NDK B)	2.1978	2.3055	2.2317	5	0	Cytoplasm
601	P61158	ACTR3 ARP3	Actin-related protein 3 (Actin-like protein 3)	0.2362	0.1118	0.1123	5	0	Cytoplasm, cytoskeleton
602	P0CG39	POTEJ	POTE ankyrin domain family member J	-1.6490	-1.8506	-1.5383	1	0	
603	Q14CN2	CLCA4 CaCC2 UNQ562/PRO1124	Calcium-activated chloride channel regulator 4 (Calcium-activated chloride channel family member 4)	1.0747	1.2181	1.0114	6	0	Cell membrane
604	P04196	HRG	Histidine-rich glycoprotein (Histidine-proline-rich glycoprotein) (HPRG)	-0.4660	-0.5312	-0.1069	4	0	Secreted

List #	UniProt ID	Gene names	Protein names	CTRL Av	BRT Av	ART Av	Peptides #	Significance Elastic Net analysis	Subcellular location
605	Q6FI13	H2AC18	Histone H2A type 2-A (Histone H2A.2) (Histone H2A/o)	-2.7134	-3.0896	-3.1079	1	0	Nucleus, Chromosome
606	P78371	CCT2 99D8.1 CCTB	T-complex protein 1 subunit beta (TCP-1-beta) (CCT-beta)	-3.0562	-3.2002	-3.2757	2	0	Cytoplasm
607	Q06323	PSME1 IFI5111	Proteasome activator complex subunit 1 (11S regulator complex subunit alpha)	-1.5906	-1.7820	-1.5680	1	0	
608	P06737	PYGL	Glycogen phosphorylase, liver form	-0.2021	-0.4358	-0.3119	3	0	
609	Q08043	ACTN3	Alpha-actinin-3 (Alpha-actinin skeletal muscle isoform 3)	-2.7149	-3.1695	-3.2249	2	0	
610	Q9BXJ4	C1QTNF3 CTRP3	Complement C1q tumor necrosis factor-related protein 3	-0.2557	-0.6857	-0.5536	3	0	Secreted
611	P16401	H1-5 H1F5 HIST1H1B	Histone H1.5 (Histone H1a) (Histone H1b) (Histone H1s-3)	1.0469	0.7178	0.4657	2	0	Nucleus
612	P05164	MPO	Myeloperoxidase (MPO)	5.7350	5.3316	5.5871	22	0	Lysosome
613	P61160	ACTR2 ARP2	Actin-related protein 2 (Actin-like protein 2)	-0.0242	0.0101	-0.1579	2	0	Cytoplasm, cytoskeleton
614	P04040	CAT	Catalase (EC 1.11.1.6)	1.3887	1.3036	1.6183	10	0	Peroxisome
615	Q9Y6R7	FCGBP	IgGFc-binding protein	2.5292	2.5590	2.9689	21	0	Secreted
616	P21333	FLNA FLN FLN1	Filamin-A (FLN-A) (Actin-binding protein 280)	-0.0189	0.0819	-0.1793	4	0	Cytoplasm, cell cortex
617	A0A0B4J1Y9	IGHV3-72	Immunoglobulin heavy variable 3-72	0.5647	0.5545	0.7883	1	0	Secreted
618	P05387	RPLP2 D11S2243E RPP2	60S acidic ribosomal protein P2	-0.4032	-0.1929	-0.2789	2	0	
619	P12814	ACTN1	Alpha-actinin-1 (Alpha-actinin cytoskeletal isoform)	-0.1868	-0.4140	-0.1464	5	0	Cytoplasm, cytoskeleton
620	P49913	CAMP CAP18 FALL39 HSD26	Cathelicidin antimicrobial peptide (18 kDa cationic antimicrobial protein) (CAP-18)	2.6773	2.2581	2.5706	5	0	Secreted
621	Q6NVY1	HIBCH	3-hydroxyisobutyryl-CoA hydrolase, mitochondrial	-3.1775	-3.1729	-3.4067	1	0	Mitochondrion
622	Q04695	KRT17	Keratin, type I cytoskeletal 17 (39.1) (Cytokeratin-17)	3.7797	3.5643	3.8740	16	0	Cytoplasm
623	P08697	SERPINF2 AAP PLI	Alpha-2-antiplasmin (Alpha-2-AP)	-4.0513	-3.6393	-3.9047	1	0	Secreted
624	P10599	TXN TRDX TRX TRX1	Thioredoxin (Trx)	3.1469	3.1130	3.0351	7	0	Nucleus
625	O60437	PPL KIAA0568	Periplakin (190 kDa paraneoplastic pemphigus antigen)	1.8592	1.7613	1.7251	13	0	Cell junction, desmosome

List #	UniProt ID	Gene names	Protein names	CTRL Av	BRT Av	ART Av	Peptides #	Significance Elastic Net analysis	Subcellular location
626	P01876	IGHA1	Immunoglobulin heavy constant alpha 1 (Ig alpha-1 chain C region)	7.8637	7.8510	8.0928	15	0	Secreted
627	P84243	H3-3A H3.3A H3F3 H3F3A PP781	Histone H3.3	-3.8350	-4.2861	-4.0399	1	0	Nucleus
628	P04843	RPN1	Ribophorin-1	-2.0788	-2.0689	-2.3074	2	0	Endoplasmic reticulum
629	P09917	ALOX5 LOG5	Arachidonate 5-lipoxygenase (5-LO) (5-lipoxygenase)	-3.7910	-3.3369	-3.5411	1	0	Cytoplasm
630	P12429	ANXA3 ANX3	Annexin A3	4.3066	4.0078	4.0552	16	0	
631	P22695	UQCRC2	Cytochrome b-c1 complex subunit 2, mitochondrial (Complex III subunit 2)	-2.8176	-2.5104	-2.6474	2	0	Mitochondrion inner membrane
632	P48643	CCT5 CCTE KIAA0098	T-complex protein 1 subunit epsilon (TCP-1-epsilon)	-2.4666	-2.6116	-2.6314	2	0	Cytoplasm
633	Q9C002	NMES1 C15orf48	Normal mucosa of esophagus-specific gene 1 protein (Protein FOAP-11)	-3.1383	-3.1868	-2.9509	1	0	Nucleus
634	P60953	CDC42	Cell division control protein 42 homolog	1.0745	1.1048	1.2741	5	0	Cell membrane
635	P04003	C4BPA C4BP	C4b-binding protein alpha chain (C4bp) (Proline-rich protein)	-2.0347	-2.0340	-2.2717	3	0	Secreted
636	P00387	CYB5R3 DIA1	NADH-cytochrome b5 reductase 3 (B5R) (Cytochrome b5 reductase)	-2.4449	-2.1749	-2.2953	1	0	[Isoform 1]: Endoplasmic reticulum membrane; [Isoform 2]: Cytoplasm
637	Q9Y2V2	CARHSP1	Calcium-regulated heat-stable protein 1 (Calcium-regulated heat-stable protein of 24 kDa)	-2.9441	-2.7875	-2.7242	1	0	Cytoplasm
638	O43242	PSMD3	26S proteasome non-ATPase regulatory subunit 3 (26S proteasome regulatory subunit RPN3)	-4.6145	-4.7297	-4.8502	1	0	
639	P15153	RAC2	Ras-related C3 botulinum toxin substrate 2 (GX) (Small G protein)	-1.2856	-1.4955	-1.0946	1	0	Cytoplasm
640	O75390	CS	Citrate synthase, mitochondrial (EC 2.3.3.1) (Citrate (Si)-synthase)	1.6160	1.6504	1.5615	5	0	Mitochondrion matrix
641	P02765	AHSG FETUA PRO2743	Alpha-2-HS-glycoprotein (Alpha-2-Z-globulin)	1.2776	1.0791	1.4557	4	0	Secreted
642	P62258	YWHAE	14-3-3 protein epsilon (14-3-3E)	1.7304	1.7264	1.6596	5	0	Nucleus
643	P04792	HSPB1 HSP27 HSP28	Heat shock protein beta-1 (HspB1) (28 kDa heat shock protein)	5.7099	5.6782	5.5332	17	0	Cytoplasm
644	P46781	RPS9	40S ribosomal protein S9	0.1308	0.3212	0.1221	2	0	Cytoplasm
645	P30085	CMPK1 CMK CMPK UCK UMK UMPK	UMP-CMP kinase (Uridine monophosphate/cytidine monophosphate kinase)	-1.7983	-1.9088	-2.0342	1	0	Nucleus

List #	UniProt ID	Gene names	Protein names	CTRL Av	BRT Av	ART Av	Peptides #	Significance Elastic Net analysis	Subcellular location
646	P18669	PGAM1 PGAMA	Phosphoglycerate mutase 1	1.4266	1.3984	1.4750	5	0	
647	P47929	LGALS7 PIG1; LGALS7B	Galectin-7 (Gal-7) (HKL-14) (PI7) (p53-induced gene 1 protein)	4.8105	4.8156	4.6194	8	0	Cytoplasm
648	Q7KZF4	SND1 TDRD11	Staphylococcal nuclease domain-containing protein 1	-2.6242	-3.0387	-2.9006	1	0	Cytoplasm
649	Q16651	PRSS8	Prostasin	0.1580	0.2065	-0.0166	2	0	Cell membrane
650	P22531	SPRR2E	Small proline-rich protein 2E (SPR-2E)	-0.0635	-0.0485	0.1935	2	0	Cytoplasm
651	P12882	MYH1	Myosin-1 (Myosin heavy chain 1)	-0.6128	-0.7842	-0.6016	8	0	Cytoplasm, myofibril
652	Q04118	PRB3	Basic salivary proline-rich protein 3 (Parotid salivary glycoprotein G1) (Proline-rich protein G1)	-0.1562	0.3613	-0.4000	2	0	Secreted
653	P21217	FUT3	Galactoside 3(4)-L-fucosyltransferase	-2.4583	-2.5983	-2.3057	1	0	Golgi apparatus
654	P20292	ALOX5AP FLAP	Arachidonate 5-lipoxygenase-activating protein (FLAP)	-0.2427	-0.4979	-0.1302	1	0	Nucleus, membrane
655	P04075	ALDOA ALDA	Fructose-bisphosphate aldolase A	3.7770	3.7133	3.6930	11	0	Cytoplasm
656	P25815	S100P S100E	Protein S100-P (Migration-inducing gene 9 protein)	1.2686	1.2730	1.4024	3	0	Cytoplasm, nucleus
657	P06730	EIF4E	Eukaryotic translation initiation factor 4E (eIF-4E)	-4.9001	-5.3484	-5.1162	1	0	Cytoplasm
658	P02533	KRT14	Keratin, type I cytoskeletal 14 (Cytokeratin-14)	5.2911	5.1893	5.4450	16	0	Cytoplasm. Nucleus
659	P01034	CST3	Cystatin-C (Cystatin-3)	2.8248	3.0473	2.8148	8	0	Secreted
660	P10163	PRB4	Basic salivary proline-rich protein 4	-1.0603	-1.4941	-1.3326	3	0	Secreted
661	P26641	EEF1G	Elongation factor 1-gamma (EF-1-gamma) (eEF-1B gamma)	0.5329	0.6297	0.6678	4	0	
662	P00915	CA1	Carbonic anhydrase 1	-0.8960	-0.9014	-0.6468	5	0	Cytoplasm
663	P61077	UBE2D3 UBC5C UBCH5C	Ubiquitin-conjugating enzyme E2 D3	-0.2514	0.2146	0.2893	1	0	Cell membrane
664	Q9NZD2	GLTP	Glycolipid transfer protein (GLTP)	-0.1246	-0.0282	-0.1491	3	0	Cytoplasm
665	Q9Y678	COPG1 COPG	Coatomer subunit gamma-1 (Gamma-1-coat protein) (Gamma-1-COP)	-3.3850	-3.3240	-3.4198	1	0	Cytoplasm

List #	UniProt ID	Gene names	Protein names	CTRL Av	BRT Av	ART Av	Peptides #	Significance Elastic Net analysis	Subcellular location
666	P04114	APOB	Apolipoprotein B-100 (Apo B-100)	1.6805	1.5137	1.7298	12	0	Cytoplasm
667	O75367	MACROH2A1 H2AFY	Core histone macro-H2A.1 (Histone macroH2A1)	0.2113	0.1497	0.0421	2	0	Nucleus
668	P13688	CEACAM1 BGP BGP1	Carcinoembryonic antigen-related cell adhesion molecule 1 (Biliary glycoprotein 1)	-1.8608	-1.9785	-2.0210	2	0	Cell membrane
669	Q14764	MVP LRP	Major vault protein (MVP)	-2.6741	-2.5995	-2.4262	1	0	Cytoplasm
670	Q9UKR0	KLK12 KLKL5	Kallikrein-12	-1.2549	-0.9330	-1.1780	2	0	Secreted
671	P49748	ACADVL VLCAD	Very long-chain specific acyl-CoA dehydrogenase, mitochondrial (VLCAD)	-0.6994	-0.8138	-0.7549	3	0	Mitochondrion inner membrane
672	Q15084	PDIA6 ERP5 P5 TXNDC7	Protein disulfide-isomerase A6	-0.6387	-0.7590	-0.6569	2	0	Endoplasmic reticulum lumen
673	P51159	RAB27A RAB27	Ras-related protein Rab-27A (Rab-27)	0.5692	0.5861	0.7159	2	0	Membrane
674	P62979	RPS27A UBA80 UBCEP1	Ubiquitin-40S ribosomal protein S27a (Ubiquitin carboxyl extension protein 80)	3.1416	3.0936	3.0929	4	0	Cytoplasm
675	P23528	CFL1 CFL	Cofilin-1 (18 kDa phosphoprotein)	2.0841	2.0430	2.0726	6	0	Nucleus matrix
676	Q5D862	FLG2 IFPS	Filaggrin-2 (FLG-2)	-2.1308	-2.3415	-2.0095	1	0	Cytoplasm
677	P61978	HNRNPK HNRPK	Heterogeneous nuclear ribonucleoprotein K (hnRNP K)	0.0967	0.1563	0.0847	3	0	Cytoplasm
678	Q15365	PCBP1	Poly(rC)-binding protein 1 (Alpha-CP1)	-2.0002	-1.8623	-1.8717	1	0	Nucleus, cytoplasm
679	Q01469	FABP5	Fatty acid-binding protein 5 (Epidermal-type fatty acid-binding protein)	4.2609	4.3649	4.3241	12	0	Cytoplasm
680	P68036	UBE2L3 UBCE7 UBCH7	Ubiquitin-conjugating enzyme E2 L3	-2.9194	-3.0727	-2.9303	1	0	Nucleus
681	P13645	KRT10 KPP	Keratin, type I cytoskeletal 10 (Cytokeratin-10)	4.8698	4.9720	4.8817	22	0	Secreted, extracellular space
682	P55058	PLTP	Phospholipid transfer protein (Lipid transfer protein II)	-0.2435	-0.1591	-0.1236	2	0	Secreted
683	P08133	ANXA6 ANX6	Annexin A6	1.8020	1.6408	1.7109	9	0	Cytoplasm
684	P47756	CAPZB	F-actin-capping protein subunit beta (CapZ beta)	0.6396	0.5836	0.6756	3	0	Cytoplasm, cytoskeleton
685	P57735	RAB25 CATX8	Ras-related protein Rab-25 (CATX-8)	-1.9059	-1.8713	-1.7805	1	0	Cell membrane
686	P62314	SNRPD1	Small nuclear ribonucleoprotein Sm D1 (Sm-D1)	-1.2124	-1.2502	-1.2634	1	0	Cytoplasm, cytosol

List #	UniProt ID	Gene names	Protein names	CTRL Av	BRT Av	ART Av	Peptides #	Significance Elastic Net analysis	Subcellular location
687	P25789	PSMA4 HC9 PSC9	Proteasome subunit alpha type-4	-1.5559	-1.5219	-1.4625	1	0	Cytoplasm
688	P28676	GCA GCL	Grancalcin	2.4802	2.5784	2.4232	5	0	Cytoplasm
689	P08865	RPSA LAMBR LAMR1	40S ribosomal protein SA	1.0583	1.0085	1.0148	4	0	Cell membrane, Cytoplasm, Nucleus
690	P09651	HNRNPA1 HNRPA1	Heterogeneous nuclear ribonucleoprotein A1 (hnRNP A1)	-0.7472	-0.8078	-0.7936	2	0	Nucleus
691	P05388	RPLP0	60S acidic ribosomal protein P0	1.3054	1.2727	1.2620	5	0	Nucleus
692	P59665	DEFA1 DEF1	Neutrophil defensin 1 (Defensin, alpha 1)	4.2059	4.2712	4.0663	2	0	Secreted
693	P02808	STATH	Statherin	-10.4194	-10.5563	-10.3099	1	0	Secreted
694	Q9P0G3	KLK14 KLKL6	Kallikrein-14 (hK14)	-2.7740	-2.7991	-2.8398	1	0	Secreted, extracellular space
695	A0M8Q6	IGLC7	Immunoglobulin lambda constant 7 (Ig lambda-7 chain C region)	-4.6331	-4.6325	-4.5928	1	0	Secreted

Supplemental Table 5: Every table (5.1; 5.2; 5.3) represents the results of the GO enrichment analysis performed per each group of proteins resulted differentially expressed from the Elastic Net analysis, the top GO entries were selected based on false discovery rate (FDR < 0.05).

Table 5.1: The enrichment table of GO terms for the target proteins involved in the network (Group1-BRT, Group2-ART, Group3-CTRL) (*Figure 45*), showing the number of proteins belonging to each term and the FDR value calculated by STRING.

Biological Process (GO)			
GO-term	*description*	*count in gene set*	*false discovery rate*
GO:0006959	humoral immune response	10 of 252	9.64e-08
GO:0019730	antimicrobial humoral response	8 of 143	3.39e-07
GO:0006955	immune response	15 of 1560	7.23e-05
GO:0009607	response to biotic stimulus	11 of 869	0.00026
GO:0061844	antimicrobial humoral immune response mediated by anti...	5 of 107	0.00066
GO:0051707	response to other organism	10 of 835	0.00077
GO:0006952	defense response	12 of 1234	0.00077
GO:0002443	leukocyte mediated immunity	9 of 632	0.00077
GO:0002252	immune effector process	10 of 927	0.0014
GO:1900229	negative regulation of single-species biofilm formation in or...	2 of 2	0.0023
GO:0035821	modification of morphology or physiology of other organism	5 of 182	0.0026
GO:0031640	killing of cells of other organism	4 of 89	0.0026
GO:0002385	mucosal immune response	3 of 31	0.0026
GO:0045055	regulated exocytosis	8 of 691	0.0028
GO:0043312	neutrophil degranulation	7 of 485	0.0028
GO:0033214	siderophore-dependent iron import into cell	2 of 4	0.0028
GO:0030162	regulation of proteolysis	8 of 742	0.0039
GO:0050896	response to stimulus	28 of 7824	0.0040
GO:0016999	antibiotic metabolic process	4 of 124	0.0041
GO:0010951	negative regulation of endopeptidase activity	5 of 242	0.0042
GO:0052548	regulation of endopeptidase activity	6 of 393	0.0043
GO:0050832	defense response to fungus	3 of 49	0.0044
GO:0042742	defense response to bacterium	5 of 250	0.0044
GO:0002576	platelet degranulation	4 of 129	0.0044
GO:1900029	positive regulation of ruffle assembly	2 of 13	0.0092
GO:0030277	maintenance of gastrointestinal epithelium	2 of 17	0.0141
GO:0034143	regulation of toll-like receptor 4 signaling pathway	2 of 19	0.0166
GO:0009617	response to bacterium	6 of 555	0.0176
GO:0009605	response to external stimulus	11 of 1857	0.0187
GO:0001775	cell activation	8 of 1024	0.0187

Cellular Component (GO)			
GO-term	*description*	*count in gene set*	*false discovery rate*
GO:0005576	extracellular region	17 of 2505	0.00045
GO:0044421	extracellular region part	12 of 1375	0.00095
GO:0035580	specific granule lumen	4 of 62	0.00095
GO:0005615	extracellular space	11 of 1134	0.00095
GO:0034774	secretory granule lumen	6 of 323	0.0019
GO:0044218	other organism cell membrane	2 of 5	0.0022
GO:1904724	tertiary granule lumen	3 of 55	0.0045
GO:0070820	tertiary granule	4 of 164	0.0059
GO:0031093	platelet alpha granule lumen	3 of 68	0.0059
GO:0005788	endoplasmic reticulum lumen	5 of 299	0.0059
GO:0044432	endoplasmic reticulum part	9 of 1294	0.0121
GO:0030141	secretory granule	7 of 828	0.0146
GO:0005783	endoplasmic reticulum	10 of 1796	0.0270
GO:0043195	terminal bouton	2 of 44	0.0353

Table 5.2: The enrichment table of GO terms for the target proteins involved in the network (Group2-ART vs Group1-BRT) (*Figure 46*), showing the number of proteins belonging to each term and the FDR value calculated by STRING.

Biological Process (GO)			
GO-term	*description*	*count in gene set*	*false discovery rate*
GO:0019730	antimicrobial humoral response	5 of 143	0.00013
GO:0061844	antimicrobial humoral immune response mediated by anti...	4 of 107	0.00049
GO:0042742	defense response to bacterium	5 of 250	0.00049
GO:0031640	killing of cells of other organism	4 of 89	0.00049
GO:0050832	defense response to fungus	3 of 49	0.0011
GO:0033214	siderophore-dependent iron import into cell	2 of 4	0.0011
GO:0051707	response to other organism	6 of 835	0.0037
GO:0050829	defense response to Gram-negative bacterium	3 of 95	0.0038
GO:0000028	ribosomal small subunit assembly	2 of 17	0.0048
GO:0044419	interspecies interaction between organisms	5 of 724	0.0136
GO:0001580	detection of chemical stimulus involved in sensory percepti...	2 of 36	0.0177
GO:0006952	defense response	6 of 1234	0.0188
GO:0009605	response to external stimulus	7 of 1857	0.0236
GO:0030490	maturation of SSU-rRNA	2 of 52	0.0291
GO:2000116	regulation of cysteine-type endopeptidase activity	3 of 243	0.0346

Cellular Component (GO)			
GO-term	*description*	*count in gene set*	*false discovery rate*
GO:0030867	rough endoplasmic reticulum membrane	2 of 23	0.0319
GO:0022627	cytosolic small ribosomal subunit	2 of 38	0.0319
GO:0005615	extracellular space	6 of 1134	0.0319
GO:0035580	specific granule lumen	2 of 62	0.0420

Table 5.3: The enrichment table of GO terms for the target proteins involved in the network (Group3-CTRL vs Group2-ART) (*Figure 47*), showing the number of proteins belonging to each term and the FDR value calculated by STRING.

Biological Process (GO)			
GO-term	*description*	*count in gene set*	*false discovery rate*
GO:0019730	antimicrobial humoral response	4 of 143	0.00045
GO:0033214	siderophore-dependent iron import into cell	2 of 4	0.00100
GO:0010951	negative regulation of endopeptidase activity	4 of 242	0.0012
GO:0030277	maintenance of gastrointestinal epithelium	2 of 17	0.0025
GO:0006955	immune response	6 of 1560	0.0030
GO:0043312	neutrophil degranulation	4 of 485	0.0034
GO:0006953	acute-phase response	2 of 45	0.0054
GO:0031640	killing of cells of other organism	2 of 89	0.0127
GO:0061844	antimicrobial humoral immune response mediated by anti...	2 of 107	0.0158
GO:2000117	negative regulation of cysteine-type endopeptidase activity	2 of 110	0.0164
GO:0002576	platelet degranulation	2 of 129	0.0192
GO:0006952	defense response	4 of 1234	0.0284
GO:0051704	multi-organism process	5 of 2222	0.0358
GO:0044419	interspecies interaction between organisms	3 of 724	0.0489

Molecular Function (GO)			
GO-term	*description*	*count in gene set*	*false discovery rate*
GO:0004866	endopeptidase inhibitor activity	4 of 169	0.00012
GO:0004869	cysteine-type endopeptidase inhibitor activity	2 of 57	0.0051
GO:0004867	serine-type endopeptidase inhibitor activity	2 of 94	0.0113
GO:0004175	endopeptidase activity	3 of 399	0.0113
GO:0098772	molecular function regulator	5 of 1793	0.0126
GO:0005506	iron ion binding	2 of 147	0.0173

Cellular Component (GO)			
GO-term	*description*	*count in gene set*	*false discovery rate*
GO:0044218	other organism cell membrane	2 of 5	0.00058
GO:0034774	secretory granule lumen	4 of 323	0.00074
GO:0005576	extracellular region	7 of 2505	0.0019
GO:0005615	extracellular space	5 of 1134	0.0028
GO:0035580	specific granule lumen	2 of 62	0.0049
GO:0031093	platelet alpha granule lumen	2 of 68	0.0051
GO:0035578	azurophil granule lumen	2 of 92	0.0077
GO:0012505	endomembrane system	7 of 4347	0.0181
GO:0070013	intracellular organelle lumen	7 of 5162	0.0420

2 INFORMED CONSENT

IMPRESO DE INFORMACIÓN Y CONSENTIMIENTO INFORMADO DE LOS SUJETOS

A INCLUIR EN EL PROYECTO DE INVESTIGACION

Título del proyecto: Cambios en los marcadores inflamatorios salivales y análisis proteómico en pacientes con carcinomas oral de células escamosas y cáncer de cabeza y cuello tratados con radioterapia.

INVESTIGADOR PRINCIPAL: Dr. José V. Bagán Sebastián

OBJETIVOS:

Realizar un estudio de investigación para determinar si existen alteraciones en la saliva de los pacientes con cáncer en la cavidad oral, así como en los tumores malignos de la cabeza y del cuello tras el tratamiento de los pacientes con radioterapia.

DESCRIPCIÓN DEL ESTUDIO

Se le va a realizar un estudio completo de la boca valorando, mediante exploración física, las lesiones orales que pudiese tener antes y tras el tratamiento con radioterapia. No realizaremos ninguna técnica cruenta en este estudio.

Se tomará una muestra de saliva en reposo del paciente, sin ningún método de estimulación química o mecánica, se hará antes de iniciar la radioterapia, y se repetirá dicha toma de su saliva tras haber realizado todo el tratamiento.

Si Ud. esta de acuerdo, libremente firme el consentimiento de participación en este estudio que para este fin se ha añadido al final de este impreso.

RIESGOS Y BENEFICIOS

No existen riesgos asociados a la toma de saliva.

Con su participación en este estudio, usted va a ayudar a conocer los cambios que se producen en la saliva tras el tratamiento con radioterapia del cáncer de la boca y de la cabeza y cuello.

Esta información podrá ser aprovechada en su propia salud.

PARTICIPACIÓN EN EL ESTUDIO

Su participación en este estudio es totalmente voluntaria y no recibirá remuneración alguna.

Como paciente, el rechazo a participar no supondrá ninguna penalización y ni afectará en modo alguno a la calidad de la asistencia sanitaria que reciba.

CONFIDENCIALIDAD

Toda la información obtenida será confidencial, los datos recogidos se introducirán, por el equipo investigador, en una base de datos para realizar el análisis estadístico pero su nombre no aparecerá en ningún documento del estudio, sólo se le asignará un número. En concreto, las muestras se identificarán con un número y se agruparan por patologías afines. En ningún caso se le identificará en las publicaciones que puedan realizarse con los resultados del estudio. Sin embargo, esta información podrá ser revisada por el Comité Ético de Investigación Clínica del Hospital General Universitario de Valencia así como por organismos gubernamentales competentes.

Puede ejercer su derecho de acceso y rectificación de sus datos. También, si así lo desea, puede ser informado de los resultados del estudio.

El estudio se realizará asegurando el cumplimiento de normas éticas y legales vigentes (Declaración de Helsinki).

Si tiene alguna duda o no entiende este texto consulte antes de firmar el documento con el Dr. José V. Bagán - teléfono 620224129 que es el médico responsable de esta investigación y le puede preguntar cualquier duda o problema que tenga relacionado con este estudio o consulte con sus familiares y, finalmente, si está de acuerdo firme este consentimiento. Se le entregará una copia.

Fdo.: José V. Bagán
Investigador Principal del Proyecto
Universidad de Valencia y Servicio
de Estomatología y Cirugía
Maxilofacial del Hospital General
Universitario de Valencia (HGUV)
TEL: 620224129

Firma del participante:
Fecha: _____

Título del estudio: Cambios en los marcadores inflamatorios salivales y análisis proteómico en pacientes con carcinomas oral de células escamosas y cáncer de cabeza y cuello tratados con radioterapia.

Yo,……..……

He leído la hoja de información anterior.

He podido hacer preguntas sobre el estudio.

He recibido suficiente información sobre el estudio.

He hablado con el Dr. José V. Bagán Sebastián y para la explicación del estudio.

Comprendo que mi participación es voluntaria.

Comprendo que puedo retirarme del estudio:

- Cuando quiera.
- Sin tener que dar explicaciones.
- Sin que esto repercuta en mis cuidados médicos.

Doy mi consentimiento para que este material aparezca en informes y artículos de revista de publicaciones médicas.

Entiendo que:

- Mi nombre no será publicado.
- El material no será utilizado para publicidad o embalaje.
- El material no será utilizado fuera de contexto.

Firmado…….. Fecha……..

CONSENTIMIENTO INFORMADO DEL REPRESENTANTE LEGAL

Título del estudio: Cambios en los marcadores inflamatorios salivales y análisis proteómico en pacientes con carcinomas oral de células escamosas y cáncer de cabeza y cuello tratados con radioterapia.

Yo, ……
en calidad de: ……
de: ……

He leído la hoja de información anterior.
He podido hacer preguntas sobre el estudio.
He recibido suficiente información sobre el estudio.

He hablado con el Dr. José V. Bagán para la explicación del estudio.
Comprendo que la participación es voluntaria.
Comprendo que puede retirarme del estudio:

- Cuando quiera.
- Sin tener que dar explicaciones.
- Sin que esto repercuta en mis cuidados médicos.

Comprendo que este material aparezca en informes y artículos de revista de publicaciones médicas.
Entiendo que:

- Mi nombre no será publicado.
- El material no será utilizado para publicidad o embalaje.
- El material no será utilizado fuera de contexto

En mi presencia se ha dado a ……
……toda la información pertinente adaptada a su nivel de entendimiento y está de acuerdo en participar.

Y presto mi conformidad con que……
…… participe en el estudio.

Firmado…….. Fecha……..

3 APPROVAL FROM THE INSTITUTIONAL ETHICAL REVIEW BOARD

VNIVERSITAT DE VALÈNCIA Vicerectorat d'Investigació i Política Científica

D. José María Montiel Company, Profesor Contratado Doctor Interino del departamento de Estomatología, y Secretario del Comité Ético de Investigación en Humanos de la Comisión de Ética en Investigación Experimental de la Universitat de València,

CERTIFICA:

Que el Comité Ético de Investigación en Humanos, en la reunión celebrada el día 12 de diciembre de 2016, una vez estudiado el proyecto de investigación titulado:
"Cambios en los marcadores inflamatorios salivales y análisis proteómico en pacientes con carcinomas oral de células escamosas y cáncer de cabeza y cuello tratados con radioterapia", *número de procedimiento H1480791009194*,
cuyo responsable es D. José V. Bagán Sebastián,
ha acordado informar favorablemente el mismo dado que se respetan los principios fundamentales establecidos en la Declaración de Helsinki, en el Convenio del Consejo de Europa relativo a los derechos humanos y cumple los requisitos establecidos en la legislación española en el ámbito de la investigación biomédica, la protección de datos de carácter personal y la bioética.

Y para que conste, se firma el presente certificado en Valencia, a catorce de diciembre de dos mil dieciséis.

Av. Blasco Ibáñez, 13 tel: 9638 64109 vicerec.investigacio@uv.es
València 46010 fax: 9639 83221 www.uv.es/cerinves

4 FUNDINGS

This project has received funding from the European Union's Horizon 2020 research and innovation programme under the Marie Sklodowska-Curie grant agreement No 721906.